Université de Montréal

Biochemical and functional characterization of the tumor suppressors BRCA1 and BAP1

par
Ian Hammond-Martel

Programmes de biologie moléculaire

Faculté de Médecine

Thèse présentée à la Faculté de Médecine
en vue de l'obtention du grade de Ph.D. en Biologie moléculaire, option générale

April, 2015

Résumé

L'ubiquitination est une modification post-traductionnelle qui joue un rôle majeur dans la régulation d'une multitude de processus cellulaires. Dans cette thèse, je discuterai de la caractérisation de deux protéines, BRCA1 et BAP1, soit deux suppresseurs de tumeurs fonctionnellement reliés. BRCA1, une ubiquitine ligase qui catalyse la liaison de l'ubiquitine à une protéine cible, est mutée dans les cancers du sein et de l'ovaire. Il est bien établi que cette protéine aide à maintenir la stabilité génomique suite à un bris double brin de l'ADN (BDB), et ce, à l'aide d'un mécanisme de réparation bien caractérisé appelé recombinaison homologue. Cependant, les mécanismes de régulation de BRCA1 suite à des stresses génotoxiques n'impliquant pas directement un BDB ne sont pas pleinement élucidés. Nous avons démontré que BRCA1 est régulée par dégradation protéasomale suite à une exposition des cellules à deux agents génotoxiques reconnus pour ne pas directement générer des BDBs, soit les rayons UV, qui provoquent la distorsion de l'hélice d'ADN, et le méthyle méthanesulfonate (MMS), qui entraîne l'alkylation de l'ADN. La dégradation de BRCA1 est réversible et indépendante des kinases associées à la voie des PI3 kinase, soit ATM, ATR et DNA-PK, protéines qui sont rapidement activées par les dommages à l'ADN. Nous proposons que la dégradation de BRCA1 prévienne son recrutement intempestif, ainsi que celui des facteurs qui lui sont associés, à des sites de dommages d'ADN qui ne sont pas des BDBs, et que cette régulation coordonne la réparation de l'ADN.

L'enzyme de déubiquitination BAP1 a initialement été identifiée comme une protéine capable d'interagir avec BRCA1 et de réguler sa fonction. Elle est également connue pour sa capacité à se lier avec les protéines du groupe Polycomb, ASXL1 et ASXL2. Cependant,

l'importance de ces interactions n'a toujours pas été établie. Nous avons démontré que BAP1 forme deux complexes protéiques mutuellement exclusifs avec ASXL1 et ASXL2. Ces interactions sont critiques pour la liaison de BAP1 à l'ubiquitine ainsi que pour la stimulation de son activité enzymatique envers l'histone H2A. Nous avons également identifié des mutations de BAP1 dérivées de cancers qui empêchent à la fois son interaction avec ASXL1 et AXSL2, et son activité de déubiquitinase, ce qui fournit un lien mécanistique direct entre la déubiquitination de H2A et la tumorigenèse.

Élucider les mécanismes de régulation de BRCA1 et BAP1 menera à une meilleure compréhension de leurs rôles de suppresseurs de tumeurs, permettant ainsi d'établir de nouvelles stratégies de diagnostic et traitement du cancer.

Mots-clés : ubiquitination, BRCA1, ADN, dommage, déubiquitination, BAP1, ASXL1, ASXL2, histone, H2A

Abstract

Ubiquitination is a post-translational modification that plays major roles in regulating a plethora of cellular processes. In this thesis, I will discuss the biochemical and functional characterization of two functionally related proteins, BRCA1 and BAP1, both of which are important tumor suppressors. BRCA1, an ubiquitin ligase that catalyzes the attachment of ubiquitin to target proteins, is mutated in breast and ovarian cancers. BRCA1 roles in maintaining genomic stability following DNA double strand breaks (DSBs) by promoting the homologous recombination repair pathway is well established. However, how BRCA1 is regulated following genotoxic stress that does not directly involve DSBs is still not fully elucidated. We showed that BRCA1 is downregulated, through proteasomal degradation, following exposure of the cells to the DNA helix distorting agent UV or the DNA alkylating agent Methyl Methanesulfonate (MMS), two DNA damaging agents that do not directly generate DSBs. BRCA1 downregulation is reversible and is independent of the PI3 kinase related kinases, ATM, ATR or DNA-PK which constitute primary responders that are rapidly activated by DNA damage. We proposed that BRCA1 downregulation prevents the untimely recruitment of BRCA1 and associated factors to DNA damage sites that are not DSBs, thus coordinating the DNA damage/repair response.

The deubiquitinating enzyme BAP1 was initially identified as an interacting protein that regulates the function of BRCA1. BAP1 is also known to interact with the Polycomb group proteins ASXL1 and ASXL2. However, the importance of this interaction was not fully understood. We showed that BAP1 forms two mutually exclusive complexes with ASXL1 and ASXL2. These interactions are critical for BAP1 binding to ubiquitin and stimulation of its

deubiquitinase activity towards histone H2A. We also identified cancer-derived mutations of BAP1 that abrogate its interaction with ASXL1 and ASXL2 and deubiquitinase activity, which provide a direct mechanistic link between H2A deubiquitination and tumorigenesis.

Elucidating how BRCA1 and BAP1 are regulated will lead to a better understanding of their roles as tumor suppressors and this will in turn help establishing improved diagnostic and therapeutic strategies to treat cancer.

Keywords: ubiquitination, BRCA1, DNA, damage, deubiquitination, BAP1, ASXL1, ASXL2, histone, H2A

Table of contents

List of figures

Introduction

Discussion

List of abbreviations

a.a or aa : amino acid

ASXL1/2 : additional sex-combs-like 1/2

ATM: Ataxia Telangiectasia Mutated

ATR: Ataxia Telangiectasia and Rad3 Related

BACH1: BRCA1-associated C-terminal helicase

BAP1: BRCA1-associated protein 1

BRCA1: Breast Cancer early onset 1

BRCC : BRCA1/BRCA2-containing complex

CC : Coiled Coil

CDK: Cyclin dependent kinase

CSA/B: Cockayne syndrome type A/ type B

CtIP : CtBP interacting protein

DDB1/2: DNA damage-binding protein ½

DNA: Deoxyribonucleic acid

DSB: DNA double strand break

DUB : Deubiquitinase

GG-NER: Global genomic NER

HCF-1 : Host cell factor 1

HECT: Homologous to the E6-AP Carboxyl Terminus

HR: homologous recombination

IR: Ionizing radiation

IRIF: IR induced foci

JAMM: JAB1/MPN/Mov34

K# : Lysine #

KO : Knockout

MDC1: Mediator of DNA damage checkpoint protein 1

MJD: Machado-Joshephin domain

MMS: Methyl methane sulfonate

MNR : Mre11-Rad50-Nbs1

MS : mass spectrometry

NHEJ: non-homologous end joining

NER: Nucleotide excision repair

PALB2 : Partner and localizer of BRCA1

PARP : poly(ADP-ribose) polymerase

PARPi : PARP inhibitor

PCNA: Proliferating cell nuclear antigen

PTM : post-translational modification

PRR: Postreplication repair

OTU: Ovarian Tumour superfamily

RING: Really Interesting New Gene

RNA: Ribonucleic acid

RNAi: RNA interference

RNF : RING finger protein

RPA : Replication protein A

ShRNA: Short hairpin RNA

SiRNA: Small interfering RNA

SSB : Single-strand break

TC-NER: Transcription coupled NER

TLS: Translesion synthesis

TS: Template switching

Ub: ubiquitin

UCH: Ubiquitin C-terminal hydrolase

UIM : Ubiquitin interaction motif

USP: Ubiquitin-specific processing protease

UV: Ultraviolet

WT : wildtype

YY1 : Yin Yang 1

Acknowledgments

I would like to begin by thanking my research director, Dr. El Bachir Affar, for accepting me into his lab as one of his first students and for teaching me almost everything I know in science. It was not always easy and we did not always see eye to eye. But in the end, we did some great research together and I will be forever greatful for all the knowledge and tools he has have given me to be a succesful scientist in the future.

I would also like to thank every student that has passed through the lab for their help and support over my years in the Affar lab, especially Helen Pak and Salima Daou, who were major contributors to the succes and publication of my research. A special thanks to two colleagues, Drs. Helen Yu and Nazar Mashtalir, for great teamwork and support. We were the first three students in the lab, and I think we all helped each other to get through what can be at times a very difficult life in science. I would also like to thank all the other contributing author that participated in my reasearch.

A special thanks to Dr. Elliot Drobetsky for taking me and Dr. Yu into his lab for the first few months before Bachir arrived at the research center and for continued guidance and support over the years. I would also like to thank Drs. Alain Verreault, Richard Bertrand and Gerardo Ferbeyre for their participation in my various commitees during my studies. I also need to mention the financial and administrative support from the Programmes de biologie moleculaire that I received during my time at the Universite de Montreal. Also a big thank you to all the students, especially the people from my new lab with Dr. Hugo Wurtele, and other researchers at the HMR research center for guidance and scientific support.

Last but not least, I would not be where I am today without the love and support of my family and friends. To my parents, Louise Martel and Ron Hammond, I love you very much. Thank you for giving me everything I ever needed to succeed in life and all your support of my career path. I also had the best grandparents, Yvon Martel and Moira McLarnon, who stimulated my intellectual abilities as a very young child every night by watching Jeopardy with me. I know you would be proud of me and I miss you very much. Thank you to all the rest of my family, especially my godfathers, Paul and Normand Martel, for their love and support. I don't have many true friends but the ones I do have I have known for close to 19 years now and will always be a part of my life. Thank you to Simon Goudreau, Jean-Philippe Pelletier, Maxime Thériault, Maxime Thériault and Gary Carillo-Lopez for all your support as friends/therapists over the years. Finally, thank you to my wife, Marie-Pier Dufresne. We started going out during my first year as a Master's student and she has never left my side since. You are everything to me and none of this would have been possible without you. Love you forever.

Chapter 1: Introduction

1.1 General principles of ubiquitination

Ubiquitin (Ub) is a small protein of 76 amino acids that was first described in 1975 by the Niall lab as an abundant and highly conserved protein[1]. Ciechanover, Hershko and Rose then described in the 1980s the enzymology of Ub conjugation through fractionation reconstitution studies using an ATP-dependent, cell-free proteolytic system from reticulocytes established by Etlinger and Goldberg[2-5]. The first step of the ubiquitination process is carried out by the Ub-activating enzyme E1 during which Ub is activated in an ATP-dependent manner and linked through a high-energy thioester bond to the E1 enzyme (Figure 1). Ub is then transferred to the Ub-conjugating enzyme E2. Ub-E2 forms an intermediate complex with the Ub-ligase E3 coupled to the protein substrate. Ub is then ligated to a lysine residue of the target protein through an isopeptide bond using the carboxy-terminal glycine residue of Ub. It was later shown that multi-Ub chains could be formed during which an Ub molecule is linked to the lysine 48 (K48) residue of another Ub molecule[6]. This classical form of polyubiquitination of protein substrates by K48 Ub linkage was shown to serve as a signal responsible for protein degradation by the 26S proteasome[7]. The final step of the ubiquitination pathway that precedes proteolysis is the recycling of free Ub which is carried out by deubiquitinases (DUBs) [8,9]. Many other forms of ubiquitination have been studied, including monoubiquitination and polyubiquitination using different lysine residues (K6, K11, K27, K29, K33 and K63), that serve to regulate a plethora of cellular processes[10,11]. The discovery of protein degradation by the the ubiquitin-proteasome system led to the 2004 Nobel Prize in Chemistry. Since the initial discovery of the ubiquitin protein, much has been

elucidated on the mechanisms and biological functions of ubiquitination. In the next sections I will briefly discuss the mechanism of action of the two major ubiquitination enzymes in link with my thesis: E3 ubiquitin ligase and DUBs.

1.1.1 E3 ubiquitin ligases

While only 1 or 2 E1-activating and a few dozen E2-conjugating enzymes exist, more than 500 human E3 ubiquitin ligases have been found throughout the genome. E3 ligases determine the specificity of the ubiquitination reaction by recognizing target proteins and play a multitude of functions in numerous cellular events including the maintenance of genome stability such as in the case with BRCA1. Two different classes of Ub ligases exist based on their catalytic domain and mechanism of ubiquitin transfer: the RING finger and HECT domain classes. The RING (Really Interesting New Gene) finger domain consists of 40-60 amino acids containing eight conserved cysteine and histidine residues[12]. RING ligases, such as BRCA1, promote the transfer of ubiquitin from the E2 to the target protein. The 350 amino acid HECT (Homologous to the E6-AP Carboxyl Terminus) domain consists of an N-terminal region that binds to the E2 and a C-terminal region containing a conserved catalytic cysteine residue allowing for direct interaction with ubiquitin[13]. HECT ligases will first bind to the E2 and form a thioester bond between the ubiquitin moiety and its catalytic cysteine and will then transfer ubiquitin to the protein substrate. An interesting example of a HECT ligase in link with BRCA1 is HERC2, which was shown to ubiquitinate BRCA1, signaling for its proteasomal degradation[14].

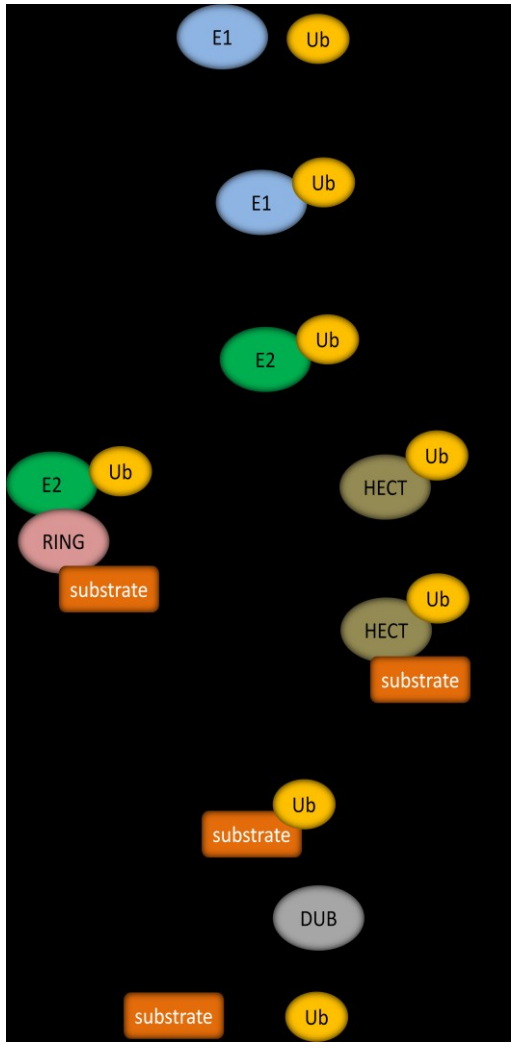

Figure 1. The ubiquitination signaling pathway. Ubiquitin is linked through a thioester bond to the E1-activating enzyme in an ATP-dependent manner and is transferred to the Ub-conjugating enzyme E2. Then the ubiquitin moiety is linked to the substrate protein through the action of two different types of E3 ubiquitin ligase. The RING ligases will bind to the E2 mediating the transfer of Ub to the substrate protein, while HECT ligases first bind to Ub and then transfer it directly to the target protein. DUB proteases are responsible for the reversibility of the ubiquitination pathway by cleaving off ubiquitin from substrate proteins.

1.1.2 Deubiquitinases (DUBs)

DUBs are proteases involved in the reversibility of the ubiquitination process by removing ubiquitin adducts from substrates through their proteolytic activity[8]. While the full range of cellular signaling events that are regulated by DUBs still remains to be fully elucidated, it is known that these enzymes (approximately 100)[15] are crucial for coordinating important cellular processes and maintaining genome integrity[16]. Two different classes of DUBs are divided in 5 different families depending on the secondary structure of their active cleft during ubiquitin binding and catalysis: cysteine proteases (USP, UCH, OTU and MJD) and metalloproteases (JAMM) [8,15]. In link with my thesis, the deubiquitinase BAP1 represents a member of the Ubiquitin C-terminal Hydrolase (UCH) DUB family whose active cleft is composed of three conserved residues (cysteine, histidine and aspartate) that form the catalytic triad[15]. UCH enzymes have a characteristic conserved papain-like catalytic domain including a flexible cross-over loop in its active site[17,18]. BAP1 is closely related to another family member, UCH-L5 (also known as UCH37), sharing an unusual C-terminal extension termed ULD, important for protein-protein interactions[19,20].

In the following section, I will describe in more detail the role of ubiquitination in the regulation of transcription. This section was originally published in Cellular Signalling as a review article that I wrote as a first co-author.

1.2 Review article: Roles of Ubiquitin Signaling in Transcription Regulation

Review on the role of ubiquitination in transcription regulation that I co-wrote with Helen Yu.

Roles of Ubiquitin Signaling in Transcription Regulation

Ian Hammond-Martel1[#], Helen Yu1[#], and El Bachir Affar[1,2]

[1]Maisonneuve-Rosemont Hospital Research Center, Department of Medicine and Department of Biochemistry, University of Montréal, Montréal, Canada

[2]Correspondence
El Bachir Affar
University of Montréal, Centre de Recherche, Hôpital Maisonneuve-Rosemont
5415 boul. de l'Assomption, Montréal, Québec, H1T 2M4, CANADA
[#] Equally contributed to this work

SUMMARY

Rivaling or cooperating with other post-translational modifications, ubiquitination plays central roles in regulating numerous cellular processes. Not surprisingly, gain- or loss-of-function mutations in several components of the ubiquitin system are causally linked to human pathologies including cancer. The covalent attachment of ubiquitin to target proteins occurs in sequential steps and involves ubiquitin ligases (E3s) which are the most abundant enzymes of the ubiquitin system. Although often associated with proteasomal degradation, ubiquitination is also involved in regulatory events in a proteasome-independent manner. Moreover, ubiquitination is reversible and specific proteases, termed deubiquitinases (DUBs), remove ubiquitin from protein substrates. While we now appreciate the importance of ubiquitin signaling in coordinating a plethora of physio-pathological processes, the molecular mechanisms are not fully understood. This review summarizes current findings on the critical functions exerted by E3s and DUBs in transcriptional control, particularly chromatin remodeling and transcription initiation/elongation.

INTRODUCTION

Ubiquitin (Ub) is an essential 76 amino acid protein ubiquitously expressed and highly conserved from yeast to humans [1, 2]. The Ub conjugation reaction, termed ubiquitination (also ubiquitinylation or ubiquitylation), is catalyzed by the sequential action of Ub-activating (E1), Ub-conjugating (E2), and Ub-ligating (E3) enzymes, and results in the attachment of a Ub moiety either to the ε-amino group of a lysine (K) residue or the amino-terminus of a polypeptide [3, 4]. Covalently attached to target proteins, Ub constitutes a signaling module that either induces proteasomal degradation or modulates protein activity depending on the nature of the modification, e.g. monomer or Ub chains [5, 6]. Indeed, Ub itself contains 7 lysines (K6, K11, K27, K29, K33, K48 and K63) that serve as attachment sites for further addition of Ub molecules allowing formation of various homo- and hetero- typic chains potentially associated with diverse signaling events [6]. Ubiquitination is a reversible modification and deubiquitinating enzymes (DUBs) catalyze the removal of Ub from targeted substrates. In addition to housekeeping functions associated with the recycling and metabolism of ubiquitin, DUBs act to spare proteins from degradation or to modulate their function [7-9]. During the last decade, E3s and DUBs have emerged as important regulators of diverse cellular processes ranging from receptor signaling at the plasma membrane, to transcription regulation and DNA damage responses in the nucleus. In this review, we describe the roles of ubiquitination in transcription regulation. We first discuss recent advances on the concerted action of E3s and DUBs in regulating chromatin structure via histone ubiquitination. In the second part, we select two examples of transcription factors whose ubiquitination plays major roles in exquisitely coordinating their function. Finally, we

summarize the state of knowledge on ubiquitin-mediated regulation of RNA polymerase II (Pol II) representing yet another level of transcriptional control.

HISTONE UBIQUITINATION IN TRANSCRIPTION REGULATION

Histones allow compaction of DNA into nucleosomes, the basic units of chromatin. The nucleosome is composed of 147 base pairs of DNA wrapped twice around an octamer of four core histones (H2A, H2B, H3 and H4) [10]. Chromatin compaction and decompaction play crucial roles in DNA-associated processes, and histone modifications (acetylation, methylation, phosphorylation and ubiquitination) represent major mechanisms of chromatin function [11]. Moreover, these histone modifications influence one another and the coexistence of specific modifications throughout the genome directs either gene expression or silencing events [12]. Histone H2A was the first ubiquitinated protein to be identified; indeed this modification is one of the most abundant in mammalian cells (5-15% of total H2A in a variety of higher eukaryotic organisms) [13]. Although polyubiquitination of H2A has been reported, monoubiquitinated K119 (H2Aub) appears to be the major form [14]. H2B is also ubiquitinated, but in contrast to H2Aub which has not been found in Saccharomyces cerevisiae, H2Bub is conserved from yeast (K123) to human (K120) [15]. A significant number of studies provided insights into the roles of H2A/B ubiquitination in transcriptional regulation, and this resulted in several mechanistic models: 1) Histone ubiquitination affects chromatin structure, which in turn regulates the accessibility of DNA to the transcriptional machinery. 2) Ub moieties constitute signaling molecules which mediate the recruitment of downstream regulators that activate or inhibit transcription. 3) Through trans-histone crosstalk, histone ubiquitination acts as a prerequisite modification for other histone

modifications that alter the structure and function of chromatin [16]. Recent findings suggest that an intricate interplay between these non-mutually exclusive mechanisms coordinates gene expression. In the following section, we discuss how ubiquitination/deubiquitination of H2B and H2A control transcription through the analysis of enzymes and cofactors catalyzing these reactions.

Ubiquitination of histone H2B

Monoubiquitination of H2B (H2Bub) is catalyzed by the E2 RAD6 and the E3 BRE1 in S. cerevisiae [17-19]. These two proteins form an E3 complex with Large cells protein 1 (Lge1) which regulates the recruitment of the complex to chromatin [18, 20]. In mammalian cells, two homologues of RAD6 (HR6A and HR6B) and BRE1 (RNF20 and RNF40) have been identified as the major mediators of H2B ubiquitination [21-23]. HR6A and HR6B might work redundantly since Hr6b knock-out mice, while displaying male sterility, are viable and exhibit a level of H2Bub comparable to wild-type mice [24, 25]. It is also possible that other E2s for H2B operate under specific conditions. For instance, UbcH6 has been found to interact with RNF20/40 and stimulate its H2B E3 activity in vitro [23]. However, its role in H2B ubiquitination in vivo is still not well defined. In providing new insight into the molecular mechanism of H2B ubiquitination, it was revealed that RNF20/RNF40 forms a complex with RAD6 and the WW domain-containing adapter protein with coiled-coil, WAC, in vivo. RNF20 is the subunit of this E3 complex that catalyzes H2Bub formation and this activity requires WAC, since depletion of the latter impairs H2B ubiquitination. WAC interacts through its C-terminal coiled-coil region with RNF20/40 and through the N-terminal WW domain with Pol II, thus appearing to directly link H2B ubiquitination to the

transcription machinery [26]. Of note, the mammalian BAF250/ARID1, a component of the SWI/SNF-A chromatin remodelling complex, assembles a cullin 2-containing E3 that also ubiquitinates H2B on K120 [27]. More studies are needed to determine the exact mechanisms that coordinate the action of H2B E3s and their cofactors.

Earlier observations indicated that H2Bub is preferentially located in transcriptionally active chromatin regions [28] and is associated with ongoing transcription and open chromatin configuration [29]. Consistent with this notion, using high-resolution tilling array coupled with chromatin immunoprecipitation using a specific antibody recognizing H2Bub, Minsky et al. demonstrated that this histone mark is localized mainly on transcribed regions of highly expressed genes [30]. H2Bub has been extensively characterized using the power of yeast genetics. The current model asserts that RAD6/BRE1 E2-E3 ligase complex is recruited to promoters by activators such as Gal4 in yeast or p53 in mammals [19, 22, 31]. Upon transcription activation, phosphorylation of serine 5 on the C-terminal domain of Pol II and recruitment of the PAF complex establish a critical platform for initiation of elongation. The recruitment of PAF allows RAD6/BRE1 to become associated with elongating Pol II, which activates the E3 activity of RAD6/BRE1 to catalyze H2B ubiquitination [32]. Moreover, the Bur1/Bur2 cyclin-dependent protein kinase complex contributes by stimulating the E3 function of RAD6/BRE1 through phosphorylation of Rad6 and promoting the recruitment of PAF [33, 34]. The PAF complex also recruits the H3K4 methyltransferase Set1-containing COMPASS complex to Pol II thereby establishing a network of interactions for cross-talk between histone ubiquitination and methylation [35, 36]. Indeed, H2Bub is required for histone marks involved in gene activation, i.e., H3K4 and H3K79 methylation by Set1 and

Dot1 respectively [37-39]. H2Bub affects di- and tri- methylation but not monomethylation of H3 -K4/-K79 [40-42]. Interestingly, it was suggested that H2Bub might be required for the transition from monomethylated to di- and tri- methylated states [42]. The authors suggested that the interaction between H2Bub and the methyltransferase might generate a conformational change allowing the latter to achieve processive methylation. However, using reconstituted nucleosomes with chemically ubiquitinated H2B, McGinty et al. revealed direct stimulation of human Dot1-mediated H3K79 mono-and di-methylation, but not trimethylation by H2Bub [43]. The Dot1 processivity model has also been challenged by kinetic analysis of H3K79 methylation indicating that Dot1 rather functions as a distributive enzyme [44]. On the other hand, the cross-talk mechanism of H2Bub and H3K4 methylation relies on Cps35, a subunit of the COMPASS complex required for its methyltransferase activity [45]. Interestingly, Cps35 also interacts with Dot1 and promotes K79 trimethylation [45]. Moreover, Rad6/Bre1 directly ubiquitinates Cps35 which in turn controls the recruitment of Spp1, another subunit of COMPASS required for H3K4 trimethylation [46].

Recent studies provided evidence for a direct influence of H2Bub on chromatin dynamics during transcription elongation independently of histone H3 methylation [47-49]. For instance H2Bub appears to stimulate the activity of the Facilitates Chromatin Transcription (FACT) complex [47]. In humans this complex catalyzes the removal of H2A/H2B dimer from nucleosomes, which decreases the nucleosomal barrier thus facilitating the progression of elongating Pol II [50]. However, studies with yeast FACT complex suggest a mechanism implying nucleosome reorganization into a looser but more dynamic form allowing chromatin accessibility [51]. On the other hand, another study demonstrated that

H2Bub functionally interacts with the histone chaperone Spt16. Together they regulate nucleosome reassembly in the wake of elongating Pol II to restore proper chromatin structure, which would prevent cryptic transcription initiation [52]. Moreover H2Bub was shown to stabilize nucleosomes at promoters [53], although it also appears to interfere with higher-order chromatin compaction and leads to an open/accessible chromatin structure [54]. It is not clear whether these effects underlie different regulatory mechanisms. Nonetheless, it appears that H2Bub regulates transcription by mechanisms independent of the cross-talk regulation of H3 methylation.

The complexity of the H2B ubiquitination pathway is reflected by the reverse reaction, as several H2B DUBs have been identified. In S. cerevisiae, UBP8 and UBP10 regulate chromatin function by specifically deubiquitinating H2B [55-58]. UBP8 is part of the histone acetyltransferase SAGA complex and its DUB activity requires assembly with regulatory factors forming a tetrameric deubiquitinating module [59-62]. UBP8 positively regulates transcription as both ubiquitination and deubiquitination of H2B are required for proper gene expression, and its depletion alters the level of H3-K4/-K36 methylation [55, 58]. So how ubiquitination and deubiquitination of H2B act together to regulate transcription? H2Bub appears to constitute a barrier to the recruitment of Ctk1 to chromatin [63]. Ctk1 is a cyclin-dependant kinase that phosphorylates serine 2 of Pol II Carboxy Terminal Domain (CTD S2P), an event required for Set2 recruitment and H3K36 methylation during elongation [64, 65]. Therefore, H2Bub must be deubiquitinated by UBP8 to allow transcription elongation [63]. USP22, the human homologue of UBP8, is also part of the human SAGA complex [66, 67] and is involved in transcription activation. Interestingly, USP22 appears to deubiquitinate

both H2B and H2A. UBP10 preferentially localizes at telomeres to reduce H2Bub as well as H3K4 and H3K79 methylation, events that promote Sir2 histone deacetylase association with telomeres and subsequent silencing [56, 57]. Of note, UBP8 is not required for gene silencing at telomeres, indicating that H2B DUBs function on distinct chromatin regions to regulate global H2B ubiquitination levels. USP7, USP3, USP12 and USP46 have also been identified as enzymes capable of deubiquitinating H2B [68-70]. However, the exact roles of these H2B DUBs in vivo remains poorly defined.

In summary, H2Bub acts as a polyvalent histone mark playing different roles in regulating gene expression. While H2Bub regulates transcription by ensuring cross-talk between histone modifications, direct regulation of chromatin dynamics and interfering with higher-order chromatin structure appears to be important mechanisms of transcription regulation. Further studies are needed to fully understand the exact roles of H2Bub as well as the upstream signaling pathways coordinating its implementation and removal.

Ubiquitination of histone H2A

The first E3 identified as catalyzing the monoubiquitination of H2A (H2Aub) is Ring1B, a component of the PcG Repressive Complex 1 (PRC1) and PRC1-like (PRC1L) [71, 72]. Since these two complexes are very similar, for convenience, we hereafter refer to these as PRC1. This repressive complex consists of several Polycomb group (PcG) proteins (Ring1A, Ring1B and Bmi-1) having a RING (Really Interesting New Gene) finger domain, a signature motif for E3 activity [73]. However, only Ring1B has E3 activity towards H2A, while the two other components (Ring1A and Bmi-1) play an important role in H2A

ubiquitination by stimulating the E3 activity of Ring1B [72, 74, 75]. Several lines of evidence indicate that H2A ubiquitination is linked to PcG silencing [72, 75]. Chromatin immunoprecipitation assays show that Ring1B and Bmi-1 colocalize with H2Aub at PcG-target genes (e.g., Hox genes) and depletion or inactivation of Ring1B induces derepression of Hox gene subsets [75]. Ring1B is also involved in X chromosome inactivation as Ring1B and H2Aub are enriched on inactive X chromosome (Xi); moreover a Ring1A/B double knockout abrogates H2Aub on Xi [74, 76]. However, the initiation of Xi silencing in embryonic cells is independent of Ring1B [77]. Recently, global occupancy studies indicated that H2Aub is present in the regulatory regions of a large number of genes suggesting its involvement in gene expression associated with several cellular processes [78].

The function of the PRC1 complex is coordinated with another PcG group complex, PRC2, which is also recruited to promoters of inactive genes and Xi. PRC2 contains EZH2, a histone methyltransferase that adds 3 methyl groups specifically to H3K27 (H3K27me3). It has been initially suggested that H3K27me3 is used as a docking site for the recruitment of PRC1 via its PcG chromodomain [79-81]. Consistently, loss of components of the PRC2 complex decreases PRC1 recruitment to chromatin [82, 83]. In addition, increase of H3K27me3 by depleting its specific demethylase UTX induces stronger recruitment of PRC1 and an increase of H2Aub on promoters [84]. However other studies have indicated that the local enrichment of H2Aub on chromatin is not limited to regions containing H3K27me3 [78, 85]. Moreover the non-requirement of the H3K27me3 mark as a docking site was also observed with the identification of another PcG group complex, L3MBTL2 containing PRC1-like 4. L3MBTL2 is required for H2A ubiquitination and transcription repression.

Interestingly, although L3MBTL2 possesses a MBT motif known to recognize H3 and H4 methylation tails, the mechanism of L3MBTL2-mediated repression seems to be independent of methylation. L3MBTL2 can interact with nucleosomes devoid of histone modifications and does not require H3K27me3 for recruitment to chromatin [86]. Therefore, methylated H3K27 is not always necessary for PRC targeting [87]. Further studies are needed to determine the exact molecular events coordinating methylated H3K27 with H2Aub.

Aside from PRC1, Ring1B is also associated with other complexes termed variations of PRC1. The BCoR, melPRC1, E2F6.com1 and PRC1L4 complexes [86, 88-90] are composed of two invariant subunits, Ring1A/B, arranged with different other subunits (reviewed in [91]). Interestingly, in addition to H2A ubiquitination, several of these complexes contain other repressive histone modifying activities and regulate different sets of genes. For instance, the BCoR complex contains the H3K36me2 demethylase Fbxl10/ KDM2B and regulates BCL6 target genes [88]. The drosophila Fbxl10/KDM2B, dKDM2 from the PcG silencing complex dRING-associated factors (dRAF) mediates H3K36 demethylation, an event required for H2A ubiquitination, revealing a crosstalk mechanism between these histone modifications [92]. On the other hand, E2F6.com1 di-methylates H3K9 by G9a/KMT1C and EuHMTase/GLP/KMT1D and controls the expression of E2F- and Myc-responsive genes in quiescent cells [90]. 2A-HUB is another E3 for histone H2A that is recruited to target gene promoters by the repressive complex NCoR which contains the histone deacetylases HDAC1/3 [93].

An important issue not completely addressed regards how H2A ubiquitination leads to gene repression or silencing? Several studies indicated that H2Aub interferes with transcription initiation [94]. For instance, through a trans-histone crosstalk mechanism, H2Aub directly inhibits the active histone marks of di- and tri- methylated H3K4 (H3K4 -me2, -me3) by MLL in vitro, during transcription initiation but not elongation [94]. However, in embryonic stem (ES) cells, PcG target genes are enriched with both repressive and active histone modifications, i.e., H3K27me3 and H3K4me3 respectively. These gene regulatory regions with opposing modifications are termed "bivalent domains". Upon ES cell differentiation, the actively transcribed genes lose H3K27me3 and retain H3K4me3. In contrast, silenced genes retain H3K27me3 and lose H3K4me3 [95, 96]. It was found that Pol II phosphorylated at Serine 5 occupies bivalent genes, and that Ring1B-mediated H2Aub regulates release of poised Pol II [97]. Upon depletion of Ring1A/B that causes loss of H2Aub, Pol II is released and subsequent gene de-repression observed. Consistent with these findings, 2A-HUB was also shown to block Pol II release at the early stage of elongation by preventing the recruitment of the FACT complex to chemokine genes [93]. Of note, Ring1B does not appear to be involved in transcription regulation for this set of genes. It has been suggested that different H2A E3s might be recruited to particular promoters, and that this specificity is further increased by selective association of the E3s with different repressive complexes [93].

How is reversal of H2A ubiquitination accomplished and how does this impact gene expression? Although the molecular mechanisms are not well defined, several H2A DUBs have been identified belonging to three subclasses of DUBs: the USP family (USP3, USP7,

USP12, Ubp-M/USP16, USP21, USP22 and USP46), the UCH family (BAP1) and the JAMM family (2A-DUB/MYSM1 and BRCC36) (partially reviewed in [98, 99]). In the following section, we integrate recent advances of known H2A DUBs that are essentially associated with transcription regulation. Using a biochemical fractionation approach, Ubp-M/USP16 was identified as a DUB for H2A [100]. Consistent with its role in counteracting PcG-mediated repression, Ubp-M appears to be required for embryonic posterior development of Xenopus laevis and regulates Hox gene expression. Of note Ubp-M is also required for proper execution of mitosis as it mediates global deubiquitination of H2A, an event prerequisite for phosphorylation of histone H3 Serine 10, a modification associated with chromosome compaction during mitosis. In addition, it was previously reported that the catalytically inactive mutant of Ubp-M is tightly associated with compacted mitotic chromatin [101]. Zhu et al. have identified 2A-DUB/MYSM1 as another specific H2A DUB that interacts with the transcription- activating histone acetyltransferase p300/CBP associated factor (P/CAF), thus suggesting crosstalk between the two modifications in gene expression control [102]. Histone acetylation appears to facilitate H2A deubiquitination by 2A-DUB in androgen receptor-dependant transcription activation. Moreover H2A deubiquitination appears to destabilize the association of linker histone H1 with nucleosomes [102]. Nakagawa et al. have found that another DUB, USP21, is capable of catalyzing the hydrolysis of H2Aub. USP21 activates transcription initiation by releasing H2Aub-mediated repression thus allowing methylation of H3K4. This process appears to operate during hepatic regeneration which is accompanied by global H2A deubiquitination as well as changes in the expression of several genes [94]. Most recently, in the course of characterizing a newly identified PcG protein Calypso, Scheuermann et al. found that this UCH domain-containing enzyme is an H2A DUB.

Complexed with another PcG protein, i.e., additional sex comb (ASX), Calypso assembles the PcG repressive DUB complex (PR-DUB) and is recruited to a large set of PcG target genes (including Hox genes) for their repression [103]. Although H2A deubiquitination is not commonly associated with gene repression, it is possible that this modification might exert a dual activation/repression function depending on the promoter context. Interestingly, the genomic binding profile of Calypso partially overlaps with Pho, another PcG protein, thereby suggesting collaboration of the two proteins in gene regulation [103]. The human orthologues of Calypso and Pho, BAP1 and Yin Yang 1 (YY1) respectively, interact physically and are recruited to chromatin to regulate transcription [104]. BAP1 is a tumor suppressor associated with several factors and cofactors of transcription, among these other PcG proteins, such as ASXL1/2 and OGT (drosophila ASX and SXC respectively) [104-107]. Thus the BAP1 complex, like PR-DUB, may well control PcG repression during development by regulating histone modifications. Indeed, like Calypso, BAP1 is capable of deubiquitinating H2A in vitro [103]. Furthermore, BAP1 also deubiquitinates its main interacting protein, Host cell factor 1 (HCF-1) [107]. The latter is a transcription coregulator that interacts with E2F transcription factors to regulate the expression of cell cycle genes [108]. Thus, deubiquitination of HCF-1 and its subsequent protection from degradation by BAP1 might be important to control HCF-1/E2F-dependant gene expression [109]. Consistent with this, depletion of BAP1 deregulates cell cycle genes and impairs cell cycle progression [104, 105, 107].

DUBs with dual-specificity for both H2A and H2B have also been identified. USP22 is an integral component of the metazoan homologue of the yeast SAGA complex, the acetyltransferase TFTC/STAGA, which plays critical roles in gene activation [67, 110, 111].

Interestingly, USP22 alone very inefficiently deubiquitinates histone H2B, and its activation requires association with TFTC/STAGA. Consistently two of its complex partners, ATXN7L3 and ENY2, are required for optimal USP22-mediated transcription activation by nuclear receptors in vivo [67]. Moreover the acetyltransferase GCN5 is required for USP22 association with TFTC/STAGA [112]. Thus USP22 DUB activity is tightly regulated by its interacting partners. Another H2A/B DUB, USP7, has been identified during purification of PRC1 complexes [113]. USP7 interacts with MEL18 and BMI1 (belonging to PRC1 complexes). Depletion of USP7 increases the ubiquitination state of MEL18 and BMI1 and reduces their protein levels, thus causing derepression of their common target gene p16INK4a. Moreover, in the same study, USP7 was found to deubiquitinate both H2A and H2B in vitro. The contribution of USP7 to histone deubiquitination in vivo requires further investigations. Interestingly, another group also found that USP7 interacts with various PcG proteins and deubiquitinates Ring1B [114]. Thus, USP7 might play important roles in gene silencing by coordinating PcG protein stability/activity. Finally, by biochemical purification, another H2A DUB activity has been observed that is independent of Ubp-M. Analysis of enzymes catalyzing this reaction led to the identification of two other DUBs (USP12 and USP46) [70] which appear to require interacting partners for efficient H2A deubiquitination. Furthermore these DUBs deubiquitinate H2B as well and regulate Xenopus laevis development [70]. It is not clear yet how different DUBs act on H2A, nonetheless it is reasonable to postulate that tissue specificity, gene regulatory regions, and interacting partners might be key determinants. Moreover, potential H2Aub “readers” might also be involved in regulating H2A ubiquitination and deubiquitination. Indeed, Richly et al. have described a new molecular mechanism for transcriptional activation of PcG-repressed genes. Through a

novel ubiquitin-interacting motif found in the zuotin domain, zuotin-related factor 1 (ZRF1) binds specifically to H2Aub, displaces PRC1, and facilitates H2Aub deubiquitination [115]. The authors suggest that this may constitute one of the first steps for derepression of silenced genes and that transcription activation might be facilitated by cooperation between ZRF1 and H2A DUBs.

Although several studies support a role of PRC1 in transcription repression via H2A ubiquitination, other studies indicated that PRC1 represses gene expression independently of histone H2A ubiquitination. In an in vitro system, PRC1 can mediate chromatin compaction on nucleosomes assembled from tail-less histones [116]. Moreover, reintroduction of a mutant Ring1B lacking E3 activity into Ring1B -/- ES cells is able to restore chromatin compaction at Hox gene loci without restoring H2Aub [117]. It is also possible that histone modification and direct chromatin compaction are not mutually exclusive, and that both mechanisms cooperate to optimize gene repression. Further investigations are needed to understand the exact roles of H2A ubiquitination in controlling chromatin dynamics and gene expression.

REGULATION OF TRANSCRIPTION VIA UBIQUITINATION OF TRANSCRIPTION FACTORS

Ub-mediated proteasomal degradation and non-degradative ubiquitination are mechanisms of regulation used by eukaryotic cells to tightly control the levels and activity of transcription factors or other chromatin associated proteins. Upstream signaling pathways act in a spatio-temporal manner to dictate not only stabilization or degradation, but also changes in protein interaction or subcellular localization, and this can profoundly impact biological

processes. Very often ubiquitination is integrated within a highly complex network of interactions involving other factors and post-translational modifications. Below, we discuss the examples of p53 and Myc which represent excellent paradigms for transcription factors subjected to diverse levels of control by ubiquitination.

Ubiquitination in the control of p53 function

The tumor suppressor p53, termed "guardian of the genome" [118], acts as a transcription factor in response to cellular stress such as DNA damage. p53 is involved in different growth-suppressive processes such as cell cycle arrest, senescence or apoptosis [119, 120]. While its steady-state levels are kept very low, p53 is stabilized and activated by cellular stress. Indeed, p53 protein levels are regulated by a gamut of post-translational modifications such as phosphorylation, acetylation, and ubiquitination [121-124]. The first observation of p53 ubiquitination came from studies on human papillomavirus (HPV) infected cells, in which p53 is degraded following association of the viral oncoprotein E6 with a cellular E3 (i.e., E6-associated protein E6AP), a mechanism that allows HPV replication in the host cell [125-127]. Other examples of viral proteins that might be critically involved in targeting p53 for degradation include the Herpes simplex virus type 1 regulatory protein ICP0 [128]; the adenovirus E1B55K and E4orf6 proteins [129]; the Latency-associated nuclear antigen (LANA) encoded by the Kaposi's sarcoma-associated herpesvirus (KSHV) [130] and BZLF1 encoded by the Epstein-Barr virus (EBV) [131]. However, mouse double-minute 2 protein (Mdm2), a cellular ring finger protein, is perhaps the most critical E3 controlling p53 stability [132-134]. In addition, Mdm2 associates with the proteasome and aids in recruiting p53 to the degradation machinery [135]. The importance of the Mdm2/p53 association is illustrated by

the fact that Mdm2-null mice are embryonically lethal, but survive in the absence of p53 [136, 137]. Interestingly, p53 also binds to responsive elements in the Mdm2 gene to increase its transcription. This sets up a negative feedback loop where active p53 promotes Mdm2 transcription, which in turns leads to p53 ubiquitination and degradation. This regulatory loop acts as a mechanism that downregulates the p53 response to allow proliferation restart [138]. In addition to polyubiquitinating p53, Mdm2 also appears to monoubiquitinate p53, representing another level of control on p53 activity [139]. At low levels of Mdm2, p53 is monoubiquitinated and exported to the cytoplasm, whereas at high levels of Mdm2, p53 is polyubiquitinated and degraded in the nucleus. It is believed that monoubiquitination of p53 represents a mechanism to control p53 activity in unstressed cells, in contrast to p53 polyubiquitination which might play a crucial function in inhibiting p53 activity at later stages of the cellular stress response.

The Mdm2 and p53 interaction is regulated by various mechanisms, most notably through post-translational modifications of p53 [121-123, 140]. p53 is phosphorylated on many sites by ATM/ATR and Chk1/Chk2 following DNA damage, thus sterically inhibiting its interaction with Mdm2, leading to p53 accumulation and subsequent expression of many target genes including p21, PUMA and Bax, involved in cell growth arrest/apoptosis. Acetylation of p53 is also associated with increased stabilization and transcriptional activity. Several histone acetyltransferases including CBP/p300, PCAF, hMOF and TIP60 acetylate p53 indicating the importance of acetylation in the control of p53 function. Interestingly, CBP/p300 shares at least 6 lysines residues targets (K370, K372, K373, K381, K382 and K386) with Mdm2, and acetylation of these sites following DNA damage blocks the

ubiquitination of p53. Other post-translational modifications of p53 such as sumoylation and methylation also impact p53 stability and activity [140, 141]. For instance, methylation of K372 by Set9 methyltransferase promotes p53 stabilization [142]. Little is known about the interplay between p53 post-translational modifications which constitutes an exciting area of investigation that would reveal how signaling pathways are coordinated in promoting or inhibiting the p53 in response to specific physio-pathological conditions. Moreover, the Mdm2-mediated ubiquitination of p53 is also regulated by post-translational modifications of Mdm2 itself, providing another layer of complexity in the control of p53 function [143-145].

In concert with post-translational modifications, several interacting proteins act to negatively or positively control p53 ubiquitination. MdmX (a homolog of Mdm2), also known as Mdm4, is a RING finger protein and forms a heterodimer with Mdm2 through interaction between their respective RING domains [144]. However, MdmX does not possess E3 activity and instead acts to enhance Mdm2 activity. In fact, Mdm2 in multimeric forms with MdmX possesses a higher level of E3 activity toward p53 than its monomeric forms. During DNA damage, post-translational modifications impacting Mdm2 interaction with MdmX, inhibit the E3 activity of the complex thus contributing to finetuning p53 function. ARF, also known as p14ARF, is a negative regulator of Mdm2. This tumor suppressor induces the p53 response by inhibiting p53 interaction with Mdm2 [146, 147]. Many other proteins, involving diverse signaling pathways, interfere with the Mdm2 and p53 interaction. These include the transcription factor YY1 which promotes p53 ubiquitination and degradation by binding both Mdm2 and p53, thereby strengthening their interaction. In addition, ARF negatively regulates the interaction between Mdm2 and YY1 [148]. Ribosomal proteins L5, L11 and L23

positively regulate p53 by inhibiting Mdm2 activity [149-152]. Recently, RFWD3, a RING finger and WD repeat domain-containing protein, was also revealed as an intriguing E3 for p53. It was found that RFWD3 interacts with Mdm2/p53 complex and stabilizes p53 [153]. RFWD3 is phosphorylated by ATM/ATR following DNA damage, an event required for p53 ubiquitination and stabilization. Importantly, RFWD3 synergizes with Mdm2 to increase p53 ubiquitination at later times of the DNA damage response. However, this ubiquitination does not signal for p53 degradation. In fact, RFWD3 was found to restrict Mdm2 to form shorter polyubiquitin chains as opposed to longer Ub chains required for degradation.

While Mdm2 is a major E3 for p53, other E3s are involved in regulating p53 stability and activity. Pirh2 [154] and COP1 [155] are both RING E3s that, similar to Mdm2, are induced by p53-dependent gene transcription as part of an autoregulatory feedback mechanism. Interestingly, COP1 is phosphorylated by ATM following ionizing radiation, which induces COP1 autodegradation that in turn promotes p53 accumulation during genotoxic stress [156]. Another E3 that targets p53 for degradation is ARF-BP1 (also known as Mule/HectH9/Huwe1) which belongs to the family of HECT domain containing E3s [157]. As with Mdm2, ARF inhibits ARF-BP1 E3 activity and hence stabilizes p53. Pirh2, COP1 and ARF-BP1 appear to signal p53 ubiquitination and degradation independently of Mdm2 thus revealing convergent signaling pathways that modulate p53 stability and transcriptional activity.

Other E3s are involved in p53 degradation indicating the major importance of tightly regulating the transcriptional activity of this tumor suppressor. CARPs (caspase 8/10-

associated RING proteins 1 and 2) induce p53 degradation irrespective of its phosphorylation status [158]. Synoviolin, also known as HRD1, is an endoplasmic reticulum-associated E3 that appears to sequester p53 in the cytoplasm and promote its ubiquitination and degradation [159]. MKRN1 (Makorin Ring Finger Protein 1) E3 signals degradation of both p53 and its target gene p21 [160]. TRIM24 (Tripartite-motif protein 24) copurifies with p53 from embryonic stem cells and ubiquitinates and degrades the latter [161]. Both β-TrCP [162] and JFK, a Kelch domain-containing F-box protein [163] induce p53 degradation as part of Skp, Cullin, F-box (SCF) containing complex. For instance IkappaB kinase 2 (IKK2) phosphorylates p53 and signals its ubiquitination by β-TrCP thus contributing to eventual attenuation of the p53 response. CHIP (carboxy terminus of Hsp70-interacting protein), a RING finger chaperone-associated E3, was observed to ubiquitinate both wild-type and mutant p53 through association with the chaperones Hsc70 and Hsp90 [164]. CHIP has been suggested to be the major E3 responsible for ubiquitination and degradation of mutant p53 [165, 166]. While its exact functional significance is still not fully understood, Topors (topoisomerase I-binding protein) was shown to act as both an Ub E3 [167] and a SUMO1 E3 [168] for p53. Ubiquitination of p53 induces its proteasomal degradation while sumoylation increases its protein levels. It would be of great interest to define the exact cellular contexts in which regulation by a specific E3 would be prevalent, and moreover to identify the signaling events that coordinate the action of these E3s to ensure precise regulation of p53 transcriptional activity.

While p53 interacts with many different E3s targeting it for proteasomal degradation, there is also a set of E3s that act on p53 in a non-proteolytic manner. E4F1, an atypical E3,

promotes p53-dependent growth arrest through small K48 Ub chain linkage [169]. E4F1, which shares homology with the SUMO E3 RanBP2, forms chains of mono-, di- or tri-ubiquitin, whereas it typically takes a chain of at least four Ub through K48 linkage to signal for proteasomal degradation. Furthermore, E4F1 ubiquitination of p53 does not induce protein destabilization or relocalization. In fact, p53 ubiquitinated by E4F1 is recruited to chromatin to induce the transcription of genes involved in cell cycle arrest but not apoptosis. Interestingly, E4F1 was demonstrated to ubiquitinate p53 on the same residue, K320, that is acetylated by the histone acetyltransferase PCAF. Since acetylation of K320 is known to lead to the activation of apoptotic genes such as PUMA and BAX, ubiquitination of this residue can switch cell fate from apoptosis to growth arrest. MLS2 (male-specific lethal-2) is a nuclear E3 that ubiquitinates p53 leading to its nuclear export without affecting its stability [170]. However, the exact physiological context of this p53 nuclear-cytoplasmic translocation remains to be elucidated. Another E3 playing a role in the cytoplasmic localization of p53 is the WW domain-containing protein 1 (WWP1), a HECT E3 [171]. WWP1 expression stabilizes p53 leading to its nuclear export which coincides with a decrease in p53 transcriptional function. It would be interesting to clarify the mechanism by which WWP1 ubiquitinates p53. There are also other cases where non-proteolytic ubiquitination of p53 induces its stabilization and inhibition of its function. Ubc13, a E2 ubiquitin-conjugating enzyme, protects p53 from Mdm2-induced degradation by promoting ubiquitination of monomeric p53 through K63 Ub chains which inhibits its multimerization (required for transcription activation) and induces its sequestration in the cytoplasm [172]. It was later demonstrated that JNK inhibits this interaction by phosphorylating p53, thereby allowing p53 multimerization and transcriptional activation [173].

Ubiquitination of p53 is also subjected to tight control by deubiquitination. It was initially observed that HAUSP (USP7) deubiquitinates and stabilizes p53 leading to inhibition of cell growth and increase of apoptosis [174]. Later it was also shown that Mdm2, known to undergo self ubiquitination, is a substrate of HAUSP and that Mdm2 becomes very unstable in HAUSP-depleted cells, which in turn leads to p53 activation [175, 176]. These results suggest the existence of a regulatory loop in which HAUSP can act as a positive or negative regulator of p53 stability. A second DUB, USP2a, positively regulates the Mdm2/p53 interaction [177]. USP2a, in contrast to HAUSP, only interacts with and deubiquitinates Mdm2 thus promoting p53 degradation. A third DUB, USP10, also deubiquitinates p53 counteracting its ubiquitination and degradation by Mdm2 [178]. It was demonstrated that in unstressed cells, USP10 is localized to the cytoplasm and inhibits p53 ubiquitination. Following DNA damage, USP10 is phosphorylated by ATM, an event necessary for its stabilization and nuclear translocation. In the nucleus, USP10 then deubiquitinates p53 leading to its activation and subsequent growth suppression. USP4 also regulates p53 stability via direct deubiquitination of the E3 ARF-BP1 [179]. As for most E3s targeting p53, it is unclear how corresponding DUB activities are coordinated. It is also expected that various DUBs, which have yet to be identified, might regulate the p53 ubiquitination pathway in a degradation-independent manner.

Ubiquitination in the control of Myc function

While proteolysis is usually engaged when the biological function of a protein is no longer required, much evidence indicates that Ub and proteolysis plays a major role in transcription activation domain (TAD) function. Transcription activators are composed of a

TAD and a DNA-binding domain. Using chimeric transcription factors composed of the GAL4 DNA binding domains and different TADs expressed in a cell line carrying a reporter gene, it was observed that the half-life of model activators, such as VP16, were inversely correlated with TAD activity [180]. Consistently, it was observed that inactivating point mutations in the TAD also protect the transcription activator from proteasomal degradation. Moreover the rapid degradation of chimeric activators was dependent on a functional GAL4 DNA binding domain, indicating that recruitment of transcription factors to DNA is essential for proteasome-mediated degradation and hence proper TAD function. Although not a general rule, the activation domains of many unstable transcription factors overlap with activator degrons [181-183]). The transcription factor c-Myc (hereafter Myc) provides an excellent model for investigating the link between TAD and degradation. Due to its oncogenic properties, cells have developed ways to tightly control Myc stability and activity. Myc has an extremely short half-life (~30 min) [184], and is a target of several E3s. The F-box protein Skp2 stimulates Myc transcription activity as well as promoting its proteasomal degradation [185, 186]. Skp2 interacts with Myc on the Myc-Box 2 (MB2) that is critical for transcription activation and oncogenic transformation. Thus, the degron and TAD overlap is consistent with the model of dependency between transcription factor potency and degradation. Moreover, the interaction between Myc and Skp2 is cell cycle regulated and is required for S phase entry during which the rate of Myc turnover is increased. Four more E3 complexes have been implicated in Myc regulation: Fbw7, HectH9, TRUSS (TRPC4AP) and β-TrCP. Whereas Skp2 acts as a positive regulator of Myc activity while still being responsible for its proteasomal degradation, Fbw7 is a negative regulator of Myc function [187-189]. The SCFFbw7 complex and its role in Myc ubiquitination has been well characterized. This

complex binds to a phosphodegron in Myc-Box 1 (MB1) and signals Myc for proteasomal degradation. Following a priming phosphorylation of serine 62 by MAP kinases, glycogen synthase kinase 3 (Gsk3) phosphorylates the threonine 58 residue in MB1 which is required for degradation by Fbw7. Cells deficient for Fbw7 have an increased steady state level and half-life of Myc [189, 190]. Consistent with the biological significance of Fbw7 interaction with Myc, mutations in the Fbw7 binding domain are found in Burkitt lymphoma [191]. More recently it was revealed through mass spectrometry of affinity-purified complexes that TRUSS interacts with Myc [192]. DDB1 and CUL4A were also found in the Myc purification suggesting that TRUSS acts as a substrate receptor (DCAF) for the DDB1-CUL4 E3 complex. TRUSS enhances Myc protein turnover, which requires both N- and C-terminal domains of Myc. Furthermore, TRUSS expression was found to be very low in many cancer cell lines suggesting that TRUSS may act as a tumor suppressor by regulating Myc protein levels and activity. One of the determining factors of protein fate is polyubiquitination using different types of Ub chain linkages. In contrast to Skp2, Fbw7, and TRUSS which signal Myc for ubiquitination and degradation, HectH9 polyubiquitinates Myc through lysine 63 linkage (K63) and does not directly play a role in its turnover [193]. It was observed that HectH9 was necessary to enhance transcription activation of Myc target genes. Consistent with its role in promoting Myc transcription, HectH9 is overexpressed in many solid tumors, and depletion of HectH9 blocks tumor cell proliferation. Adding to the complexity of Myc ubiquitination, SCFβ-TrCP inhibits SCFFbw7– mediated turnover of Myc through different Ub chains, and this promotes Myc stabilization [194]. Using single substitutions of the different Ub lysines, it was observed that K33, K48 and K63 mutants hindered β-TrCP stabilization of Myc suggesting that this E3 forms heterotypic chains, whereas only the K48 mutant abrogated

Fbw7 degradation of Myc supporting homotypic polyubiquitin chain formation. Consistent with a positive role of β-TrCP in regulating Myc, it was observed that ubiquitination of Myc by β-TrCP is necessary for cell cycle progression. Further studies are required to fully elucidate the mechanism of Myc ubiquitination by β-TrCP.

Similar to p53, Myc is also regulated by DUBs. Usp28 was identified through a RNAi screen as a protein involved in Myc function [195]. Expression of Usp28, but not of its catalytic inactive mutant, increased levels of Myc and its half-life. Interestingly, Usp28 antagonizes the action of Fbw7 without directly binding Myc. There are three isoforms of Fbw7 (α, β, and γ). The nuclear Fbw7α and the nucleolar Fbw7γ both degrade Myc, while Fbw7β is cytosolic and does not interact with Myc [187]. Usp28 is nuclear and was found to interact with Fbw7α, thus preventing Myc degradation only in the nucleus. This explains why Myc is very unstable in the nucleolus. Moreover, Usp28 was found to be highly expressed in colon and breast carcinomas. Since Fbw7 is a tumor suppressor gene and that Usp28 blocks Fbw7-mediated Myc ubiquitination rendering Myc more stable, Usp28 could be considered in this context as an oncogene.

Although, less documented than p53, the involvment of several E3 complexes and a DUB in regulating Myc strongly supports the essential role of ubiquitination in controlling the stability and activity of this oncogene. Due to the important role of Myc in tumorogenesis, it will be crucial to determine potential crosstalks between the different E3s and define the upstream signaling pathways that control Myc function.

Regulation of RNA polymerase II by ubiquitination

Regulation of the recruitment and activity of Pol II constitutes another major mode of transcriptional control. When actively transcribed DNA is exposed to genotoxic agents such as UV, resulting DNA lesions are repaired via the transcription-coupled nucleotide excision repair (TC-NER) pathway which is triggered through blockage of Pol II progression. Following this lesion recognition event, at some point Pol II must be removed from the template to allow recruitment of the repair machinery. It was initially found that following UV exposure, the large subunit of Pol II, Rpb1, is ubiquitinated; moreover this modification appeared deficient in cells derived from Cockayne syndrome A and B (CSA and CSB), a rare disorder where TC-NER is abrogated [196]. It was later shown that UV-induced ubiquitination of Pol II targets this enzyme for proteasomal degradation [197]. A direct link between TC-NER and Pol II degradation was provided by Rad26, a yeast functional homologue of human CSB, that interacts with Def1, a protein necessary for Pol II ubiquitination and degradation following DNA damage [198]. It was observed that the fraction of Rpb1 that was ubiquitinated and degraded by the proteasome is hyperphosphorylated [197]. On the other hand, other findings suggested that the hypophosphorylated form of Pol II might also be targeted for degradation [199, 200]. Studies involving the use of specific CTD kinase inhibitors support the notion that phosphorylation of the CTD of Pol II is required for its ubiquitination and degradation [201, 202]. Consistently, using an antibody recognizing all forms of Pol II (ARNA-3), it was observed that Pol II becomes hyperphosphorylated following UV exposure and this is concomitant with its degradation [202]. Interestingly, the authors reported that degradation of Pol II was not significantly different in CSA or CSB cells compared to repair-competent cells, although

these proteins participate in Pol II ubiquitination [202]. The discovery of the first E3 required for Pol II ubiquitination came from a biochemical approach to identify subtrates of Rsp5, an essential HECT E3 in S. cerevisiae. It was found that Rsp5 is in stable complex with, and ubiquitinates, Rpb1 [203]. It was further demonstrated that degradation of Rpb1 following treatment with UV or the UV-mimetic compound 4-nitroquinoline-1-oxide (4-NQO) depends on Rsp5 [199]. The authors also observed that human Nedd4, closely related to yeast Rsp5, was able to bind and ubiquitinate human Rpb1. In agreement, it was recently shown that DNA damage-induced Pol II ubiquitination depends on Nedd4 [204]. With the discovery of the E3 for Pol II, it became possible to investigate the involvement of CTD phosphorylation in Pol II ubiquitination using an in vitro assay [205]. Using Uba1 (E1), Ubc5 (E2) and Rsp5, it was demonstrated that the Pol II/DNA/RNA ternary complex is more efficiently ubiquitinated than free Pol II, and moreover the preferred substrate for ubiquitination is the damage-stalled Pol II ternary complex. In addition, it was demonstrated that Serine 5 phosphorylation of the CTD blocks Pol II ubiquitination, whereas Serine 2 phosphorylation promotes its ubiquitination [205].

Following the discovery of Rsp5, it was found that the von Hippel-Lindau tumor suppressor protein (VHL)-associated E3 complex (containing Elongin B, Elongin C, Cullin 2 and Rbx1 (Roc1)), interacts with hyperphosphorylated Pol II and is required for its ubiquitination and degradation following DNA damage [206]. Ela1 (Elongin A), Elc1 (Elongin C) and Cul3 are necessary for DNA damage-induced Rpb1 ubiquitination and degradation in S. cerevisiae [207, 208]. It was later demonstrated that, in mammalian cells, another complex containing Elongin A/B/C, Cul5 and Rbx2 is also involved in the

ubiquitination and degradation of Pol II following DNA damage [209]. The tumor suppressor BRCA1 and its stoichiometric partner BARD1 assemble a Ring finger E3 complex that appears to target Pol II. One study reported that the elongating form of the enzyme, possibly stalled at DNA damage sites, is the preferential target of the BRCA1/BARD1 E3 complex [210]. On the other hand, it was also shown that BRCA1/BARD1 E3 complex ubiquitinates Serine 5 phosphorylated Pol II [211]. This appears to prevent stable association of Pol II with TFIIE and TFIIH, and thus blocks the initiation of mRNA synthesis rather than elongation. In addition, this process does not appear to target for degradation as the Ub moiety itself interferes with the assembly of basal transcription factors at the promoter [212]. These data can be reconciled by taking into account that BRCA1 might interact with several E2s to promote the assembly of degradative Ub chains or non-degradative Ub chains depending on the stage of transcription. Clearly, the exact role of BRCA1-mediated ubiquitination in regulating Pol II function requires further studies.

Regulation of Pol II by ubiquitination does not appear to be solely regulated in response to DNA damage. Indeed it was found that the HECT domain E3 WWP2, targets Pol II for ubiquitin-mediated degradation in a DNA-damage independent manner, and moreover, this interaction does not rely on the phosphorylation state of Pol II [213]. It was also observed using an in vitro transcription system that Pol II is ubiquitinated via lysine-63 linked chains following transcription inhibition with α-amanitin, indicating that stalled or arrested Pol II induces Ub signaling cascades to rescue transcription [214]. The identity of this E3 activity as well as the mechanism of its recruitment to the transcriptional machinery have yet to be revealed.

A major issue yet to be resolved concerns how distinct E3s act on Pol II. Recent studies have begun to shed light on the intricate mechanisms of Pol II ubiquitination. For instance Rsp5 and Elc1/Cul3 act on Pol II ubiquitination in a sequential fashion with different Ub chains [215]. Using a yeast in vitro reconstituted system for Pol II ubiquitination, it was demonstrated that Rsp5 is required for the monoubiquitination of Pol II or polyubiquitination through K63-linked Ub chains. Following this first step, Elc1 and Cul3 are then recruited for Pol II polyubiquitination through K48 Ub chains. In addition, the requirement for Rsp5 could be bypassed by using pre-monoubiquitinated Pol II. These findings were further confirmed using human purified factors showing that Nedd4 is required for monoubiquitination of Pol II followed by polyubiquitination by the ElonginABC/Rbx1/Cullin5 complex. This two-step mechanism is suggested to allow sufficient proofreading capacity during Pol II ubiquitination to tightly control its proteolysis.

As would be expected, deubiquitination represents another form of Pol II control by ubiquitination. The DUB Ubp3 co-purifies with Pol II and elongation factors such as Spt5 and reverses its ubiquitination [216]. Moreover, it was demonstrated that Ubp3 mutant yeast cells have increased hyper-ubiquitinated Pol II and were also sensitive to treatment with the elongation inhibitor 6-azauracil (6-AU). Consistently, Ubp3 efficiently deubiquitinates the polymerase in vitro. However another DUB, Ubp2, interacts with and antagonizes Rsp5 by deubiquitinating Rpb1 [215, 217]. In contrast to the mechanism of Ubp3 action, Ubp2 efficiently hydrolyzes Ub chains but is unable to break the bond between Ub and Pol II. Furthermore, Ubp2 deubiquitinates K63 polyubiquitinated Pol II, consistent with a previous study demonstrating that this DUB regulates formation of K63-linked Ub chains [218]. These

studies clearly show that deubiquitination plays an important role in Pol II stability and function through the action of different DUBs.

In conclusion, ubiquitination is an integral part of the transcription process and exerts positive or negative regulatory effects on gene expression depending on the enzymes and the substrates involved. Ubiquitination of the same substrate could have seemingly opposite effects depending on the nature of the modification. Indeed ubiquitination of components of the transcription apparatus can induce degradation, activation, and assembly or disassembly of multi-protein complexes. Further studies are needed to address the biological roles of components of the Ub system. Moreover, understanding the molecular mechanisms of ubiquitination/deubiquitination is likely to reveal novel principles of signaling. Undoubtedly, with the advent of new approaches and technologies, the years lying ahead will certainly herald exciting new insight into this post-translational modification.

Acknowledgements

This work was supported by grants to E.B.A. from the Terry Fox Foundation (grant#018144) and The Natural Sciences and Engineering Research Council of Canada. E.B.A. is a scholar of the Canadian Institutes of Health Research and Le Fonds de la Recherche en Santé du Québec (FRSQ). H.Y. is a scholar of Canadian Institutes of Health Research. We thank Drs Elliot Drobetsky and Haider H. Dar for critical reading of the manuscript. We apologize to colleagues whose work has not been cited due to space limitations.

REFERENCES

[1] Hochstrasser M, Annu Rev Genet. 1996;30:405-439.

[2] Hershko A, Ciechanover A, Annu Rev Biochem. 1998;67:425-479.

[3] Pickart CM, Eddins MJ, Biochim. Biophys. Acta. 2004;1695:55-72.

[4] Varshavsky A, Genes Cells. 1997;2:13-28.

[5] Welchman RL, Gordon C, Mayer RJ, Nat. Rev. Mol. Cell Biol. 2005;6:599-609.

[6] Ikeda F, Dikic I, EMBO Rep. 2008;9:536-542.

[7] Nijman SM, Luna-Vargas MP, Velds A, Brummelkamp TR, Dirac AM, Sixma TK, Bernards R, Cell. 2005;123:773-786.

[8] Reyes-Turcu FE, Ventii KH, Wilkinson KD, Annu Rev Biochem. 2009;78:363-397.

[9] Komander D, Clague MJ, Urbe S, Nat Rev Mol Cell Biol. 2009;10:550-563.

[10] Luger K, Mader AW, Richmond RK, Sargent DF, Richmond TJ, Nature. 1997;389:251-260.

[11] Kouzarides T, Cell. 2007;128:693-705.

[12] Jenuwein T, Allis CD, Science. 2001;293:1074-1080.

[13] Goldknopf IL, Taylor CW, Baum RM, Yeoman LC, Olson MO, Prestayko AW, Busch H, J Biol Chem. 1975;250:7182-7187.

[14] Nickel BE, Davie JR, Biochemistry. 1989;28:964-968.

[15] West MH, Bonner WM, Nucleic Acids Res. 1980;8:4671-4680.

[16] Zhang Y, Genes Dev. 2003;17:2733-2740.

[17] Robzyk K, Recht J, Osley MA, Science. 2000;287:501-504.

[18] Hwang WW, Venkatasubrahmanyam S, Ianculescu AG, Tong A, Boone C, Madhani HD, Mol Cell. 2003;11:261-266.

[19] Wood A, Krogan NJ, Dover J, Schneider J, Heidt J, Boateng MA, Dean K, Golshani A, Zhang Y, Greenblatt JF, Johnston M, Shilatifard A, Mol Cell. 2003;11:267-274.

[20] Song YH, Ahn SH, J Biol Chem. 2010;285:2361-2367.

[21] Koken MH, Reynolds P, Jaspers-Dekker I, Prakash L, Prakash S, Bootsma D, Hoeijmakers JH, Proc Natl Acad Sci U S A. 1991;88:8865-8869.

[22] Kim J, Hake SB, Roeder RG, Mol Cell. 2005;20:759-770.

[23] Zhu B, Zheng Y, Pham AD, Mandal SS, Erdjument-Bromage H, Tempst P, Reinberg D, Mol Cell. 2005;20:601-611.

[24] Roest HP, van Klaveren J, de Wit J, van Gurp CG, Koken MH, Vermey M, van Roijen JH, Hoogerbrugge JW, Vreeburg JT, Baarends WM, Bootsma D, Grootegoed JA, Hoeijmakers JH, Cell. 1996;86:799-810.

[25] Baarends WM, Wassenaar E, Hoogerbrugge JW, Schoenmakers S, Sun ZW, Grootegoed JA, J Cell Sci. 2007;120:1841-1851.

[26] Zhang F, Yu X, Mol Cell. 2011;41:384-397.

[27] Li XS, Trojer P, Matsumura T, Treisman JE, Tanese N, Mol Cell Biol. 2010;30:1673-1688.

[28] Nickel BE, Allis CD, Davie JR, Biochemistry. 1989;28:958-963.

[29] Davie JR, Murphy LC, Biochemistry. 1990;29:4752-4757.

[30] Minsky N, Shema E, Field Y, Schuster M, Segal E, Oren M, Nat Cell Biol. 2008;10:483-488.

[31] Kao CF, Hillyer C, Tsukuda T, Henry K, Berger S, Osley MA, Genes Dev. 2004;18:184-195.

[32] Xiao T, Kao CF, Krogan NJ, Sun ZW, Greenblatt JF, Osley MA, Strahl BD, Mol Cell Biol. 2005;25:637-651.

[33] Laribee RN, Krogan NJ, Xiao T, Shibata Y, Hughes TR, Greenblatt JF, Strahl BD, Curr Biol. 2005;15:1487-1493.

[34] Wood A, Schneider J, Dover J, Johnston M, Shilatifard A, Mol Cell. 2005;20:589-599.

[35] Krogan NJ, Dover J, Wood A, Schneider J, Heidt J, Boateng MA, Dean K, Ryan OW, Golshani A, Johnston M, Greenblatt JF, Shilatifard A, Mol Cell. 2003;11:721-729.

[36] Ng HH, Robert F, Young RA, Struhl K, Mol Cell. 2003;11:709-719.

[37] Sun ZW, Allis CD, Nature. 2002;418:104-108.

[38] Briggs SD, Xiao T, Sun ZW, Caldwell JA, Shabanowitz J, Hunt DF, Allis CD, Strahl BD, Nature. 2002;418:498.

[39] Ng HH, Xu RM, Zhang Y, Struhl K, J Biol Chem. 2002;277:34655-34657.

[40] Dehe PM, Pamblanco M, Luciano P, Lebrun R, Moinier D, Sendra R, Verreault A, Tordera V, Geli V, J Mol Biol. 2005;353:477-484.

[41] Schneider J, Wood A, Lee JS, Schuster R, Dueker J, Maguire C, Swanson SK, Florens L, Washburn MP, Shilatifard A, Mol Cell. 2005;19:849-856.

[42] Shahbazian MD, Zhang K, Grunstein M, Mol Cell. 2005;19:271-277.

[43] McGinty RK, Kim J, Chatterjee C, Roeder RG, Muir TW, Nature. 2008;453:812-816.

[44] Frederiks F, Tzouros M, Oudgenoeg G, van Welsem T, Fornerod M, Krijgsveld J, van Leeuwen F, Nat Struct Mol Biol. 2008;15:550-557.

[45] Lee JS, Shukla A, Schneider J, Swanson SK, Washburn MP, Florens L, Bhaumik SR, Shilatifard A, Cell. 2007;131:1084-1096.

[46] Vitaliano-Prunier A, Menant A, Hobeika M, Geli V, Gwizdek C, Dargemont C, Nat Cell Biol. 2008;10:1365-1371.

[47] Pavri R, Zhu B, Li G, Trojer P, Mandal S, Shilatifard A, Reinberg D, Cell. 2006;125:703-717.

[48] Shukla A, Bhaumik SR, Biochem Biophys Res Commun. 2007;359:214-220.

[49] Tanny JC, Erdjument-Bromage H, Tempst P, Allis CD, Genes Dev. 2007;21:835-847.

[50] Belotserkovskaya R, Oh S, Bondarenko VA, Orphanides G, Studitsky VM, Reinberg D, Science. 2003;301:1090-1093.

[51] Xin H, Takahata S, Blanksma M, McCullough L, Stillman DJ, Formosa T, Mol Cell. 2009;35:365-376.

[52] Fleming AB, Kao CF, Hillyer C, Pikaart M, Osley MA, Mol Cell. 2008;31:57-66.

[53] Chandrasekharan MB, Huang F, Sun ZW, Proc Natl Acad Sci U S A. 2009;106:16686-16691.

[54] Fierz B, Chatterjee C, McGinty RK, Bar-Dagan M, Raleigh DP, Muir TW, Nat Chem Biol. 2011;7:113-119.

[55] Henry KW, Wyce A, Lo WS, Duggan LJ, Emre NC, Kao CF, Pillus L, Shilatifard A, Osley MA, Berger SL, Genes Dev. 2003;17:2648-2663.

[56] Emre NC, Ingvarsdottir K, Wyce A, Wood A, Krogan NJ, Henry KW, Li K, Marmorstein R, Greenblatt JF, Shilatifard A, Berger SL, Mol Cell. 2005;17:585-594.

[57] Gardner RG, Nelson ZW, Gottschling DE, Mol Cell Biol. 2005;25:6123-6139.

[58] Daniel JA, Torok MS, Sun ZW, Schieltz D, Allis CD, Yates JR, 3rd, Grant PA, J Biol Chem. 2004;279:1867-1871.

[59] Lee KK, Florens L, Swanson SK, Washburn MP, Workman JL, Mol Cell Biol. 2005;25:1173-1182.

[60] Ingvarsdottir K, Krogan NJ, Emre NC, Wyce A, Thompson NJ, Emili A, Hughes TR, Greenblatt JF, Berger SL, Mol Cell Biol. 2005;25:1162-1172.

[61] Kohler A, Zimmerman E, Schneider M, Hurt E, Zheng N, Cell. 2010;141:606-617.

[62] Samara NL, Datta AB, Berndsen CE, Zhang X, Yao T, Cohen RE, Wolberger C, Science. 2010;328:1025-1029.

[63] Wyce A, Xiao T, Whelan KA, Kosman C, Walter W, Eick D, Hughes TR, Krogan NJ, Strahl BD, Berger SL, Mol Cell. 2007;27:275-288.

[64] Krogan NJ, Kim M, Tong A, Golshani A, Cagney G, Canadien V, Richards DP, Beattie BK, Emili A, Boone C, Shilatifard A, Buratowski S, Greenblatt J, Mol Cell Biol. 2003;23:4207-4218.

[65] Xiao T, Hall H, Kizer KO, Shibata Y, Hall MC, Borchers CH, Strahl BD, Genes Dev. 2003;17:654-663.

[66] Zhang XY, Pfeiffer HK, Thorne AW, McMahon SB, Cell Cycle. 2008;7:1522-1524.

[67] Zhao Y, Lang G, Ito S, Bonnet J, Metzger E, Sawatsubashi S, Suzuki E, Le Guezennec X, Stunnenberg HG, Krasnov A, Georgieva SG, Schule R, Takeyama K, Kato S, Tora L, Devys D, Mol Cell. 2008;29:92-101.

[68] van der Knaap JA, Kumar BR, Moshkin YM, Langenberg K, Krijgsveld J, Heck AJ, Karch F, Verrijzer CP, Mol Cell. 2005;17:695-707.

[69] Nicassio F, Corrado N, Vissers JH, Areces LB, Bergink S, Marteijn JA, Geverts B, Houtsmuller AB, Vermeulen W, Di Fiore PP, Citterio E, Curr Biol. 2007;17:1972-1977.

[70] Joo HY, Jones A, Yang C, Zhai L, Smith ADt, Zhang Z, Chandrasekharan MB, Sun ZW, Renfrow MB, Wang Y, Chang C, Wang H, J Biol Chem. 2011;286:7190-7201.

[71] Levine SS, Weiss A, Erdjument-Bromage H, Shao Z, Tempst P, Kingston RE, Mol Cell Biol. 2002;22:6070-6078.

[72] Wang H, Wang L, Erdjument-Bromage H, Vidal M, Tempst P, Jones RS, Zhang Y, Nature. 2004;431:873-878.

[73] Joazeiro CA, Weissman AM, Cell. 2000;102:549-552.

[74] de Napoles M, Mermoud JE, Wakao R, Tang YA, Endoh M, Appanah R, Nesterova TB, Silva J, Otte AP, Vidal M, Koseki H, Brockdorff N, Dev Cell. 2004;7:663-676.
[75] Cao R, Tsukada Y, Zhang Y, Mol Cell. 2005;20:845-854.
[76] Fang J, Chen T, Chadwick B, Li E, Zhang Y, J Biol Chem. 2004;279:52812-52815.
[77] Leeb M, Wutz A, J Cell Biol. 2007;178:219-229.
[78] Kallin EM, Cao R, Jothi R, Xia K, Cui K, Zhao K, Zhang Y, PLoS Genet. 2009;5:e1000506.
[79] Cao R, Wang L, Wang H, Xia L, Erdjument-Bromage H, Tempst P, Jones RS, Zhang Y, Science. 2002;298:1039-1043.
[80] Fischle W, Wang Y, Jacobs SA, Kim Y, Allis CD, Khorasanizadeh S, Genes Dev. 2003;17:1870-1881.
[81] Min J, Zhang Y, Xu RM, Genes Dev. 2003;17:1823-1828.
[82] Boyer LA, Plath K, Zeitlinger J, Brambrink T, Medeiros LA, Lee TI, Levine SS, Wernig M, Tajonar A, Ray MK, Bell GW, Otte AP, Vidal M, Gifford DK, Young RA, Jaenisch R, Nature. 2006;441:349-353.
[83] Wang L, Brown JL, Cao R, Zhang Y, Kassis JA, Jones RS, Mol Cell. 2004;14:637-646.
[84] Lee MG, Villa R, Trojer P, Norman J, Yan KP, Reinberg D, Di Croce L, Shiekhattar R, Science. 2007;318:447-450.
[85] Schoeftner S, Sengupta AK, Kubicek S, Mechtler K, Spahn L, Koseki H, Jenuwein T, Wutz A, Embo J. 2006;25:3110-3122.
[86] Trojer P, Cao AR, Gao Z, Li Y, Zhang J, Xu X, Li G, Losson R, Erdjument-Bromage H, Tempst P, Farnham PJ, Reinberg D, Mol Cell. 2011;42:438-450.
[87] Simon JA, Kingston RE, Nat Rev Mol Cell Biol. 2009;10:697-708.
[88] Gearhart MD, Corcoran CM, Wamstad JA, Bardwell VJ, Mol Cell Biol. 2006;26:6880-6889.
[89] Elderkin S, Maertens GN, Endoh M, Mallery DL, Morrice N, Koseki H, Peters G, Brockdorff N, Hiom K, Mol Cell. 2007;28:107-120.
[90] Ogawa H, Ishiguro K, Gaubatz S, Livingston DM, Nakatani Y, Science. 2002;296:1132-1136.
[91] Kerppola TK, Trends Cell Biol. 2009;19:692-704.

[92] Lagarou A, Mohd-Sarip A, Moshkin YM, Chalkley GE, Bezstarosti K, Demmers JA, Verrijzer CP, Genes Dev. 2008;22:2799-2810.
[93] Zhou W, Zhu P, Wang J, Pascual G, Ohgi KA, Lozach J, Glass CK, Rosenfeld MG, Mol Cell. 2008;29:69-80.
[94] Nakagawa T, Kajitani T, Togo S, Masuko N, Ohdan H, Hishikawa Y, Koji T, Matsuyama T, Ikura T, Muramatsu M, Ito T, Genes Dev. 2008;22:37-49.
[95] Azuara V, Perry P, Sauer S, Spivakov M, Jorgensen HF, John RM, Gouti M, Casanova M, Warnes G, Merkenschlager M, Fisher AG, Nat Cell Biol. 2006;8:532-538.
[96] Bernstein BE, Mikkelsen TS, Xie X, Kamal M, Huebert DJ, Cuff J, Fry B, Meissner A, Wernig M, Plath K, Jaenisch R, Wagschal A, Feil R, Schreiber SL, Lander ES, Cell. 2006;125:315-326.
[97] Stock JK, Giadrossi S, Casanova M, Brookes E, Vidal M, Koseki H, Brockdorff N, Fisher AG, Pombo A, Nat Cell Biol. 2007;9:1428-1435.
[98] Vissers JH, Nicassio F, van Lohuizen M, Di Fiore PP, Citterio E, Cell Div. 2008;3:8.
[99] Atanassov BS, Koutelou E, Dent SY, FEBS Lett. 2010.
[100] Joo HY, Zhai L, Yang C, Nie S, Erdjument-Bromage H, Tempst P, Chang C, Wang H, Nature. 2007;449:1068-1072.
[101] Cai SY, Babbitt RW, Marchesi VT, Proc Natl Acad Sci U S A. 1999;96:2828-2833.
[102] Zhu P, Zhou W, Wang J, Puc J, Ohgi KA, Erdjument-Bromage H, Tempst P, Glass CK, Rosenfeld MG, Mol Cell. 2007;27:609-621.
[103] Scheuermann JC, de Ayala Alonso AG, Oktaba K, Ly-Hartig N, McGinty RK, Fraterman S, Wilm M, Muir TW, Muller J, Nature. 2010;465:243-247.
[104] Yu H, Mashtalir N, Daou S, Hammond-Martel I, Ross J, Sui G, Hart GW, Rauscher FJ, 3rd, Drobetsky E, Milot E, Shi Y, Affar EB, Mol Cell Biol. 2010.
[105] Machida YJ, Machida Y, Vashisht AA, Wohlschlegel JA, Dutta A, J Biol Chem. 2009.
[106] Sowa ME, Bennett EJ, Gygi SP, Harper JW, Cell. 2009;138:389-403.
[107] Misaghi S, Ottosen S, Izrael-Tomasevic A, Arnott D, Lamkanfi M, Lee J, Liu J, O'Rourke K, Dixit VM, Wilson AC, Mol Cell Biol. 2009;29:2181-2192.
[108] Tyagi S, Chabes AL, Wysocka J, Herr W, Mol Cell. 2007;27:107-119.
[109] Eletr ZM, Wilkinson KD, Cell Biochem Biophys. 2011;60:3-11.

[110] Zhang XY, Varthi M, Sykes SM, Phillips C, Warzecha C, Zhu W, Wyce A, Thorne AW, Berger SL, McMahon SB, Mol Cell. 2008;29:102-111.
[111] Lang G, Bonnet J, Umlauf D, Karmodiya K, Koffler J, Stierle M, Devys D, Tora L, Mol Cell Biol. 2011;31:3734-3744.
[112] Atanassov BS, Evrard YA, Multani AS, Zhang Z, Tora L, Devys D, Chang S, Dent SY, Mol Cell. 2009;35:352-364.
[113] Maertens GN, El Messaoudi-Aubert S, Elderkin S, Hiom K, Peters G, EMBO J. 2010;29:2553-2565.
[114] de Bie P, Zaaroor-Regev D, Ciechanover A, Biochem Biophys Res Commun. 2010;400:389-395.
[115] Richly H, Rocha-Viegas L, Ribeiro JD, Demajo S, Gundem G, Lopez-Bigas N, Nakagawa T, Rospert S, Ito T, Di Croce L, Nature. 2010;468:1124-1128.
[116] Francis NJ, Kingston RE, Woodcock CL, Science. 2004;306:1574-1577.
[117] Eskeland R, Leeb M, Grimes GR, Kress C, Boyle S, Sproul D, Gilbert N, Fan Y, Skoultchi AI, Wutz A, Bickmore WA, Mol Cell. 2010;38:452-464.
[118] Lane DP, Nature. 1992;358:15-16.
[119] Levine AJ, Cell. 1997;88:323-331.
[120] Vogelstein B, Lane D, Levine AJ, Nature. 2000;408:307-310.
[121] Brooks CL, Gu W, Curr Opin Cell Biol. 2003;15:164-171.
[122] Brooks CL, Gu W, Protein Cell. 2011;2:456-462.
[123] Meek DW, Anderson CW, Cold Spring Harb Perspect Biol. 2009;1:a000950.
[124] Dai C, Gu W, Trends Mol Med. 2010;16:528-536.
[125] Scheffner M, Werness BA, Huibregtse JM, Levine AJ, Howley PM, Cell. 1990;63:1129-1136.
[126] Huibregtse JM, Scheffner M, Howley PM, Mol Cell Biol. 1993;13:775-784.
[127] Scheffner M, Huibregtse JM, Vierstra RD, Howley PM, Cell. 1993;75:495-505.
[128] Boutell C, Everett RD, J Biol Chem. 2003;278:36596-36602.
[129] Querido E, Blanchette P, Yan Q, Kamura T, Morrison M, Boivin D, Kaelin WG, Conaway RC, Conaway JW, Branton PE, Genes Dev. 2001;15:3104-3117.
[130] Cai QL, Knight JS, Verma SC, Zald P, Robertson ES, PLoS Pathog. 2006;2:e116.

[131] Sato Y, Kamura T, Shirata N, Murata T, Kudoh A, Iwahori S, Nakayama S, Isomura H, Nishiyama Y, Tsurumi T, PLoS Pathog. 2009;5:e1000530.
[132] Haupt Y, Maya R, Kazaz A, Oren M, Nature. 1997;387:296-299.
[133] Honda R, Tanaka H, Yasuda H, FEBS Lett. 1997;420:25-27.
[134] Kubbutat MH, Jones SN, Vousden KH, Nature. 1997;387:299-303.
[135] Kulikov R, Letienne J, Kaur M, Grossman SR, Arts J, Blattner C, Proc Natl Acad Sci U S A. 2010;107:10038-10043.
[136] Montes de Oca Luna R, Wagner DS, Lozano G, Nature. 1995;378:203-206.
[137] Jones SN, Roe AE, Donehower LA, Bradley A, Nature. 1995;378:206-208.
[138] Barak Y, Juven T, Haffner R, Oren M, EMBO J. 1993;12:461-468.
[139] Li M, Brooks CL, Wu-Baer F, Chen D, Baer R, Gu W, Science. 2003;302:1972-1975.
[140] Bode AM, Dong Z, Nat Rev Cancer. 2004;4:793-805.
[141] Huang J, Berger SL, Curr Opin Genet Dev. 2008;18:152-158.
[142] Chuikov S, Kurash JK, Wilson JR, Xiao B, Justin N, Ivanov GS, McKinney K, Tempst P, Prives C, Gamblin SJ, Barlev NA, Reinberg D, Nature. 2004;432:353-360.
[143] Meek DW, Knippschild U, Mol Cancer Res. 2003;1:1017-1026.
[144] Wade M, Wang YV, Wahl GM, Trends Cell Biol. 2010;20:299-309.
[145] Wang X, Taplick J, Geva N, Oren M, FEBS Lett. 2004;561:195-201.
[146] Zhang Y, Xiong Y, Yarbrough WG, Cell. 1998;92:725-734.
[147] Kamijo T, Weber JD, Zambetti G, Zindy F, Roussel MF, Sherr CJ, Proc Natl Acad Sci U S A. 1998;95:8292-8297.
[148] Sui G, Affar el B, Shi Y, Brignone C, Wall NR, Yin P, Donohoe M, Luke MP, Calvo D, Grossman SR, Shi Y, Cell. 2004;117:859-872.
[149] Zhang Y, Wolf GW, Bhat K, Jin A, Allio T, Burkhart WA, Xiong Y, Mol Cell Biol. 2003;23:8902-8912.
[150] Lohrum MA, Ludwig RL, Kubbutat MH, Hanlon M, Vousden KH, Cancer Cell. 2003;3:577-587.
[151] Dai MS, Zeng SX, Jin Y, Sun XX, David L, Lu H, Mol Cell Biol. 2004;24:7654-7668.
[152] Dai MS, Lu H, J Biol Chem. 2004;279:44475-44482.

[153] Fu X, Yucer N, Liu S, Li M, Yi P, Mu JJ, Yang T, Chu J, Jung SY, O'Malley BW, Gu W, Qin J, Wang Y, Proc Natl Acad Sci U S A. 2010;107:4579-4584.
[154] Leng RP, Lin Y, Ma W, Wu H, Lemmers B, Chung S, Parant JM, Lozano G, Hakem R, Benchimol S, Cell. 2003;112:779-791.
[155] Dornan D, Wertz I, Shimizu H, Arnott D, Frantz GD, Dowd P, O'Rourke K, Koeppen H, Dixit VM, Nature. 2004;429:86-92.
[156] Dornan D, Shimizu H, Mah A, Dudhela T, Eby M, O'Rourke K, Seshagiri S, Dixit VM, Science. 2006;313:1122-1126.
[157] Chen D, Kon N, Li M, Zhang W, Qin J, Gu W, Cell. 2005;121:1071-1083.
[158] Yang W, Rozan LM, McDonald ER, 3rd, Navaraj A, Liu JJ, Matthew EM, Wang W, Dicker DT, El-Deiry WS, J Biol Chem. 2007;282:3273-3281.
[159] Yamasaki S, Yagishita N, Sasaki T, Nakazawa M, Kato Y, Yamadera T, Bae E, Toriyama S, Ikeda R, Zhang L, Fujitani K, Yoo E, Tsuchimochi K, Ohta T, Araya N, Fujita H, Aratani S, Eguchi K, Komiya S, Maruyama I, Higashi N, Sato M, Senoo H, Ochi T, Yokoyama S, Amano T, Kim J, Gay S, Fukamizu A, Nishioka K, Tanaka K, Nakajima T, EMBO J. 2007;26:113-122.
[160] Lee EW, Lee MS, Camus S, Ghim J, Yang MR, Oh W, Ha NC, Lane DP, Song J, EMBO J. 2009;28:2100-2113.
[161] Allton K, Jain AK, Herz HM, Tsai WW, Jung SY, Qin J, Bergmann A, Johnson RL, Barton MC, Proc Natl Acad Sci U S A. 2009;106:11612-11616.
[162] Xia Y, Padre RC, De Mendoza TH, Bottero V, Tergaonkar VB, Verma IM, Proc Natl Acad Sci U S A. 2009;106:2629-2634.
[163] Sun L, Shi L, Li W, Yu W, Liang J, Zhang H, Yang X, Wang Y, Li R, Yao X, Yi X, Shang Y, Proc Natl Acad Sci U S A. 2009;106:10195-10200.
[164] Esser C, Scheffner M, Hohfeld J, J Biol Chem. 2005;280:27443-27448.
[165] Lukashchuk N, Vousden KH, Mol Cell Biol. 2007;27:8284-8295.
[166] Muller P, Hrstka R, Coomber D, Lane DP, Vojtesek B, Oncogene. 2008;27:3371-3383.
[167] Rajendra R, Malegaonkar D, Pungaliya P, Marshall H, Rasheed Z, Brownell J, Liu LF, Lutzker S, Saleem A, Rubin EH, J Biol Chem. 2004;279:36440-36444.
[168] Weger S, Hammer E, Heilbronn R, FEBS Lett. 2005;579:5007-5012.

[169] Le Cam L, Linares LK, Paul C, Julien E, Lacroix M, Hatchi E, Triboulet R, Bossis G, Shmueli A, Rodriguez MS, Coux O, Sardet C, Cell. 2006;127:775-788.
[170] Kruse JP, Gu W, J Biol Chem. 2009;284:3250-3263.
[171] Laine A, Ronai Z, Oncogene. 2007;26:1477-1483.
[172] Laine A, Topisirovic I, Zhai D, Reed JC, Borden KL, Ronai Z, Mol Cell Biol. 2006;26:8901-8913.
[173] Topisirovic I, Gutierrez GJ, Chen M, Appella E, Borden KL, Ronai ZA, Proc Natl Acad Sci U S A. 2009;106:12676-12681.
[174] Li M, Chen D, Shiloh A, Luo J, Nikolaev AY, Qin J, Gu W, Nature. 2002;416:648-653.
[175] Cummins JM, Rago C, Kohli M, Kinzler KW, Lengauer C, Vogelstein B, Nature. 2004;428:1 p following 486.
[176] Li M, Brooks CL, Kon N, Gu W, Mol Cell. 2004;13:879-886.
[177] Stevenson LF, Sparks A, Allende-Vega N, Xirodimas DP, Lane DP, Saville MK, Embo J. 2007.
[178] Yuan J, Luo K, Zhang L, Cheville JC, Lou Z, Cell. 2010;140:384-396.
[179] Zhang X, Berger FG, Yang J, Lu X, EMBO J. 2011.
[180] Molinari E, Gilman M, Natesan S, EMBO J. 1999;18:6439-6447.
[181] Salghetti SE, Muratani M, Wijnen H, Futcher B, Tansey WP, Proc Natl Acad Sci U S A. 2000;97:3118-3123.
[182] Salghetti SE, Caudy AA, Chenoweth JG, Tansey WP, Science. 2001;293:1651-1653.
[183] Muratani M, Tansey WP, Nat Rev Mol Cell Biol. 2003;4:192-201.
[184] Hann SR, Eisenman RN, Mol Cell Biol. 1984;4:2486-2497.
[185] Kim SY, Herbst A, Tworkowski KA, Salghetti SE, Tansey WP, Mol Cell. 2003;11:1177-1188.
[186] von der Lehr N, Johansson S, Wu S, Bahram F, Castell A, Cetinkaya C, Hydbring P, Weidung I, Nakayama K, Nakayama KI, Soderberg O, Kerppola TK, Larsson LG, Mol Cell. 2003;11:1189-1200.
[187] Welcker M, Orian A, Grim JE, Eisenman RN, Clurman BE, Curr Biol. 2004;14:1852-1857.

[188] Welcker M, Orian A, Jin J, Grim JE, Harper JW, Eisenman RN, Clurman BE, Proc Natl Acad Sci U S A. 2004;101:9085-9090.
[189] Yada M, Hatakeyama S, Kamura T, Nishiyama M, Tsunematsu R, Imaki H, Ishida N, Okumura F, Nakayama K, Nakayama KI, EMBO J. 2004;23:2116-2125.
[190] Onoyama I, Tsunematsu R, Matsumoto A, Kimura T, de Alboran IM, Nakayama K, Nakayama KI, J Exp Med. 2007;204:2875-2888.
[191] Welcker M, Clurman BE, Nat Rev Cancer. 2008;8:83-93.
[192] Choi SH, Wright JB, Gerber SA, Cole MD, Genes Dev. 2010;24:1236-1241.
[193] Adhikary S, Marinoni F, Hock A, Hulleman E, Popov N, Beier R, Bernard S, Quarto M, Capra M, Goettig S, Kogel U, Scheffner M, Helin K, Eilers M, Cell. 2005;123:409-421.
[194] Popov N, Schulein C, Jaenicke LA, Eilers M, Nat Cell Biol. 2010;12:973-981.
[195] Popov N, Wanzel M, Madiredjo M, Zhang D, Beijersbergen R, Bernards R, Moll R, Elledge SJ, Eilers M, Nat Cell Biol. 2007;9:765-774.
[196] Bregman DB, Halaban R, van Gool AJ, Henning KA, Friedberg EC, Warren SL, Proc Natl Acad Sci U S A. 1996;93:11586-11590.
[197] Ratner JN, Balasubramanian B, Corden J, Warren SL, Bregman DB, J Biol Chem. 1998;273:5184-5189.
[198] Woudstra EC, Gilbert C, Fellows J, Jansen L, Brouwer J, Erdjument-Bromage H, Tempst P, Svejstrup JQ, Nature. 2002;415:929-933.
[199] Beaudenon SL, Huacani MR, Wang G, McDonnell DP, Huibregtse JM, Mol Cell Biol. 1999;19:6972-6979.
[200] Rockx DA, Mason R, van Hoffen A, Barton MC, Citterio E, Bregman DB, van Zeeland AA, Vrieling H, Mullenders LH, Proc Natl Acad Sci U S A. 2000;97:10503-10508.
[201] Mitsui A, Sharp PA, Proc Natl Acad Sci U S A. 1999;96:6054-6059.
[202] Luo Z, Zheng J, Lu Y, Bregman DB, Mutat Res. 2001;486:259-274.
[203] Huibregtse JM, Yang JC, Beaudenon SL, Proc Natl Acad Sci U S A. 1997;94:3656-3661.
[204] Anindya R, Aygun O, Svejstrup JQ, Mol Cell. 2007;28:386-397.
[205] Somesh BP, Reid J, Liu WF, Sogaard TM, Erdjument-Bromage H, Tempst P, Svejstrup JQ, Cell. 2005;121:913-923.

[206] Kuznetsova AV, Meller J, Schnell PO, Nash JA, Ignacak ML, Sanchez Y, Conaway JW, Conaway RC, Czyzyk-Krzeska MF, Proc Natl Acad Sci U S A. 2003;100:2706-2711.

[207] Ribar B, Prakash L, Prakash S, Mol Cell Biol. 2006;26:3999-4005.

[208] Ribar B, Prakash L, Prakash S, Mol Cell Biol. 2007;27:3211-3216.

[209] Yasukawa T, Kamura T, Kitajima S, Conaway RC, Conaway JW, Aso T, EMBO J. 2008;27:3256-3266.

[210] Kleiman FE, Wu-Baer F, Fonseca D, Kaneko S, Baer R, Manley JL, Genes Dev. 2005;19:1227-1237.

[211] Starita LM, Horwitz AA, Keogh MC, Ishioka C, Parvin JD, Chiba N, J Biol Chem. 2005;280:24498-24505.

[212] Horwitz AA, Affar el B, Heine GF, Shi Y, Parvin JD, Proc Natl Acad Sci U S A. 2007;104:6614-6619.

[213] Li H, Zhang Z, Wang B, Zhang J, Zhao Y, Jin Y, Mol Cell Biol. 2007;27:5296-5305.

[214] Lee KB, Sharp PA, Biochemistry. 2004;43:15223-15229.

[215] Harreman M, Taschner M, Sigurdsson S, Anindya R, Reid J, Somesh B, Kong SE, Banks CA, Conaway RC, Conaway JW, Svejstrup JQ, Proc Natl Acad Sci U S A. 2009;106:20705-20710.

[216] Kvint K, Uhler JP, Taschner MJ, Sigurdsson S, Erdjument-Bromage H, Tempst P, Svejstrup JQ, Mol Cell. 2008;30:498-506.

[217] Kee Y, Lyon N, Huibregtse JM, EMBO J. 2005;24:2414-2424.

[218] Kee Y, Munoz W, Lyon N, Huibregtse JM, J Biol Chem. 2006;281:36724-36731.

Figure Legends

Figure 1. Model of the mechanism of action of H2B ubiquitination in gene activation.

Bre1/Rad6/Lge1 E3 complex is recruited by activators to promoters. Phosphorylated at serine 5 of the CTD domain (CTDS5P), Pol II recruits PAF elongation factor complex, which in turn, allows the activation of Bre1/Rad6/Lge1 for the ubiquitination of H2B. BUR complex acts as a stimulator of the Bre1/Rad6/Lge1 complex activity. H2Bub activates transcription by different mechanisms. H2Bub promotes ubiquitination of Cps35, a subunit of COMPASS complex, which allow the chromatin recruitment of Spp1 to COMPASS and activation of COMPASS for the tri-methylation of H3K4 by Set1. H2Bub is deubiquitinated by Ubp8, a component of the SAGA complex. This event allows the recruitment of Ctk1 for the phosphorylation of Pol II CTD on Serine 2 which in turn promotes Set2 recruitement for H3K36 methylation. H2Bub stimulates the activity of the FACT complex to facilitate the passage of Pol II.

Figure 2. Model of the mechanism of action of H2A ubiquitination in gene repression.

At repressed gene promoters, PRC2 is recruited to tri-methylate H3K27, and this in turn, recruits PRC1 to catalyze H2A ubiquitination. There are different variations of PRC1 complexes, all containing the subunit Ring1B that is responsible for the ubiquitination activity of the complex. At selective promoters (e.g. chemokines genes), 2A-HUB is recruited by the repressive NCoR complex to catalyze the ubiquitination of H2A. This histone modification is able to inhibit H3K4 methylation and FACT recruitment for gene repression. To activate H2Aub-repressed genes, ZRF1 binds to H2Aub, displaces PRC1 and facilitates H2Aub

deubiquitination. Eight H2A DUBs associated with transcription regulation have been identified and interact with different proteins to form diverse complexes.

Figure 3. Regulation of p53 stability and localization by ubiquitination.

p53 is regulated by various E3s leading to diverse effects on its stability and localization. Several E3s, including Mdm2 and Pirh2, negatively regulate p53 protein levels by polyubiquitination-mediated proteasomal degradation, a process enhanced or inhibited by DUBs such as HAUSP and USP10 respectively. Mdm2 can further monoubiquitinate p53 which leads to its cytoplasmic localization. Other E3s positively affect p53 through stabilization such as RFWD3 or cytoplasmic and chromatin localization by WWP1 and E4F1 respectively.

Figure 4. Regulation of Myc oncogene activity and function by ubiquitination.

Myc is polyubiquitinated through K48 linkage by the E3 Skp2 leading first to Myc activation followed by its proteasomal degradation, representing a mechanism to control Myc function. In contrast to Skp2, the E3s TRUSS and Fbw7 also polyubiquitinate Myc through K48 linkage but instead inhibit Myc and signal for its degradation. In the case of Fbw7, its effect on Myc can be blocked by the actions of the USP28 DUB and by the β-TrCP E3 which ubiquitinates Myc through heterotypic Ub chains leading to Myc stabilization and function in cell cycle progression. Finally, Hect H9 (Huwe1) activates Myc through K63 poly-Ub linkage.

Figure 5. RNA Pol II function is regulated by ubiquitination.

The major subunit of Pol II, Rpb1, is ubiquitinated in a controlled manner to ensure the proper function of the polymerase. In a first step, Rpb1 is monoubiquitinated by Rsp5 (Nedd4), a modification reversed by the action of the DUB Ubp3. Furthermore, this step is regulated by the phosphorylation status of the CTD of Rpb1. While phosphorylation on Serine 2 (elongation) of the CTD signals for mono-Ub by Rsp5, Serine 5 (initiation) inhibits the action of the E3. Following this priming ubiquitination step, Rpb1 is polyubiquitinated through K48 Ub linkage by an Elongin/Cullin complex signaling Pol II for proteasomal degradation, which can be blocked by the DUB Ubp2.

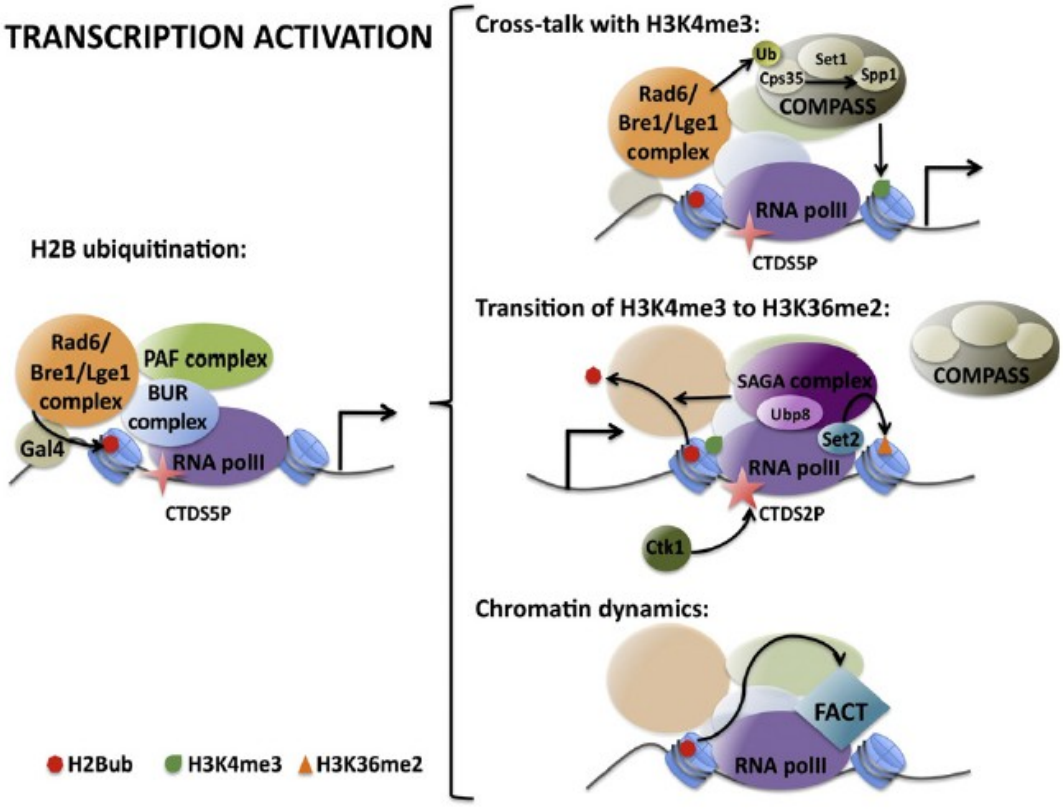
TRANSCRIPTION ACTIVATION
H2B ubiquitination:
Rad6/
Bre1/Lge1
complex
PAF complex
BUR
complex
Gal4
RNA polII
CTDS5P
Cross-talk with H3K4me3:
Ub
Set1
Cps35
Spp1
COMPASS
Rad6/
Bre1/Lge1
complex
RNA polII
CTDS5P
Transition of H3K4me3 to H3K36me2:
COMPASS
SAGA complex
Ubp8
Set2
RNA polII
CTDS2P
Ctk1
Chromatin dynamics:
FACT
RNA polII
H2Bub
H3K4me3
H3K36me2

Figure 1

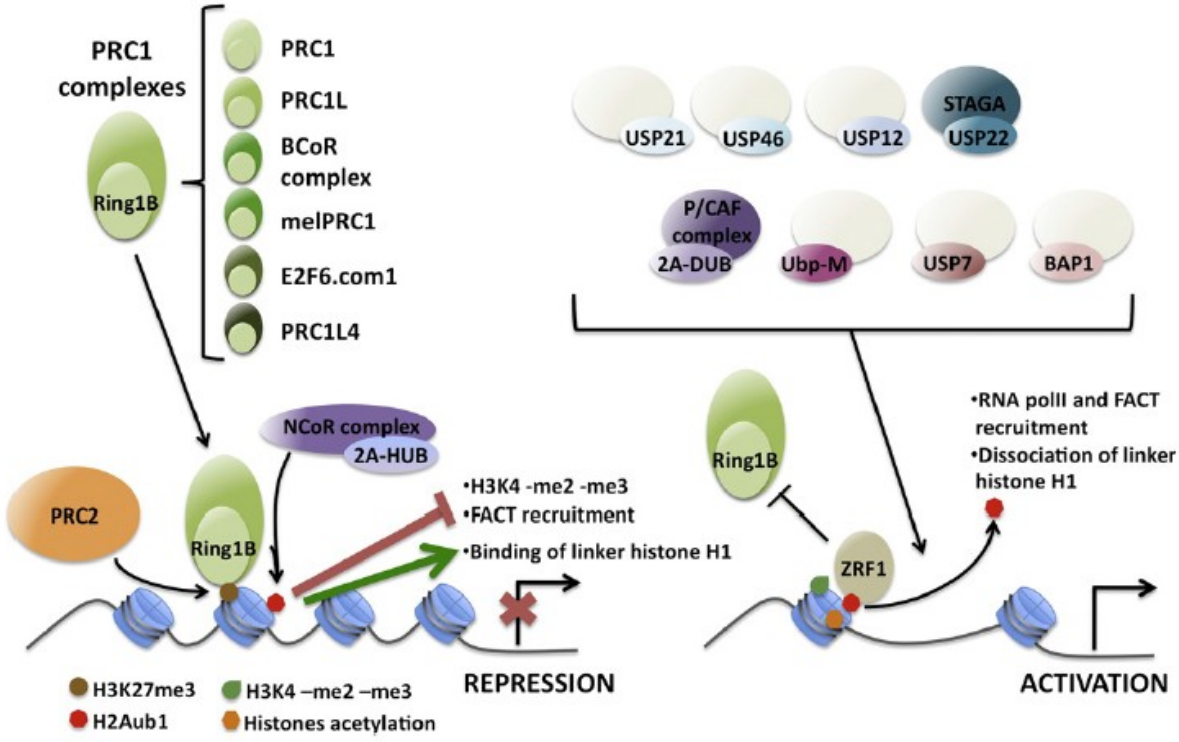
PRC1 complexes
Ring1B
PRC1
PRC1L
BCoR complex
melPRC1
E2F6.com1
PRC1L4
NCoR complex
2A-HUB
PRC2
Ring1B
•H3K4 -me2 -me3
•FACT recruitment
•Binding of linker histone H1
H3K27me3
H2Aub1
H3K4 –me2 –me3
Histones acetylation
REPRESSION
USP21
USP46
USP12
STAGA
USP22
P/CAF complex
2A-DUB
Ubp-M
USP7
BAP1
Ring1B
•RNA polII and FACT recruitment
•Dissociation of linker histone H1
ZRF1
ACTIVATION

Figure 2

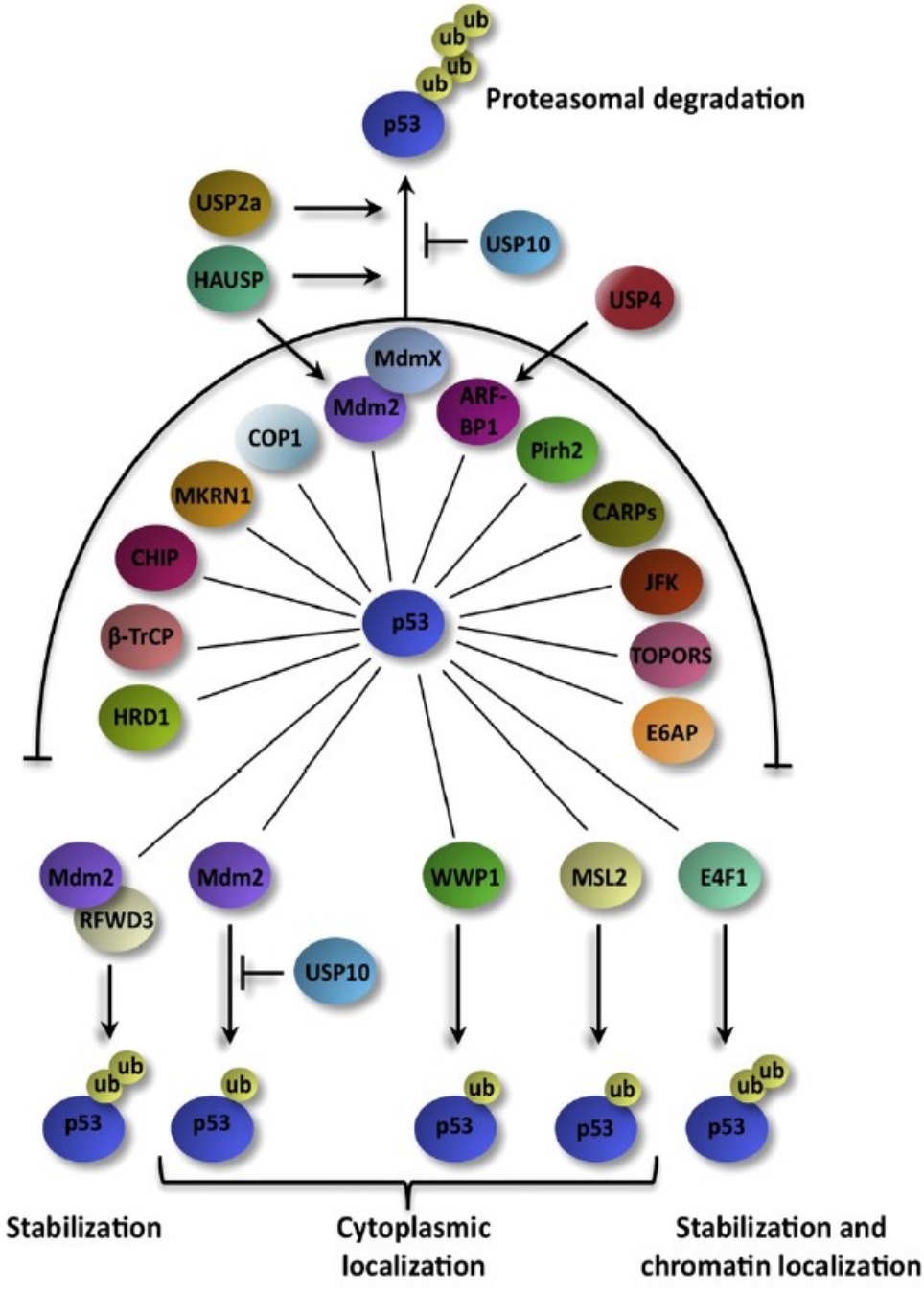
ub
ub
ub
ub
p53
Proteasomal degradation
USP2a
HAUSP
USP10
USP4
MdmX
Mdm2
ARF-BP1
COP1
Pirh2
MKRN1
CARPs
CHIP
JFK
p53
β-TrCP
TOPORS
HRD1
E6AP
Mdm2
RFWD3
Mdm2
WWP1
MSL2
E4F1
USP10
Stabilization
Cytoplasmic localization
Stabilization and chromatin localization

Figure 3

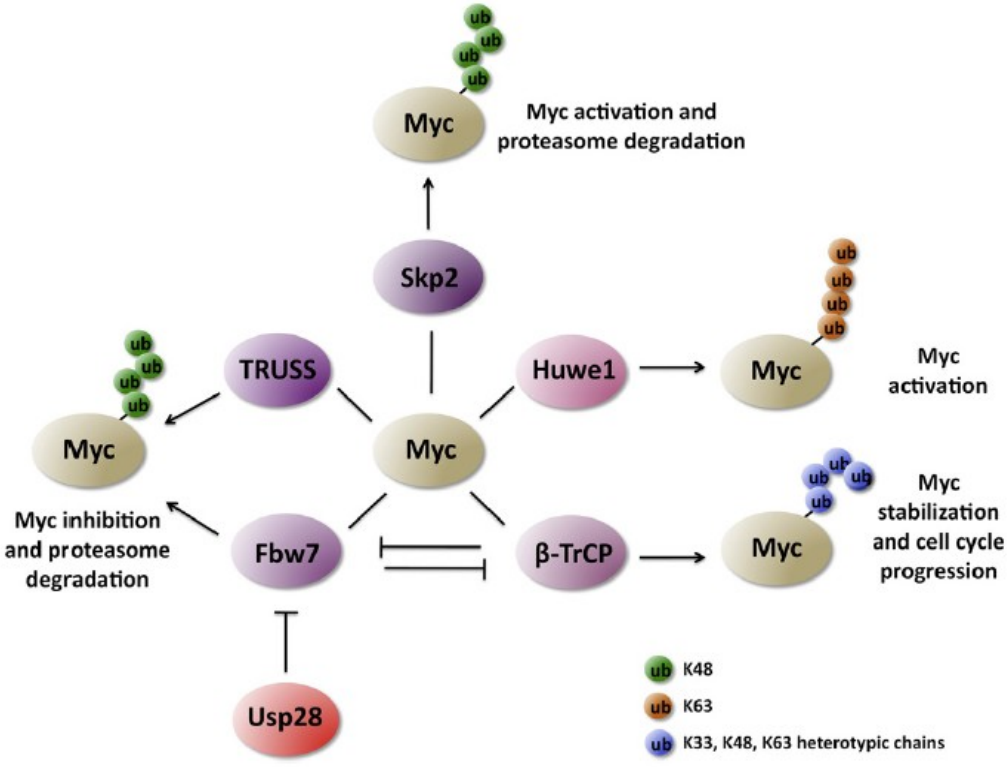
ub
Myc
Myc activation and
proteasome degradation
Skp2
TRUSS
Huwe1
Myc
Myc
activation
Myc
Myc inhibition
and proteasome
degradation
Fbw7
β-TrCP
Myc
Myc
stabilization
and cell cycle
progression
Usp28
K48
K63
K33, K48, K63 heterotypic chains

Figure 4

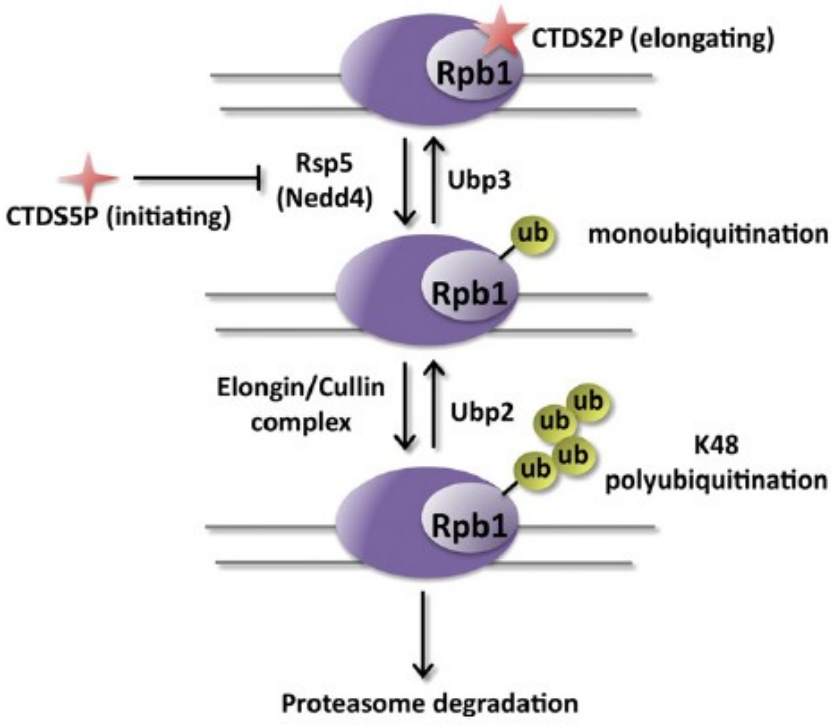
CTDS2P (elongating)
Rpb1
Rsp5
(Nedd4)
Ubp3
CTDS5P (initiating)
ub
monoubiquitination
Rpb1
Elongin/Cullin
complex
Ubp2
ub
ub
ub
ub
K48
polyubiquitination
Rpb1
Proteasome degradation

Figure 5

1.3 Ubiquitination and DNA repair

Exogenous DNA-damaging agents, such as ionizing (IR) and ultraviolet (UV) radiations, as well as endogenous DNA damage caused by reactive oxygen species or defects in DNA replication, continuously challenge our cells and cause genomic instability and cancer. To maintain genome integrity, cells utilize a complex network of signaling cascades that collectively constitute the DNA damage response (DDR)[21]. Activation of DDR ensures detection, signaling and repair of different forms of DNA damage. The nature of the DNA lesion determines which specific DNA repair pathway need to be activated during the DDR. For example, DNA bulky adducts caused by UV radiation are repaired by nucleotide-excision repair (NER). Furthermore, DNA double strand breaks (DSBs) are repaired mostly by non-homologous end joining (NHEJ) or homologous recombination (HR).

It is now widely accepted that ubiquitination plays an essential role in the DDR. In this section, I will briefly discuss examples of DNA repair pathways that use ubiquitination in their signaling cascades. Of note, the role of ubiquitination in the repair of DSBs will be developed in more detail in a later section.

1.3.1 Ubiquitination in NER

Bulky DNA adducts caused by UV radiation are highly genotoxic since they inhibit the progression of the replication and transcription machineries. These lesions are efficiently and faithfully repaired through the NER pathway. NER is composed of two subpathways that differ in the recognition of the lesion: global genome repair (GG-NER) and transcription-coupled repair (TC-NER)[22,23] (Figure 2). In respect to GG-NER, which is responsible of

repair throughout the whole genome, lesions are recognized by two different complexes, DDB1-DDB2 (XPE) and XPC-RAD23[24]. DDB1-DDB2 functions as an adapter protein in the CUL4 E3 ligase complex which is inhibited by the COP9 signalosome (CSN) [25]. Following DNA damage, CUL4 is dissociated from COP9 and is recruited to the lesion where it monoubiquitinates histones to generate a relaxed chromatin environment to allow for proper repair[26]. In addition, CUL4 also polyubiquitinates DDB2 leading to the dissociation of the XPE complex from DNA and ultimately its proteasomal degradation[25]. Moreover, XPC is also polyubiquitinated by CUL4 through K63 chain linkage which promotes its binding to DNA and hence NER[27]. With TC-NER, repair is activated by the stalling of RNA polymerase II (RNAP II) at the site of a DNA lesion on a transcribed strand only. TC-NER requires the recruitment of CSB and CSA, with CSA forming an E3 ligase with CUL4, at a UV lesion site[23,28]. The exact ligase activity CUL4-CSA is still not fully elucidated. However, it has been suggested that CSB is ubiquitinated and degraded at later stages of TC-NER to permit transcription to resume[29]. In addition, the DUB USP7 is recruited to lesion sites by binding to UVSSA, which interacts with stalled RNAP II[30-32], and delays CSB degradation. Following recognition, the transcription factor TFIIH and the helicases XPB and XPD are recruited which promotes DNA unwinding to allow for the recruitment of XPA and RPA to bind and protect single stranded DNA ends. The endonucleases XPF and XPG are then brought in to excise the lesion allowing for the DNA polymerase to fill the gap followed by ligation by DNA ligase I.

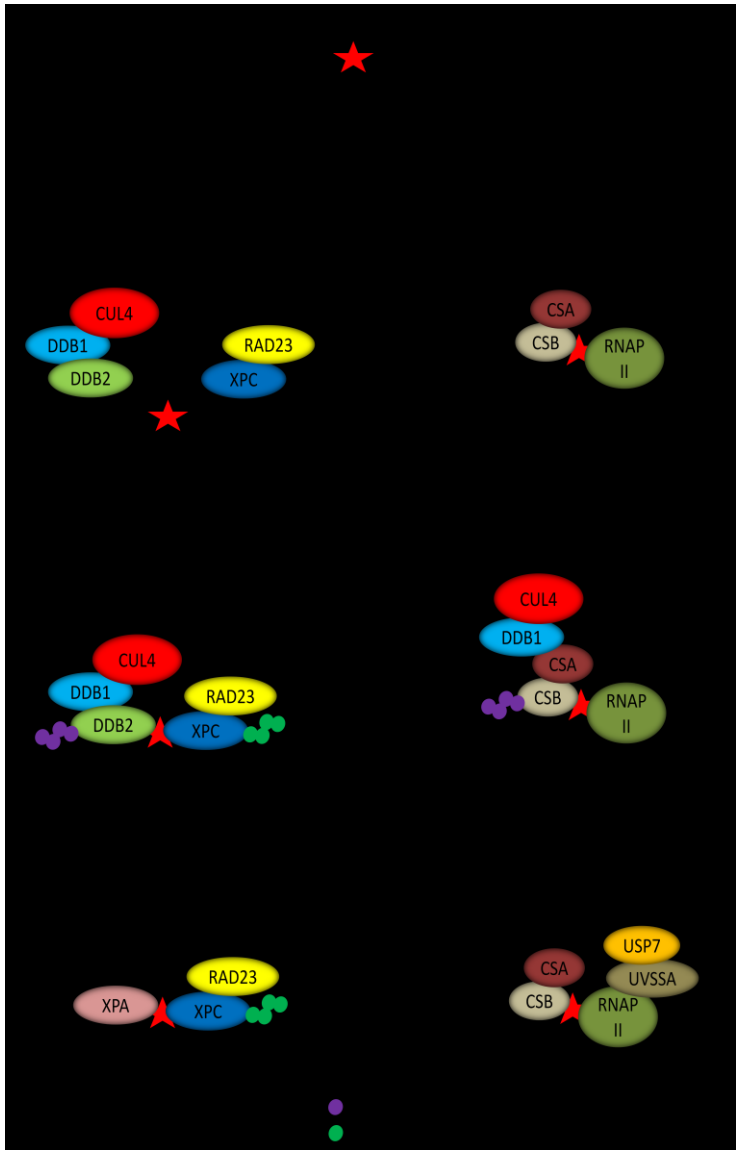

Figure 2. Role of ubiquitination in NER. In GG-NER, lesions are recognized by two different complexes, DDB1-DDB2 (XPE) and XPC-RAD23. DDB1-DDB2 recruits the CUL4 E3 ligase complex, leading to DDB2 and XPC polyubiquitination through K48 and K63 ubiquitin chains respectively. DDB2 is then dissociated from the lesion site and degraded, while XPA and the remaining NER machinery is recruited to complete repair. In TC-NER, CSA and CSB are recruited after RNAP II stalling at a DNA lesion induced by UV. CSA then binds to DDB1-CUL4 leading to CSB ubiquitination and its dissociation allowing for DNA replication to resume. CSB degradation can be delayed by the DUB USP7 through binding to UVSSA, which interacts with RNAP II.

1.3.2 Ubiquitination and postreplication repair

Postreplication repair (PRR) is an evolutionarily conserved pathway that permits replication beyond bulky DNA lesions through DNA damage-tolerance pathways coordinated by the ubiquitination (as well as sumoylation) of the DNA clamp Proliferating cell nuclear antigen (PCNA) which functions as a processivity factor in DNA replication[22]. Eukaryotic PRR is divided into two subpathways: translesion synthesis (TLS) and template switching (TS)[33]. TLS allows for DNA synthesis past a lesion through the action of specialized polymerases of the Y family such as Polη, Polι, Polκ, and Polζ[34]. However, unlike high-fidelity DNA polymerases, TLS polymerases are error prone. Template switching uses newly synthesized sister chromatids, in combination with the HR machinery, to allow for error-free bypass of a DNA lesion. An initial step in PRR in yeast is the monoubiquitination of PCNA, primarily on K164, by the E2-E3 enzymes Rad6-Rad18[35-37]. This modification is then recognized by TLS polymerases through their ubiquitin-binding domains (UBDs) and allow for DNA replication passed the lesion[38]. While still unclear, PCNA is then possibly deubiquitinated by USP1-UAF1 in vertebrates which would allow for the switch back to DNA polymerases to continue replication[39]. Template switching, on the other hand, involves the polyubiquitination of PCNA by Rad5 on K164[37]. Rad5, in conjunction with the dimeric E2 Ubc13-Mms2, induces the formation of K63-linked ubiquitin chains on PCNA, which support TS through still undefined mechanisms.

Many more studies are required to fully understand the magnitude of the role of ubiquitination in the DDR. In further sections, I will discuss the role of BRCA1 and ubiquitination in the repair of DSBs.

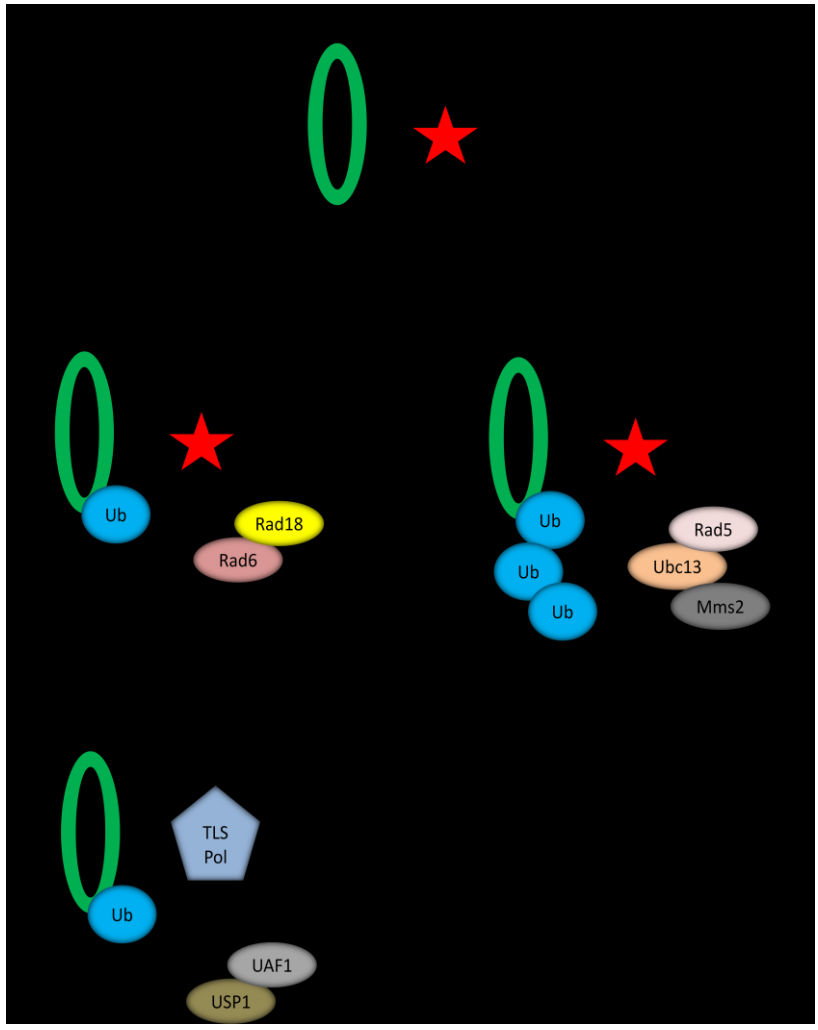

Figure 3. Role of ubiquitination in PRR. Eukaryotic PRR is divided into two pathways: translesion synthesis (TLS) and template switching (TS). An initial step in PRR is the monoubiquitination of PCNA, primarily on K164. During TLS, this modification is carried out by Rad6-Rad18, which signals for the recruitment of the error-prone TLS polymerases to bypass the lesion. PCNA is also deubiquitinated by USP1-UAF1 to possibly switch back to high-fidelity DNA polymerases to continue replication following lesion bypass. TS involves the polyubiquitination of PCNA by Rad5-Ubc13-Mms2 on K164 inducing the formation of K63-linked ubiquitin chains on PCNA, which support TS through still undefined mechanisms.

1.4 The breast cancer tumor suppressor BRCA1

1.4.1 Genetic predisposition to cancer

Family history is one of the most important risk factor during the development of breast cancer. In fact 5-10% of all breast cancers are genetically linked to mutations in high-penetrance susceptibility genes[40-43]. The *Breast Cancer early onset gene 1* (*BRCA1*) was originally mapped and cloned twenty years ago[44] and can account, with *BRCA2*, for approximately 15-25% of all hereditary breast cancers[41,45]. Mutations of these two tumor suppressors, that play major roles in the DNA damage response, lead to increased risk of cancers of the breast and of the gynaecological tract such as ovarian cancer[41]. The risk of developing cancer in women with genetic defects in BRCA1 reaches 80% by age 70, which is considerably higher than the 1 in 8 risk for all women[46]. Since BRCA1 has been studied for many years, the amount of information on this protein is quite impressive even though much still needs to be understood to fully establish the function and regulation of this protein. In the next sections, I will focus on the major interacting partners for BRCA1, its role in double strand break (DSB) repair and what is known about its interaction with BAP1.

1.4.2 General principles of DSB repair

DSBs are thought to be the most cytotoxic forms of DNA damage since both DNA strands are compromised[47,48]. Homologous recombination (HR) and Non-homologous end joining (NHEJ) are the two main mechanisms to repair DSBs (reviewed in [48-50]) (Figure 2). HR repair, which occurs in the S and G2 phases of the cell cycle, is more accurate since it relies on homologous DNA on a sister chromatid as a template to repair the break[51]. Briefly, when a DSB occurs, the MRN complex (Mre11-Rad50-Nbs1) binds to DNA on either side of

the break which recruits helicases and nucleases that serve the initial processing of the ends of the break[52,53]. It is at this point in the signalling cascade that BRCA1-CtIP is recruited for further end resection, which will be discussed in more detail in further sections. Following end processing, RPA binds with high affinity to single-stranded DNA (ssDNA) 3' overhangs. Then the BRCA2/PALB2 (Partner and localizer of BRCA2) complex displaces RPA from ssDNA leading to the recruitment of Rad51 and nucleoprotein filament formation[54-57]. After homology searching, this nucleoprotein filament then invades the other sister chromatid. Finally, DNA synthesis and crossover of genetic information occurs leading to error-free repair. NHEJ is less accurate since it mainly occurs during G0- and G1-phases of the cell cycle when sister chromatids are not present and involves direct ligation of broken ends[58,59]. Briefly, the Ku70/80 heterodimeric ATP-dependent DNA helicase binds to the ends of the break and recruits other NHEJ proteins including DNA-PK_{CS} which binds to each end and interact with each other forming a synaptic complex thus stabilizing DSB ends. Following end processing by Artemis[60], DNA ligase IV religates the broken ends.

1.4.3 Activation of BRCA1 by phosphorylation is response to a DSB

BRCA1 is phosphorylated and activated by two major members of the phosphoinositide 3-kinase (PI3K)-related protein kinase (PIKK) family: ataxia telangiectasia mutated (ATM) and ataxia telangiectasia and Rad3 related (ATR)[61,62]. These kinases can phosphorylate BRCA1 directly on SQ and TQ motifs found in its SQ cluster domain. ATM can also indirectly activate BRCA1 through phosphorylation of Chk2, a downstream checkpoint kinase. Activated Chk2 will then phosphorylate BRCA1 at serine 988[63,64]. In addition, both ATM and ATR can indirectly activate BRCA1 by phosphorylating Chk1[65].

Instead of phosphorylating BRCA1 itself, Chk1 rather binds BRCA1 through interaction with its BRCT domains (which will be discussed later). BRCA1 in turn will control the activation of Chk1 which is important for proper G2/M checkpoint activation following genotoxic stress[66].

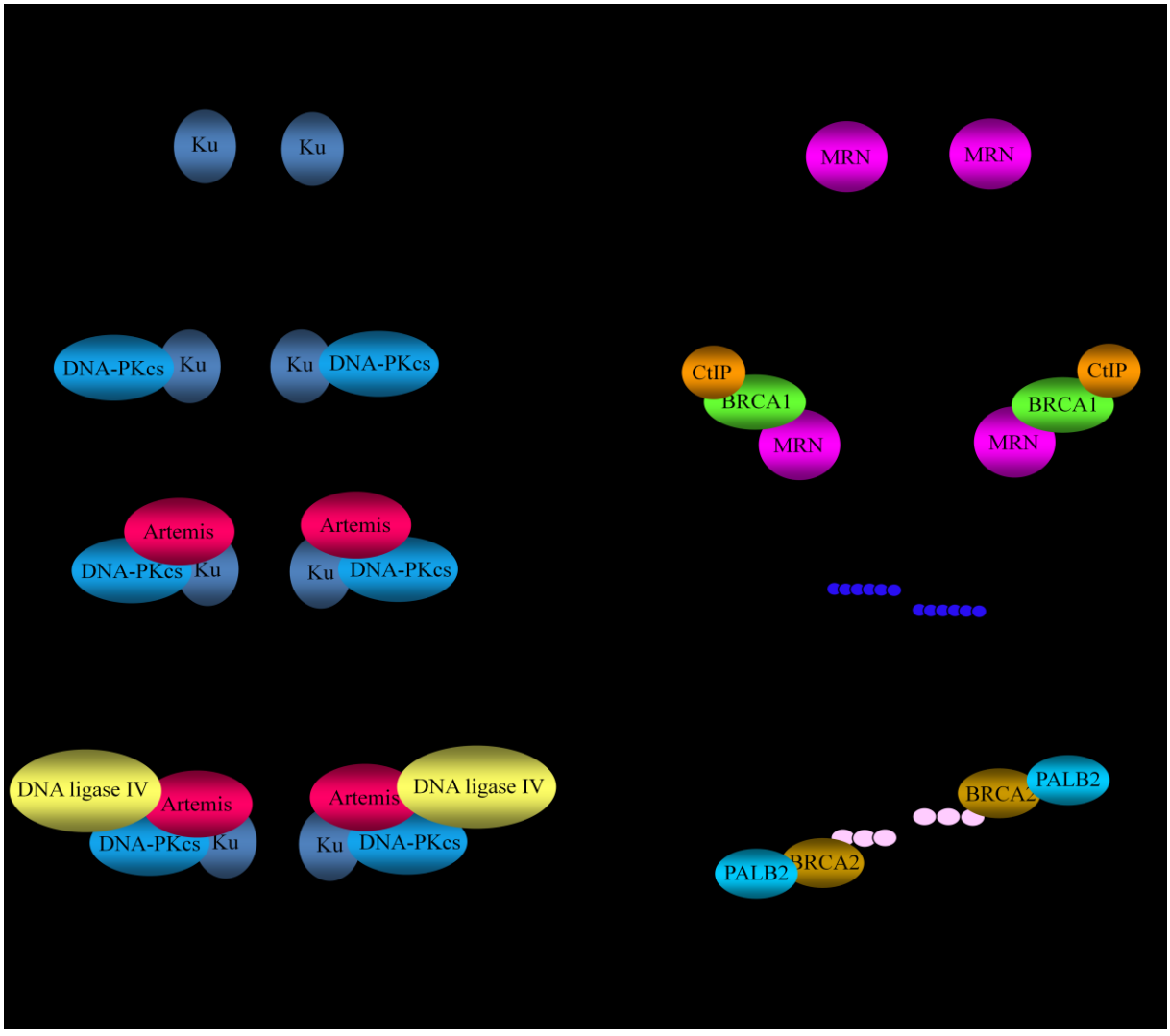

Figure 4. General principles of DSB repair. HR repair occurs in the S and G2 phases of the cell cycle when sister chromatids are present. The MRN complex (Mre11-Rad50-Nbs1) binds to DNA on either side of the break and leads to the recruitment of BRCA1-CtIP that serves to resect the ends of the break. RPA binds with high affinity to single-stranded DNA (ssDNA) 3' overhangs. BRCA2/PALB2 complex then displaces RPA from ssDNA leading to the recruitment of Rad51, strand invasion and ligation. NHEJ is less accurate since it mainly occurs during the G1 cell cycle phase when sister chromatids are not present and involves direct ligation of broken ends. The Ku70/80 heterodimeric DNA helicase binds to the ends of the break and recruits DNA-PK_{CS} which binds and stabilizes the ends. Following end processing by Artemis, DNA ligase IV religates the broken ends leading to repair.

1.4.4 BRCA1 protein domains and interacting partners

In the following section, I will discuss the major protein domains of BRCA1 as well as the different proteins that interact with these domains.

1.4.4.1 RING domain and the BRCA1 interaction with BARD1

The BRCA1 gene encodes an 1863 amino acid nuclear protein (BRCA1 contains a nuclear localization sequence, NLS[67]) containing several important domains. First, the N-terminal region of BRCA1 contains the evolutionary conserved Really interesting new gene (RING) domain, commonly found in E3 ligases, required for binding to BRCA1-associated RING domain protein 1 (BARD1)[68]. BRCA1 forms a heterodimer with BARD1, a stoichiometric partner, through binding of their respective RING domains. This interaction stabilizes BRCA1 and is required for its E3 ligase activity, which was originally thought to play a major role in tumor suppression[69]. In fact, the BRCA1-BARD1 heterodimer generates noncanonical K6-Ub chains when associated to the Ubch5c E2 enzyme *in vitro*[70,71]. These chains are present at sites of double strand breaks (DSBs) and appear to depend on BRCA1[72]. It is well established that BRCA1-BARD1 can be autoubiquitinated, but the function of this modification is still unclear. However, identification of other substrates of the BRCA1-BARD1 ubiquitin ligase has remained difficult with CtIP and histone H2A representing possible targets[73,74]. The importance of the RING domain for the tumor suppressor function of BRCA1 has been put into question recently. BRCA1-null mice die between embryonic day 5.5 and 8.5[75-78]. BRCA1-RING mutant knock-in mice show different phenotypes depending on the nature of the mutation. Mice with the I26A substitution, a synthetic RING mutation

not found in humans disrupting BRCA1 interaction with E2 conjugating enzymes but allowing interaction with BARD1, are viable, proficient for HR and are not susceptible to cancer[79,80]. However, mice harboring the C61G substitution, found in human cancer patients and disrupting the interaction with BARD1[68], show DNA repair defects and are embryonic lethal similar to *Brca1*-null mice[81]. Therefore, the role of the RING domain in BRCA1 tumor suppression is still unclear and it is now thought that BRCA1 C-terminal repeats (BRCT domains) are equally important for tumor inhibition[80].

1.4.4.2 BRCT domains and recruitment to DSB sites

BRCT repeats recognize phosphoserine residues and allow binding between BRCA1 and Abraxas, BRCA1-interacting protein C-terminal helicase 1 (BACH1) and CtIP all of which are required for BRCA1 function in DSB repair[82,83].

1.4.4.2.1 BRCA1-A (Abraxas) complex is recruited to DSB sites through an ubiquitination signaling cascade

Following exposure to ionizing radiation (IR) causing DSB lesions, the histone H2A variant H2AX is phosphorylated (γ-H2AX) on serine 139 by ATM and ATR[50,84]. Mediator of DNA damage checkpoint 1 (MDC1) is then recruited and phosphorylated[85,86] which serves as a scaffold for the E3 ligase RING finger protein 8 (RFN8). RNF8 mediates ubiquitination of chromatin-associated proteins around the DSB through K63 Ub-linkage[87-90]. RNF168 is then recruited and ubiquitinates, with the E2 conjugating enzyme UBC13, H2A on K13 and K15 residues[91,92]. Of note, RNF168 is regulated positively and negatively by the DUBs USP34[93] and OTUB1[94,95] respectively. H2Aub then serves as a platform for the recruitment of

receptor-associated protein 80 (RAP80), which possesses two ubiquitin-interacting motifs (UIMs) that have been shown to preferentially bind to K6 and K63 ubiquitin chains[96,97]. RAP80 is responsible for recruiting Abraxas, BRCC36, MERIT40 and BRCC45, all of which are necessary for efficient BRCA1 localization to DSB lesions[98,99]. Abraxas, also known as coiled-coil domain-containing protein 98 (CCDC98), directly binds to the BRCT domains of BRCA1 and functions as a linker between BRCA1 and RAP80[100]. The BRCA1/BRCA2-containing complex subunit 36 (BRCC36) deubiquitinase specifically hydrolyses K63 ubiquitin chains, thereby restricting K63-Ub around a DSB, and is required for BRCA1 recruitment to DSB sites[101]. The two other members of the BRCA1-A complex, MERIT40 and BRCC45, are required for the stability of the complex[102,103]. In addition to RNF8/168, BRCA1 recruitment to DSBs is also dependent on the E3 ligases RNF20 and RNF40, through a still undefined mechanism. RNF20 and RNF40 are suggested to play a role in histone eviction by ubiquitinating histone H2B on lysine 120 and 125, which would promote end resection and DNA repair[104,105]. Altogether, it is clear that proper BRCA1 localization to DSB lesions requires an upstream ubiquitination signaling cascade.

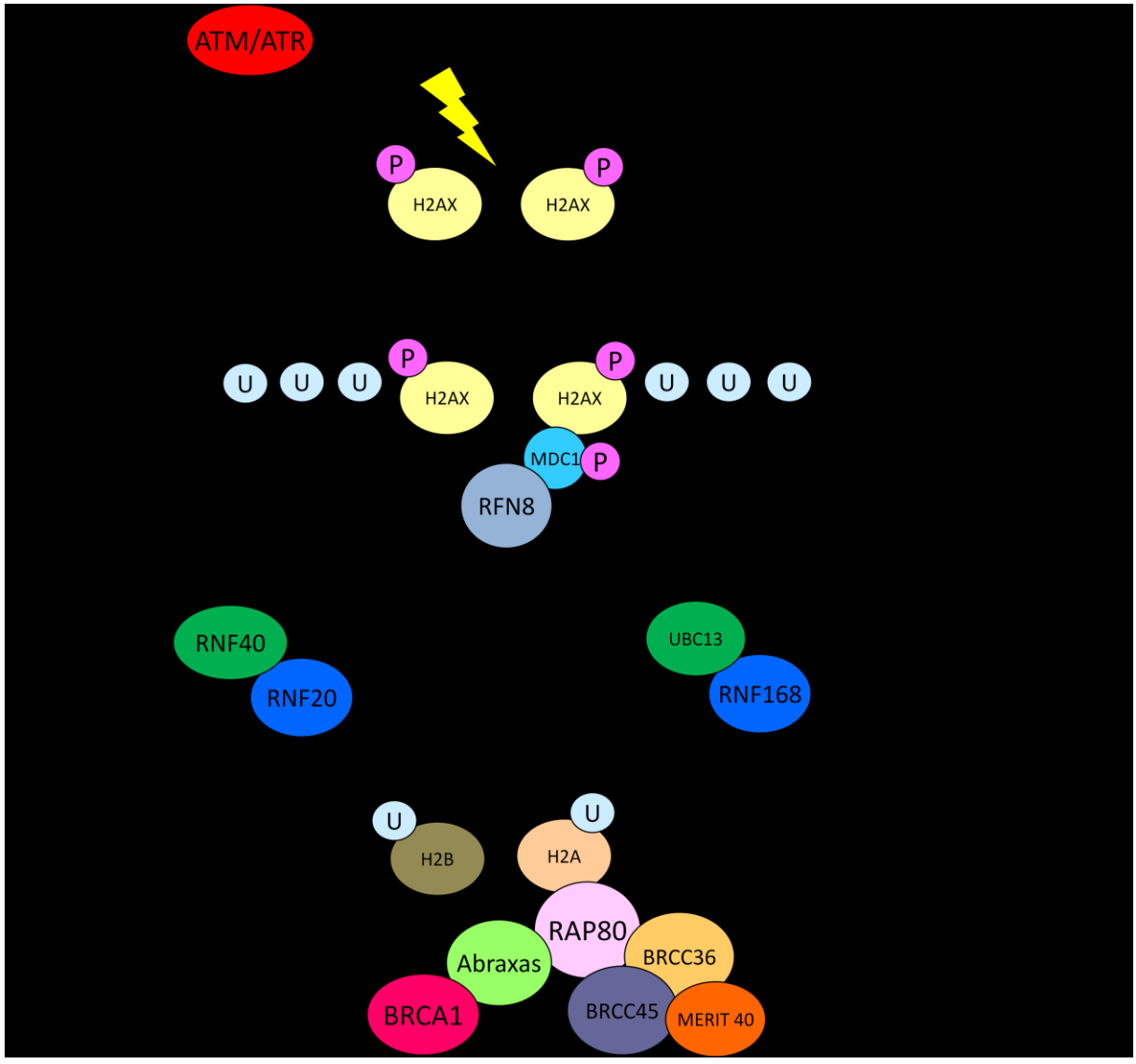

Figure 5. Recruitment of the BRCA1-A complex to DSB sites. Following DSB-inducing DNA damage, H2AX is phosphorylated by ATM/ATR signaling for MDC1 recruitment and phosphorylation, which is required for RNF8 localization. Then, RNF8 ubiquitinates chromatin-associated proteins around the lesion through K63-Ub linkage, which serves as a platform for RNF168 recrutiment. RNF168 then monoubiquitinates H2A on K13 and K15. RAP80, using its ubiquitin-interacting motifs, then binds H2Aub, and functions to recruit the BRCA1-A complex. BRCA1 is also recruited by RNF20/40, which ubiquitinates H2B on K120/125, through undefined mechanisms.

1.4.4.2.2 BRCA1-B (BACH1) complex

Chromatin remodeling during HR is essential since it modifies chromatin structure giving access to repair protein. BRCA1 BRCT motifs bind to the BRCA1-associated C-terminal helicase (BACH1). BACH1 is phosphorylated by ATM following DNA damage and forms foci reminiscent of BRCA1 IRIFs that also colocalize with γ-H2AX[106]. BACH1 was shown to regulate Rad51 displacement which is required for efficient HR repair[107]. As previously discussed, Rad51 is required for HR repair by forming a nucleoprotein filament necessary for strand invasion. Therefore, the main function of BRCA1 interaction with BACH1 might be to restrain its activity of promoting Rad51 displacement. Moreover, cells expressing a dominant negative mutation of BACH1 which inhibits its helicase activity show genomic instability. The second member of the BRCA1-B complex is the topoisomerase IIB binding protein 1 (TopBP1). TopBP1 is thought to interact indirectly with BRCA1 through BACH1[108]. While not fully elucidated, the main function of TopBP1 appears to be activating ATR via binding to the ATR-interacting protein (ATRIP). Stimulation of ATR would be in turn important for activation of BRCA1 and HR repair[109,110].

1.4.4.2.3 BRCA1-C (CtIP) complex

The cell cycle protein CtBP interacting protein (CtIP) interacts with BRCA1 through its BRCT domains in a cell-cycle dependant manner. CtIP is phosphorylated at serine 327 by ATM which is required for binding to BRCA1[111]. CtIP then links BRCA1 to the Nbs1 subunit of the MRN (Mre11-Rad50-Nbs1) complex. Nbs1, also known as Nibrin, which functions as a regulator of the MRN complex, is also phosphorylated by ATM and localized to DSB sites[112]. Another member of the MRN complex, meiotic recombination 11 (Mre11), is a 3'-5'

exonuclease capable of generating ssDNA through resection of DSB ends[113]. The BRCA1-CtIP-MRN complex is therefore essential during S/G2 for proper end resection and HR repair, which will be further discussed in the section on DSB repair pathway choice[114].

1.4.4.3 Coiled-coil domain and PALB2

BRCA1 interacts with PALB2 through binding of their respective coiled-coil (CC) domains[56,115]. PALB2 plays a major role during the displacement of RPA by loading BRCA2 and Rad51 to DSB repair sites during HR[116]. While not fully understood, BRCA1 is thought to aid in strand invasion by interacting indirectly with BRCA2/Rad51 through PALB2. In fact, mutation of both genes severely inhibits Rad51 HR foci formation. Moreover, missense mutations found in cancer patients affecting the CC of BRCA1, thereby blocking its interaction with PALB2, lead to inefficient HR. However, foci formation capacity of BRCA1 and PALB2 following DSBs seem to be independent of each other. In fact, BRCA1 mutated in its CC was still capable of forming IRIFs following DNA damage. In addition, PALB2 foci are found in HCC1937 cells that express a truncated BRCA1 lacking its CC domain. Further studies are needed to fully address the inter-dependency of BRCA1 and PALB2, and how it affects HR repair.

1.4.5 DSB repair: battle between 53BP1-RIF1 and BRCA1-CtIP

In this section, I will discuss the role BRCA1 plays in determining DSB repair choice through its interplay with 53BP1. Furthermore, I will emphasize the notion of synthetic lethality between BRCA1 deficiency and PARP inhibitors as a strategy for selective killing of cancer cells.

1.4.5.1 DSB repair pathway choice

The timing in the cell cycle and how the ends of a DSB are initially processed determine the choice of the repair pathway (reviewed in [47,48]). In the G1 phase DSBs are protected from end resection which favors recruitment of NHEJ proteins. Once cells enter the S phase, end resection is activated to promote HR. Recently these processes have been shown to implicate two complexes, 53BP1-RIF1 and BRCA1-CtIP, which are both recruited to DSB sites through the actions of the E3 ligases RNF8 and RNF168[117-121]. In fact, 53BP1 is ubiquitinated by RNF168, a modification required for its role in DSB repair[122]. While the exact mechanisms are still unclear, it is widely accepted that BRCA1 is essential for HR repair through its role in end resection and recruitment of BRCA2/PALB2 to repair sites during S and G2. This is supported by the fact the cells deficient for BRCA1 show cytogenetic characteristics of defective HR repair. In contrast, 53BP1 promotes NHEJ in G1 by inhibiting 5' end resection of DSBs. *53bp1*$^{-/-}$ avian DT40 cells are sensitive to ionizing radiation (IR) specifically in G1, which is similar to Ku70 deletion[123]. Originally believed to act independently, it is now known that BRCA1 and 53BP1 compete for the choice of the pathway used to repair a DSB. Following its phosphorylation by ATM, 53BP1 binds and recruits RIF1 to DSB sites. RIF1 then inhibits end resection and Rad51 nucleoprotein filament thereby promoting NHEJ. In S and G2, RIF1 accumulation is inhibited by BRCA1 and its interacting partner CtIP. In fact, depletion of CtIP resulted in RIF1 foci in S/G2. Inhibition of RIF1 activity was dependent on CtIP CDK-phosphorylation leading to end resection. This has led to the "real estate" model where the choice of DSB repair pathway depends on the chromatin occupancy of RIF1 and CtIP (Figure 6A).

1.4.5.2 Interplay between BRCA1, 53BP1 and PARP inhibitors

1.4.5.2.1 Ablation of 53BP1 and/or RIF1 rescue lethality and HR defects induced by loss of BRCA1

Homozygous mice for *Brca1*-null mutation are embryonic lethal due to genomic instability[76]. While deletion of another tumor suppressor, p53, is able to delay the embryonic lethality, it is not capable of inhibiting all of the proliferation defects caused by loss of BRCA1[124]. Interestingly, the embryonic lethality and HR defects seen in *Brca1*-deficient mice can also be rescued through deletion of 53BP1 or RIF1[125-127]. In fact, in $Brca1^{\Delta 11/\Delta 11}$ cells, that contain an in-frame deletion of exon 11 resulting in defective HR repair, loss of 53BP1 was able to reverse the tumor phenotype of these cells. Furthermore, embryonic stem (ES) cells deficient in BRCA1 were able to survive following concomitant deletion of 53BP1. Moreover, RIF1 deletion also was found to inhibit BRCA1 deficiency phenotypes[117-120]. Therefore, loss of 53BP1 and/or RIF1 is "synthetically viable" with deletion of BRCA1. The mechanism behind this synthetic viability involves end resection and DSB repair pathway choice. In BRCA1-deficient cells, the 53BP1-RIF1 complex is not inhibited by BRCA1 in S/G2 therefore leading to a restraint in CtIP end resection activity (Figure 6B). 53BP1-RIF1 is then able to promote NHEJ repair in S/G2 which leads to genomic instability and loss of viability in BRCA1-deficient cells. When 53BP1-RIF1 is also deleted in BRCA1-deficient cells, CtIP is then recruited to DSB sites in S/G2 thereby promoting end resection and HR, which supports genome stability.

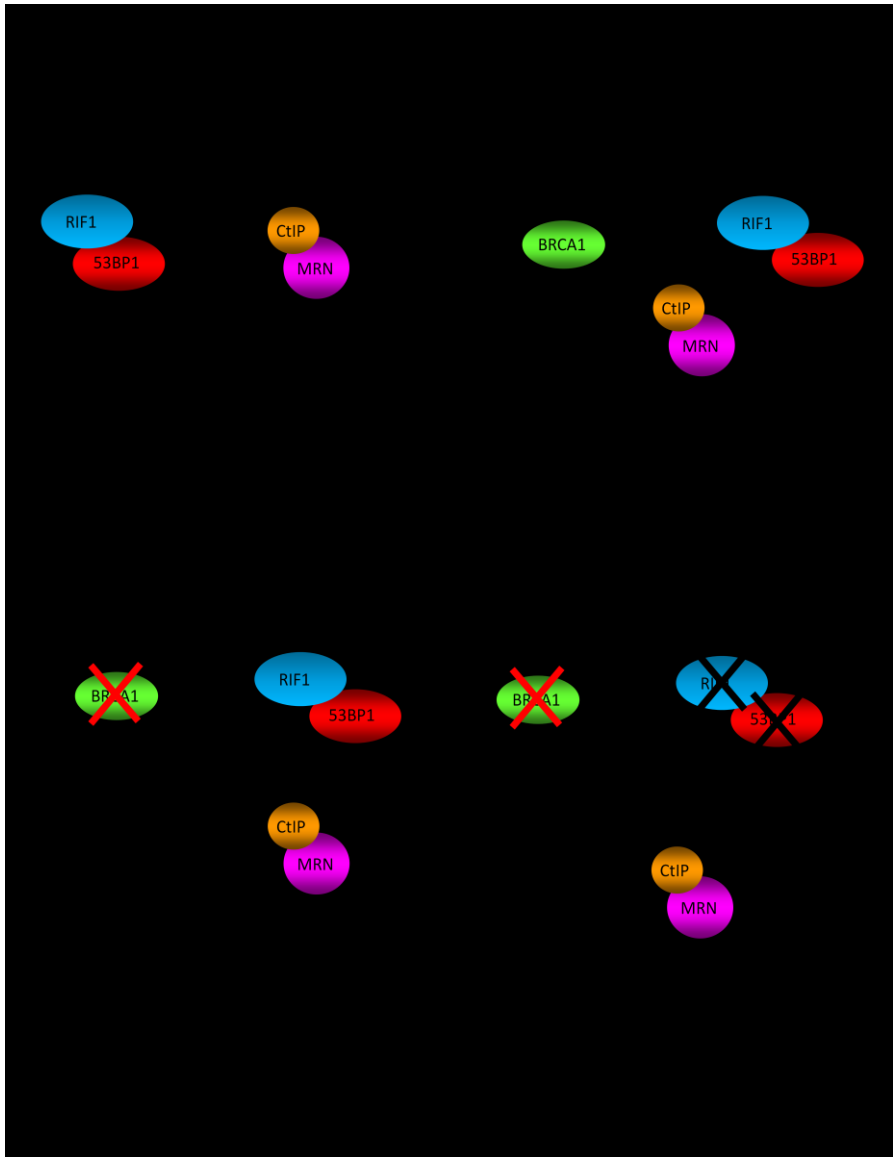

Figure 6. DSB repair pathway choice. A) In G0/G1, 53BP1-RIF1 inhibits end resection by CtIP thereby promoting NHEJ repair of a DSB. In S/G2, BRCA1 counteracts 53BP1-RIF1 activity giving way to CtIP recruitment and DSB end processing promoting HR repair. B) Deletion of 53BP1 or RIF1 can rescue *BRCA1*$^{-/-}$ background from lethality and genomic instability. In S/G2, BRCA1 deletion will promote 53BP1-RIF1 activity and NHEJ which will lead to error-prone repair and genomic instability. However, if 53BP1 and RIF1 are also deleted, end processing by CtIP is still functional allowing for error-free HR repair and genome stability.

1.4.5.2.2 Conditional synthetic lethality between loss of BRCA1 and PARP inhibitors

Studies showing that BRCA1-deficient cells are sensitive to the inhibition of poly (ADP-ribose) polymerase (PARP) were an interesting advance in the treatment of BRCA1-deficient cancers[128,129]. In fact, many potential PARP inhibitors (PARPi), such as Olaparib, have been developed to treat BRCA1-dependent cancers[130]. PARP plays a role in single-strand break repair (SSB) where it is required for processing the break and recruitment of multiple repair factors[131-133]. In the absence of PARP, SSBs accumulate in S phase leading to replication fork collapse and DSBs[134,135]. These DSBs are then repaired through BRCA1-dependent HR which gives way to cell survival. In BRCA1-depleted cells, PARP inhibition causes unrepaired SSBs that cannot be repaired by HR leading to catastrophic failure of replication fork restart and therefore cell death[129,136]. However, this "conditional synthetic lethality" between BRCA1 and PARPi can be prevented by deletion of 53BP1 (Figure 7)[137]. In $BRCA1^{-/-}$ $53BP1^{+/+}$ cells treated with PARPi, NHEJ is the primary pathway to repair the DSBs resulting from SSBs in S phase leading to replication fork collapse. NHEJ being less accurate can lead to genomic instability. In contrast, $BRCA1^{-/-}$ $53BP1^{-/-}$ cells are HR repair proficient and can repair the damage generated by PARPi. Unfortunately, BRCA1-mutant cells can become resistant to PARPi through reversion mutations where BRCA1-depleted cells acquire secondary mutations that restore a partially functional gene[138-142]. Therefore, while PARPi have been approved recently for patient treatment[130], the importance of PARPi in the treatment of BRCA1-deficient cancers still remains uncertain.

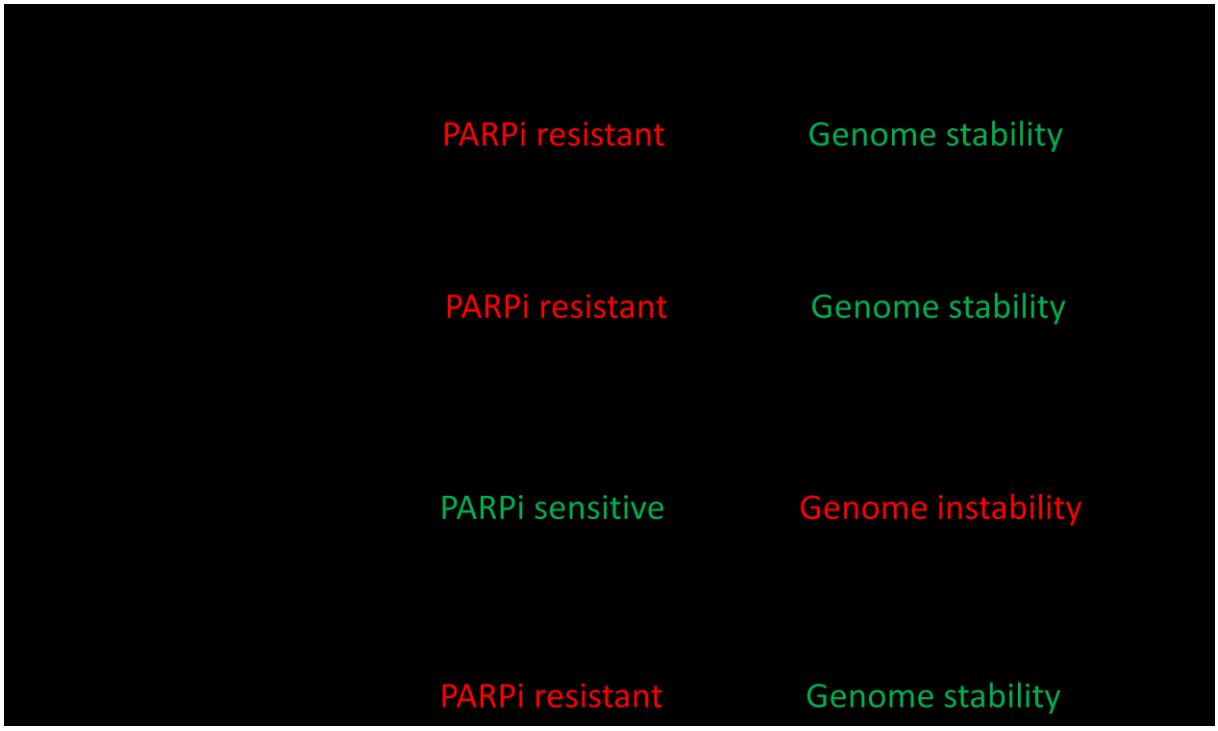

Figure 7. Interplay between BRCA1, 53BP1 and PARP inhibitors. A) In WT cells, both HR and NHEJ are balanced therefore SSBs generated by PARP inhibition are correctly repaired which maintains genome stability. B) In $BRCA1^{+/+}$ $53BP1^{-/-}$ cells, HR is favored which also promotes efficient repair of PARPi-induced SSBs. C) However, in a $BRCA1^{-/-}$ $53BP1^{+/+}$ background, NHEJ becomes the primary repair pathway. SSBs caused by PARPi are therefore repaired by error-prone repair leading to genome instability. D) PARPi sensitivity can be rescued by deleting both BRCA1 and 53BP1, which promotes end resection and HR through still undefined mechanisms.

1.4.6 Role of BRCA1 in the ultraviolet (UV)-damage response

In contrast to the situation for IR, how BRCA1 is regulated in response to genotoxic agents that do not directly induce DSBs is poorly understood. Ultraviolet (UV)-light exposure leads to the formation of DNA bulky adduct helix-distorting lesions such as 6-4 photoproducts and cyclobutane pyrimidine dimers[143]. These lesions are potentially mutagenic when the replication fork is stalled by the unrepaired bulky adducts leading to fork collapse and possibly a cytotoxic DSB. DNA lesions induced by UV are repaired by nucleotide excision repair (NER) which involves the generation of ssDNA gaps filled by DNA polymerases. A recent study showed that *BRCA1*$^{-/-}$ human breast cancer cell lines are UV hypersensitive[144]. In fact, it was suggested that BRCA1 is recruited to sites of UV damage where it plays a role in UV repair through the excision of UV lesions, generation of RPA-coated ssDNA gaps and recruitment of PCNA and DNA polymerase δ. However, as we will discuss in Chapter 2, we found that following UV or MMS exposure, BRCA1 is degraded concomitant with a loss of BRCA1 nuclear foci.

1.5 The BAP1 deubiquitinase

1.5.1 BAP1 interaction with BRCA1 and its role in HR repair

BAP1 was initially found to interact with wild-type (WT), but not with cancer mutations-containing BRCA1, using a yeast two-hybrid screen for BRCA1 RING finger interacting proteins[20]. Disruption of the BAP1 coiled-coil domain inhibited its interaction with BRCA1. Therefore, it was postulated that BAP1 interacts with BRCA1 through its C-terminal domain. In addition, co-expression of BAP1 in MCF7 breast cancer cells, known to exhibit growth suppression with BRCA1 overexpression, increased the capacity of BRCA1 to limit colony growth of these cells. The importance of the BAP1-BRCA1 interaction was initially refuted by a study showing that the deubiquitinase activity of BAP1 had no impact on the function of the BRCA1/BARD1 complex[145]. However, a second study demonstrated that BAP1 can inhibit BRCA1/BARD1 E3 ligase activity[146]. In this paper it was shown in fact that BAP1 interacts mainly with BARD1 and that BRCA1 acts more as an enhancer of the interaction. Moreover, contrary to BRCA1 that was shown to interact with the C-terminus of BAP1, BARD1 interacts with the region (amino acids 182-365) following the N-terminal UCH domain in BAP1. In addition, it was shown by GST-pulldown that BAP1 interferes with the BRCA1/BARD1 heterodimer by binding to BARD1. Since BRCA1 and BARD1 form an active E3 ligase, it was hypothesized that BAP1 interaction with BARD1 could interfere with this activity. In fact, through an *in vitro* ubiquitin ligation assay BAP1 was shown to inhibit the BRCA1/BARD1 ligase activity. BAP1 inhibits BRCA1 ligase activity by binding to BARD1 in a deubiquitinase activity independent manner. Furthermore, BAP1 knockdown led to hypersensitivity to ionizing radiation (IR), suggesting that BAP1 through its interaction with the BRCA1/BARD1 complex regulates ubiquitination following DNA damage.

However, the biological significance of the direct interaction between BAP1 and BRCA1/BARD1 is still not fully understood.

Our lab[147] recently demonstrated a role of BAP1 in HR repair, in which I participated in performing some of the experiments. I mainly contributed in the DUB RNAi screen to identify regulators of HR protein assembly following DNA damage (Figure 8, Fig. 1 in ANNEX 2). In this screen, U2OS cells were transfected with siRNA pools targeting most known DUBs to determine the impact of DUB depletion on BRCA1 and Rad51 foci formation following ionizing radiation. Interestingly, one of the DUBs whose depletion negatively affected foci formation was BAP1, which we further investigated in detail. Knockout (KO) chicken DT40 cells for BAP1 were generated and were more sensitive to IR and other DSB-inducing agents. Also, we identified IR-induced phosphorylation sites in BAP1. I contributed in generating cell lines stably expressing BAP1 mutated for the phosphorylation sites as well as its catalytic site (C91S) (Fig. 5 in ANNEX 2). Both BAP1 DUB activity and phosphorylation were found to be essential in promoting cell recovery from IR-induced DSBs. This data was of major importance since it linked BAP1 function to HR repair providing a possible mechanism for its tumor suppression function. Shortly after our lab published this data, another group supported our findings by showing that BAP1 is phosphorylated by ATM after ionizing radiation treatment and that BAP1 promotes HR repair of DSBs[148]. Moreover, they found that BAP1 is recruited to DSB sites in a RNF8/RNF168-dependent manner and that BAP1 mediates the recruitment of ASXL1 to DNA damage sites.

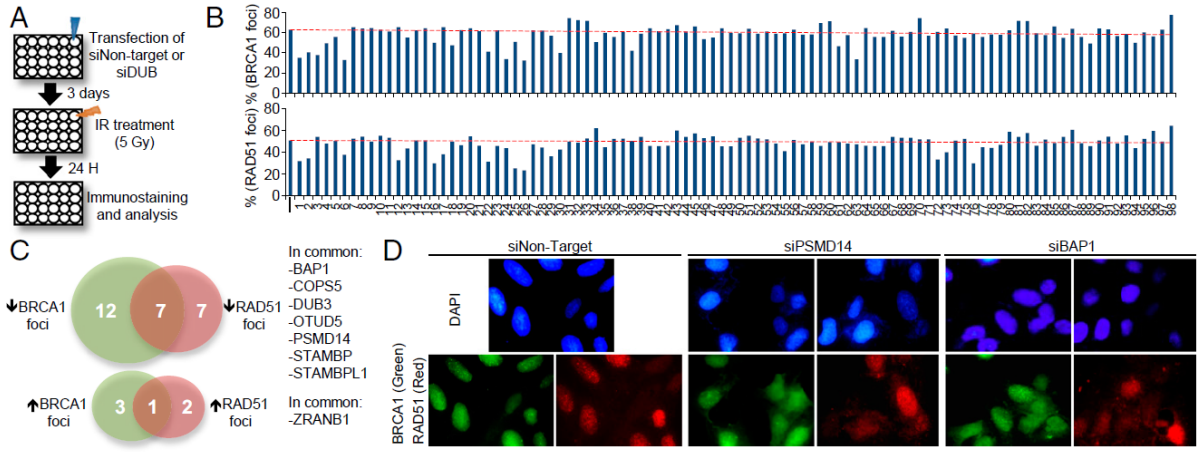

Figure 8. DUB screen identifies novel regulators of HR protein assembly at IRIF. A) Schematic representation of DUB loss-of-function screen for IRIF regulators. U2OS cells were transfected with individual siRNA pool targeting DUBs, exposed to IR and collected for staining. B) Graphs represent the percentage of cells with more than 10 foci of BRCA1 or RAD51. Dashed red line shows the percentage of cells with protein foci for the control sample. C) Venn diagrams showing DUBs associated with reduced or increased percentage of cells with foci. DUBs having the same phenotype with both BRCA1 and RAD51 foci are indicated. D) Representative staining of BRCA1 and RAD51 foci in PSMD14- and BAP1-depleted cells.[147] (taken from reference 147)

1.5.2 Overview of the BAP1 protein

Human BAP1 is a 729 amino acid residue nuclear protein that contains an N-terminal catalytic domain (UCH) responsible for its deubiquitinase activity. The importance of its enzymatic activity is highlighted by the fact that cancer-associated mutations found in the UCH domain were shown to inhibit BAP1-mediated deubiquitination. BAP1 also harbors a protein binding motif (HBM, residues 363-366) required for its interaction with the transcription regulator host cell factor-1 (HCF-1). Mutation of the HBM does not impact BAP1 enzymatic activity. The BAP1 C-terminal domain (CTD) contains a coiled-coil motif that we found to be important for BAP1 interaction with the polycomb group proteins ASXL1 and ASXL2.

1.5.3 BAP1 and tumor suppression

After its initial discovery in 1998[20], it took nearly ten years before more substantial research surfaced on the function of BAP1. While early evidence pointed to BAP1 acting as a tumor suppressor, *in vivo* data supporting this was still missing. Ventii et al. investigated the *in vivo* growth suppressive function of BAP1[149,150]. First, they demonstrated that previously identified mutations in the BAP1 UCH domain found in lung cancers[151] (e.g., A95D and G178V) as well as the catalytic cystein mutant C91A, were unable to deubiquitinate Ub-AMC as opposed to the WT BAP1. This result suggested that BAP1 DUB activity could be required for its tumor suppressor function. In addition, a homozygous 8-bp deletion in BAP1 resulting in a truncated protein at residue 393 found in the non-small cell lung carcinoma cell line NCI-H1466[20] was shown to disrupt BAP1 nuclear localization suggesting that loss of BAP1 function in the nucleus could also be an important determinant for cancer pathogenesis. To

confirm the requirement of BAP1 DUB activity and nuclear localization for tumor suppression *in vivo*, NCI-H226[20] cells, another non-small lung carcinoma cell line harboring a deletion in the BAP1 gene leading to a truncated protein that lost the nuclear localization signal, was used in xenograft studies. These cells expressing the WT or mutant BAP1 were injected into nude mice which were analyzed for tumor formation. The WT BAP1 was capable of inhibiting the tumorigenicity of the H226 cells, whereas mutants lacking either DUB activity (C91A) or nuclear localization still formed tumors in nude mice. Moreover, it was shown that expression of the WT BAP1 caused significant alterations in the cell cycle of H226 cells, leading to cell death by both apoptosis and necrosis. This was the first study clearly linking BAP1 DUB activity and its nuclear localization to its growth suppressive function *in vivo* and provided evidence supporting the notion that BAP1 is a tumor suppressor.

1.5.4 The BAP1 multi-protein complex

Our lab[152] and another group[153] have identified, using affinity purification and mass spectrometry, proteins that interact with BAP1. While the data from both groups are similar, I will focus on the results from our lab. We initially used glycerol density gradient fractionation of nuclear extracts and found that BAP1 assembles into high-molecular-weight multiprotein complexes. Therefore, we generated stable cell lines expressing Flag-HA-BAP1 and purified BAP1 through double immunopurification to identify interacting partners (Figure 9, Fig. 1. in ANNEX 1). Many proteins were found in the BAP1 protein complex including the transcriptional regulator host cell factor-1 (HCF-1), the polycomb group proteins additional sex combs-like 1 and 2 (ASXL1 and ASXL2) and the transcription factor YY1. Also found

interacting with BAP1 are the E2 enzyme UBE2O, the O-linked *N*-acetylglucosamine transferase (OGT), the forkhead transcription factors FOXK1 and FOXK2, the ETS-related transcription factors ELF-1 and ELF-2 and the histone H3K4 demethylase KDM1B. Interestingly, we found that BAP1 enzymatic activity is not required for the assembly of BAP1 complexes. Of note, we did not find BRCA1 in our BAP1 complex, but did find BARD1, the major interacting partner of BRCA1, which is relevant for the role of BAP1 in homologous recombination repair.

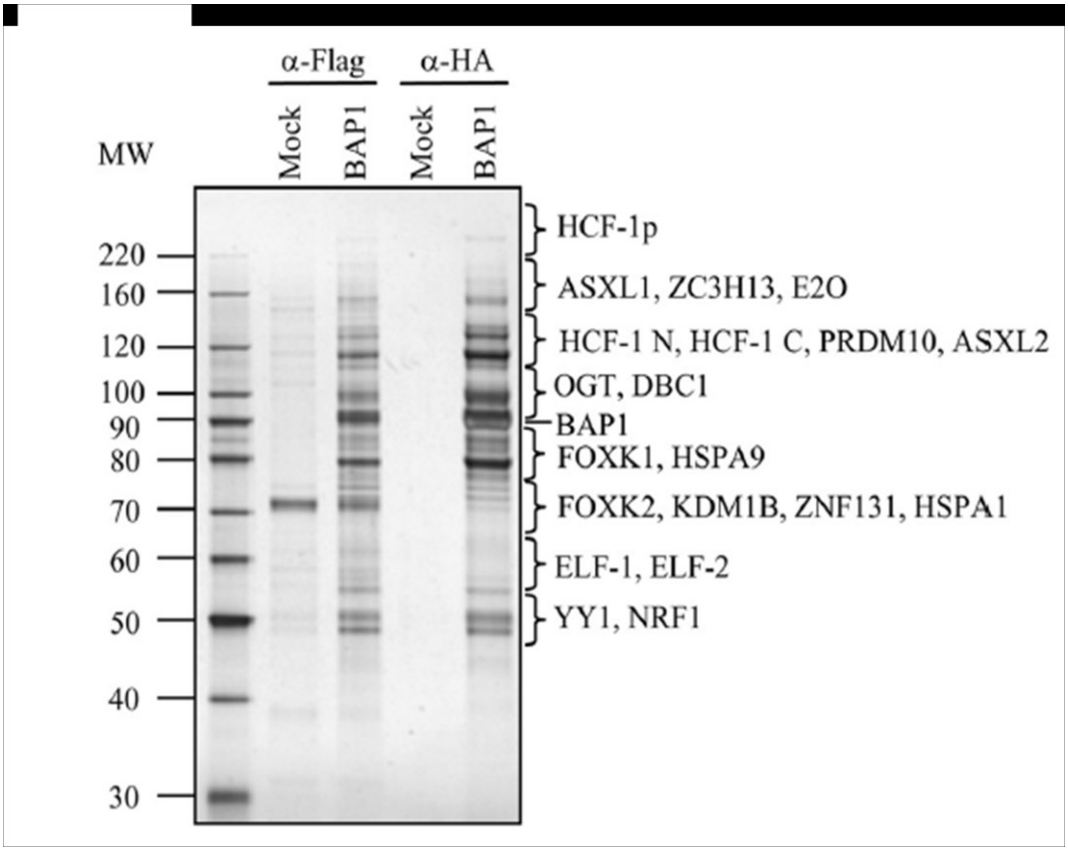

Figure 9. Purification of the BAP1 protein complex. Purification of BAP1-associated proteins. A HeLa cell line stably expressing Flag-Ha-BAP1 was used for sequential double immunopurification using anti-Flag antibody and anti-HA antibody columns. The Flag- or HA-eluted proteins were separated by SDS-PAGE and detected by silver staining. The mock purification was conducted using a stable cell line generated with the empty vector. Several regions were cut from the gel, and the polypeptides were identified by mass spectrometry. MW, molecular weight (in thousands) [152] (taken from reference 152)

1.5.4.1 BAP1 interaction with HCF-1

HCF-1 is a transcriptional regulator originally found to activate viral gene expression during herpes simplex virus infection[154-156]. HCF-1 interacts with diverse transcription factors suggesting that HCF-1 regulates the expression of a variety of genes[157]. HCF-1 can act as either an activator or repressor, as this chromatin-associated protein was shown to regulate cell cycle progression via interaction with E2F4 or E2F1, which can respectively repress or activate E2F target genes[158]. Interestingly, HCF-1 is synthesized as a precursor that undergoes proteolytic cleavage in its middle region referred to as the proteolytic processing domain (PPD) [159,160]. This cleavage results in the generation of two fragments: the HCF-1_N subunit required for proper G1/S transition during the cell cycle and the HCF-1_C subunit required for progression through mitosis[161].

A series of research articles provided insights into the significance of the interaction between BAP1 and HCF-1 (reviewed in [162]). The first study[163] identified HCF-1 as a BAP1-interacting partner through immunoprecipitation of Flag-epitope tagged BAP1, in which BAP1 and its associated proteins were visualized by silver stain and identified by mass spectrometry (MS). This interaction was confirmed by other approaches, and was found to occur in the nucleus where both proteins are known to localize. However, they did not show immunopurification or MS data for other BAP1-associated proteins and specified that BRCA1, which was originally identified as interacting with BAP1, was not detected in the Flag-BAP1 immunoprecipitation. Moreover, BAP1 interacts with the β-propeller domain in the HCF-1_N subunit independently of its DUB activity. Of note, the β-propeller domain of HCF-1 mediates many protein interactions, including its association with the viral coactivator

VP16, through a consensus D/EHXY motif[164-166]. However, BAP1 does not have this motif, but contains the sequence Asn-His-Asn-Tyr (NHNY, amino acids 363 to 366) which is fully conserved among other vertebrate BAP1 proteins. In fact, it was shown, using a mutant Flag-BAP1 in which the four residues were substituted with alanine, that BAP1 interacts with HCF-1 through this motif. Thereafter, this tetrapeptide sequence of BAP1 was referred to as the HCF-1 binding motif (HBM). Of note, the BAP1 NHNY/AAAA mutant was still enzymatically active. Furthermore, HCF-1 was shown to be ubiquitinated by both K48- and K63-linkage, with BAP1 selectively removing K48-linked Ub from HCF-1 suggesting that BAP1 might positively control HCF-1 protein levels. However, cells depleted of BAP1 by siRNA showed a slight increase in HCF-1 levels. This would seem counterintuitive considering that depleting BAP1 is predicted to lead to more K48-linked Ub on HCF-1 which would promote its proteasomal degradation. Moreover, since HCF-1 is known to play an important role in cell cycle progression, the effect of BAP1 knockdown on the cell cycle was also studied. In fact, BAP1 depletion induced increase in the percentage of cells in S and G_2/M phases, with a concomitant decrease of the percentage of cells in G1. These results led to hypothesize that BAP1 is recruited, via its interaction with HCF-1, to gene regulatory regions to regulate the transcription of genes involved in cell cycle control, a mechanism possibly linked to BAP1 tumor suppressor function.

A second very similar article was published shortly after, in which the interaction between BAP1 and HCF-1 and its implication in cell growth was investigated[153]. In fact, BAP1 depletion was found to promote growth retardation. Moreover, through overexpression experiments using WT or catalytic dead BAP1 (C91S), it was determined that BAP1 DUB

activity is required for proper cell proliferation. They also found that the NHNY sequence (HBM) in BAP1 is required for intercation with HCF-1. They also showed that the HCF-1_N is ubiquitinated *in vivo* on the Kelch domain and determined that K48 is the major form of polyubiquitin chain linkage on HCF-1. Moreover, BAP1 WT, but not the C91S mutant, was capable of deubiquitinating HCF-1 *in vivo*. In addition, BAP1 ΔHBM, which no longer interacts with HCF-1, was unable to deubiquitinate HCF-1. A weakness of this study is the fact that the authors almost completely disregarded the role of the HCF-1_C subunit in the interaction with BAP1 and the possibility that it is also ubiquitinated like the HCF-1_N subunit. Furthermore, all their experiments were performed by protein overexpression, therefore data with endogenous proteins was lacking. Nonetheless, taking into account the results of both studies[153,163], it was now clear that BAP1 interacts with HCF-1, which appears to be important for the growth suppressive function of BAP1. However, the exact mechanism of action of BAP1 as a tumor suppressor and how it relates to HCF-1 remained poorly understood.

1.5.4.2 BAP1 forms a ternary complex with YY1 and HCF-1 and regulates transcription

I contributed to a study showing that BAP1, through interaction with HCF-1 and the transcription factor Yin Yang 1 (YY1), mediates control of gene expression[152]. YY1, similar to HCF-1, can act as either an activator or repressor of gene expression depending on its interactions with different coactivators and corepressors at specific promoters[167,168]. Using nuclear extracts, we determined through immunodepletion experiments using an excess of a specific antibody that all cellular BAP1 is complexed to HCF-1, suggesting that HCF-1 acts as the major scaffold protein for BAP1. Furthermore, we showed that endogenous BAP1 interacts with HCF-1 and YY1. We then mapped the domains required for YY1 interaction

with BAP1 and HCF-1 through GST-pulldown experiments. BAP1 interacts with YY1 through its C-terminal coiled-coil (CC) domain, a motif commonly found in proteins involved in gene expression. This indicates that BAP1 can simultaneously interact with HCF-1, through the HBM motif, and with YY1. Moreover, we showed that HCF-1 can directly interact with the central region (amino acids 142 to 260) of YY1 that contains a GA/GK-rich domain[169], whereas BAP1 binds the C-terminal zinc finger domain (amino acids 331 to 414) of YY1. Interestingly, BAP1 ΔHBM interacted much less with YY1 when compared to BAP1 WT. This result was confirmed by depleting HCF-1, using a shRNA approach, which led to a major decrease in BAP1 interaction with YY1. These results taken altogether suggest a model in which BAP1, HCF-1 and YY1 form a ternary complex using binary binding of each protein (Figure 10, Fig. 8 in ANNEX 1).

We then focused on the biological importance of this ternary complex. We found that BAP1 is associated with transcriptionally active genomic regions with HCF-1 and YY1. Furthermore, in a luciferase reporter assay, Gal4-BAP1 WT activated transcription, while Gal4-BAP1 ΔHBM and Gal4-BAP1 C91S had respectively less or no transcriptional activity, suggesting that BAP1 DUB activity is required for its role in transcription. We identified up- and down-regulated genes by global mRNA expression profiling using microarrays following shRNA depletion of BAP1 in U2OS cells. BAP1 depletion led to significant increase or decrease in the expression of approximately 250 genes involved in many cellular processes including cell cycle control, DNA repair and cell metabolism. Importantly, the expression of many E2F target genes, such as *cdc6*, *p107* and *cdc25a*, was decreased following BAP1 depletion. Finally, we analyzed the *cox7c* gene, highly downregulated in the microarray data,

as a possible model target gene of BAP1. Using ChIP assays, it was determined that BAP1, HCF-1 and YY1 are enriched on the *cox7c* promoter (Figure 10, Fig. 8 in ANNEX 1). YY1 depletion by shRNA abrogated the enrichment of BAP1 and HCF-1, suggesting a critical role for YY1 in BAP1 and HCF-1 recruitment to promoter regions. In fact, the bovine *cox7c* promoter had previously been shown to have two YY1 binding sites, conserved in mammalians, that when mutated inhibited promoter activity[170]. In addition, BAP1 regulation of *cox7c* expression was dependent on its DUB activity, since BAP1 C91S overexpression inhibited *cox7c* expression. In summary, we showed that BAP1 interacts with HCF-1 and YY1 to function as a regulator of gene transcription. In addition, our results supported previous studies showing that BAP1 was required for proper cell cycle progression, notably during the G1/S transition[163]. Indeed, BAP1 depletion affected the expression of many genes involved in cell cycle regulation, which would be important for its role as a tumor suppressor.

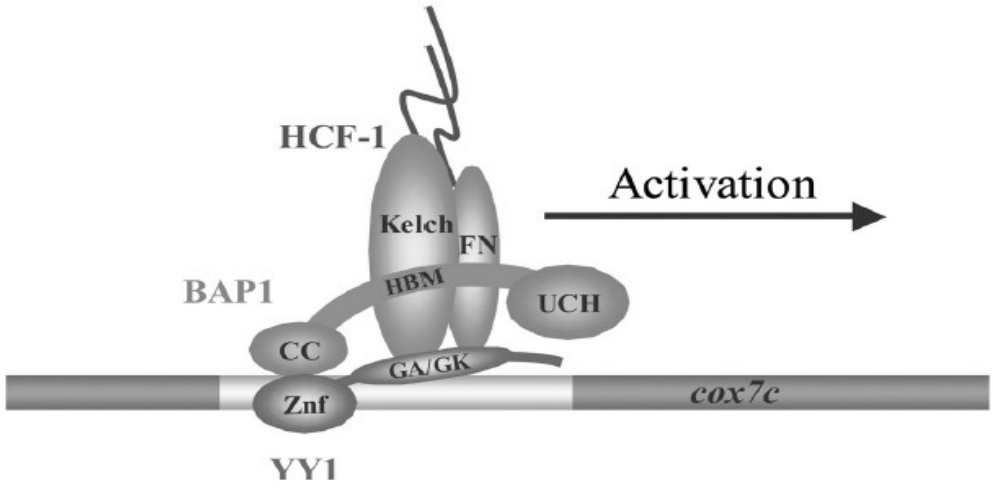

Figure 10. YY1 recruits BAP1 and HCF-1 to coactivate *cox7c* expression. BAP1 interacts with YY1 through its coiled-coil (CC) domain while also interacting with HCF-1 through the HBM motif. Both BAP1 and HCF-1 are recruited to the *cox7c* gene promoter by YY1. HCF-1 directly interacts with the central region of YY1 containing a GA/GK-rich domain, while BAP1 binds to the C-terminal zinc finger (Znf) domain. BAP1, HCF-1 and YY1 form a ternary complex required for the activation of the *cox7c* gene.[152] (taken from reference 152)

1.5.4.3 BAP1 interaction with ASXL1 and ASXL2

1.5.4.3.1 Polycomb repressive deubiquitinase (PR-DUB) complex

Drosophila additional sex combs (ASX) was initially shown to enhance the functions of both Polycomb group (PcG) and Trithorax group (trxG) proteins in the coordination of proper Hox gene expression patterns[171]. *Asx* deletion leads to a homeotic phenotype with characteristics of both PcG and Trithorax deletions, suggesting that ASX acts as a dual activator and repressor of Hox genes[172]. *Drosophila* ASX was found to interact *in vivo* with Calypso, whose mammalian ortholog is BAP1. Calypso interacted with N-terminal 337 amino acids of ASX. Interestingly, BAP1 also interacted with the N-terminal (amino acids 2-365) of ASXL1, the human homologue (with ASXL2) of *Drosophila* ASX. Furthermore, a catalytic inactive mutant of Calypso also interacted with ASX, suggesting that this interaction does not depend on DUB activity. The Calypso-ASX heterodimer was termed the Polycomb repressive deubiquitinase (PR-DUB) complex. Using an Ub-AMC substrate, the authors showed that the interaction between Calypso and ASX is required for DUB activity. Furthermore, both the *Drosophila* and human PR-DUB complexes were shown to deubiquitinate monoubiquitinated histone H2A but not histone H2B in the *in vitro* context of nucleosomes. As mentioned in the introduction, monoubiquitination of H2A is required for PcG gene repression. Therefore, it would be counterintuitive that the PR-DUB complex, by removing ubiquitin from histone H2A, would be required for gene repression. However, PR-DUB was in fact shown to be necessary for repression of the PcG target gene *Ubx* in *Drosophila*. This was the first study to characterize the interaction between BAP1 and ASXL1. We decided to further elucidate the link between BAP1 and both PcG proteins ASXL1 and ASXL2, and the importance of this interaction in humans through an extensive biochemical study discussed in Chapter 3.

1.5.4.3.2 Opposing roles of ASXL1 and ASXL2 in transcription

ASXL1 and ASXL2 are suggested to play opposing roles in transcription[173]. Studies on the peroxisome proliferator-activated receptor γ (PPARγ), a ligand-dependent transcription factor that functions mainly in adipogenesis, showed that ASXL1 and ASXL2 control adipogenesis through regulation of PPARγ activity[174]. In fact, both ASXL1 and ASXL2 were shown to interact *in vitro* and *in vivo* with PPARγ. Furthermore, PPARγ regulates the expression of genes with promoters containing a PPARγ-response element, such as the adipocyte lipid-binding 2 (*aP*2) gene. Through ChIP experiments, ASXL1 was shown to be recruited to the *aP2* promoter with the repressive histone mark H3K9me3, whereas ASXL2 occupied the same promoter with the active histone marks H3K9ac and H3K4me3 as well as the MLL1 methytransferase. Moreover, microarray analysis showed that ASXL1 and ASXL2 differentially regulated the expression of adipogenic genes, further suggesting that both PcG proteins play opposing roles in transcription regulation. In addition, another study showed that ASXL1 and ASXL2 regulate lipid homeostasis through differential Liver X receptor alpha (LXRα)-dependent gene expression[175]. The opposing functions in transcription of ASXL1 and ASXL2 are very interesting since, as we will see in Chapter 3, BAP1 forms two mutually exclusive complexes with ASXL1 and ASXL2, which could potentially explain that BAP1 has been suggested to act as both an activator and repressor of gene expression.

1.5.4.3.3 ASXL1 and ASXL2 cancer mutations

ASXL1 mutations, as is the case with BAP1 mutations, have been linked to myeloid transformation[176,177]. In fact, ASXL1 is mutated in approximately 20% of patients with myelodysplastic syndrome and in 10-15% of patients with AML[178]. Earlier studies[179]

using ASXL1 KO mice showed that it is required for hematopoiesis. A second study more extensively described the role of ASXL1 in myeloid transformation[176]. They showed that most AXSL1 mutations were somatic nonsense and insertion/deletion mutations found near the C-terminal PHD domain leading to a loss of ASXL1 expression and upregulation of *HOXA* gene expression. Interestingly, they also showed that ASXL1 interacts with BAP1 in leukemia cells, but that knockdown of BAP1 had no impact on *HOXA* gene expression, which led the authors to suggest that ASXL1 promotes myeloid transformation in a BAP1-independent manner. Furthermore, this group did not find any BAP1 mutations in patients with AML, while BAP1 has been linked to hematopoietic cancers[180]. Since ASXL1 is a PcG protein, they then decided to look at how ASXL1 mutations affect known PcG-associated histone modifications. They found that loss of ASXL1 was concomitant with a global loss of the repressive H3K27me3 mark. Furthermore, through ChIP-seq analysis, it was shown that genes overexpressed following ASXL1 knockdown contained bivalent activating H3K4me3 and repressive H3K27me3 histone marks. This is interesting, since as we will discuss in Chapter 3, ASXL1 and ASXL2 engage mutually exclusive interactions with BAP1 and might play an important role in coordinating the expression of BAP1-target genes.

Until recently not much was known about the extent of ASXL2 mutations found in human cancers[177], however a study on t(8;21) translocated RUNX1 gene in acute myeloid leukemia (AML) identified somatic mutations in ASXL2[181]. Most of these mutations were frameshift mutations occurring in an uncharacterized region of the gene. In addition, mutations in ASXL1 associated to myelodysplastic syndromes were also found in this study. Interestingly, ASXL2 mutations were mutually exclusive with ASXL1 mutations in AML.

1.5.5 Link between BAP1 mutations and cancer

Since the initial study highlighting its role as a tumor suppressor[149], important findings have linked BAP1 somatic and germline mutations to various human malignancies (reviewed in[182]). I will briefly discuss some of these findings.

1.5.5.1 BAP1 mutations and uveal melanoma

One of the first studies focused on BAP1 mutations in metastasizing uveal melanomas (UM)[183]. UM is the most frequent cancer of the eye with a strong tendency for metastasis that is often fatal[184]. Through parallel exome sequencing coupled to Sanger resequencing, it was found that BAP1 is mutated in UM, which included mutations leading to premature protein termination, missense mutations and in-frame deletions that were found in different domains of BAP1. Furthermore, while most mutations were somatic in origin, one germline BAP1 mutation was found when comparing the tumor to normal DNA from the patient. These results were the first to strongly suggest that BAP1 mutational inactivation is required for metastasis and that the BAP1 pathway could be a therapeutic target for UM cancer treatment.

1.5.5.2 BAP1 mutations and mesothelioma

Two studies reported BAP1 inactivating mutations in malignant mesotheliomas. These aggressive tumors are associated with the use of asbestos and cause approximately 3000 deaths annually in the USA[185]. The first group[186] used an integrated genomics approach to find genomic copy number alterations (CNAs) in malignant pleural mesotheliomas (MPMs). The three most common deletions were at chromosome positions 9p21, 22q and 3p21. The first two have been previously linked to genetic alterations in CDKN2A and NF2. BAP1

which is located at 3p21.1 was found to be either mutated of lost in 42% of the MPM tumors tested. BAP1 mutations included nonsense, missense and frameshift mutations, with the majority being somatic in nature. Purification of Flag-tagged BAP1 mutant proteins with missense mutations and then tested in an *in vitro* DUB assay showed that these mutants had decreased enzymatic activity compared to BAP1 WT. In addition, the interaction between BAP1 and ASXL1 in MPM was also studied. It was confirmed that BAP1 and ASXL1 do indeed interact *in vivo*, but several BAP1 point mutations tested did not affect this interaction and the domains required for BAP1-ASXL1 binding were not determined.

Shortly after, a second group[187] published their results focusing on germline BAP1 mutations that predispose to malignant mesothelioma. They studied two families with a higher than expected incidence of mesothelioma. Using array-comparative genomic hybridization (CGH) analysis, they found genetic alterations of the BAP1 locus at 3p21.1 in tumors from both families. This led them to sequence BAP1 in germline DNA from both families. In the first family, it was found that six members (four with mesothelioma, one with breast cancer and one with renal cancer) had the identical BAP1 mutation at the intron 6/exon 7 boundary resulting in a frameshift leading to a premature stop codon. As for the second family, sequencing of germline DNA from three members with mesothelioma (including one also treated for uveal melanoma) and two affected by skin carcinomas showed C/G to T/A transition in exon 16 of BAP1 leading to a premature stop codon. Interestingly, significant amounts of tremolite and chrysotile asbestos were found in all the homes where affected members of both families had lived. However, 30 million US homes are built using asbestos and living in this type of houses is associated with only a small level of exposure[185]. Therefore

genetic mutations in BAP1 might explain the high predisposition to develop mesothelioma in both families. Also, DNA from 26 patients with sporadic mesothelioma that had reported to have been exposed to asbestos was also sequenced for germline BAP1 mutations. Two patients that had been treated for uveal melanoma before been diagnosed with mesothelioma had germline BAP1 deletions. The importance of this study was linking BAP1 germline mutations to both uveal melanomas and mesotheliomas. Furthermore, since the incidence of both cancers is approximately 5-7/100,000 in the US[188], the likelihood that both cancers arise in the same person by chance would be extremely rare. This suggests that a person diagnosed with uveal melanoma harboring a germline mutation in BAP1 would have a high predisposition to develop mesothelioma, which proposes the presence of a hereditary BAP1 mutations-associated cancer syndrome.

Following these studies on BAP1 mutations in mesothelioma, a group decided to generate a *BAP1*$^{+/-}$ mouse model, since homozygous deletion of BAP1 is embryonically lethal[180], to further study the predisposition to cancer following asbestos exposure[189]. In fact, *BAP1*$^{+/-}$ mice had a higher incidence of mesothelioma (73%) after chronic exposure to crocidolite asbestos fibers compared to the WT littermates (32%). Furthermore, *BAP1*$^{+/-}$ mesothelioma cancer mouse cells showed biallelic inactivation of *BAP1*, which is consistent with loss of heterozygosity. Moreover, protein levels of the tumor suppressor Retinoblastoma (Rb) were decreased in malignant mesothelioma cells from *BAP1*$^{+/-}$ mice, suggesting that loss of Rb might contribute to increased incidence of asbestos-related cancer in *BAP1*$^{+/-}$ mice. This is very interesting since Rb binds and inhibits transcription factors of the E2F family, which are found on the promoters of genes involved in cell cyle progression[190]. In addition, as

already mentioned, our lab showed that the expression of many E2F target genes, such as *cdc6*, *p107* and *cdc25a*, was decreased following BAP1 depletion[152]. More studies are required to fully elucidate the link between BAP1 and Rb/E2F in transcription regulation.

1.5.5.3 BAP1 and myeloid transformation

More recently BAP1 was shown to play a role in hematopoiesis[180]. Dey et al. reported that *Bap1*$^{-/-}$ mice embryos die at E9.5. However, when they restricted BAP1 loss using a tamoxifen-inducible system to hematopoietic cells, the mice were viable but displayed characteristics of human myelodysplastic syndrome (MDS). In fact, the mice developed splenomegaly due to expansion of the myeloid lineage. Blood from these mice showed cytological features of myelodysplasia and had elevated leukocytes as seen in human chronic myelomonocytic leukemia (CMML)-like disease. They then investigated the mechanism behind BAP1 tumor suppression by affinity-purifying Flag-tagged BAP1 from mouse spleen and brain to identify BAP1-interacting proteins. They found as already shown in a paper from our lab[152] that BAP1 interacts with HCF-1, OGT, ASXL1 and ASXL2, FOXK1 and KDM1B. Interestingly, in contrast to our data using shRNA and siRNA knockdown of BAP1, HCF-1 levels were decreased in BAP1 KO splenocytes. Furthermore, OGT and global O-GlcNAcylation levels were also decreased. The authors then show that OGT is a substrate for the DUB activity of BAP1. They then investigated BAP1 regulated genes through ChIP-seq studies on promoter occupancy of HCF-1, OGT and BAP1 in bone marrow-derived macrophages. They found that most promoters with BAP1 are also occupied by HCF-1, which is not surprising since our lab showed that all of BAP1 is in complex with HCF-1[152]. In addition, OGT, while not on as many promoters, is found mostly with BAP1 and HCF-1.

However, the authors did not discuss in details the different BAP1 target genes found through their ChIP-seq experiment. More importantly, they found a MDS patient containing a somatic frameshift mutations leading to premature termination within the UCH domain of BAP1. This patient showed similar characteristics as in the BAP1 KO mice. This was the first study to link the tumor suppressor function of BAP1 to the development of hematopoietic cancer.

1.6 General objective of the thesis

The main objective of the thesis was to further elucidate the cellular functions and regulation of BRCA1 and BAP1, an ubiquitin ligase and a deubiquitinase that act as tumor suppressors. While each of the two parts of the thesis are not directly linked, they shed new light on how BAP1 and BRCA1, both involved in HR repair, act to promote genomic stability and prevent cancer progression.

1.6.1 Objective 1

The function of BRCA1 in response to IR leading to DSBs requiring HR repair as described earlier has been extensively characterized. However, how BRCA1 functions in response to genotoxic stress that does not directly cause DSBs is poorly understood. Because of the fundamental and clinical importance of understanding BRCA1 function, we sought to rigorously evaluate the role of this tumor suppressor in response to diverse forms of genotoxic stress. Experiments done to answer this question led to the publication of an article entitled "PI 3 Kinase Related Kinases-Independent Proteolysis of BRCA1 Regulates Rad51 Recruitment during Genotoxic Stress in Human Cells" published in PLoS One in 2010, in which I am the first author.

1.6.2 Objective 2

While over the last few years many research articles highlighting the importance of BAP1 in cancer development, few have elucidated the cellular mechanisms by which BAP1 acts as a tumor suppressor. Since our lab and other groups found that BAP1 interacts with polycomb group proteins ASXL1 and ASXL2, we sought to further study the role of the

BAP1/ASXL1/ASXL2 relationship during tumor progression. Research performed to elucidate the importance of their interaction led to the production of a complete manuscript (not yet published) entitled “Deubiquitination of Histone H2A by the BAP1/ASXL Axis is Disrupted by Multiple Cancer-Associated Mechanisms” in which I am a first co-author.

Chapter 2: PI 3 Kinase Related Kinases-Independent Proteolysis of BRCA1 Regulates Rad51 Recruitment during Genotoxic Stress in Human Cells

Ian Hammond-Martel[1], Helen Pak[1], Helen Yu[1], Raphael Rouget[1], Andrew A. Horwitz[2,3], Jeffrey D. Parvin[2,4], Elliot A. Drobetsky[1] and El Bachir Affar[1,5]

[1]Maisonneuve-Rosemont Hospital Research Center, Department of Medicine, University of Montréal, Montréal H1T 2M4, Québec, Canada

[2]Department of Pathology, Harvard Medical School and Brigham and Women's Hospital, Boston, MA, USA

[3]Current address: University of California San Francisco, San Francisco, CA, USA

[4]Current address: The Ohio State University Department of Biomedical Informatics, OSU Comprehensive Cancer Center, Columbus, OH 43210, USA

[5]Correspondence: Fax (514)-252-3430

Short Title: Regulation of BRCA1/BARD1 stability

Key words: DNA damage, BRCA1, BARD1, BACH1, Rad51, proteasome, ubiquitin

Abstract

Background: The function of BRCA1 in response to ionizing radiation, which directly generates DNA double strand breaks (DSBs), has been extensively characterized. However several previous investigations have produced conflicting data on mutagens that initially induce other classes of DNA adducts, e.g., bulky lesions and alkylated bases. Because of the fundamental and clinical importance of understanding BRCA1 function, we sought to rigorously evaluate the role of this tumor suppressor in response to diverse forms of genotoxic stress.

Methodology/Principal Findings: We investigated BRCA1 stability and localization in various human cells treated with model mutagens that trigger different DNA damage signaling pathways. We firmly established that, unlike ionizing radiation, either UVC or methylmethanesulfonate (generating bulky DNA adducts or alkylated bases respectively) induces a transient downregulation of BRCA1 protein. We also further reveal novel aspects pertaining to the mechanism underlying this event. BRCA1 downregulation is, unexpectedly, neither prevented nor enhanced by inhibition of preeminent DNA damage-induced activators of BRCA1 function including ATM, ATR and DNA-PK. Moreover, we find that the proteasome mediates early degradation of BRCA1, BARD1, BACH1, and Rad52 implying that critical components of the homologous recombination machinery need to be functionally abrogated as part of the early response to UV or methylmethanesulfonate. In support of this, following methylmethanesulfonate exposure, the BRCA1-interacting protein Abraxas is also downregulated, albeit by a different mechanism. Significantly, we found that inhibition of BRCA1/BARD1 downregulation is accompanied by the unscheduled recruitment of both proteins to chromatin along with Rad51. Consistently, treatment of cells with

methylmethanesulfonate engendered complete disassembly of Rad51 from pre-formed ionizing radiation-induced foci concomitantly with BRCA1/BARD1 downregulation. Following the initial phase of BRCA1/BARD1 downregulation, we found that the recovery of these proteins in foci coincides with the formation of RPA and Rad51 foci. This indicates that homologous recombination is reactivated at the later stage of the cellular response to MMS, most likely to repair DSBs generated by replication blocks.

Conclusion/Significance: Taken together our results demonstrate that (i) the stabilities of BRCA1/BARD1 complexes are regulated in a mutagen-specific manner, and (ii) indicate the existence of mechanisms which may be required to prevent the simultaneous recruitment of conflicting signaling pathways to sites of DNA damage.

Introduction

Germline mutations in BRCA1 cause extremely high predisposition to breast and ovarian cancers. BRCA1 is a large protein with a well-established modular structure. It contains two BRCT domains at the C-terminus, i.e., phospho-peptide binding modules also carried by several proteins involved in the DNA damage response. The N-terminus of BRCA1 is characterized by the presence of a ring finger domain conferring ubiquitin ligase activity via stable complex formation with another ring finger protein, BRCA1-associated RING domain 1 (BARD1). Although the precise role(s) of BRCA1/BARD1 in tumor suppression have not been fully established, ample evidence indicates that this heterodimer is required to maintain genomic stability following DNA damage (see reviews [1,2]). During periods of genotoxic stress BRCA1 is rapidly phosphorylated and thus activated by the primary responders Ataxia-Telangiectasia-Mutated kinase (ATM) or ATM- and Rad3-Related kinase (ATR), which in turn promotes cellular recovery through induction of DNA damage checkpoints [3-7]. Moreover, recent studies indicate that BRCA1/BARD1 selectively associates with several components of the DNA damage response forming mutually exclusive complexes. Indeed, through the BRCT domain, BRCA1/BARD1 interacts with either Abraxas, BACH1, or CtIP, along with other distinct cofactors, to form multiprotein complexes termed A, B, and C, respectively. These complexes play important roles in the DNA damage response by exerting specific although overlapping functions in cell cycle arrest and DNA repair [2,8].

The role of BRCA1 has been studied mostly in the context of ionizing radiation (IR), which directly induces highly-genotoxic DNA double-strand breaks (DSBs). Following

exposure to IR, several proteins are rapidly recruited to DSB sites to form IR-Induced Foci (IRIF). IRIFs are characterized by ATM-mediated phosphorylation of the histone variant H2AX (γH2AX) [9], which is required for the subsequent highly coordinated assembly of checkpoint/ repair proteins. The precise mechanism of IRIF formation is not completely understood, although recent studies have shed light on the dynamics and orchestration of this process. The DNA damage mediator MDC1 promotes recruitment of the E3 ligases RNF8 and RNF168 that ubiquitinate specific substrates including histones. These events are required for interaction with the ubiquitin binding protein RAP80, which then recruits additional factors including BRCA1 and BARD1. At the IRIF, BRCA1/BARD1 in turn attracts other proteins such as Rad51 and BRCA2 that mediate cell cycle checkpoints and DNA repair (reviewed recently in [2,8,10]).

In contrast to the situation for IR, the manner in which BRCA1 responds to genotoxic agents that do not directly induce DSBs is poorly understood. BRCA1 was initially reported to be rapidly dispersed from constitutive foci (i.e., normally-occurring S-phase foci as opposed to IRIF) following treatment with various non-clastogenic mutagens [11,12]. The manner in which BRCA1 dispersion occurs, and the significance of this event, remain to be elucidated. In particular it has been unclear whether there might be a relationship between this dispersion and changes in protein stability during DNA damage. Although it is often assumed that the phosphorylation state, rather than absolute levels, of BRCA1 changes in response to DNA damage [3,5-7,13-15], some studies reported that BRCA1 and/or BARD1 are upregulated following treatment with UV or the topoisomerase II inhibitor doxorubicin [16-20]. In sharp contrast, other investigations reported that these proteins are downregulated

following treatment with the same agents [21,22]. Recently, it was shown that BARD1 is downregulated in a proteasome-dependent manner following treatment with an extremely cytotoxic dose of UV (70 J/m2) that induces substantial levels of apoptosis [23]. However, under the same conditions, significant changes in BRCA1 levels were not consistently observed. It is also critical to emphasize that BRCA1 was shown to be rapidly cleaved during apoptosis induced by high dose UV, thereby possibly accounting for the aformentioned inconsistency [24-26]. BRCA1 protein levels and subnuclear localization have also been investigated following treatment of cells with DNA alkylating agents. One study reported that this protein accumulates in nuclear foci following treatment with methylmethanesulfonate [27], whereas another showed that BRCA1 is actually downregulated by this agent [28]. In summary, it is not yet clear how BRCA1/BARD1 stability and subcellular localization are regulated in response to diverse classes of DNA adducts, other than DSBs, which trigger unique though overlapping signaling pathways.

Defining how BRCA1 participates in the DNA damage response is of a major importance not only for understanding breast and ovarian cancer development, but also towards helping to improve current cancer therapeutic protocols. For example several promising clinical trials are based on the use of inhibitors of the DNA damage-responsive enzyme PARP1 as a means to selectively target BRCA1-deficient tumor cells [29,30]. In view of the importance of BRCA1 in cancer development and treatment, and the conflicting data in the literature as cited above, we were prompted to carefully evaluate BRCA1 stability and localization in the cellular response to diverse-acting DNA damaging agents. We conclusively demonstrate that BRCA1 stability is regulated in a mutagen-specific manner. Indeed, in the

early response to UV and methylmethanesulfonate (MMS), but not to IR, dispersion of BRCA1/BARD1 from nuclear foci is accompanied by ubiquitin-mediated degradation of both tumor suppressors. Significantly, BRCA1 downregulation does not involve the major DNA damage-activated PI3K or MAPK pathways, suggesting that other yet to be identified signaling mechanisms regulate BRCA1 stability/function following DNA damage. Furthermore, we reveal that BACH1 and Rad52 are also degraded in a proteasome-dependent manner indicating that critical components of the homologous recombination (HR) machinery are selectively targeted for degradation. Finally, data is provided suggesting that DNA damage signaling pathways might need to be coordinated in order to forestall the untimely recruitment of potentially conflicting DNA damage responses.

Results

BRCA1 is downregulated in response to UVC or methylmethanesulfonate, but not IR.

Towards understanding the mechanisms that coordinate regulation of BRCA1 stability and localization following genotoxic stress, we initially treated HeLa cells with 30 J/m2 of 254-nm UV (UVC) which induces rapid ATR-dependent phosphorylation of BRCA1 [3,13]. Using an antibody recognizing the N-terminal region of BRCA1, we found that UVC induced a substantial decrease in levels of this protein at 3 hrs post-treatment, which became more marked by 6 hrs (Fig.1A, top panel). Of note, this occurred simultaneously with depletion of BRCA1 from nuclear foci (Fig.1A. bottom panel). Thus, the previously-described phenomenon of BRCA1 "dispersion" from constitutive foci after UVC irradiation [11,12] appears to be associated with actual depletion of the protein. Interestingly, IR treatment which has been shown to result in early dispersion of BRCA1 from constitutive foci [11], did not significantly affect BRCA1 protein levels (Fig.1B). We also conducted immunoblotting with other anti-BRCA1 antibodies that map to the middle and C-terminal regions and found that in each case a substantial fraction of the protein is downregulated post-UVC (Supp. Fig.1). It is important to emphasize that BRCA1 is downregulated following treatment with doses as low as 10 J/m2 of UVC (Supp. Fig.2). Next, in investigating an additional diverse-acting genotoxin, we revealed that BRCA1 is downregulated in a dose-dependent manner following treatment with the DNA alkylating agent methylmethanesulfonate (MMS) (Fig.1C and Supp. Fig.3). The above data demonstrate that control of BRCA1 stability varies significantly in a mutagen-specific manner. We also show (Fig.1D) that BRCA1 downregulation (i) is not cell-type specific, as it occurs in various tumor cell lines and moreover (ii) was observed in

primary human fibroblasts, revealing that the downregulation is not specific to transformed or tumor-derived cells.

BRCA1 downregulation is independent of apoptosis and is reversible

To determine whether DNA damage-induced BRCA1 downregulation might be a consequence of cell death, HeLa cells were treated with 200 μM MMS and harvested at various time points for immunostaining. BRCA1 protein exhibited maximal decrease at 3-6 hrs followed by its reappearance (reaching nearly 100% of basal levels) by 24 hrs post-treatment indicating that this decrease is transient (Fig.2A). Under the above MMS treatment conditions, we did not observe cell death as indicated by the absence of any nuclear condensation typical of apoptosis (see nuclear staining by DAPI). Consistently, immunoblotting experiments also revealed a transient downregulation of BRCA1 (Fig.2B, top panel). Densitometric quantification of BRCA1 protein levels confirmed these results (Fig.2B, low panel). In addition, no cleavage of either PARP-1 or caspase-3, two hallmarks of apoptosis, were detected in MMS-treated cells (Fig.2B), and moreover no change in cell viability was observed during the treatments (~100 % viability at all time points as determined by trypan blue exclusion assay). Of note, to ensure that we were able to actually detect apoptosis in our experimental system, we treated cells with UVC (100 J/m2), and found that this highly toxic dose induced substantial apoptotic cleavage of caspase-3 or PARP-1 after only 6 hrs post-treatment (Fig.2B, right panel). The above results indicate that downregulation of BRCA1 is not a consequence of apoptosis, suggesting that a unique signaling process may underlie the temporal and spatial regulation of this protein.

BRCA1 downregulation occurs in S and G2 phases of the cell cycle.

Since (i) downregulation of BRCA1 after DNA damage is partial (Fig. 2), suggesting that this process might be specific to a distinct cell population, and (ii) BRCA1 is known to be expressed primarily during S and G2 phases [31], we evaluated whether DNA damage-induced BRCA1 downregulation might be triggered in a cell cycle-specific manner. HeLa cells were synchronized at the G1/S border using thymidine double block and treated with MMS for 3 hrs at different times post-release. Cell cycle profiles with or without MMS exposure reveal that more than 90% of cells were in S phase at 5 hrs, and ~ 80 % in G2 at 11 hrs (Fig.3A top panel). In accord with previous studies [31], BRCA1 protein levels were dramatically increased in S phase-enriched populations (Fig.3A bottom panel, compare 5 hrs versus Asyn). We found that BRCA1 was downregulated at all time points examined after MMS treatment. Since under thymidine block the G2 population is not highly enriched (i.e., contaminated with S phase cells), we synchronized cells using other methods. G2 cells were highly purified (~95%) after 16 hrs by pre-treatment with the mitotic inhibitor nocodazole in conjunction with mitotic shake-off to remove M cells (Supp. Fig.4 left panel). G2 cells treated with MMS exhibited substantial downregulation of BRCA1 at 3 and 6 hrs (Supp. Fig.4 right panel). We also synchronized primary human foreskin fibroblasts in G0 through a physiological process, i.e., contact inhibition, followed by release for various time points to allow progression through the cell cycle (Fig.3B). We found that following UVC treatment, at any time during cell cycle progression up to 32 hr, BRCA1 is downregulated (Fig.3B). The above data taken together conclusively demonstrate that the primary signal triggering BRCA1 downregulation during periods of genotoxic stress is not dependent upon cell cycle as might be expected a priori.

The PI3 kinase related kinases (PIKKs) family members ATM, ATR and DNA-PK, and the canonical MAPKs, are not required for signaling BRCA1 downregulation following DNA damage.

ATM, ATR, and DNA-PK initiate multiple signaling cascades including the phosphorylation-mediated activation, stabilization, or degradation of various proteins that participate in coordinating the DNA damage response [32,33]. Since BRCA1 is directly and rapidly phosphorylated by ATM and/or ATR, we evaluated the likely possibility of a link between PIKKs signaling and BRCA1 downregulation during genotoxic stress. We first treated HeLa cells with IR or MMS for short time periods and analyzed BRCA1 protein. We found that while IR did not significantly affect BRCA1 protein levels, it induced a substantial shift of protein mobility strongly suggestive of phosphorylation (Fig.4A). In contrast, MMS induced mainly a downregulation of the protein with a less significant effect on protein mobility (Fig.4A). Thus, phosphorylation is not correlated with BRCA1 degradation. Next, we used caffeine, a well-characterized inhibitor of ATM and ATR [34], and found that while MMS-induced H2AX phosphorylation is strongly inhibited, BRCA1 downregulation is unaffected (Fig.4B). Similar conclusions could be drawn using the specific ATM inhibitor KU-55933 [35] (Fig.4C) or ATM-deficient human fibroblasts (Fig.4D and Supp. Fig.5). As control for pharmacological inhibition of ATM, abrogation of Chk2 phosphorylation was evaluated and shown to be reduced (Fig.4C). To specifically address the role of ATR, we used an shRNA construct which induces efficient knockdown of this protein (Fig.4E, left panel). Following treatment with MMS, BRCA1 is downregulated to a similar extent in cells whether depleted or not for ATR (Fig.4E, right panel). Finally, paired glioblastoma cell lines deficient or not in DNA-PK were employed to probe the potential requirement for the latter in BRCA1

downregulation. BRCA1 levels were decreased equally in DNA-PK deficient (MO59J) or proficient (MO59K) cells exposed to MMS, indicating that this kinase is dispensable for DNA damage-mediated downregulation of BRCA1 (Fig.4F and Supp Fig.5). Finally, we investigated the involvement of the canonical mitogen-activated protein kinases (MAPKs), including extracellular signal-related kinase (ERK1/2), c-Jun N-terminal kinase (JNK1/2), and p38 /β kinase which are rapidly activated by phosphorylation following exposure to genotoxic agents. These kinases in turn phosphorylate numerous downstream effectors that influence DNA damage-induced apoptosis, cell cycle checkpoints, and repair [36-38]. We found that inhibition of MAPK signaling using highly specific pharmacological inhibitors does not affect BRCA1 downregulation by MMS (Supp. Fig.6). The overall data suggest that kinases other than PIKKs or MAPK family members, or possibly signals other than phosphorylation, are involved in signaling BRCA1 downregulation.

Identification of BRCA1 domains required for DNA-damage induced BRCA1 downregulation

To provide additional insight into the mechanism of BRCA1 downregulation, we next conducted functional mapping studies using expression constructs encoding BRCA1 variants lacking major functional domains (Fig.5A). All the fragments used are expressed in HeLa cells at protein levels quite similar or below the levels of endogenous BRCA1. We observed that BRCA1 deleted for the N-terminal region (Δ 1-302 aa) is downregulated to a similar extent as endogenous BRCA1 following MMS treatment (Fig.5B). This demonstrates that the ring finger is dispensable for downregulation, thereby excluding the involvement of BRCA1 ubiquitin ligase activity, and also indicates that interaction with BARD1 is not prerequisite for

degradation. On the other hand, we found that BRCA1 deficient in the C-terminal region (Δ 1527-1863 aa) is completely resistant to proteasomal degradation, strongly suggesting a requirement for the BRCT domains. We also noted that BRCA1 missing the aa residues 305-770 is degraded following MMS treatment. This region contains domains required for interaction with chromatin remodeling and transcription regulators such as the SWI/SNF complex and ZBRK1 repressor [39,40], indicating that these latter interacting partners do not play a role in BRCA1 downregulation following DNA damage. Interestingly, we found that the middle region (aa 775-1292) which encompasses the Rad51 interaction domain is essential for degradation [41]. Finally, BRCA1 lacking either the BRCT motifs or the region spanning aa 775-1292 consistently exhibited stabilization following MMS exposure, supporting the involvement of these regions in regulating BRCA1 stability following genotoxic stress.

DNA damage-dependent downregulation of BRCA1, BARD1, BACH1 or Rad52 is mediated by the proteasome.

To provide insight into the mechanism of BRCA1 downregulation, in cells treated with MMS, we investigated the stability or activation of major DNA damage response proteins known to be involved in the BRCA1 pathway (Fig.6A). We first analyzed BARD1, the stochiometric partner of BRCA1, and found that the former is also downregulated following MMS treatment and moreover is depleted from the same foci as BRCA1 (Fig.9). In addition levels of the MRN complex proteins (MRE11, NBS1 and Rad50), BRCC36, RAP80, CtIP and Rad51 all known to assemble various complexes with BRCA1/BARD1 heterodimer are not affected by MMS treatment (Fig.6A). Moreover, no major changes of RPA32 protein,

a marker for DNA end-resection, were observed at early time points of BRCA1/BARD1 downregulation. Strikingly however, this protein was hyperphosphorylated at the later stage of MMS exposure, as indicated by the typical shift of protein electrophoretic mobility (Fig.6A) [42-44]. On the other hand, we did observe downregulation of Abraxas and BACH1, two other BRCT motif-interacting proteins that define the A and B complexes respectively (Fig.6A). Interestingly, while Abraxas showed a downregulation profile similar to BRCA1 and BARD1, BACH1 exhibited a biphasic downregulation. Moreover, we found that levels of the HR protein Rad52, known to act downstream BRCA1, were significantly reduced. In addition, a slight shift in Rad52 protein gel mobility was consistently observed at the later stage of treatment (12 and 24 hours). We also observed that phosphorylation of the checkpoint kinases CHK1, CHK2, and of the histone variant H2AX appear to be temporally correlated with reduction in BRCA1/BARD1/BACH1 and Rad52 protein levels (Fig.6A). These results indicate that specific components of the HR machinery are downregulated at the early stage of the cellular response to MMS exposure and then recovered totally or partially at later times. Since RPA is hyperphosphorylated at 12 and 24 hours post-treatment, we sought to investigate the subnuclear localization of critical components of the HR pathway, i.e., BRCA1, γH2AX, RPA32 and Rad51. As expected from immunobloting experiments, γH2AX was strongly induced (Fig.6B). Of note, IR treatment is known to induce the formation of relatively large γH2AX foci to which BRCA1/BARD1 is rapidly recruited (Fig.8B). In contrast, MMS induced the assembly of a substantial number of relatively small γH2AX foci that, at the early stage of treatment (3-6 hours), exhibited no staining for the HR proteins BRCA1, Rad51 or RPA (Fig.6B and Supp Fig.8). Interestingly, at the later stage (12-24 hours post-treatment), BRCA1, as well as RPA and Rad51, formed foci indicating DSBs processing.

We next evaluated the possibility that MMS-induced downregulation of BRCA1 and associated partners occurs at the level of protein stability. First, a cycloheximide chase revealed that BRCA1 stability is significantly decreased in response to MMS versus cycloheximide alone, suggesting an active degradation mechanism (Fig.7A). In contrast, the abundance of Cdc6, a protein with short half-life, is substantially decreased by treatment with cycloheximide, but not with MMS. This result prompted us to investigate the involvement of active protein degradation in regulating the stability of BRCA1 and associated partners. We found that the proteasome inhibitor MG132 completely blocks downregulation of BRCA1 (Fig. 7B). Similar results were obtained for BRCA1 following pre-treatment of HCT116 or HeLa cells with proteasome inhibitors prior to either MMS or UVC exposure (Supp. Fig.7). Next, we analyzed additional components and found that the proteasome is also required for downregulation of BARD1, BACH1, and Rad52 in HeLa cells treated with MMS (Fig. 7B). Surprisingly, Abraxas downregulation is not blocked by MG132 suggesting that a proteasome-independent mechanism regulates levels of this protein. To demonstrate the involvement of ubiquitination per se, BRCA1 immunoprecipitated from either mock- or MMS-treated HeLa cells was shown to be readily ubiquitinated following DNA damage (Fig. 7C, left panel). A densitometric quantification indicated that the ubiquitin signal is increased by ~ 3-fold following MMS treatment. We confirmed these results in HEK293T, i.e., MMS induced a 3-fold increase in BRCA1 ubiquitination (Fig. 7C, right panel). In summary, our results indicate that proteasomal-mediated degradation of BRCA1/BARD1/BACH1 and of Rad52 is a normal physiological response to DNA damaging agents that do not directly generate DSBs, and suggest the existence of a yet-to-be characterized regulatory mechanism controlling the BRCA1 pathway.

BRCA1/BARD1 downregulation prevents their recruitment, along with Rad51, to chromatin following MMS treatment

In response to IR-induced DSBs, phosphorylation of H2AX engenders a cascade of protein recruitment that culminates in the assembly of the BRCA1/BARD1/Rad51 HR repair complex at the IRIF. The primary types of DNA damage induced by UVC and MMS are pyrimidine dimers and alkylated bases, respectively. These agents also significantly induce γH2AX (Fig.6 and discussion). Thus we postulate that early BRCA1/BARD1 downregulation might be needed to prevent their recruitment to UV- or MMS-damaged chromatin, as this might otherwise interfere with mutagen specific-signaling events or -repair processes, i.e., nucleotide excision repair of UV-induced pyrimidine dimers or base excision repair of alkylated DNA bases. To investigate this possibility, we analyzed the recruitment of BRCA1, BARD1, and Rad51 to chromatin following inhibition of BRCA1/BARD1 downregulation using the proteasome inhibitor MG132. As control, we used IR treatment which is known to rapidly induce the assembly of BRCA1/BARD1/RAD51 on chromatin (Fig.8A). We found, in sharp contrast to treatment with MMS or MG132 alone, that combined treatment with MMS and MG132 resulted in a highly significant recruitment of BRCA1/BARD1/RAD51 proteins to chromatin. However, it was previously shown that proteasome inhibitors block BRCA1 and Rad51 recruitment to IRIF [45]. Thus, we sought to resolve this apparent discrepancy. First, we treated HeLa cells with MG132 and found that neither BRCA1 or Rad51 formed foci following IR, thus reproducing in our experimental setting, the previously published findings (Supp Fig.9). Next, we investigated the subnuclear localization of these proteins in response to MG132, MMS or combined treatments. As control, we used IR to induce BRCA1 or Rad51 foci formation (Fig 8B, left panel and Supp Fig.10). We found that BRCA1 exhibited a

strong, but diffuse, nuclear staining following treatment with either MG132 or MG132/MMS. As expected, a very low BRCA1 signal was detected in cells treated with MMS only. Rad51 staining was diffuse for all treatments except for IR, which induced its assembly at IRIF. Foci formation was observed for BRCA1/RAD51/γH2AX following IR, but only for γH2AX in the case of MMS (Fig 8B, right panel). Altogether, these results suggest that BRCA1 and Rad51 might be loaded on the chromatin in response to MG132/MMS without forming distinct foci. To further demonstrate this, we permeabilized the cells post-treatment to remove soluble cytoplasmic and nuclear proteins [46] and conducted immunostaining as above. As a control for the cell permeabilization procedure, we analyzed the nuclear protein BAP1 [47] and we observed a substantial decrease of its nuclear staining (Supp Fig.11). We found that RAD51 and BRCA1 signals remained high with MG132/MMS, and to a lesser extent with MG132 alone, following cell permeabilization (Fig 8C, left panel and Supp Fig.10). In contrast, Rad51 signal was significantly decreased in the untreated cells and following MMS, most likely due to its diffusion from the nuclei. Again, foci formation for BRCA1 and Rad51 was not observed with MG132 or MG132/MMS, as shown above for intact cells (Fig 8C, right panel).

We next tested whether exposure to MMS might affect pre-assembled BRCA1/BARD1/RAD51 at IRIF. Cells were first treated with IR in order to induce IRIF (as revealed by immunostaining for γH2AX/BRCA1/BARD1/RAD51), which was followed by treatment with MMS. This treatment resulted in a dramatic decrease of BRCA1/BARD1/RAD51 foci, but not of γH2AX foci (Fig.9A, top and bottom panels). As

expected, immunoblotting indicated that although BRCA1 and BARD1 are substantially downregulated, Rad51 protein levels remain unchanged (Fig.9B).

Discussion

A critical role for BRCA1/BARD1 in the HR branch of DSB repair following IR exposure is now well established. However previous studies have reported conflicting results on the regulation and functionality of this heterodimer in response to genotoxic agents which induce (i) DNA adducts other than DSBs, and therefore also (ii) unique signaling pathways relative to the situation for IR (see Introduction). Here, we resolved these discrepancies by demonstrating that BRCA1 is actually downregulated rather than simply relocalized.

Indeed, the previously described dispersion of BRCA1 from constitutive foci following UVC exposure [11,12], or following MMS exposure (this study), is associated with active degradation of the protein. However IR, which was shown to induce early dispersion of BRCA1 from constitutive foci prior to IRIF formation [11], does not induce BRCA1 downregulation. Thus, distinct signaling mechanisms are ostensibly responsible for controlling BRCA1 relocalization and/or levels during periods of genotoxic stress depending upon the nature of the DNA damage. We note that during our investigation of BRCA1 downregulation following treatment with UVC or MMS, several critical factors were taken into consideration that might account for discrepancies between previous studies and our own: (i) Total cell extracts prepared in 2% SDS, sonicated, and boiled prior to immunoblotting were used to exclude the possibility of selective extraction. (ii) Different antibodies recognizing several regions of BRCA1 were employed, thus excluding potential artifacts due to epitope masking that might be caused by post-translational modifications. (iii) Diverse human strains including primary human fibroblasts were investigated, thus controlling for potential cell-type specific responses. (iv) We showed that BRCA1 is downregulated

following exposure to relatively low mutagen doses, i.e, 50 μM of MMS or 10 J/m2 of UVC, where within the time frame of our analysis cell viability is not compromised and apoptosis is not induced. This is important because a previous study had indicated that BRCA1 is cleaved by caspase-3 during apoptosis, as early as 3 hrs following treatment with a very high dose of UV [24]. In addition BRCA1 downregulation is fully reversible, strongly arguing against any involvement of caspases in this early event. We also emphasize that 10 J/m2 of UVC is physiologically relevant as this dose induces a level of DNA photoproducts equivalent to that which can be obtained during 1 hr of exposure to natural sunlight [48,49].

Regulation of protein stability by the ubiquitin-proteasome system is a critical determinant of protein function. Several lines of evidence presented here indicate that BRCA1 is degraded via the proteasome: (i) UVC or MMS treatment induces dramatic downregulation of BRCA1 within 2-3 hrs, and this cannot be explained by a decline of protein levels as a consequence of transcription/translation arrest since complete inhibition of protein synthesis by cycloheximide revealed that the half-life of BRCA1 is ~ 4h ([31] and this study). In addition, downregulation of BRCA1 in response to MMS treatment cannot be enhanced by pretreatment with cycloheximide, indicating that an active degradation process predominates with respect to constitutive turnover of BRCA1. (ii) Importantly, two different proteasome inhibitors (ZL3VS [50] and MG132 [51]) were used to minimize the possibility of non-specific effects. (iii) We established that BRCA1 is ubiquitinated following MMS treatment. It should be emphasized that an ubiquitination signal is also observed below that of full length BRCA1, as degradation occurs during the process of immunoprecipitation (Fig.7C). Moreover other interacting partners of BRCA1, including BARD1 and BACH1, would also be expected

to contribute to the ubiquitination signal, since these proteins are co-regulated in a proteasome-dependent manner. Building on the above firm conclusions, we decided to further elucidate novel aspects pertaining to the mechanism and significance of BRCA1/BARD1 degradation following genotoxic stress.

One preeminent event requiring consideration in the context of the current study is the rapid phosphorylation of BRCA1 by PI3K family members following genotoxic insult. Indeed the notion that PI3K signaling is required for transient proteasome-mediated downregulation of critical DNA damage responsive proteins is not without precedent. For example it was previously observed that the cyclin-dependent kinase inhibitor p21waf1 is downregulated by UVC and MMS, but not by IR, and this depends upon functional ATR kinase [52,53]. Also the very rapid phosphorylation of BRCA1 by ATR following UV is temporally associated with BRCA1 degradation observed here. Despite these considerations, we found that inhibition of ATR, ATM, or DNA-PK does not either block or enhance BRCA1 downregulation, supporting the notion that PI3K-mediated BRCA1 phosphorylation, and degradation of the protein, represent distinct signaling processes acting to control BRCA1 function. It is noteworthy that in addition to ATM, ATR, DNA-PK and MAPK, we also investigated, using specific chemical inhibitors, the potential involvement of several other kinases implicated in the DNA damage response including Casein Kinase 2 and Cyclin-Dependent Kinase 2 each known to phosphorylate BRCA1 [54,55]. Using various inhibitor concentrations, we failed to observe any interference with BRCA1 downregulation by MMS (data not shown). Taken together our data strongly suggest that phosphorylation might not be involved in triggering BRCA1 degradation. Thus, the possible involvement of other post-

translational modifications or signaling events in triggering BRCA1 degradation appears quite plausible. In this respect, our work sets the stage for further studies focused on unraveling the novel signaling mechanism mediating BRCA1 downregulation following UVC- or MMS-induced DNA damage.

Interestingly we found that BRCA1 variants lacking BRCT motifs or the region spanning aa 775-1292 were not only completely resistant to degradation, but also consistently exhibited stabilization following MMS treatment. This suggests that i) the aforementioned domains contain protein interaction motifs or sites for post-translational modifications (including ubiquitination sites) that induce degradation, and ii) along with the engagement of active degradation, a feedback process of BRCA1 stabilization might also be concomitantly induced by MMS, and this later event becomes effective only when the signaling responsible for degradation is terminated or inhibited. This feedback loop would contribute to the re-establishment of BRCA1 protein levels at the appropriate time post-genotoxic stress. Further investigations are required to address the molecular mechanism underlying this dynamic regulation of BRCA1 stability.

It appears counterintuitive that the function of a tumor suppressor is abrogated during periods of genotoxic stress. We postulate that the biological significance of BRCA1 downregulation likely reflects a necessity to temporally coordinate DNA damage signaling and repair pathways in response to specific classes of DNA adducts. Such coordination has been proposed for other tumor suppressors involved in the maintenance of genomic integrity including the checkpoint kinase CHK1 and the DNA damage binding protein DDB2 [56-58].

Of particular note the early transient, proteasome-dependent degradation of p21waf1 mentioned above was shown to be required for efficient repair of DNA damage after UV irradiation [52,53]. IR is well known to directly generate DSBs leading to rapid ATM/DNA-PK activation followed by phosphorylation of H2AX and subsequent DSB repair via non-homologous end-joining or HR. On the other hand neither UVC nor MMS generates DSBs as primary lesions, although both induce replication stress resulting in a delayed formation of DSBs at collapsed replication forks, which in turn induces ATM-dependent phosphorylation of H2AX [59-61]. Interestingly, it has also been reported that alkylation base damage can induce γH2AX in the complete absence of replication blockage [62]. In addition, it was clearly shown that γH2AX is upregulated by UVC treatment in the absence of DSBs and moreover associates with sites of nucleotide excision repair [63]. The exact significance of H2AX phosphorylation under such conditions is not yet clear. However since this histone modification might promote the recruitment of DSB repair proteins per se, it appears reasonable that critical compensatory mechanisms would be engaged to prevent the initiation of conflicting DNA damage/repair responses, i.e., in instances where no DSBs are actually induced. In fact we provide evidence that BRCA1/BARD1 degradation might prevent the untimely association of HR repair proteins with MMS-damaged chromatin, which would otherwise interfere with specific signaling events induced by alkylated DNA bases or with the execution of base excision repair. In support of this, following MMS treatment, we observed downregulation of the HR proteins Rad52, BACH1 and Abraxas, which are not immediately required to process DNA alkylation damage. For example, Rad52 interacts with Rad51, associates with single-stranded DNA ends, and promotes the annealing of complementary DNA strands [64]. Thus, its association with DNA repair intermediates generated during the

processing of alkylated bases might very well compromise the efficiency of base excision repair. We emphasize that downregulation of components of the HR machinery during the initial period of MMS treatment is followed by a second phase of recovery. We note that unlike BRCA1 and BARD1, Rad52 downregulation by MMS is not followed by complete recovery at 24 hours. This might suggest that only a small portion of Rad52 is needed at the later stage of MMS response, time at which HR pathway is activated. Consistent with this, a shift in Rad52 protein mobility was observed at 12 and 24 hours likely reflecting phosphorylation that might modulate its function in HR. Indeed, we observed at later stages of MMS that typical HR foci are formed and are highly enriched in BRCA1, RPA and Rad51. Importantly, foci formation was also concomitant with RPA hyperphosphorylation, a maker for DSBs processing. Clearly, the process of repair takes place after the initial phase of BRCA1/BARD1 downregulation, most likely to repair DSBs generated by replication blocking lesions. We propose a model integrating our findings, which highlight the biphasic response of HR machinery to MMS (Fig.10).

In conclusion we have demonstrated that BRCA1/BARD1 stability and hence function is tightly regulated by ubiquitination-mediated proteasomal degradation in response to UV or MMS exposure, in a manner entirely distinct to that observed following treatment with IR. It would be extremely interesting to identify the ubiquitin ligase mediating BRCA1/BARD1 downregulation, as well as to determine how defects in this pathway affect tumor suppressor function.

Materials and Methods

Chemicals, plasmids and antibodies

The pharmacological kinase inhibitors U0126, SP600125, and SB202190 were from Cell Signaling. Nocodazole, caffeine, cycloheximide and MG132 were from Sigma-Aldrich and KU-55933 from Calbiochem. GFP-tagged full-length BRCA1 and BRCA1 deletion mutants were provided by Dr. N. Chiba [65]. ZL3VS proteasome inhibitor was a generous gift of Dr. B.M. Kessler [50].

Cell culture and DNA damage treatments

HeLa cervical cancer, U2OS osteosarcoma, HEK293 embryonic kidney, HCT116 colon carcinoma and low passage primary human foreskin fibroblasts (CCD-2056) were from ATCC, and ATM-deficient primary skin fibroblasts (HDSF, AG04405A) from the Coriell Institute. The MO59K (DNA-PK proficient) and MO59J (DNA-PK null) glioblastoma cell lines were provided by Dr. M.J. Allalunis-Turner [66]. All strains were cultured in DMEM supplemented with 10 % foetal bovine serum, L-glutamine and antibiotics. Cell monolayers were washed with phosphate-buffered saline (PBS), covered with PBS, and irradiated with UVC using a crosslinker (CL-1000, VWR) at a fluency of 5 J/m2/s and returned to culture medium. IR exposure was performed using a cesium-137 source (Gamma Cell; Atomic Energy Canada) at a dose rate of 6.3 rad/s. Methylmethanesulfonate (Sigma-Aldrich) was added to the culture medium at the indicated concentrations.

Synchronization and cell cycle analysis

Primary fibroblasts we synchronized in G0/G1 by contact inhibition [31]. HeLa and U2OS cells were synchronized at the G1/S border using a thymidine double block protocol [67]. G2/M populations were obtained following 16 hours (hrs) of treatment with nocodazole (200 ng/ml) used to prevent cells from cycling. G2 cells were separated from M cells by mitotic shake off. Cell cycle analysis was carried out as described [68] using a FACScan flow cytometer fitted with CellQuestPro software (BD Biosciences).

shRNA knockdowns

shRNA targeting ATR (TRC0000039615) was purchased from Sigma-Aldrich. The non-target control shRNA was described [69]. Cells were transfected with either shRNA and selected in medium containing puromycin for 2 days as described [68].

Immunostaining and immunoblotting

All antibodies are described in Supplemental Table 1. Western blotting using total cell extracts was performed as described [68]. The band signals were directly acquired with a LAS-3000 LCD camera coupled to MultiGauge software (Fuji, Stamford, CT, USA). Immunostaining was performed as described [68] except that the secondary antibodies Alexa Flour 488 goat anti-mouse IgG or an Alexa Fluor 594 goat anti-rabbit IgG (Invitrogen) were used. Nuclei were counterstained with DAPI. Nuclei permabilization was essentially conducted as previously descibed [46]. Fluorescence was visualized with a Leica DMRE microscope, and the data acquired using a RETIGA EX digital camera (QIMAGING) coupled with OpenLab 3.1.1 software (OpenLab).

Immunoprecipitation

Cell extracts from control or MMS-treated cells were prepared as described [68] except that 20 mM of N-EthylMaleimide (NEM) was added to the lysis buffer. After sonication and centrifugation, lysates were incubated with anti-BRCA1 or a control IgG for 5 to 6 hrs. Immunocomplexes were recovered following 2 hrs incubation with protein G-sepharose, extensively washed with the lysis buffer, and eluted with Laemmli sample buffer for immunoblotting.

Isolation of chromatin

Following DNA damage treatments, cells were washed with PBS and then resuspended in high-detergent containing buffer (50 mM Tris-HCl, pH 7.3; 5 mM EDTA; 150 mM KCl; 10 mM NaF, 1 % Triton X-100; 1 mM phenylmethylsulfonyl fluoride (PMSF); and protease inhibitors cocktail (Sigma). Following 3 successive extractions for 15 minutes each with the same buffer, the chromatin fraction was recovered by centrifugation at 6000g/10 min. Chromatin and total cell extracts were then used for determination of protein concentration and western blotting.

Acknowledgements

This work was supported by a grant (018144) to EBA from the Terry Fox Foundation (Canadian Cancer Society Research Institute). EBA is a scholar of Le Fonds de la Recherche en Santé du Québec (FRSQ). HY is supported by a PhD fellowship from the Cole foundation. JP was supported by NCI award CA111480. AH was a predoctoral fellow with the Dept of Defense Breast Cancer Research Program. We are grateful to Natsuko Chiba for the generous gift of BRCA1 deletion constructs.

References

1. Narod, S.A. and Foulkes, W.D. (2004) BRCA1 and BRCA2: 1994 and beyond. Nat Rev Cancer, 4, 665-76.

2. Huen, M.S., Sy, S.M. and Chen, J. (2010) BRCA1 and its toolbox for the maintenance of genome integrity. Nat Rev Mol Cell Biol. 11, 138-148

3. Tibbetts, R.S., Cortez, D., Brumbaugh, K.M., Scully, R., Livingston, D., Elledge, S.J. and Abraham, R.T. (2000) Functional interactions between BRCA1 and the checkpoint kinase ATR during genotoxic stress. Genes Dev, 14, 2989-3002.

4. Xu, B., O'Donnell, A.H., Kim, S.T. and Kastan, M.B. (2002) Phosphorylation of serine 1387 in Brca1 is specifically required for the Atm-mediated S-phase checkpoint after ionizing irradiation. Cancer Res, 62, 4588-91.

5. Cortez, D., Wang, Y., Qin, J. and Elledge, S.J. (1999) Requirement of ATM-dependent phosphorylation of brca1 in the DNA damage response to double-strand breaks. Science, 286, 1162-6.

6. Xu, B., Kim, S. and Kastan, M.B. (2001) Involvement of Brca1 in S-phase and G(2)-phase checkpoints after ionizing irradiation. Mol Cell Biol, 21, 3445-50.

7. Lin, S.Y., Li, K., Stewart, G.S. and Elledge, S.J. (2004) Human Claspin works with BRCA1 to both positively and negatively regulate cell proliferation. Proc Natl Acad Sci U S A, 101, 6484-9.

8. O'Donovan, P. and Livingston, D.M. (2010) BRCA1 and BRCA2: breast/ovarian cancer susceptibility gene products and participants in DNA double strand break repair. Carcinogenesis. 6, 961-7

9. Burma, S., Chen, B.P., Murphy, M., Kurimasa, A. and Chen, D.J. (2001) ATM phosphorylates histone H2AX in response to DNA double-strand breaks. J Biol Chem, 276, 42462-7.

10. Panier, S. and Durocher, D. (2009) Regulatory ubiquitylation in response to DNA double-strand breaks. DNA Repair (Amst), 8, 436-43.

11. Scully, R., Chen, J., Ochs, R.L., Keegan, K., Hoekstra, M., Feunteun, J. and Livingston, D.M. (1997) Dynamic changes of BRCA1 subnuclear location and phosphorylation state are initiated by DNA damage. Cell, 90, 425-35.

12. Thomas, J.E., Smith, M., Tonkinson, J.L., Rubinfeld, B. and Polakis, P. (1997) Induction of phosphorylation on BRCA1 during the cell cycle and after DNA damage. Cell Growth Differ, 8, 801-9.

13. Gatei, M., Zhou, B.B., Hobson, K., Scott, S., Young, D. and Khanna, K.K. (2001) Ataxia telangiectasia mutated (ATM) kinase and ATM and Rad3 related kinase mediate phosphorylation of Brca1 at distinct and overlapping sites. In vivo assessment using phospho-specific antibodies. J Biol Chem, 276, 17276-80.

14. Johnson, N., Cai, D., Kennedy, R.D., Pathania, S., Arora, M., Li, Y.C., D'Andrea, A.D., Parvin, J.D. and Shapiro, G.I. (2009) Cdk1 participates in BRCA1-dependent S phase checkpoint control in response to DNA damage. Mol Cell, 35, 327-39.

15. Ray, A., Mir, S.N., Wani, G., Zhao, Q., Battu, A., Zhu, Q., Wang, Q.E. and Wani, A.A. (2009) Human SNF5/INI1, a component of the human SWI/SNF chromatin remodeling complex, promotes nucleotide excision repair by influencing ATM recruitment and downstream H2AX phosphorylation. Mol Cell Biol, 29, 6206-19.

16. Clarkin, C.E., Zhang, H. and Weber, B.L. (2000) Kinetics of BRCA1 regulation in response to UVC radiation. Cell Mol Life Sci, 57, 1126-34.

17. Irminger-Finger, I., Leung, W.C., Li, J., Dubois-Dauphin, M., Harb, J., Feki, A., Jefford, C.E., Soriano, J.V., Jaconi, M., Montesano, R. and Krause, K.H. (2001) Identification of BARD1 as mediator between proapoptotic stress and p53-dependent apoptosis. Mol Cell, 8, 1255-66.

18. Feki, A., Jefford, C.E., Berardi, P., Wu, J.Y., Cartier, L., Krause, K.H. and Irminger-Finger, I. (2005) BARD1 induces apoptosis by catalysing phosphorylation of p53 by DNA-damage response kinase. Oncogene, 24, 3726-36.

19. Yan, Y., Black, C.P., Cao, P.T., Haferbier, J.L., Kolb, R.H., Spieker, R.S., Ristow, A.M. and Cowan, K.H. (2008) Gamma-irradiation-induced DNA damage checkpoint activation involves feedback regulation between extracellular signal-regulated kinase 1/2 and BRCA1. Cancer Res, 68, 5113-21.

20. Rusin, M., Zajkowicz, A. and Butkiewicz, D. (2009) Resveratrol induces senescence-like growth inhibition of U-2 OS cells associated with the instability of telomeric DNA and upregulation of BRCA1. Mech Ageing Dev, 130, 528-37.

21. Fan, S., Twu, N.F., Wang, J.A., Yuan, R.Q., Andres, J., Goldberg, I.D. and Rosen, E.M. (1998) Down-regulation of BRCA1 and BRCA2 in human ovarian cancer cells exposed to adriamycin and ultraviolet radiation. Int J Cancer, 77, 600-9.

22. Kranz, D., Dohmesen, C. and Dobbelstein, M. (2008) BRCA1 and Tip60 determine the cellular response to ultraviolet irradiation through distinct pathways. J Cell Biol, 182, 197-213.

23. Brodie, K.M. and Henderson, B.R. (2010) Differential modulation of BRCA1 and BARD1 nuclear localisation and foci assembly by DNA damage. Cell Signal, 22, 291-302.

24. Zhan, Q., Jin, S., Ng, B., Plisket, J., Shangary, S., Rathi, A., Brown, K.D. and Baskaran, R. (2002) Caspase-3 mediated cleavage of BRCA1 during UV-induced apoptosis. Oncogene, 21, 5335-45.

25. Yang, W.W., Wang, Z.H., Zhu, Y. and Yang, H.T. (2007) E2F6 negatively regulates ultraviolet-induced apoptosis via modulation of BRCA1. Cell Death Differ, 14, 807-17.

26. Dizin, E., Ray, H., Suau, F., Voeltzel, T. and Dalla Venezia, N. (2008) Caspase-dependent BRCA1 cleavage facilitates chemotherapy-induced apoptosis. Apoptosis, 13, 237-46.

27. Au, W.W. and Henderson, B.R. (2007) Identification of sequences that target BRCA1 to nuclear foci following alkylative DNA damage. Cell Signal, 19, 1879-92.

28. Bennett, C.B., Westmoreland, T.J., Verrier, C.S., Blanchette, C.A., Sabin, T.L., Phatnani, H.P., Mishina, Y.V., Huper, G., Selim, A.L., Madison, E.R., Bailey, D.D., Falae, A.I., Galli, A., Olson, J.A., Greenleaf, A.L. and Marks, J.R. (2008) Yeast screens identify the RNA polymerase II CTD and SPT5 as relevant targets of BRCA1 interaction. PLoS One, 3, e1448.

29. Bolderson, E., Richard, D.J., Zhou, B.B. and Khanna, K.K. (2009) Recent advances in cancer therapy targeting proteins involved in DNA double-strand break repair. Clin Cancer Res, 15, 6314-20.

30. Drew, Y. and Plummer, R. (2010) The emerging potential of poly(ADP-ribose) polymerase inhibitors in the treatment of breast cancer. Curr Opin Obstet Gynecol, 22, 67-71.

31. Choudhury, A.D., Xu, H. and Baer, R. (2004) Ubiquitination and proteasomal degradation of the BRCA1 tumor suppressor is regulated during cell cycle progression. J Biol Chem, 279, 33909-18.

32. Abraham, R.T. (2001) Cell cycle checkpoint signaling through the ATM and ATR kinases. Genes Dev, 15, 2177-96.

33. Durocher, D. and Jackson, S.P. (2001) DNA-PK, ATM and ATR as sensors of DNA damage: variations on a theme? Curr Opin Cell Biol, 13, 225-31.

34. Sarkaria, J.N., Busby, E.C., Tibbetts, R.S., Roos, P., Taya, Y., Karnitz, L.M. and Abraham, R.T. (1999) Inhibition of ATM and ATR kinase activities by the radiosensitizing agent, caffeine. Cancer Res, 59, 4375-82.

35. Hickson, I., Zhao, Y., Richardson, C.J., Green, S.J., Martin, N.M., Orr, A.I., Reaper, P.M., Jackson, S.P., Curtin, N.J. and Smith, G.C. (2004) Identification and characterization of a novel and specific inhibitor of the ataxia-telangiectasia mutated kinase ATM. Cancer Res, 64, 9152-9.

36. Liu, Z.G., Baskaran, R., Lea-Chou, E.T., Wood, L.D., Chen, Y., Karin, M. and Wang, J.Y. (1996) Three distinct signalling responses by murine fibroblasts to genotoxic stress. Nature, 384, 273-6.

37. Dent, P., Yacoub, A., Fisher, P.B., Hagan, M.P. and Grant, S. (2003) MAPK pathways in radiation responses. Oncogene, 22, 5885-96.

38. Thornton, T.M. and Rincon, M. (2009) Non-classical p38 map kinase functions: cell cycle checkpoints and survival. Int J Biol Sci, 5, 44-51.

39. Zheng, L., Pan, H., Li, S., Flesken-Nikitin, A., Chen, P.L., Boyer, T.G. and Lee, W.H. (2000) Sequence-specific transcriptional corepressor function for BRCA1 through a novel zinc finger protein, ZBRK1. Mol Cell, 6, 757-68.

40. Bochar, D.A., Wang, L., Beniya, H., Kinev, A., Xue, Y., Lane, W.S., Wang, W., Kashanchi, F. and Shiekhattar, R. (2000) BRCA1 is associated with a human SWI/SNF-related complex: linking chromatin remodeling to breast cancer. Cell, 102, 257-65.

41. Scully, R., Chen, J., Plug, A., Xiao, Y., Weaver, D., Feunteun, J., Ashley, T. and Livingston, D.M. (1997) Association of BRCA1 with Rad51 in mitotic and meiotic cells. Cell, 88, 265-75.

42. Shao, R.G., Cao, C.X., Zhang, H., Kohn, K.W., Wold, M.S. and Pommier, Y. (1999) Replication-mediated DNA damage by camptothecin induces phosphorylation of RPA by DNA-dependent protein kinase and dissociates RPA:DNA-PK complexes. Embo J, 18, 1397-406.

43. Manthey, K.C., Opiyo, S., Glanzer, J.G., Dimitrova, D., Elliott, J. and Oakley, G.G. (2007) NBS1 mediates ATR-dependent RPA hyperphosphorylation following replication-fork stall and collapse. J Cell Sci, 120, 4221-9.

44. Vassin, V.M., Anantha, R.W., Sokolova, E., Kanner, S. and Borowiec, J.A. (2009) Human RPA phosphorylation by ATR stimulates DNA synthesis and prevents ssDNA accumulation during DNA-replication stress. J Cell Sci, 122, 4070-80.

45. Jacquemont, C. and Taniguchi, T. (2007) Proteasome function is required for DNA damage response and fanconi anemia pathway activation. Cancer Res, 67, 7395-405.

46. Tang, Y. and DeFranco, D.B. (1996) ATP-dependent release of glucocorticoid receptors from the nuclear matrix. Mol Cell Biol, 16, 1989-2001.

47. Jensen, D.E., Proctor, M., Marquis, S.T., Gardner, H.P., Ha, S.I., Chodosh, L.A., Ishov, A.M., Tommerup, N., Vissing, H., Sekido, Y., Minna, J., Borodovsky, A., Schultz, D.C., Wilkinson, K.D., Maul, G.G., Barlev, N., Berger, S.L., Prendergast, G.C. and Rauscher, F.J., 3rd (1998) BAP1: a novel ubiquitin hydrolase which binds to the BRCA1 RING finger and enhances BRCA1-mediated cell growth suppression. Oncogene, 16, 1097-1112.

48. Kuluncsics, Z., Perdiz, D., Brulay, E., Muel, B. and Sage, E. (1999) Wavelength dependence of ultraviolet-induced DNA damage distribution: involvement of direct or indirect mechanisms and possible artefacts. J Photochem Photobiol B, 49, 71-80.

49. Yoon, J.H., Lee, C.S., O'Connor, T.R., Yasui, A. and Pfeifer, G.P. (2000) The DNA damage spectrum produced by simulated sunlight. J Mol Biol, 299, 681-93.

50. Kessler, B.M., Tortorella, D., Altun, M., Kisselev, A.F., Fiebiger, E., Hekking, B.G., Ploegh, H.L. and Overkleeft, H.S. (2001) Extended peptide-based inhibitors efficiently target the proteasome and reveal overlapping specificities of the catalytic beta-subunits. Chem Biol, 8, 913-29.

51. Lee, D.H. and Goldberg, A.L. (1998) Proteasome inhibitors: valuable new tools for cell biologists. Trends Cell Biol, 8, 397-403.

52. Bendjennat, M., Boulaire, J., Jascur, T., Brickner, H., Barbier, V., Sarasin, A., Fotedar, A. and Fotedar, R. (2003) UV irradiation triggers ubiquitin-dependent degradation of p21(WAF1) to promote DNA repair. Cell, 114, 599-610.

53. Soria, G. and Gottifredi, V. (210) PCNA-coupled p21 degradation after DNA damage: The exception that confirms the rule? DNA Repair (Amst), 9, 358-64.

54. O'Brien, K.A., Lemke, S.J., Cocke, K.S., Rao, R.N. and Beckmann, R.P. (1999) Casein kinase 2 binds to and phosphorylates BRCA1. Biochem Biophys Res Commun, 260, 658-64.

55. Ruffner, H., Jiang, W., Craig, A.G., Hunter, T. and Verma, I.M. (1999) BRCA1 is phosphorylated at serine 1497 in vivo at a cyclin-dependent kinase 2 phosphorylation site. Mol Cell Biol, 19, 4843-54.

56. Zhang, Y.W., Otterness, D.M., Chiang, G.G., Xie, W., Liu, Y.C., Mercurio, F. and Abraham, R.T. (2005) Genotoxic stress targets human Chk1 for degradation by the ubiquitin-proteasome pathway. Mol Cell, 19, 607-18.

57. Rapic-Otrin, V., McLenigan, M.P., Bisi, D.C., Gonzalez, M. and Levine, A.S. (2002) Sequential binding of UV DNA damage binding factor and degradation of the p48 subunit as early events after UV irradiation. Nucleic Acids Res, 30, 2588-98.

58. Fitch, M.E., Cross, I.V., Turner, S.J., Adimoolam, S., Lin, C.X., Williams, K.G. and Ford, J.M. (2003) The DDB2 nucleotide excision repair gene product p48 enhances global genomic repair in p53 deficient human fibroblasts. DNA Repair (Amst), 2, 819-26.

59. Ward, I.M. and Chen, J. (2001) Histone H2AX is phosphorylated in an ATR-dependent manner in response to replicational stress. J Biol Chem, 276, 47759-62.

60. Ward, I.M., Minn, K. and Chen, J. (2004) UV-induced ataxia-telangiectasia-mutated and Rad3-related (ATR) activation requires replication stress. J Biol Chem, 279, 9677-80.

61. Staszewski, O., Nikolova, T. and Kaina, B. (2008) Kinetics of gamma-H2AX focus formation upon treatment of cells with UV light and alkylating agents. Environ Mol Mutagen, 49, 734-40.

62. Liu, J.S., Kuo, S.R. and Melendy, T. (2003) Comparison of checkpoint responses triggered by DNA polymerase inhibition versus DNA damaging agents. Mutat Res, 532, 215-26.

63. Marti, T.M., Hefner, E., Feeney, L., Natale, V. and Cleaver, J.E. (2006) H2AX phosphorylation within the G1 phase after UV irradiation depends on nucleotide excision repair and not DNA double-strand breaks. Proc Natl Acad Sci U S A, 103, 9891-6.

64. Symington, L.S. (2002) Role of RAD52 epistasis group genes in homologous recombination and double-strand break repair. Microbiol Mol Biol Rev, 66, 630-70, table of contents.

65. Wei, L., Lan, L., Hong, Z., Yasui, A., Ishioka, C. and Chiba, N. (2008) Rapid recruitment of BRCA1 to DNA double-strand breaks is dependent on its association with Ku80. Mol Cell Biol, 28, 7380-93.

66. Anderson, C.W., Dunn, J.J., Freimuth, P.I., Galloway, A.M. and Allalunis-Turner, M.J. (2001) Frameshift mutation in PRKDC, the gene for DNA-PKcs, in the DNA repair-defective, human, glioma-derived cell line M059J. Radiat Res, 156, 2-9.

67. Harper, J.V. (2005) Synchronization of cell populations in G1/S and G2/M phases of the cell cycle. Methods Mol Biol, 296, 157-66.

68. Affar, E.B., Gay, F., Shi, Y., Liu, H., Huarte, M., Wu, S., Tucker, C., Li, E. and Shi, Y. (2006) Essential dosage-dependent functions of the transcription factor Yin Yang 1 in late embryonic development and cell cycle progression. Mol. Cell Biol., 26, 3565-3581.

69. Sui, G., Affar el, B., Shi, Y., Brignone, C., Wall, N.R., Yin, P., Donohoe, M., Luke, M.P., Calvo, D., Grossman, S.R. and Shi, Y. (2004) Yin Yang 1 is a negative regulator of p53. Cell, 117, 859-872.

Figure Legends

Figure 1. Downregulation of BRCA1 protein during genotoxic stress. A) Top, BRCA1 expression in HeLa cells treated with UVC (30 J/m2) was detected by immunoblotting after harvesting at the indicated times. Bottom, immunostaining of BRCA1 at 4 hrs post-treatment. DNA was counterstained with DAPI. B) BRCA1 levels in HeLa cells treated with IR (10 Gy) for the indicated times. C) BRCA1 levels in HeLa cells treated with the DNA alkylating agent, methylmethanesulfonate (MMS, 200 μM) for the indicated times. D) BRCA1 levels in various cell types treated with 200 μM MMS for the indicated times. All immunoblottings were conducted using total cell extracts. β-actin was detected to ensure equal protein loading.

Figure 2. BRCA1 downregulation is independent of apoptosis and is reversible. A) Immunostaining of BRCA1 in HeLa cells treated with 200 μM MMS. Cells were harvested at 3 and 6 hrs or changed to MMS free medium for the later times. The nuclei were counterstained with DAPI. B) Top left, immunoblotting of BRCA1 and apoptosis markers, PARP-1 and Caspase-3, in HeLa cells treated as indicated above. Bottom left, BRCA1 band intensity was quantified and data are expressed as percentage of untreated cells. Right, immunoblotting for PARP-1 and Caspase-3 following treatment with high dose of UVC (100 J/m2).

Figure 3. Downregulation of BRCA1 occurs independently of the cell cycle phases. A) Synchronized HeLa cells using a thymidine double block (TDB) method were treated with 200 μM MMS for 3 hrs at various time points post-release. Cell cycle analysis (top panel) and immunoblotting (low panel) were conducted at the indicated time points. B) Downregulation

of BRCA1 during cell cycle progression in primary cells. Top, human primary fibroblasts were synchronized in G0/G1 by contact inhibition and were released by replating at low density. Bottom, following UVC (30 J/m2) treatment for the last 2 hrs, cell were harvested at the indicated times for immunoblotting. β-actin immunodetection was used as loading control.

Figure 4. The DNA damage-activated PIKKs family members ATM, ATR and DNA-PK are not required for downregulation of BRCA1. A) Immunoblotting detection of BRCA1 in HeLa cells treated with 10 Gy IR or 200 μM MMS. B) BRCA1 downregulation is not blocked by caffeine. Immunoblotting detection of BRCA1 in HeLa cells pre-treated with 10 mM caffeine for 30 min prior to 200 μM MMS treatment for 6 hrs. C) The downregulation of BRCA1 is not prevented by the ATM inhibitor (KU-55933). Immunoblotting detection of BRCA1 in HeLa cells pre-treated with 10 μM KU-55933 for 30 min prior to 200 μM MMS treatment for 6 hrs. γH2AX and pCHK2 detection were used as controls to confirm inhibition of ATM and/or ATR kinases. D) BRCA1 is downregulated in ATM-deficient human fibroblasts. Cells were treated with 200 μM MMS treatment for 6 hrs and harvested for immunoblotting. E) Depletion of ATR by RNAi does not prevent BRCA1 downregulation by MMS. Left, immunodetection of ATR following transfection and selection. Right, ATR-depleted cells were treated with 200 μM MMS and harvested at the indicated times for immunoblotting. F) BRCA1 is downregulated in DNA-PKcs deficient cells. Glioblastoma DNA-PKcs proficient (MO59K) or deficient (MO59J) were treated with 200 μM MMS and harvested at the indicated times for immunoblotting.

Figure 5. The BRCT motif, but not the ring finger domain, is required for MMS-induced BRCA1 downregulation. A) schematic view of the deletion constructs used in this study. B) HeLa cells were transfected with various expression constructs for BRCA1 and 2 days post-transfection, cells were treated with 200 μM MMS and harvested at the indicated times for immunoblotting to detect either endogenous BRCA1 or mutant forms using anti-BRCA1 or anti-GFP respectively. β-actin immunodetection was used as a loading control.

Figure 6. MMS induces a biphasic response of homologous recombination proteins. A) Immunodetection of various BRCA1-associated and DNA damage/repair proteins following treatment of HeLa cells with 200 μM MMS. HeLa cells were treated with 200 μM MMS and harvested at the indicated times for immunoblotting. The star indicates the specific protein band detected with a given antibody. B) Foci formation of HR proteins following MMS treatment. HeLa cells were treated with 200 μM MMS and harvested at the indicated times for immunostaining. Bottom, cells with more than 10 foci were counted and the data are presented as percentage of cells with foci under each condition. The values represent the average ± SD of three independent experiments

Figure 7. The proteasome mediates BRCA1 and BARD1 downregulation following MMS treatment. A) Cells were incubated with 20 μg/ml of cycloheximide alone or with 200 μM MMS (with or without cycloheximide) and harvested at the indicated times for immunoblotting. B) Cells were pre-treated with 20 μM proteasome inhibitor MG132 for 30 min and then incubated with MMS in the presence of the inhibitor and harvested at 6 hrs for immunoblotting. C) Detection of BRCA1 ubiquitination following DNA damage in Hela cells

(left panel) or HEK293T cells (right panel). Following MMS treatment for 3 hrs, cell extracts were used for immunoprecipitation with an anti-BRCA1 antibody. A non-related polyclonal antibody was used as a control. The immunoprecipitates were used for immunoblotting using anti-BRCA1 or anti-ubiquitin antibodies. Densitometric quantification was conducted on BRCA1 and ubiquitin and the ratio ubiquitin/BRCA1 is shown.

Figure 8. BRCA1/BARD1 downregulation prevents recruitment of these proteins along with Rad51 to chromatin following MMS treatment. A) HeLa cells were treated for 6 hrs with IR (10 Gy) or 200 μM MMS (with or without pretreatment with MG132). Chromatin from control or treated cells was prepared as described in material and methods and proteins were detected by western blotting. B) HeLa cells were treated as in panel A and harvested for immunostaining (left panel). Cells with more than 10 foci were counted and the data are presented as percentage of cells with foci under each condition (Right panel). The values represent the average ± SD of three independent experiments. C) Hela cells were treated as in A except that a premeabilization step was added before fixation and immunostaining (left panel). Cells with more than 10 foci were counted and the data are presented as percentage of cells with foci under each condition (Right panel). The values represent the average ± SD of three independent experiments.

Figure 9. The DNA alkylating agent MMS induces the disassembly of BRCA1/BARD1/Rad51 from IRIF. A) U2OS cells were pre-treated with IR (10 Gy) for 12 hrs and then with or without 200 μM MMS for 6 hrs and harvested for immunostaining. Bottom, cells with more than 10 foci were counted and the data are presented as percentage of

cells with foci under each condition. The values represent the average ± SD of three independent experiments. B) Immunoblotting detection of BRCA1, BARD1 and Rad51 in HeLa cells pre-treated with IR (10 Gy) for 12 hrs and then left untreated or exposed to 200 μM MMS for 3 and 6 hrs.

Figure 10. Model indicating a biphasic response of the homologous recombination pathway induced by the alkylating agent MMS. In response to MMS, human cells induce a signaling pathway that culminate in BRCA1/BARD1 downregulation. This prevents the unwanted assembly of the HR machinery at the early stage of the MMS-induced DNA damage response. At the second stage, recovery and assembly of HR proteins ensure the repair of DSBs generated by replication blocks.

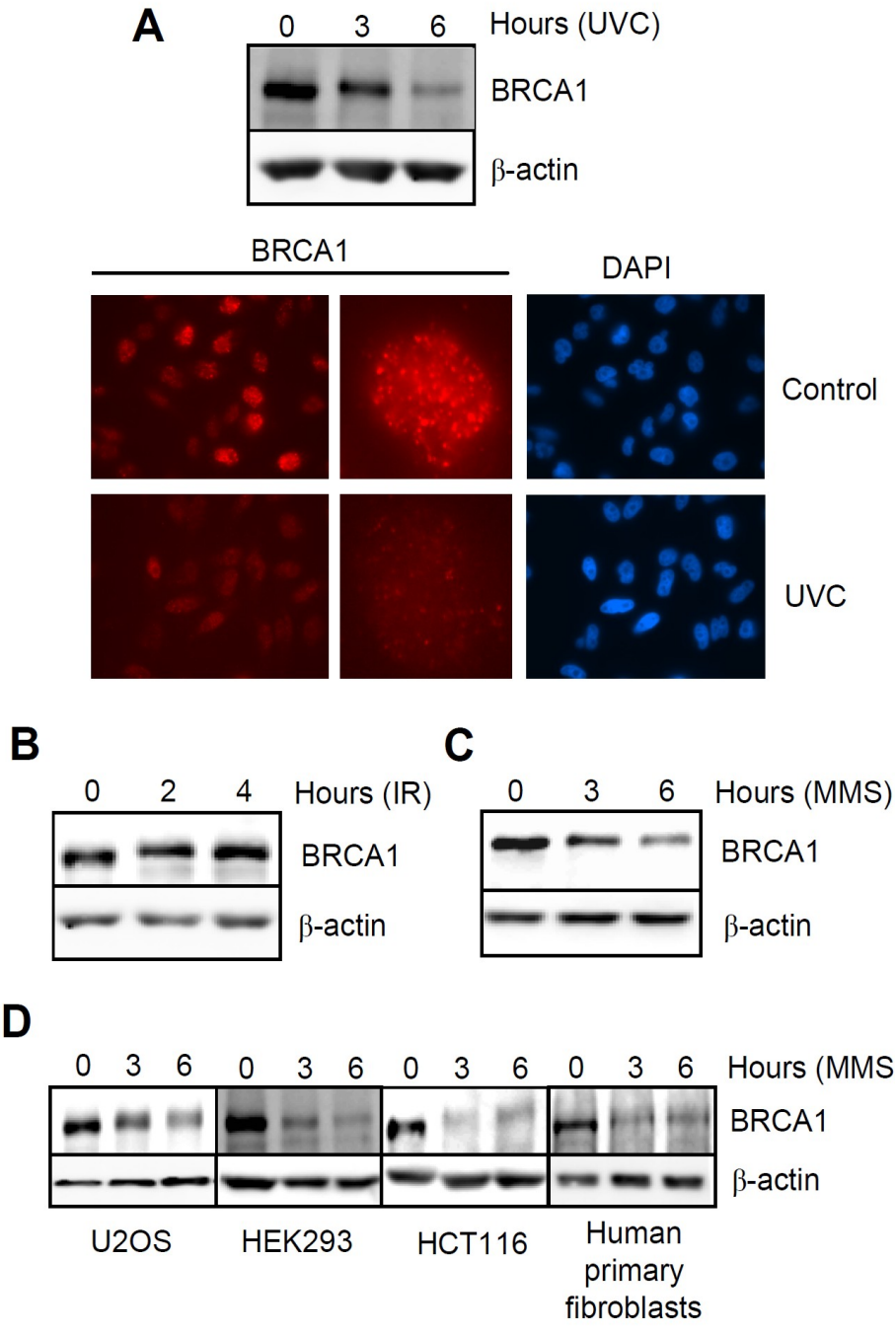
A
0 3 6
Hours (UVC)
BRCA1
β-actin
BRCA1
DAPI
Control
UVC
B
0 2 4
Hours (IR)
BRCA1
β-actin
C
0 3 6
Hours (MMS)
BRCA1
β-actin
D
0 3 6 0 3 6 0 3 6 0 3 6
Hours (MMS
BRCA1
β-actin
U2OS
HEK293
HCT116
Human primary fibroblasts

Figure 1

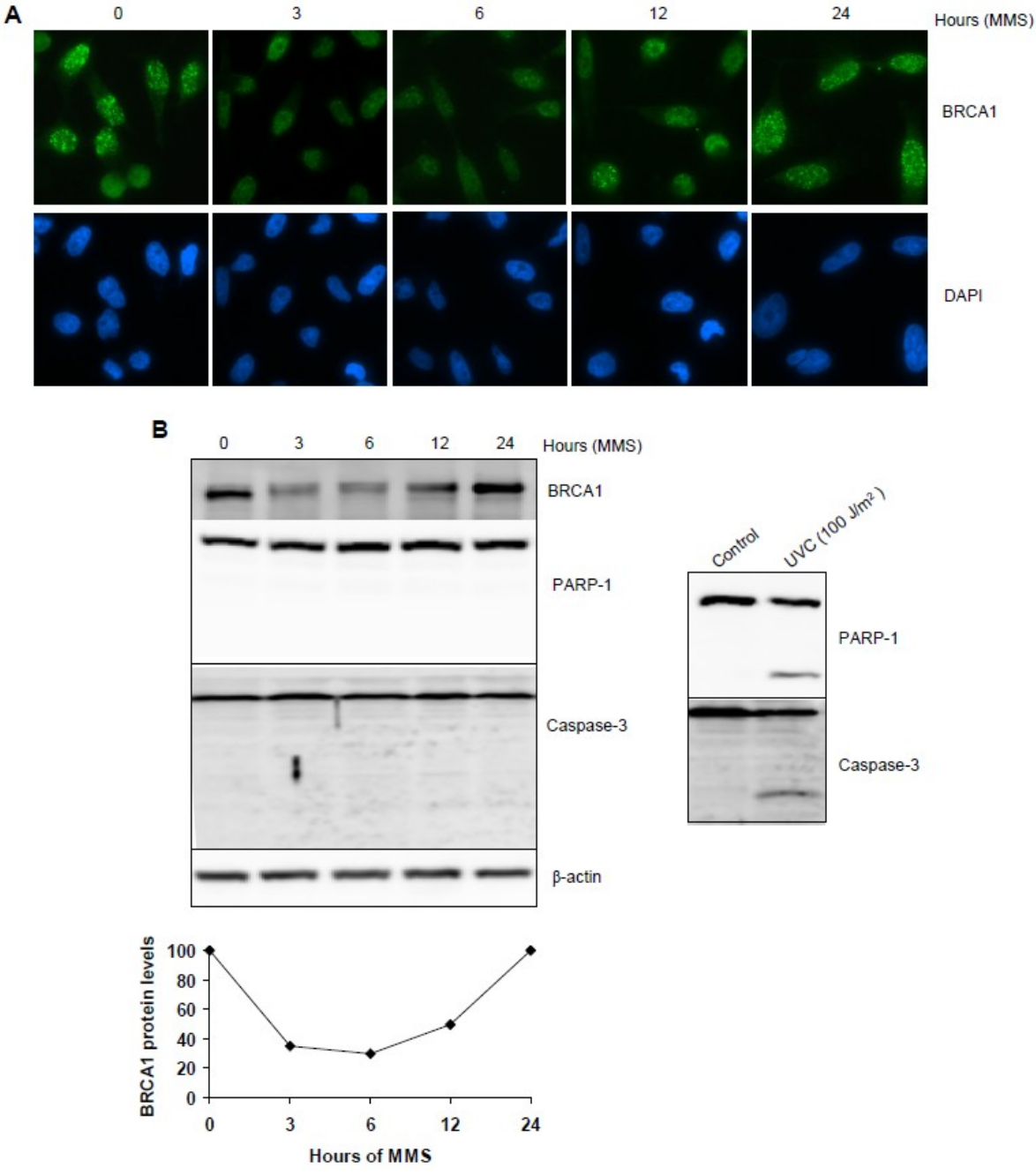
A
0
3
6
12
24
Hours (MMS)
BRCA1
DAPI
B
0
3
6
12
24
Hours (MMS)
BRCA1
PARP-1
Caspase-3
β-actin
Control
UVC (100 J/m²)
PARP-1
Caspase-3
BRCA1 protein levels
100
80
60
40
20
0
0
3
6
12
24
Hours of MMS

Figure 2

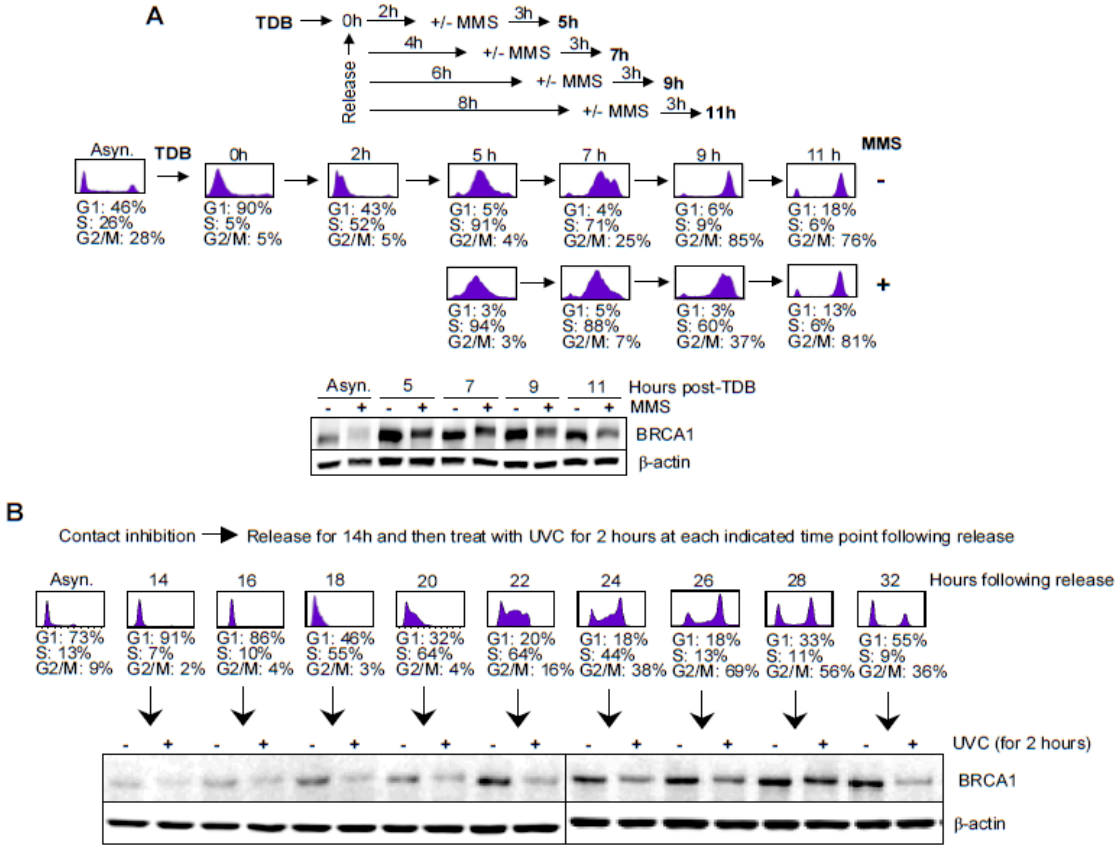
A
TDB
0h
2h
+/- MMS
3h
5h
4h
+/- MMS
3h
7h
6h
+/- MMS
3h
9h
8h
+/- MMS
3h
11h
Release
Asyn.
TDB
0h
2h
5 h
7 h
9 h
11 h
MMS
-
G1: 46%
S: 26%
G2/M: 28%
G1: 90%
S: 5%
G2/M: 5%
G1: 43%
S: 52%
G2/M: 5%
G1: 5%
S: 91%
G2/M: 4%
G1: 4%
S: 71%
G2/M: 25%
G1: 6%
S: 9%
G2/M: 85%
G1: 18%
S: 6%
G2/M: 76%
+
G1: 3%
S: 94%
G2/M: 3%
G1: 5%
S: 88%
G2/M: 7%
G1: 3%
S: 60%
G2/M: 37%
G1: 13%
S: 6%
G2/M: 81%
Asyn.
5
7
9
11
Hours post-TDB
MMS
BRCA1
β-actin
B
Contact inhibition
Release for 14h and then treat with UVC for 2 hours at each indicated time point following release
Asyn.
14
16
18
20
22
24
26
28
32
Hours following release
G1: 73%
S: 13%
G2/M: 9%
G1: 91%
S: 7%
G2/M: 2%
G1: 86%
S: 10%
G2/M: 4%
G1: 46%
S: 55%
G2/M: 3%
G1: 32%
S: 64%
G2/M: 4%
G1: 20%
S: 64%
G2/M: 16%
G1: 18%
S: 44%
G2/M: 38%
G1: 18%
S: 13%
G2/M: 69%
G1: 33%
S: 11%
G2/M: 56%
G1: 55%
S: 9%
G2/M: 36%
UVC (for 2 hours)
BRCA1
β-actin

Figure 3

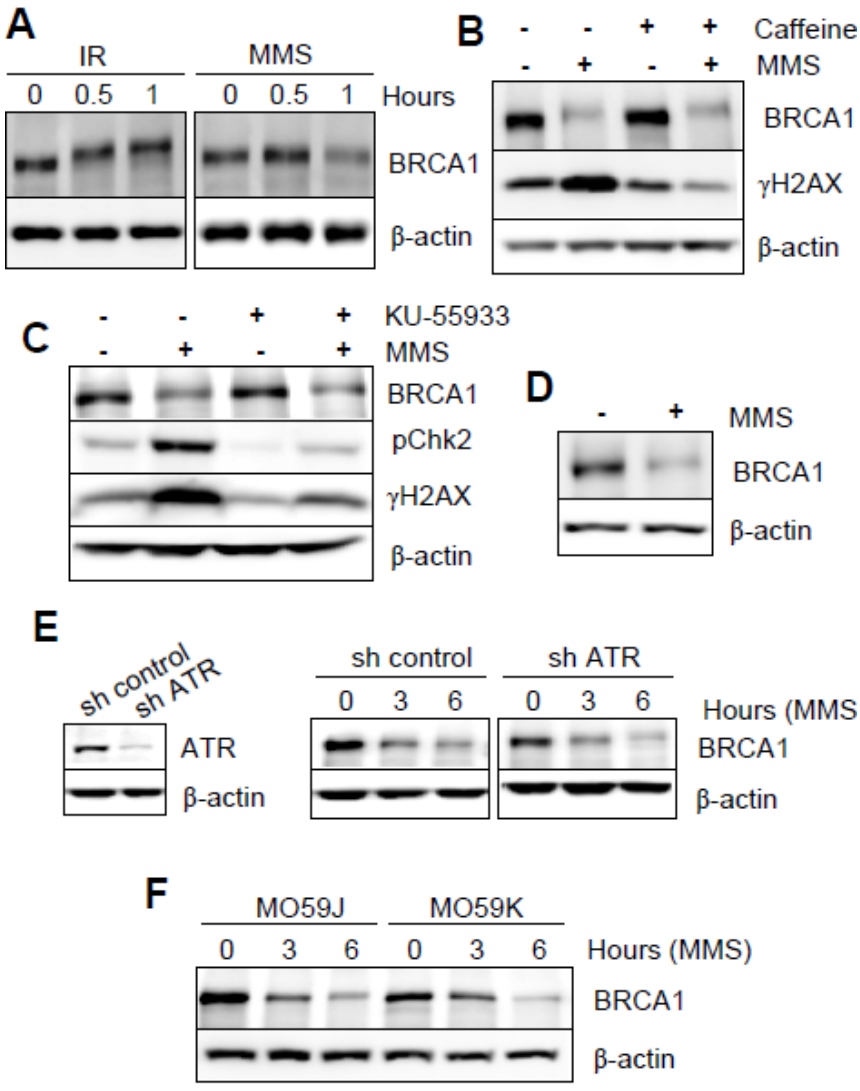
A
IR
MMS
0 0.5 1 0 0.5 1
Hours
BRCA1
β-actin
B
- - + + Caffeine
- + - + MMS
BRCA1
γH2AX
β-actin
C
- - + + KU-55933
- + - + MMS
BRCA1
pChk2
γH2AX
β-actin
D
- + MMS
BRCA1
β-actin
E
sh control
sh ATR
ATR
β-actin
sh control
sh ATR
0 3 6 0 3 6
Hours (MMS
BRCA1
β-actin
F
MO59J
MO59K
0 3 6 0 3 6
Hours (MMS)
BRCA1
β-actin

Figure 4

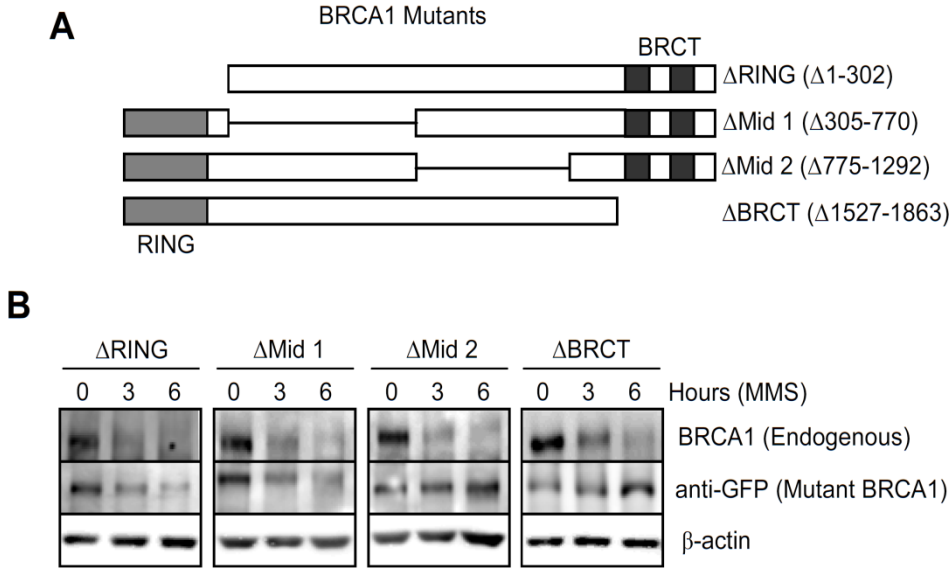
A
BRCA1 Mutants
BRCT
ΔRING (Δ1-302)
ΔMid 1 (Δ305-770)
ΔMid 2 (Δ775-1292)
ΔBRCT (Δ1527-1863)
RING
B
ΔRING
ΔMid 1
ΔMid 2
ΔBRCT
0 3 6 0 3 6 0 3 6 0 3 6
Hours (MMS)
BRCA1 (Endogenous)
anti-GFP (Mutant BRCA1)
β-actin

Figure 5

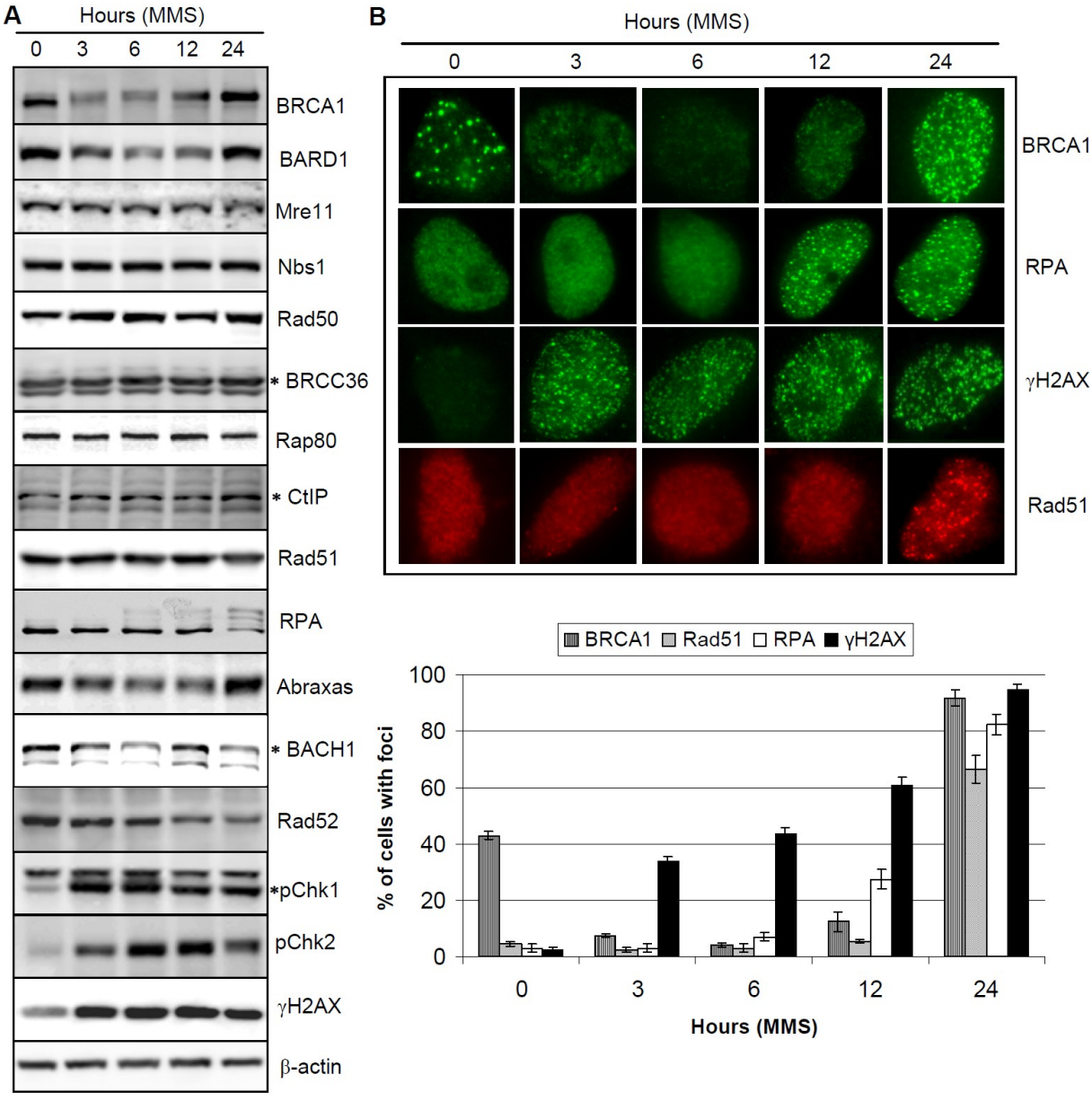
A
Hours (MMS)
0 3 6 12 24
BRCA1
BARD1
Mre11
Nbs1
Rad50
* BRCC36
Rap80
* CtIP
Rad51
RPA
Abraxas
* BACH1
Rad52
*pChk1
pChk2
γH2AX
β-actin
B
Hours (MMS)
0 3 6 12 24
BRCA1
RPA
γH2AX
Rad51
BRCA1 Rad51 RPA γH2AX
% of cells with foci
100
80
60
40
20
0
0 3 6 12 24
Hours (MMS)

Figure 6

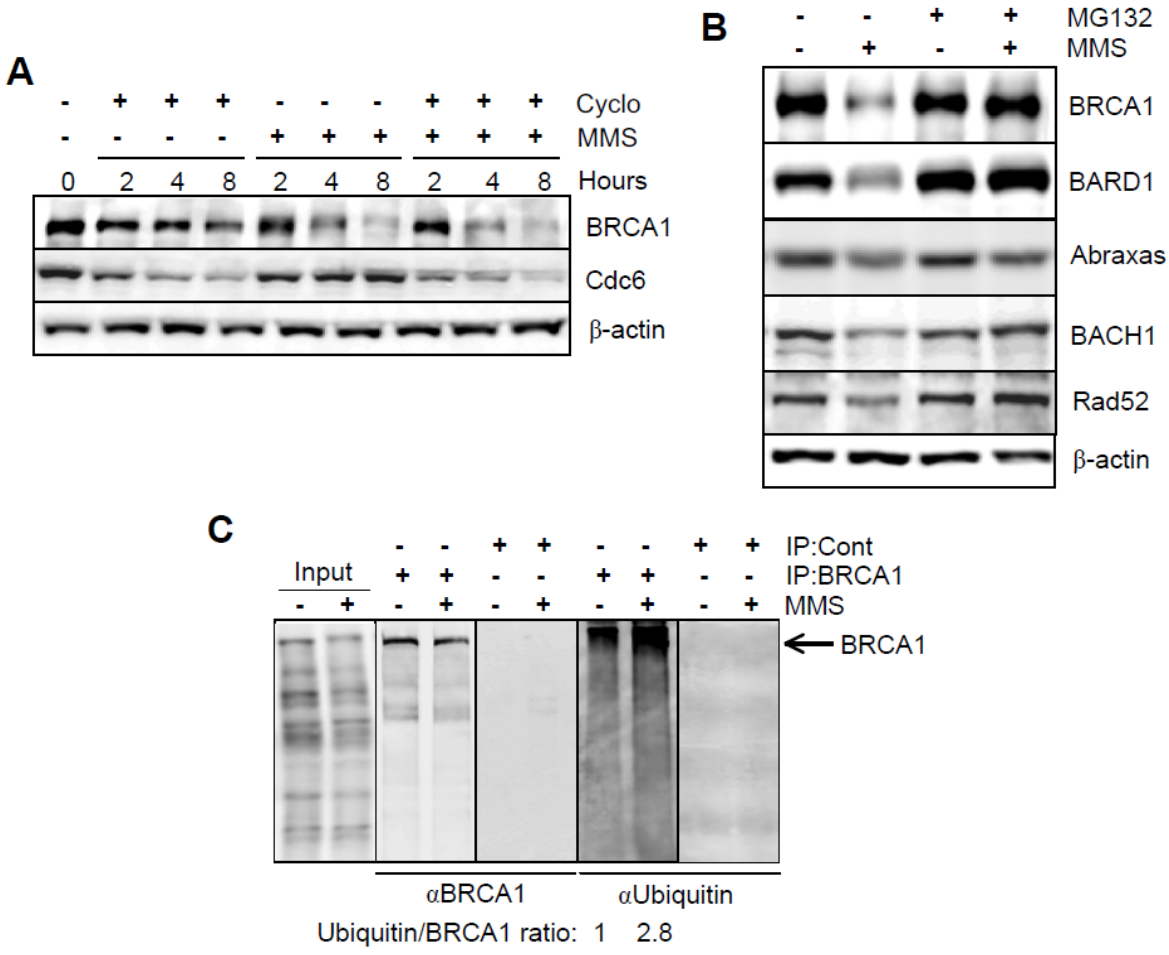
A
Cyclo
MMS
Hours
0 2 4 8 2 4 8 2 4 8
BRCA1
Cdc6
β-actin
B
MG132
MMS
BRCA1
BARD1
Abraxas
BACH1
Rad52
β-actin
C
IP:Cont
IP:BRCA1
MMS
Input
BRCA1
αBRCA1
αUbiquitin
Ubiquitin/BRCA1 ratio: 1 2.8

Figure 7

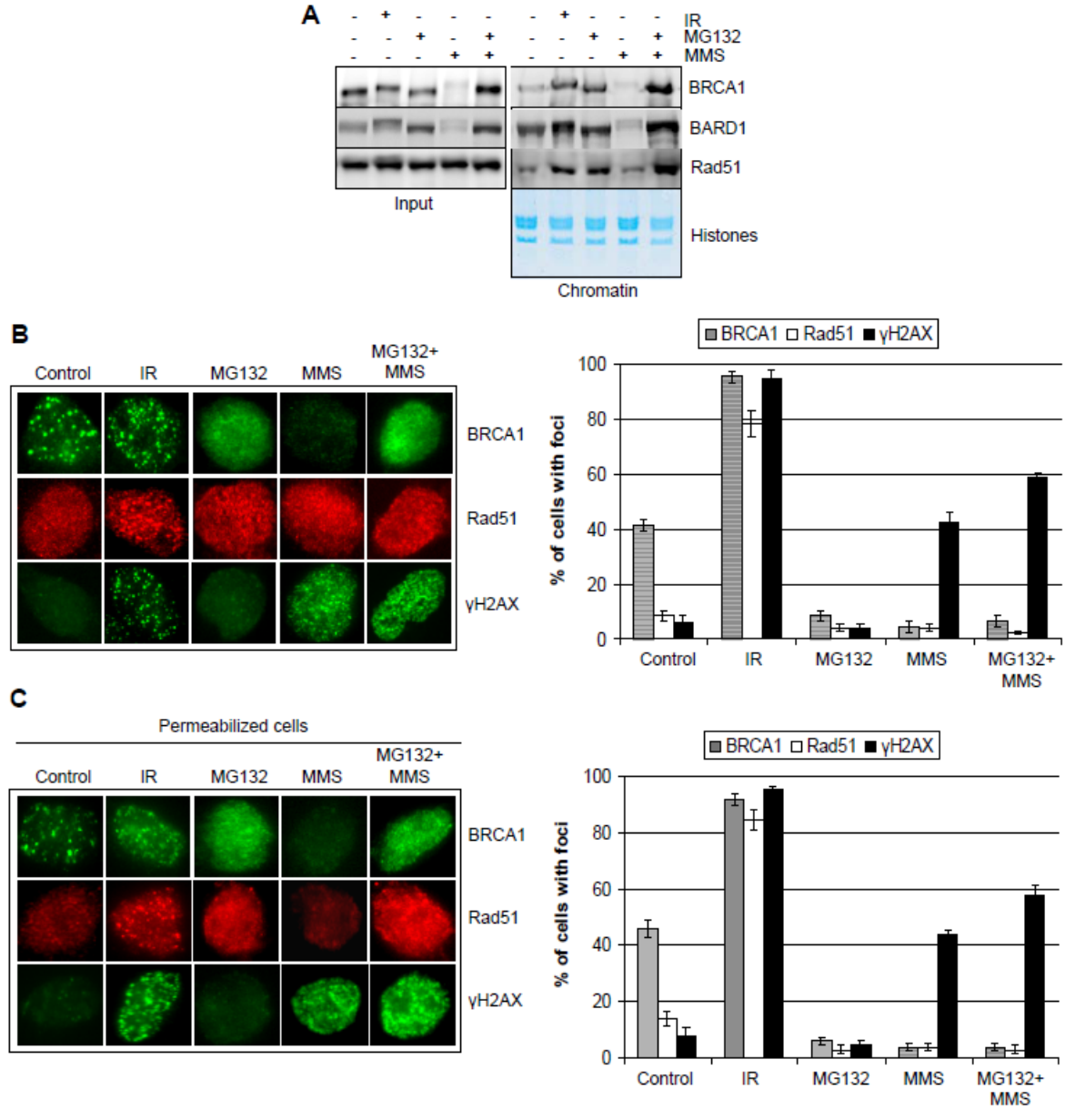
A
IR
MG132
MMS
BRCA1
BARD1
Rad51
Histones
Input
Chromatin
B
Control
IR
MG132
MMS
MG132+ MMS
BRCA1
Rad51
γH2AX
BRCA1 Rad51 γH2AX
% of cells with foci
100
80
60
40
20
0
Control
IR
MG132
MMS
MG132+ MMS
C
Permeabilized cells
Control
IR
MG132
MMS
MG132+ MMS
BRCA1
Rad51
γH2AX
BRCA1 Rad51 γH2AX
% of cells with foci
100
80
60
40
20
0
Control
IR
MG132
MMS
MG132+ MMS

Figure 8

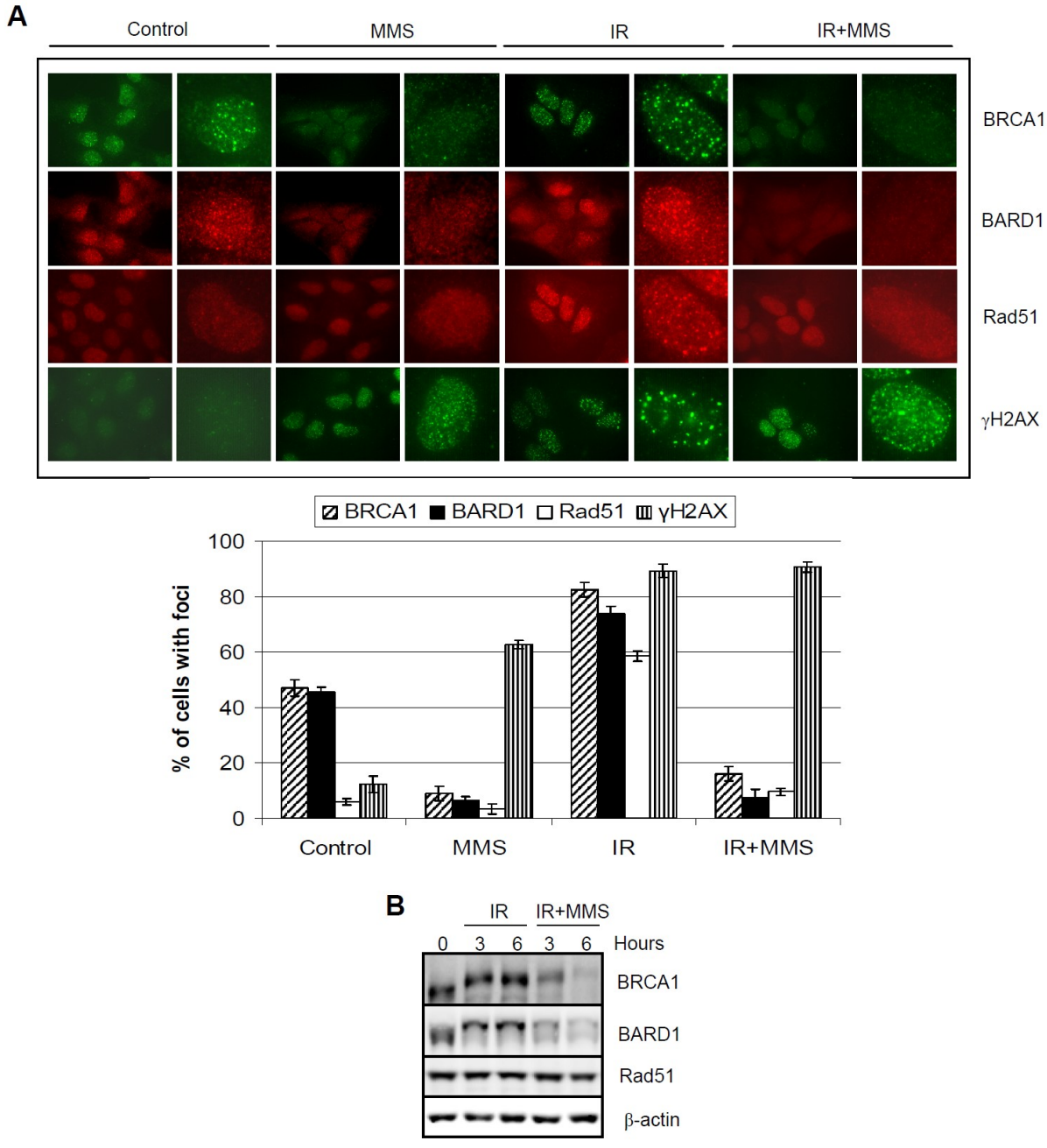
A
Control
MMS
IR
IR+MMS
BRCA1
BARD1
Rad51
γH2AX
BRCA1 BARD1 Rad51 γH2AX
% of cells with foci
100
80
60
40
20
0
Control
MMS
IR
IR+MMS
B
IR
IR+MMS
0 3 6 3 6 Hours
BRCA1
BARD1
Rad51
β-actin

Figure 9

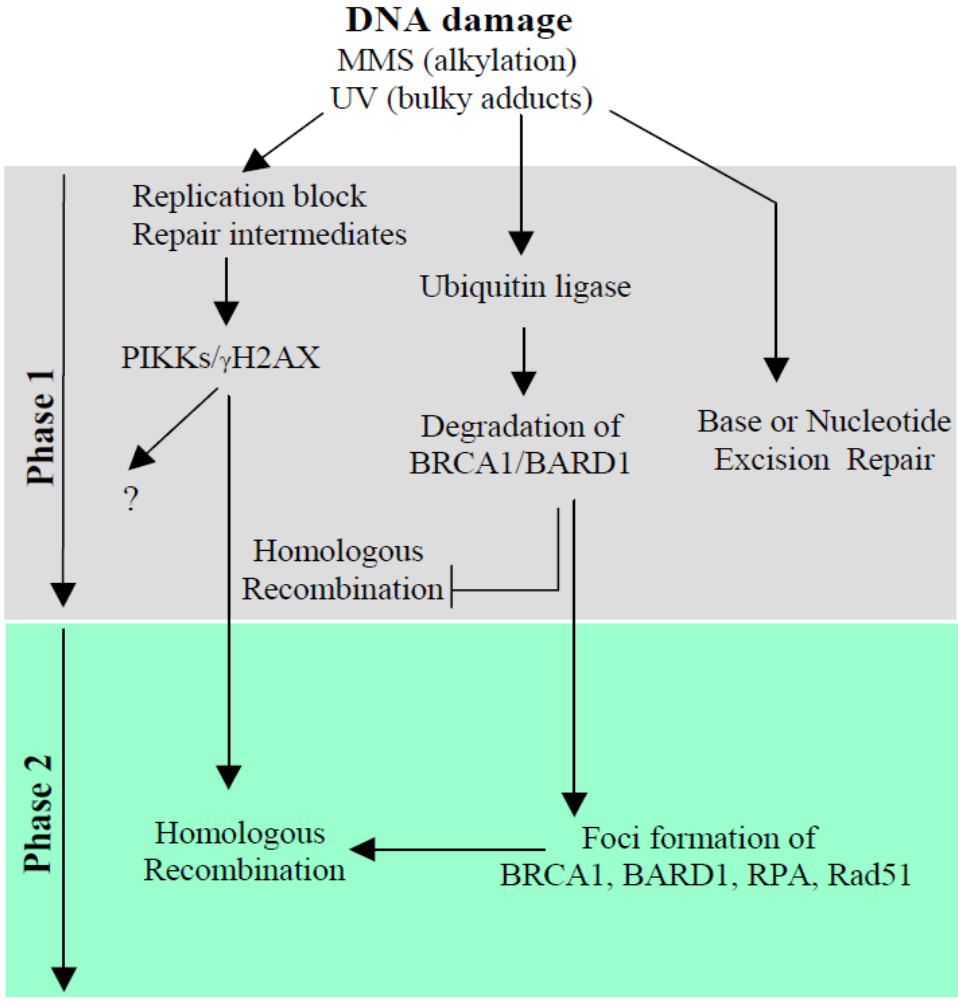
DNA damage
MMS (alkylation)
UV (bulky adducts)
Replication block
Repair intermediates
Ubiquitin ligase
PIKKs/γH2AX
Degradation of
BRCA1/BARD1
Base or Nucleotide
Excision Repair
?
Homologous
Recombination
Phase 1
Phase 2
Homologous
Recombination
Foci formation of
BRCA1, BARD1, RPA, Rad51

Figure 10

Supplementary Information contains one table for the antibodies used and 11 figures

Supplemental Table 1. Antibodies used in this study

Proteins	Name of antibodies	Company or Reference	Catalogue number	Application and Dilution
BRCA1	MS110 (Ab-1) (mono)	Calbiochem	OP92	Western (1/100) and Immunofluorescence (1/100)
BRCA1	SD118 (mono)	Livingston (1)	N/A	Western (1/20)
BRCA1	Rabbit poly	(2)	N/A	Western (1/2000) and Immunofluorescence (1/9000)
BRCA1	I-20 (rabbit poly)	Santa Cruz	sc-646	Immunoprecipitation (1/25)
BARD1	2059C4a (mono)	Santa Cruz	sc-81195	Western (1/200)
BARD1	H-300 (poly)	Santa Cruz	sc-11438	Immunofluorescence (1/200)
BACH1	A300-561A	Bethyl Laboratories	A300-561A	Western (1/1000)
CtIP	A300-488A	Bethyl Laboratories	A300-488A	Western (1/500)
βActin	Anti-actin, clone 4 (mono)	Millipore	MAB1501	Western (1/500 000)
Mre11	C-16 (goat poly)	Santa Cruz	sc-5859	Western (1/200)
Nbs1	1D7 (mono)	Santa Cruz	Sc-56166	Western (1/200)
Rad50	13B3/2C6 (mono)	Santa Cruz	sc-56209	Western (1/500)
Rad51	H-92 (rabbit poly)	Santa Cruz	sc-8349	Western (1/200) and Immunofluorescence (1/500)
Rad52	H-300 (rabbit poly)	Santa Cruz	sc-8350	Western (1/200)
Cdc6	H-304 (rabbit poly)	Santa Cruz	sc-8341	Western (1/200)
pCHK1	Phospho-Chk1 (Ser317) (rabbit poly)	Cell signaling	2344	Western (1/1000)
pCHK2	Phospho-Chk2 (Thr387) (rabbit poly)	Cell signaling	2688	Western (1/1000)
γH2AX	Anti-phospho-Histone H2A.X (Ser139), clone JBW301 (mono)	Millipore	05-636	Western (1/1000) and Immunofluorescence (1/1000)
PARP-1	F2 (mono)	Santa Cruz	sc-8007	Western (1/1000)
Caspase-3	H-277 (rabbit poly)	Santa Cruz	sc-7148	Western (1/200)
Ubiquitin	P4D1 (mono)	Santa Cruz	sc-8017	Western (1/200)
pERK	ERK1/2 [pTpY185/187] (rabbit poly)	Biosource (Invitrogen)	44-680G	Western (1/1000)
pJNK	JNK (SAPK) [pTpY183/185] (rabbit poly)	Biosource (Invitrogen)	44-682G	Western (1/1000)
MAPKAP2	N/A	Cell signaling	3042	Western (1/1000)
DNA-PK	G-4 (mono)	Santa Cruz	sc-5282	Immunofluorescence (1/200)
ATM	2C1 (mono)	Santa Cruz	sc-23921	Western (1/200)
ATR	N19 (goat poly)	Santa Cruz	sc-1887	Western (1/200)
Abraxas	FAM175A	Novus Biologicals	NBP1-22977	Western (1/1000)
GFP	B-2 (mono)	Santa Cruz	sc-9996	Western (1/200)
BRCC36	ab62075	Abcam	Ab62075	Western (1/1000)
RPA	9H8 (mono)	Abcam	Ab2175	Western (1/1000 and Immunofluorescence (1/500)

1. Wilson, C. A., Ramos, L., Villasenor, M. R., Anders, K. H., Press, M. F., Clarke, K., Karlan, B., Chen, J. J., Scully, R., Livingston, D., Zuch, R. H., Kanter, M. H., Cohen, S., Calzone, F. J., and Slamon, D. J. Localization of human BRCA1 and its loss in high-grade, non-inherited breast carcinomas. Nat Genet, *21:* 236-240, 1999.
2. Sankaran, S., Starita, L. M., Simons, A. M., and Parvin, J. D. Identification of domains of BRCA1 critical for the ubiquitin-dependent inhibition of centrosome function. Cancer Res, *66:* 4100-4107, 2006.

Supplementary Figure 1. Immunoblotting detection of BRCA1 at various times post-UV using additional specific antibodies. (A-B) HeLa cells were treated with UVC (30 J/m^2) and harvested at the indicated times for immunodetection with anti-BRCA1 antibodies. The monoclonal SD118 antibody which recognizes the C-terminus (A), or the polyclonal rabbit specific for the middle region (Sankaran et al. 2006) (B), were used. Immunodetection of β-actin was used as loading control.

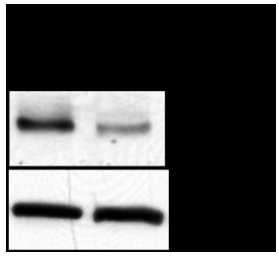

Supplementary Figure 2. Downregulation of BRCA1 with low dose of UVC. Immunoblotting detection of BRCA1 in HeLa cells following treatment with UVC (10 J/m^2). Immunodetection of PARP-1 was used as loading control.

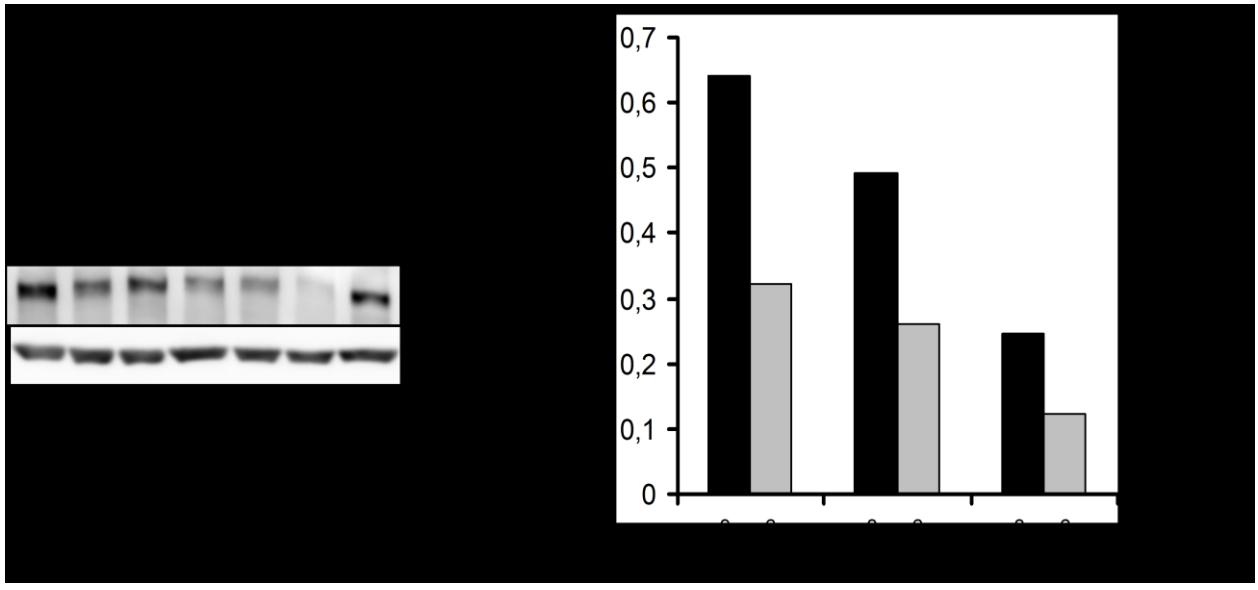

Supplementary Figure 3. Dose-dependent downregulation of BRCA1 following MMS treatment. HEK293 Cells were harvested at the indicated time points for immunoblotting with anti-BRCA1 and anti-β-actin antibodies (left panel). The band signals were directly acquired with a LAS-3000 LCD camera (Fuji, Stamford, CT, USA) coupled to MultiGauge software (Fuji). The protein levels are relative values and are expressed as a ratio BRCA1/β-actin (right panel).

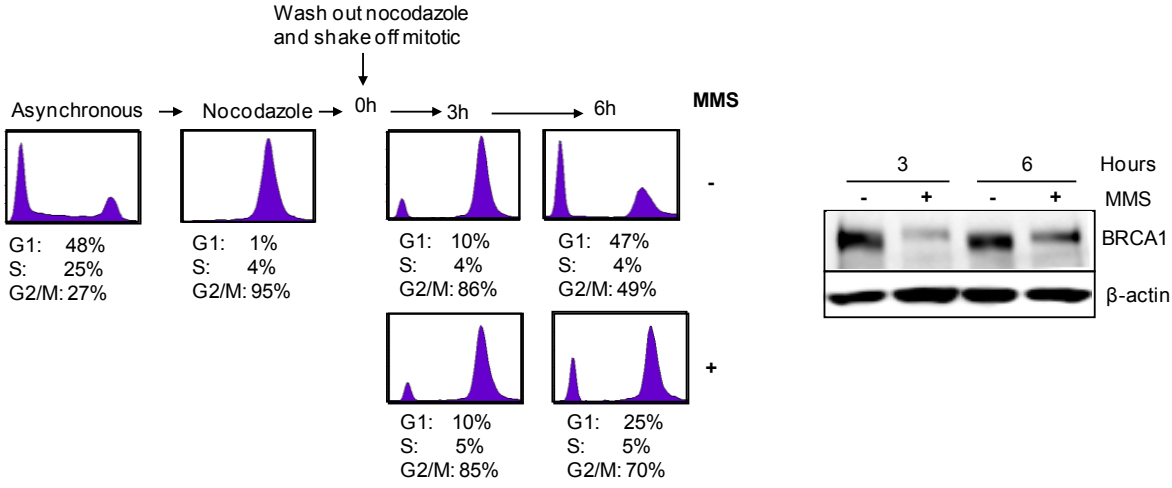

Supplementary Figure 4. Downregulation of BRCA1 occurs in G2 phase. HeLa cells were synchronized in G2/M after 16 hrs exposure to nocodazole. Mitotic cells were removed by shake off and the purified G2 population was treated with 200 μM MMS for 3 hrs at various time points post-removal of nocodazole. Cell cycle analysis (left panel) and immunoblotting (right panel) were conducted at the indicated time points.

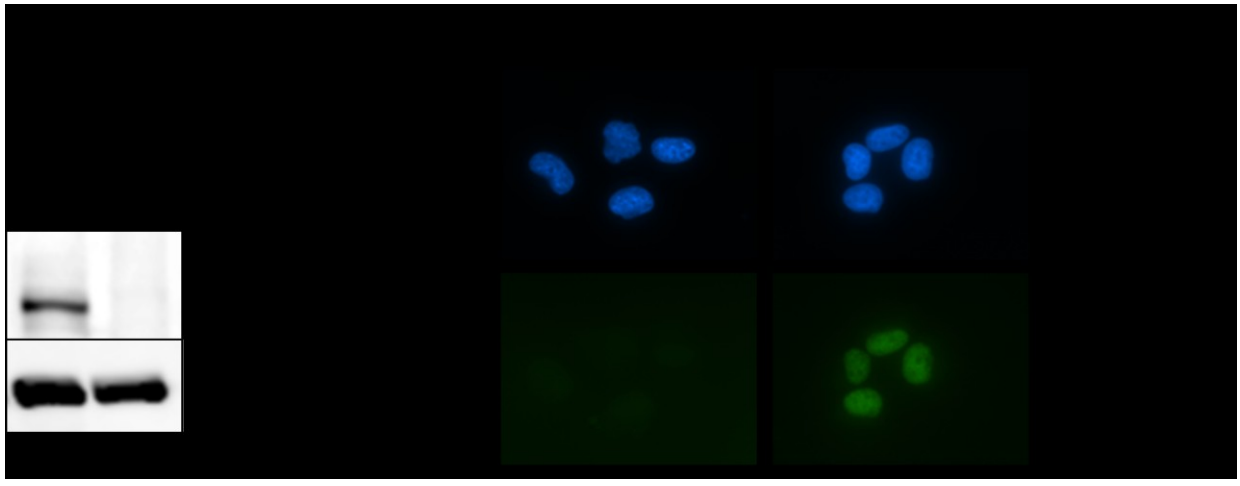

Supplementary Figure 5. Immunodetection of ATM or DNA-PK in the cell lines used. *Left*, HeLa or ATM-deficient fibroblasts were used for immunodetection with anti-ATM antibody. *Right*, Immunostaining detection of DNA-PKcs in glioblastoma cell lines, proficient (MO59K) or deficient (MO59J).

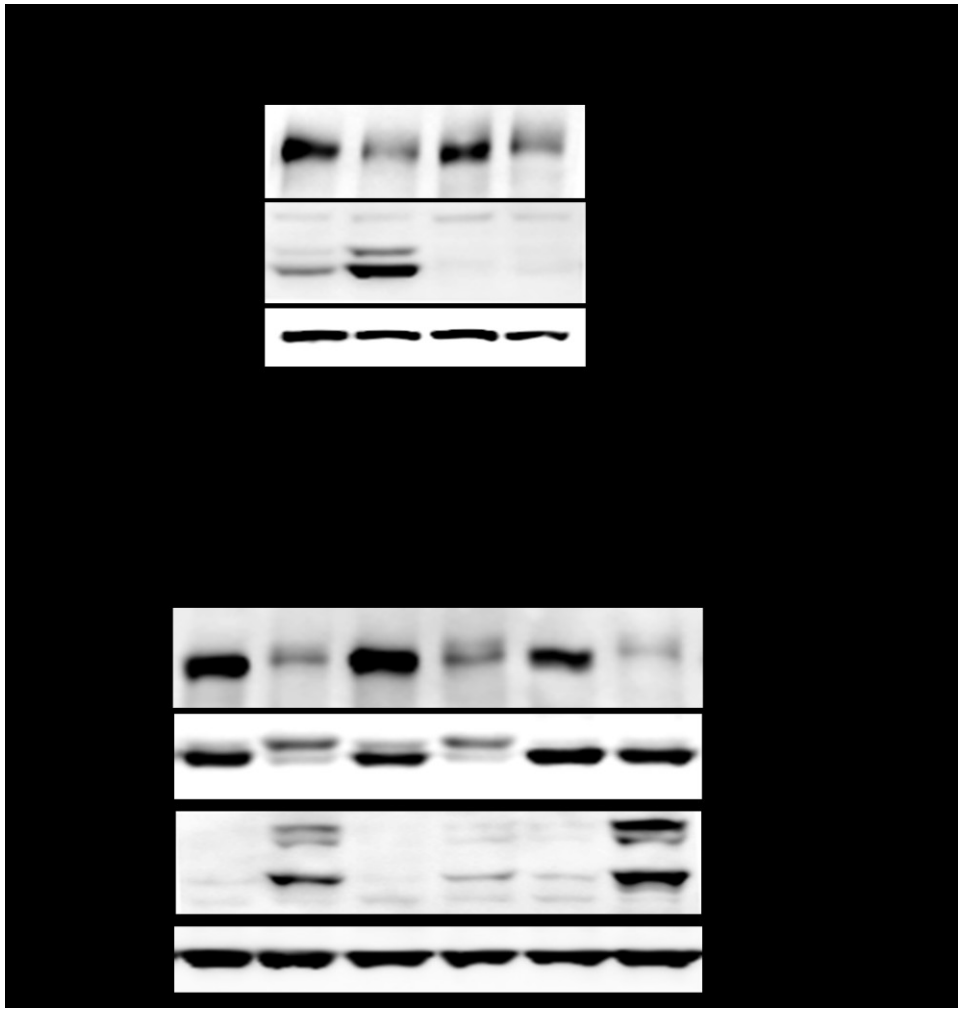

Supplementary Figure 6. DNA damage-activated MAPKs are not required for downregulation of BRCA1. Cells were pre-treated with 20 μM U0126, 30 μM SP600125, or 20 μM SB202190 for 30 min to inhibit signaling pathways involving ERK1/2, JNK1/2, or p38α/β, respectively (Rouget et al. 2008). Cells were then treated with 200 μM MMS and harvested after 3 hrs. Abrogation of MAPK signaling following MMS treatment was evaluated by quantification of MAPK phosphorylation using anti-phospho-ERK1/2, -JNK1/2 antibodies. The inhibition of p38α/β activity was assessed by levels of phosphorylated form of its substrate MAPKAPK2 (MK2), which can be readily distinguished from the unphosphorylated form by band shift using anti-MK2 antibody. β-actin immunodetection was used as a loading control.

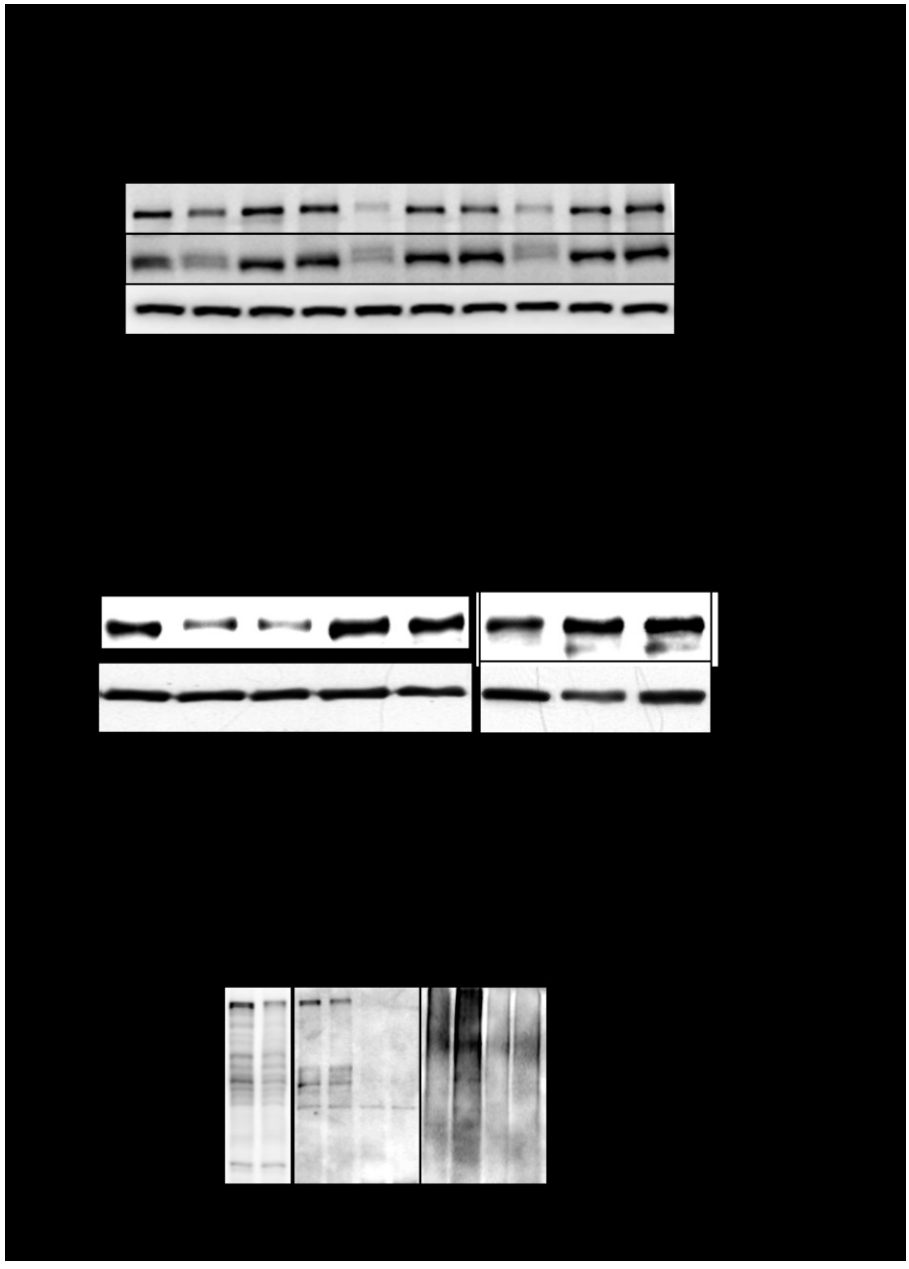

Supplementary Figure 7. The proteasome mediates BRCA1 downregulation in response to DNA damage. (A) HCT116 cells were pre-treated with 20 μM of the proteasome inhibitor MG132 for 30 min and then treated with 200 μM MMS in the presence of the inhibitor, and then harvested at the indicated times for immunoblotting. (B) HeLa cells were pre-treated with 20 μM of another proteasome inhibitor ZL3VS for 30 min and then treated with 30 J/m^2 UVC in the presence of the inhibitor and harvested at the indicated times for immunoblotting.

PARP-1 was used as a loading control. (C) Detection of BRCA1 ubiquitination following DNA damage in HeLa cells. Following MMS treatment for 3 hrs, cell extracts were used for immunoprecipitation with an anti-BRCA1 antibody. A non-related polyclonal antibody was used as a control. The immunoprecipitates were used for immunoblotting using anti-BRCA1 or anti-ubiquitin antibodies. Densitometric quantification was conducted on BRCA1 and ubiquitin and the ratio ubiquitin/BRCA1 is shown.

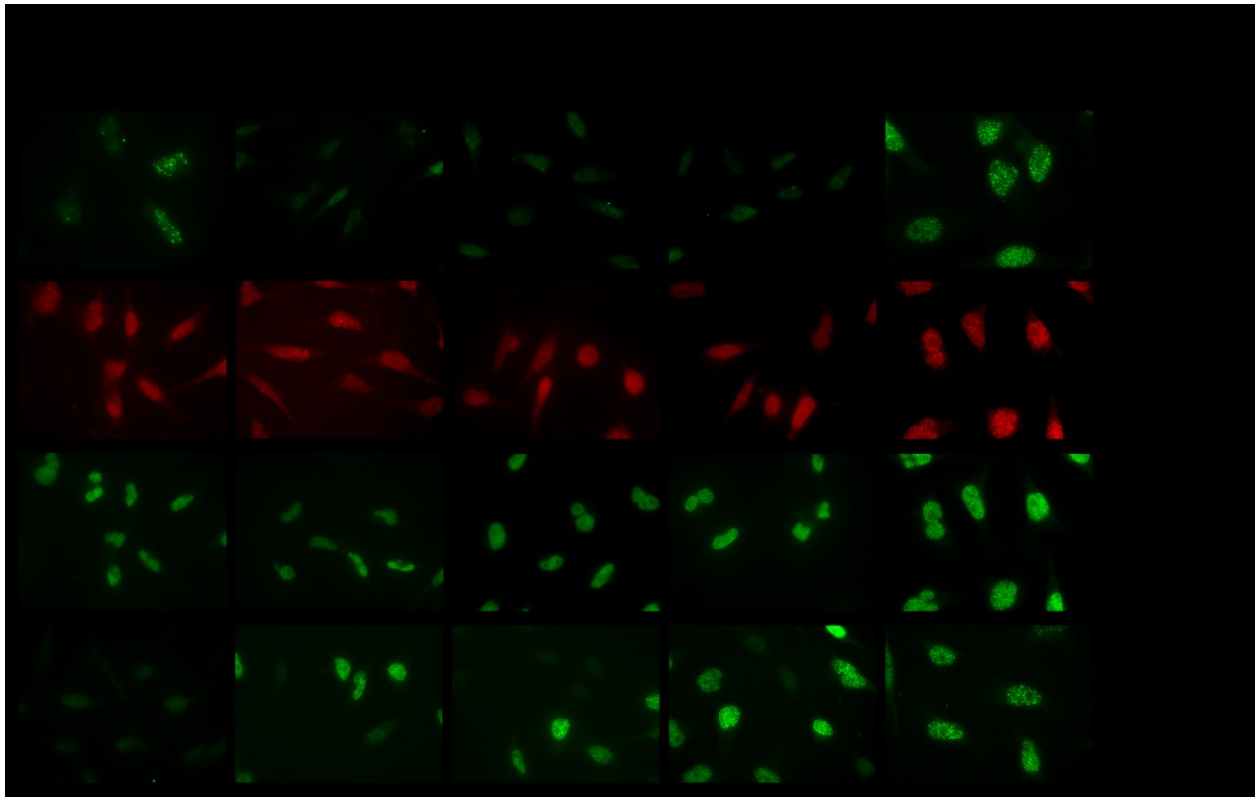

Supplementary Figure 8. Immunostaining for BRCA1, Rad51, RPA or γH2AX following MMS treatment. HeLa cells were treated with 200 μM MMS and harvested for immunostaining.

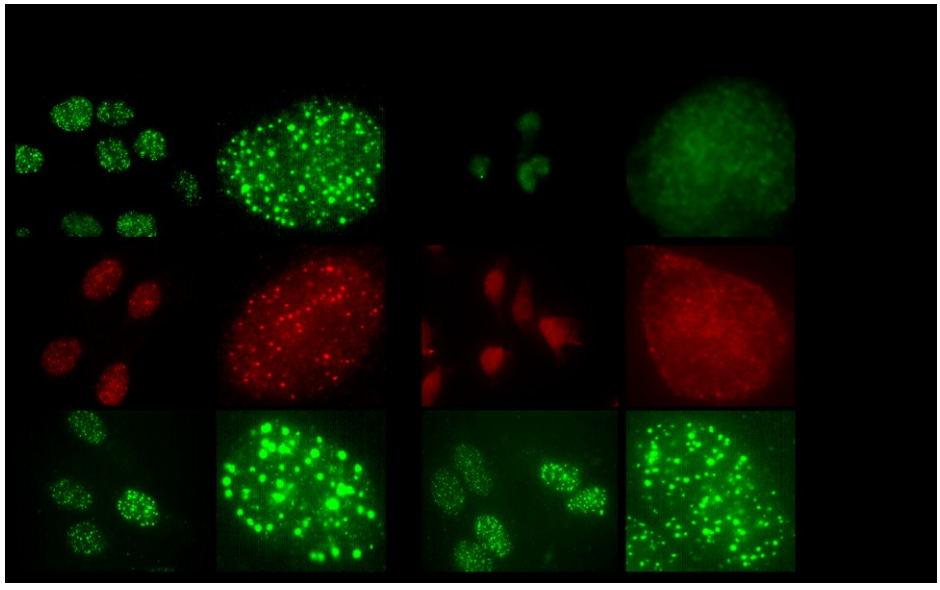

Supplementary Figure 9. Immunostaining for BRCA1, Rad51 and γH2AX Following IR and proteasome inhibition. HeLa cells were treated for 6 hrs with IR (10 Gy) (with or without pretreatment with MG132) and harvested for immunostaining.

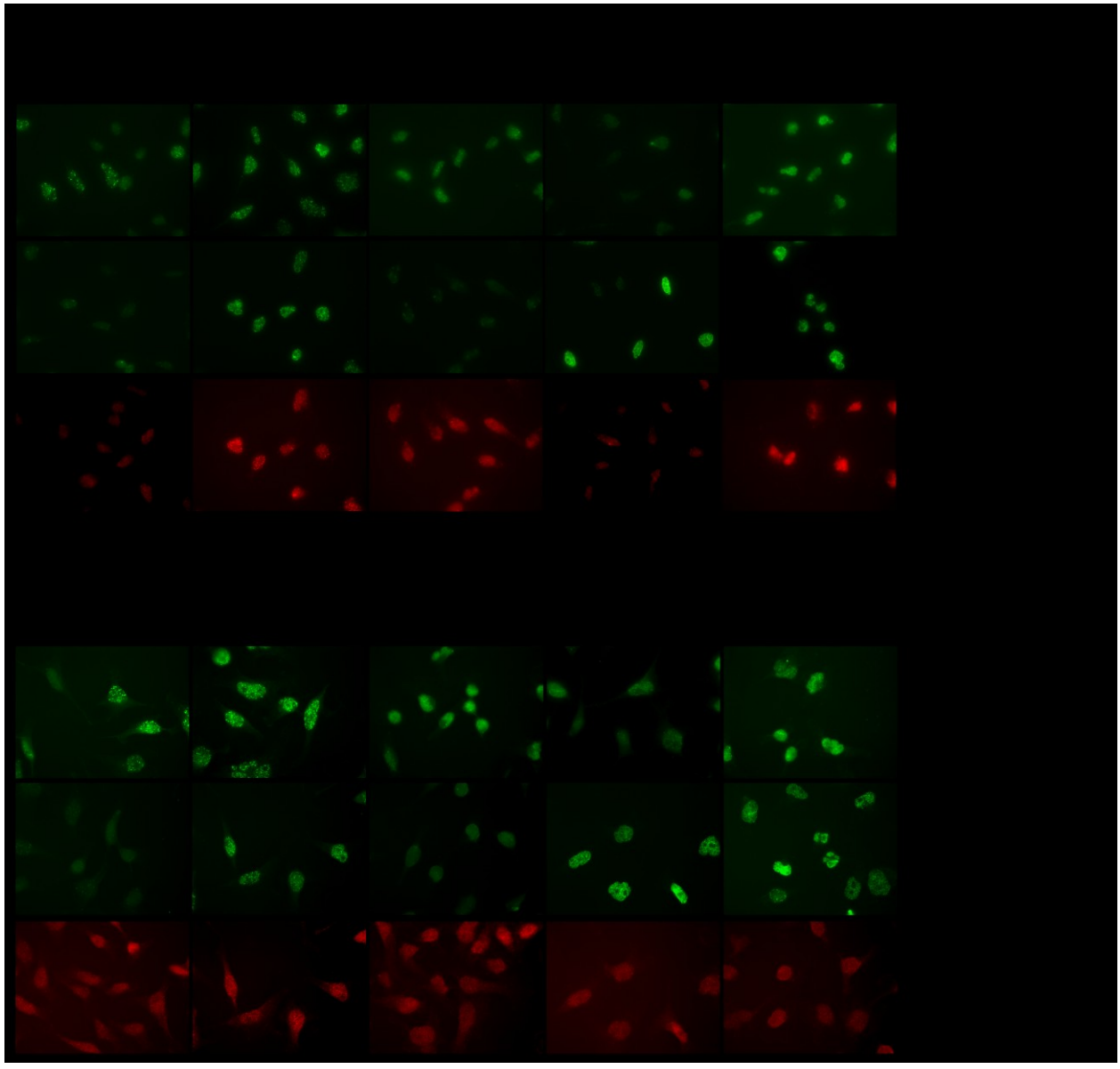

Supplementary Figure 10. Immunostaining for BRCA1, Rad51 and γH2AX in various conditions. HeLa cells were treated for 6 hrs with IR (10 Gy) or 200 μM MMS (with or without pretreatment with MG132) and harvested for immunostaining with *(top panel)* or without (*bottom panel*) a permeabilization step.

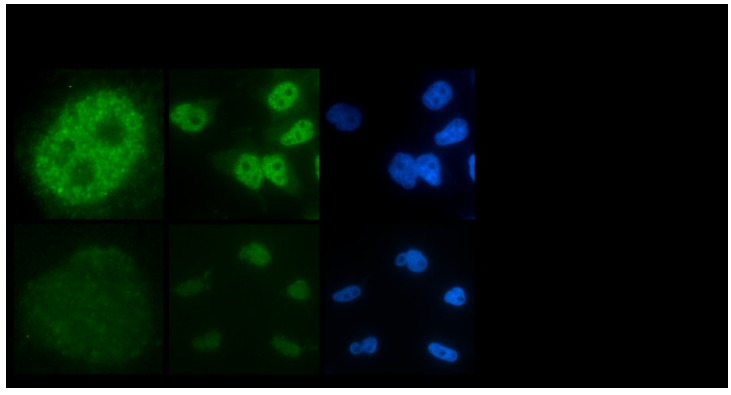

Supplementary Figure 11. Immunostaining for BAP1 following permeabilization. HeLa cells were harvested for immunostaining with *(botton panel)* or without (*top panel*) a permeabilization step.

Chapter 3: Deubiquitination of Histone H2A by the BAP1/ASXL Axis is disrupted by Multiple Cancer-Associated Mechanisms

Salima Daou[#], Ian Hammond-Martel[#], Nazar Mashtalir, Haithem Barbour, Jessica Gagnon, Nadine Sen Nkwe, Nicholas V.G. Ianantuono, Helen Yu, Helen Pak, Alena Motorina, Frédérick A. Mallette and El Bachir Affar[1]

Maisonneuve-Rosemont Hospital Research Center and Department of Medicine, University of Montréal, Montréal H3C 3J7, Québec, Canada

# Equal contribution

[1]Correspondence

El Bachir Affar

Running title: ASXL1 and ASXL2 coordinate BAP1 function

Contributions: S.D, I.H.M., N.M., H.B, J.G., F.A.M. and E.B.A. designed the experiments. S.D., I.H.M., N.M., H.B J.G., N.N.S, N. V.G.I, H.Y., H.P., A.M., F.A.M. and E.B.A. conducted the experiments and performed data analysis. S.D, I.H.M. and E.B.A. wrote the manuscript.

SUMMARY

Monoubiquitination of histone H2A (H2Aub) is a critical epigenetic modification involved in transcriptional repression. In Drosophila, H2Aub is reversed by the deubiquitinase (DUB) and Polycomb group protein Calypso, which associates with Additional Sex Comb (ASX) and forms the Polycomb Repressive DUB (PR-DUB) complex. Here, we report that the tumor suppressor and mammalian ortholog of Calypso, BAP1, forms two mutually exclusive complexes with ASXL1 and ASXL2, two orthologs of ASX. ASXL1 and ASXL2 use their highly conserved ASXM domain to interact with the C-terminal domain (CTD) of BAP1, and these factors regulate each other's protein stability. Significantly, through mutational analysis, we defined two distinct functions of the ASXM, namely enhancing BAP1 binding to ubiquitin and stimulating its DUB activity. Importantly, these functions require intramolecular interactions in BAP1 that generate a composite ubiquitin binding interface (CUBI). Gain and loss of function studies indicated that BAP1, ASXL1 and ASXL2 play critical roles in the coordination of cell cycle progression. Notably, BAP1 is required for ASXL2 protein stability and overexpression of both proteins trigger the p53/p21 DNA damage response and cellular senescence, and these effects are abolished by mutations of the CTD or ASXM interaction domains. Next, we identified cancer-derived mutations of BAP1 and ASXL2 that inhibit H2A DUB activity by multiple mechanisms. Furthermore, we showed that cancer-associated inactivation of BAP1/ASXL1/2 DUB activity disrupts coordination of cell proliferation. Our results indicate that BAP1 and ASXL1/2 exert a tight control on cell cycle progression, and provide a direct mechanistic link between H2A deubiquitination and tumorigenesis.

INTRODUCTION

Ubiquitin attachment can influence protein stability and function, and as such this post-translational modification exerts major roles in diverse cellular processes including cell cycle control, transcription and DNA repair (1-3). Ubiquitination is tightly regulated by the concerted action of ubiquitin E3 ligases and deubiquitinases (DUBs), thus ensuring the proper and timely initiation, propagation or termination of cellular signaling events (4, 5).

The nuclear DUB BAP1 is a tumor suppressor either deleted or mutated in an increasing number of cancers of diverse origins (6, 7). BAP1 somatic or germinal inactivating mutations were found in mesothelioma, uveal melanoma, cutaneous melanocytic tumors, clear cell renal cell carcinoma, breast and lung cancers. Genetic ablation of BAP1 in mice is embryonic lethal, demonstrating the importance of this DUB in embryonic development, and selective inactivation of BAP1 in the adult mice induced severe defects in the myeloid cell lineage, recapitulating key features of the myelodysplastic syndrome (8). Recently, it was also shown that *BAP1+/-* heterozygous mice are more prone to asbestos-induced mesothelioma than wild type animals (9). At the molecular level, we and others recently isolated BAP1 as a chromatin-associated protein that assembles large multi-protein complexes containing transcription factors and co-factors including, the Host Cell Factor (HCF-1), the O-linked N-acetyl-Glucosamine Transferase (OGT), the Lysine Specific Demethylase KDM1B, the Additional Sex Comb Like proteins ASXL1 and ASXL2 (ASXL1/2), the Forkhead Box transcription factors FOXK1 and FOXK2 as well as the zinc finger transcription factor Yin Yang 1 (YY1) (10-12). We found that BAP1 regulates the expression of genes involved in cell proliferation and is recruited to gene regulatory regions to activate transcription (12).

BAP1 is also recruited to the site of DNA double strand breaks to promote repair by homologous recombination (13, 14). Moreover, this DUB appears to be also finely regulated by post-translational modifications including phosphorylation and ubiquitination (13, 15).

The deubiquitination of histone H2AK118 by Calypso/ASX in *Drosophila* (16) was also observed for vertebrate BAP1 in vitro and vivo (13, 15, and 16). Additionally, it was shown that a minimal complex containing BAP1 and the N-terminal region of ASXL1 efficiently deubiquitinates H2A in vitro (16). The Drosophila ASX protein is an atypical Polycomb group (PcG) factor required for maintenance of transcriptional silencing and activation (17, 18). Vertebrate ASXL1/2 are ASX paralogs, and were reported to function with both co-repressors and co-activators, notably the Lysine-Specific Demethylase KDM1A, the PcG complex PRC2 and the Trithorax Group (TrxG) epigenetic regulators (19-25). Interestingly, similar to BAP1, ablation of ASXL1 in mice also results in myelodysplastic syndrome-like disease (24, 26).

Since ASXL1/2 are also targeted by point and truncating mutations as well as chromosomal translocations in various cancer types (27-29), we sought to determine whether ASXL1/2 coordinate the H2A DUB activity of BAP1 in vivo, and the relevance of these factors to BAP1 tumor suppressor function.

RESULTS

BAP1 assembles two mutually exclusive protein complexes with ASXL1/2.

We initially sought to define how ASXL1/2 interact with BAP1. ASXL1/2 contain two uncharacterized N-terminal domains, ASXN and ASXM, and a C-terminal Plant Homeo Domain (PHD) finger (Fig. 1A). These factors co-purify with BAP1 (10-12), and mass spectrometry peptide counts suggest that they are associated with BAP1 at similar levels (Fig. S1A). Immunoprecipitation (IP) of ASXL2 from purified BAP1 complexes did not show interaction with ASXL1 (Fig. 1B), and ASXL1 and ASXL2 failed to interact following overexpression (Fig. 1C). BAP1 was shown to interact with the N-terminal region of ASXL1 (1-337 a.a.), containing the ASXN and ASXM domains in addition to a linker region (16). To identify the domain responsible for this interaction, we conducted GST-pull down assays and found that in vitro translated N-terminal fragment of ASXL1/2, containing the ASXM domain (ASXM1: 253-391 a.a., ASXM2: 246-401 a.a. of ASXL1 and ASXL2 respectively) strongly interacted with GST-BAP1 (Fig. 1D). Sequence alignment of human ASXL1/2 proteins with Drosophila ASX indicated that the ASXM domain is highly conserved (Fig. 1A and Fig. S1B). Next, we found that ASXL2 lacking the BAP1-interacting domain ($ASXL2^{\Delta ASXM}$), but not $ASXL1^{\Delta ASXM}$, was less expressed following transfection (Fig. S1C). When the amounts of transfected plasmids were adjusted to obtain comparable expression for ASXL1/2 wild type or mutants, both ASXL1/2 mutants lacking their respective ASXM domain hardly interacted with BAP1 or formed protein complexes (Fig. 1E).

BAP1 contains notably a UCH catalytic domain and a conserved C-terminal domain (CTD), in addition to an HCF-1-Binding Motif (HBM) (Fig. 1F and Fig. S2A). BAP1

physical interaction with ASXL1/2 was not affected by the loss of HCF-1 and OGT, two major subunits of the BAP1 core complex associated through BAP1 HBM (Fig. S2B). GST-tagged fragments of BAP1 containing its C-terminal domain (CTD) interacted with ASXM domains of ASXL1/2 (Fig 1F, right panel). Thus, BAP1 can interact with either ASXL1 or ASXL2, but is unable to engage interactions with these co-factors simultaneously. To gain insights into the significance of BAP1/ASXL1/2 interactions, we constructed BAP1 mutants disrupted in the CTD region (Fig. S2A, top panel). We initially conducted transfections in 293T cells and found that the $BAP1^{\Delta CTD}$ mutant was less expressed than the wild type form (Fig. S2C). We also generated BAP1 lacking most of the CTD sequence except for the KRKKFK which might function as a nuclear localization signal ($BAP1^{\Delta CTD1}$) (30) (Fig. S2A, top panel). We note that both constructs have been used and produced similar results. Next, we generated HeLa cells stably expressing BAP1 or $BAP1^{\Delta CTD1}$ for complex purification. Silver staining of immunopurified complexes, adjusted for similar amounts of BAP1, revealed that BAP1 and $BAP1^{\Delta CTD1}$ complexes were quite similar (Fig. 1G). However, immunoblotting showed that the interaction between $BAP1^{\Delta CTD1}$ and ASXL1/2 was abolished (Fig. 1G). In contrast, association of BAP1 with other major components, including HCF-1 and OGT, remained unchanged (Fig. 1G). To further confirm that ASXL1 and ASXL2 compete for interaction with BAP1, we overexpressed increasing amounts of ASXL1 with constant amounts of BAP1 and ASXL2 in 293T cells, and observed that ASXL2 was displaced from binding BAP1 (Fig. 1H). Based on these results altogether, we therefore concluded that BAP1 assembles mutually exclusive complexes with either ASXL1 or ASXL2.

BAP1 and ASXL1/2 are co-regulated and loss of BAP1 in cancer is concomitant with the destabilization of ASXL2.

To further investigate the functional relationship between BAP1 and ASXL1/2, 293T cells were transfected with BAP1 and increasing amounts of Myc-tagged ASXL1/2. As suspected from the results obtained with the expression of interaction-deficient mutants (Fig. S1C and Fig. S2C), BAP1 protein levels were increased by ASXL1/2 in a dose-dependent manner (Fig. 2A). ASXL1/2 protein levels were also increased following expression of BAP1 (Fig. 2B). In support of these results, siRNA knockdown of either ASXL1 or ASXL2 resulted in a significant decrease of BAP1 protein levels (Fig. 2C, Fig. S6C). Combined knockdown of ASXL1/2 caused an even stronger decrease of BAP1 than depletion of individual proteins (Fig. 2C), indicating that ASXL1/2 are required for maintaining proper protein levels of this DUB. We also observed that depletion of ASXL1 resulted in a noticeable decrease of ASXL2 protein levels, while knockdown of ASXL2 caused an increase of ASXL1 (Fig. 2C, Fig. S6C). Knockdown of BAP1, most notably, affected ASXL2 protein levels (Fig. 2C, Fig. S6C). This effect is independent of BAP1 DUB activity, as the decrease of ASXL2 protein in U2OS cells was prevented by re-expression of siRNA-resistant BAP1 either wild type or catalytically dead (C91S) (Fig. 6D). The strict dependency of ASXL2 protein levels on BAP1 abundance suggests that ASXL2/BAP1 is an obligate complex. Consistent with this assumption, immunodepletion of endogenous proteins from nuclear extracts revealed that the majority of ASXL2 is associated with BAP1 (Fig. 2D). However, only about half the amount of BAP1 is in complex with ASXL2 (Fig. 2D). Significantly, ASXL2 was downregulated in BAP1-deficient H28 mesothelioma and H226 lung carcinoma cells, and re-expression of BAP1or $BAP1^{C91S}$ restored ASXL2 protein levels in these cells, without affecting its mRNA

levels (Fig. 2E,F). These data suggest that BAP1/ASXL1/2 interactions are highly regulated and that loss of BAP1 during cancer development results in the concomitant loss of ASXL2.

ASXL1/2 regulate BAP1 DUB activity in an ASXM-dependent manner.

Several DUBs including BAP1 were shown to target H2AK119 (H2Aub) in mammals (2, 31). However, it is not clear what is the relative contribution of each enzyme in H2A deubiquitination in vivo. We conducted a siRNA screen using a library that covers the human DUB repertoire by analyzing the global increase of H2AubK119 with a specific antibody. Depletion of BAP1 produced the most significant increase of H2Aub indicating that this enzyme is a major DUB for this histone modification, under normal growth conditions (Fig. 3A). Next, to determine how ASXL1/2 regulates BAP1 DUB activity in vivo, we conducted RNAi-mediated knockdown of these factors. Neither ASXL1 nor ASXL2 individual knockdown induced noticeable global changes of H2Aub (Fig. S3A). However, combined knockdown of ASXL1/2 resulted in a significant increase of H2Aub, similar to the effect induced by BAP1 depletion (Fig. S3A). This prompted us to determine the respective contribution of ASXL1 and ASXL2 to the H2A DUB activity of BAP1. A striking BAP1-mediated deubiquitination of H2A was observed upon its co-expression with either ASXL1 or ASXL2, and this effect was dependent on BAP1 catalytic activity (Fig. S3B). Consistently, ASXL1 or ASXL2 lacking ASXM were unable to activate H2A deubiquitination (Fig. 3B). Based on these results, we concluded that BAP1 deubiquitinates H2A, in vivo, in an ASXL1/2-dependent manner. Next, we found that BAP1 also deubiquitinates K118 of H2A, a site that is also used by the PRC1 ubiquitin E3 ligase complex in vertebrate in addition to the

major site K119 (Fig. S4A). Moreover, BAP1 also deubiquitinates the histones variants H2AX and H2AZ, both of which are also catalyzed by the PRC1 complex (Fig. S4A). Interestingly, the nucleosomal structure is not prerequisite for BAP1 activity, as digestion of DNA with benzonase or denaturation of nucleosomes did not impact H2A deubiquitination (Fig. S4B,C). Furthermore, we note that BAP1 is unable to deubiquitinate H2AK13/K15 (Fig. S4D), sites that are ubiquitinated by the DNA damage-associated E3 Ligase RNF168 (32). On the other hand, using different antibodies against H2Bub K120, we did not detect changes in the observed immunoblot signals following BAP1 depletion in mammalian cells (Fig. S4E). Significantly, H28 mesothelioma BAP1-deficient cells exhibited high H2Aub levels and reconstitution of these cells with BAP1 induced about a 3-fold decrease in H2Aub levels in a catalytic activity-dependent manner, whereas no changes were detected for H2Bub (Fig. S4E). Finally, while a striking deubiquitination could be observed on H2A in vitro using the BAP1 complexes, no changes were observed for H2Bub in the same enzymatic reactions (Fig. S4F).

The ASXM domain ensures two distinct functions of BAP1: ubiquitin binding and DUB activity.

To further dissect the mechanistic of H2A deubiquitination by BAP1, we used an in vitro DUB assay and found that the ASXM domain of ASXL1 or ASXL2, but not GST-CTD used as a control, is sufficient for stimulating BAP1-mediated deubiquitination of nucleosomal H2A (Fig.3C). By conducting ubiquitin interaction pull down assays, we found that both ASXM of ASXL1 and ASXL2 strongly enhanced BAP1 binding to ubiquitin

(Fig.3D). Since the ASXM of ASXL1 or ASXL2 acted similarly in DUB and ubiquitin binding assays, we selected ASXM of ASXL2 for further studies (hereafter ASXM2). We generated several constructs encompassing several regions and highly conserved motifs of ASXM2 (Fig. 3E). We found that the 246-347 a.a. region interacted with BAP1 as efficiently as the full length ASXM2 (246-401 a.a.), while no interaction was observed for the 316-401 a.a. region (Fig. 3E,F). The 246-313 a.a. and 300-401 a.a. regions interacted only poorly with BAP1. These results suggest that critical interaction motifs are located within or overlapping with the 300-347 a.a. region (Fig. 3E,F). Only the ASXM2 full length and the 246-347 a.a. fragment that strongly interacted with BAP1 promoted its DUB activity (Fig 3E,F). Unexpectedly, the 246-347 a.a., which efficiently interacted with BAP1 and activated its DUB activity, failed to enhance BAP1 binding to ubiquitin. Thus, stimulating BAP1 deubiquitination and promoting its binding to ubiquitin appear to be two distinct functions of the ASXM2 domain. Next, we generated discrete mutations in several highly conserved residues of ASXM2 (Fig. 3G), and found that ASXM2 interaction with BAP1 and ubiquitin binding are maintained for most mutants except for the LLLL303-306AAAA hydrophobic stretch mutant which lost interaction with BAP1 (Fig. S1B, Fig. 3H,I). As expected, the LLLL303-306AAAA mutant failed to stimulate DUB activity. Interestingly, while the L286A and NN328-329AA mutants were essentially efficient in promoting BAP1 binding to ubiquitin, they were unable of promoting efficient DUB activity, once again separating BAP1/ASXM binding to ubiquitin from BAP1/ASXM-mediated enzymatic catalysis (Fig. 3H,I).

Intramolecular interactions in BAP1 create a Composite Ubiquitin Binding Interface (CUBI) and enable DUB activity.

The CTD of BAP1 is necessary and sufficient for interaction with ASXL1/2 (Fig.1F,G). This domain contains a Coiled-Coil (CC2) domain that engages an intramolecular interaction with the CC1 domain that is distal to the UCH domain in order to ensure auto-deubiquitination (15). Interestingly, recent structural studies showed that a similar intramolecular interaction occurs in a close family homolog of BAP1, UCH37, and that the corresponding domain of CTD, UCH37-like domain (ULD), establishes a direct contact with ubiquitin (33). Thus, we sought to investigate the requirements of these domains for ASXM-mediated ubiquitin binding and H2A deubiquitination. Indeed, BAP1 lacking all the CTD sequence ($BAP1^{\Delta CTD}$) failed to deubiquitinate H2A in vitro (Fig. 4A,B) and in vivo (Fig. S5A). Deletion of CC2 within the CTD ($BAP1^{\Delta CC2}$) also disrupts BAP1-mediated H2A deubiquitination (Fig. S5B). Moreover, deletion of CC1 abolished H2A deubiquitination similar to deletion of UCH or mutation of the catalytic cysteine of BAP1 (C91S) (Fig.4B). Of note, deletion of HBM which abrogates BAP1 binding with the major component of the complex, HCF-1, did not impact H2A deubiquitination (Fig. S5C). Next, we sought to determine the effect of these domains on ASXM2-mediated ubiquitin binding by BAP1. ASXM2 promoted binding to ubiquitin of both wild type and catalytic dead $BAP1^{C91S}$ mutant (Fig. 4C). In contrast, ASXM2 failed to enhance ubiquitin binding of BAP1 lacking the UCH, the CC1 or the CTD. Thus, in concert with ASXM2, BAP1 forms a Composite Ubiquitin Binding Interface (hereafter CUBI) that requires multiple domains of BAP1 (Fig. 4C). Ubiquitin uses various interfaces, notably the L8/I44/V70 (VLI) hydrophobic patch, for interaction with diverse ubiquitin binding motifs contained within components of the

ubiquitin proteasome system (1). We generated several ubiquitin constructs containing mutations in critical residues and tested their ability to bind BAP1/ASXM2. Indeed, binding to ubiquitin lacking the hydrophobic patch VLI by BAP1/ASXM2 is completely abrogated (Fig. 4D, left panel). Mutation of I44, which constitutes the center of the hydrophobic recognition patch, also significantly reduced the binding of ubiquitin by BAP1/ASXM2 (Fig. 4D, right panel). Finally, mutation of the polar patch D58 did not affect ubiquitin binding by BAP1/ASXM2 (Fig. 4D, right panel). Thus, although we could not exclude that other regions of ubiquitin are involved, the CUBI interacts essentially with the VLI hydrophobic patch of ubiquitin.

Cancer-derived mutations abolish BAP1 interaction with ASXL1/2, ubiquitin binding and DUB activity toward histone H2A.

PcG proteins are deregulated in cancer (34, 35), and BAP1 is inactivated by various cancer-associated mutations directly impacting its catalytic activity or cellular localization (7, 15). However, it is not well known how the spectrum of mutations of *BAP1* could disrupt specific functions of the subunits that compose its complexes. We sought to investigate whether mutations of BAP1 could result in a selective loss of its interacting partners, notably ASXL1/2. Thus, we analyzed the previously reported mutation landscape of BAP1 and found several mutations within or near its critical domains UCH (E31K, Y33D), CC1 (L230Q, Q253K) and CTD (K656N, K658R, D663H, R666-H669del) (Fig. 5A and Fig. S2A). We also included additional mutations, not found in cancer, but correspond to highly conserved amino acids in the vicinity of these cancer mutations (F228A, N670A). Interestingly, the Y33 and

F228 of BAP1 UCH correspond to V34 and F216 in tsUCH37 of the worm *Trichinella spiralis*, two residues that were shown to establish contact with the hydrophobic VLI patch of ubiquitin (33). The K658 and D663 residues of BAP1 CTD were also involved in ubiquitin binding by the tsUCH37 UDL (33). First, we co-expressed these BAP1 mutants with ASXL2 and found that protein interaction is essentially unaffected for most mutants except for R666-H669 mutant whose interaction with ASXL2 is strongly reduced (Fig. 5A). Significantly, several of these mutants, e.g., L230Q, K658R and R666-H669del were strongly affected in their ability to bind ubiquitin following addition of ASXM2 (Fig. 5B). Most mutants were greatly disrupted in their ability to stimulate BAP1-mediated H2A deubiquitination by the ASXM2 domain in vitro (Fig. 5B). Interestingly, the D663H mutant was efficient in binding ASXM2 and ubiquitin but failed to promote efficient DUB activity, again supporting the notion that ASXM2/BAP1 interaction ensures two separate functions, ubiquitin docking and deubiquitination. Since the deletion of the amino acids R666-H669 (hereafter BAP1$^{R666\text{-}H669}$) abolished the interaction with ASXL2, ubiquitin binding and DUB activity, we selected this mutant for further biochemical and functional studies. First, we generated HeLa cells stably expressing Flag-HA-BAP1$^{R666\text{-}H669}$ and conducted TAP affinity purification from total cell extracts. Although the BAP1$^{R666\text{-}H669}$ mutant was less stable than the wild type form (Fig. S2C), silver staining indicated that their complexes were very similar, with the most noticeable difference being the missing ASXL2 band in the purified BAP1$^{R666\text{-}H669}$ complexes (Fig. 5C, left panel). ASXL1 co-migrates with other high M.W. proteins, and could not be discerned as a distinct band. Strikingly, western blot analysis of the complexes indicated that BAP1$^{R666\text{-}H669}$ does not interact with both ASXL1/2, while interaction with HCF-1/OGT were not affected (Fig. 5C, right panel). Indeed, neither full length ASXL1 nor ASXL2 are capable

of stimulating BAP1$^{R666\text{-}H669}$ DUB activity in vivo (Fig. S5D). This effect is direct since the purified BAP1$^{R666\text{-}H669}$ complex was unable to deubiquitinate nucleosomal histone H2A or to bind ubiquitin in vitro (Fig. 5D). Significantly, the BAP1-null cancer cell line H226 displays high levels of H2Aub, and re-introduction of BAP1, but not the BAP1$^{R666\text{-}H669}$ nor the BAP1^{C91S}, in these cells promoted substantial H2A deubiquitination (Fig. 5E). Next, we selected several reported cancer-associated point mutations in ASXM2 (Fig. 5F), and found that almost all these mutations do not disrupt ASXM2 interaction with BAP1 or BAP1/ASXM2 binding to ubiquitin except the P274L mutant (Fig. 5G,H). However, three of these mutants (P274L, E330Q, F331L) showed significantly reduced DUB activity toward H2A indicating that ASXL2 is also targeted by mutations that disrupt BAP1 DUB activity (Fig. 5H).

Altogether, these results indicate that several cancer-associated mechanisms target the interaction of BAP1 with ASXL1/2 inducing loss of ubiquitin binding and/or H2A DUB activity.

ASXL1 and ASXL2 exert opposite effects on cell cycle progression.

Since BAP1 is a tumor suppressor implicated in the control of cell proliferation (10, 30), we assessed the role of its interaction with ASXL1/2 in cell cycle control. First, we sought to compare BAP1 complexes composition between cycling and quiescent (G0) primary skin fibroblasts (LF1). Since ASXL1/2 form two mutually exclusive complexes with BAP1, we initially hypothesized that these complexes might be differentially required to coordinate gene expression in proliferating versus G0 cells. LF1 cells stably expressing Flag-

HA-BAP1 were synchronized in G0 by contact inhibition and used for immunopurification (Fig. 6A, Fig S6A). We observed a substantial loss of interaction between BAP1 and its partners including ASXL1/2, and this was concomitant with cell cycle exit (Fig. 6A). This led us to hypothesize that both BAP1/ASXL1/2 complexes are necessary for cell cycle progression. We initially noticed that ASXL2 knockdown in U2OS induced an apparent delay in cell proliferation (Fig. S6B). We also observed that ASXL1 knockdown in LF1 cells induced a medium color change, i.e., acidification that might indicate increased cell proliferation (Fig. S6D). To further assess the role of these complexes in regulating cell proliferation, we conducted cell cycle synchronization in conjunction with siRNA knockdown of these factors. Strikingly, we found that knockdown of ASXL1 in U2OS followed by double thymidine block synchronization and release resulted in a faster progression through G1/S, while ASXL2 knockdown delayed this progression (Fig. 6C, top panel). BAP1 knockdown also delayed cell cycle progression, although to a lesser extent than that of ASXL2. To further confirm this dual function of ASXL1/2 in regulating cell cycle progression, we conducted RNAi of BAP1, ASXL1 and ASXL2 followed by nocodazole treatment to block the cells in M, thus enabling the visualization of the progression from G1 to M. The results confirmed that ASXL2 knockdown causes G1/S transition delay, while ASXL1 knockdown caused a faster progression through the cell cycle (Fig. 6C, bottom panel). Again, BAP1 knockdown induced a less pronounced effect than ASXL2. Next, we asked whether ASXL1/2 and BAP1 coordinate cell cycle progression through protein interactions. We generated U2OS cells stably expressing siRNA-resistant BAP1, $BAP1^{C91S}$, $BAP1^{\Delta CTD}$ or $BAP1^{R666\text{-}H669}$ (Fig. 6D, Fig. S7A), and conducted RNAi depletion of endogenous BAP1 followed by the double thymidine block/release protocol. We found that, while expression of BAP1 rescues the defect

induced by knockdown of endogenous BAP1, this was not observed with the catalytic dead $BAP1^{C91S}$ or ASXL1/2-interaction deficient mutants ($BAP1^{R666\text{-}H669}$ or $BAP1^{\Delta CTD}$) (Fig. 6E and Fig. S7A,B). Note the rescue of H2Aub levels by BAP1, but not by the ASXL1/2-interaction deficient BAP1 mutant (Fig. 6D). Thus, a tight collaboration, through physical interaction, between ASXL1/2 and BAP1 is required for the proper control of cell cycle progression.

To define how BAP1/ASXL1/ASXL2 regulates cell proliferation, we analyzed the protein levels of several major regulators of cell cycle including p53, p21 and pRB. The replication-promoting factor *CDC6* was also included, since this prototypical E2F target gene is also regulated by HCF-1 and YY1 (36, 37), two partners of BAP1 (12). We found that knockdown of ASXL1 or ASXL2 induced an increase or a decrease of CDC6 protein levels, respectively (Fig. 6B and Fig. S6C), while BAP1 knockdown hardly affected CDC6 protein levels. In addition, ASXL2, but not ASXL1, depletion induced the DNA damage response as the levels of γH2AX and p53/p21 proteins were significantly increased (Fig. 6B and Fig. S6C). An increase of p21 mRNA indicative of p53 induction was also observed (Fig. S6E). We also noticed a substantial decrease of pRB and its phosphorylated form following ASXL2 knockdown (Fig. 6B). Of note, knockdown of BAP1 had a less pronounced effect than that of ASXL2 knockdown on the p53/p21 induction. Altogether, these results are consistent with the observed differential roles of BAP1, ASXL1 and ASXL2 in regulating cell cycle progression.

Enforced expression of BAP1 and ASXL2 induce cellular senescence and the p53/p21 tumor suppressor pathway.

Cellular senescence-associated cell cycle exit is a potent tumor suppressor mechanism. Since we established that BAP1 function is coordinated with ASXL1 and ASXL2 in regulating cell cycle progression, we enquired if BAP1/ASXL1/2 might influence cellular senescence. Of note, PcG proteins, notably BMI1, are known to be involved in senescence (38-40). Therefore, we evaluated whether enforced expression of BAP1, ASXL1 or ASXL2 trigger senescence in the normal diploid human fibroblasts IMR90 cell line model. Strikingly, retroviral overexpression of ASXL2, but not ASXL1, strongly induced senescence-associated β-galactosidase (SA-β-gal) activity and reduced cell proliferation (Fig. 7A,B). This effect is dependent on BAP1 as ASXL2 lacking ASXM2 failed to induce senescence or to reduce cell proliferation. Moreover overexpression of BAP1 induced senescence (Fig. 7A,B). Interestingly, overexpression of $BAP1^{C91S}$ mutant also induced senescence with a more pronounced effect than the wild type form (Fig.7A,B and Fig. S8). To probe whether this effect is due to BAP1 ability to interact with ASXL1/2, we evaluated the effect of $BAP1^{\Delta CTD}$ as well as $BAP1^{R666\text{-}H669}$ on cellular senescence. Indeed, these mutations prevented BAP1 from inducing senescence (Fig 7A,B). Similar effects were observed for the double mutants $BAP1^{C91S\text{-}R666\text{-}H669}$, although only a partial rescue was noted for $BAP1^{C91S\text{-}\Delta CTD}$ (Fig. S8). To provide further insights into the molecular mechanism that orchestrate BAP1/ASXL2-mediated senescence, we evaluated the expression levels of known proteins that induce cellular senescence upon overexpression of BAP1, $BAP1^{C91S}$ and corresponding mutants (Fig. 7C). We found that, although the effect of BAP1 was less pronounced than the $BAP1^{C91S}$ form, overexpression of this DUB induced the p53/p21 tumor suppressor pathway.

Overexpression of $BAP1^{\Delta CTD}$, $BAP1^{R666\text{-}H669}$, $BAP1^{C91S\text{-}\Delta CTD}$ or $BAP1^{C91S\text{-}R666\text{-}H669}$ did not upregulate p53/p21 indicating the requirement for ASXL1/2 in BAP1-mediated senescence (Fig. 7C). We also observed a concomitant decrease of CDC6 and pRB following overexpression of BAP1 or $BAP1^{C91S}$, and these effects required interaction with ASXL1/2. In contrast, no significant changes were observed on $p16^{INK4a}$ cell cycle inhibitor and the p53 E3 ligase MDM2.

Altogether, there results indicate that the fine balance between components of BAP1/ASXL1/2 complexes and their coordination of H2A deubiquitination are required for proper progression of cell cycle in mammals.

DISCUSSION

Although, BAP1 has emerged as the most highly mutated DUB in human malignancies, its mechanism of action is still not fully defined. In this study, we provided novel insights into the mechanism by which BAP1 deubiquitinates histone H2A K119 and acts as a tumor suppressor. First, we revealed that BAP1 and ASXL1/2 protein levels are tightly regulated by each other. Notably, BAP1 protein levels are reduced by about half following ASXL1 or ASXL2 depletion, and almost completely following concomitant depletion of ASXL1 and ASXL2. This regulation is highly conserved since deletion of drosophila ASX destabilizes Calypso (16). In addition, depletion or loss of BAP1 destabilizes ASXL2. These findings demonstrate the importance of complex assembly in coordinating BAP1 function. Thus, developmental or disease-associated inactivation or loss of expression of one component would result in a profound functional impact on the other partners. Indeed, loss of BAP1 in two tumor types of different origins, i.e., mesothelioma and non-small lung carcinoma, caused a severe reduction of ASXL2 levels. Second, we demonstrated that BAP1 assembles two mutually exclusive complexes with either ASXL1 or ASXL2. Although ASXL1/2 compete for BAP1 binding, both subunits can stimulate BAP1 binding to ubiquitin as well as its DUB activity toward H2Aub. Third, we found that the BAP1/ASXL1/ASXL2 axis tightly regulates cell cycle progression and impact cellular senescence. Fourth, we identified cancer mutations that directly abolish the BAP1 interaction with ASXL1/2 or selectively target ubiquitin binding and/or DUB activity of BAP1/ASXL1/2 complexes and hence abrogate the dynamic coordination of H2A ubiquitination as well as cell proliferation.

Interaction mapping studies revealed that the highly conserved ASXM/CTD domains govern the ASXL1/2 interaction with BAP1. Thus, ASXM-CTD interactions define an interaction platform distinct from OGT/HCF-1/BAP1 which uses the Kelch domain and HBM motif of HCF-1 and BAP1 respectively (10, 41). It is worth mentioning that since BAP1 acquired the middle region (containing the HBM) later during evolution, BAP1/ASXL1/ASXL2 and BAP1/OGT/HCF-1 constitute two major regulatory axes with distinct but complementary and coordinated chromatin-associated functions.

One of the salient findings of this study is the effect of ASXM in promoting BAP1 binding to ubiquitin that appears to be independent of stimulating histone H2A deubiquitination by this DUB. Indeed, we isolated a region of ASXM (246-347 a.a) that strongly interacts with BAP1, is efficient in stimulating enzymatic activity, but unable to enhance binding to ubiquitin by this DUB. Conversely, we also isolated mutants of ASXM, including cancer mutants, that efficiently interact with and promote BAP1 binding to ubiquitin, but are essentially unable to stimulate DUB activity (e.g., N328A/N329A, E330Q). Moreover, we also isolated a BAP1 mutant (i.e., D663H) that interacts with ubiquitin in ASXM-dependent manner, but is inefficient in H2A deubiquitination. Separation of these two functions can have major functional implications for the BAP1 complexes. Binding to ubiquitin could facilitate the tethering of the complex to chromatin, and deubiquitination can take place only when other biochemical requirements are met. For instance, BAP1/ASXL1/2 binding to H2Aub might promote the recruitment of additional factors or ensure the removal or addition of other histones modifications prior to H2A deubiquitination. In addition, the BAP1 complexes could also promote transcriptional regulation in an H2Aub-dependent, but catalytic activity-independent manner. For instance, both wild type and catalytic dead BAP1

induce senescence in an ASXL1/2-dependent manner. Although, additional studies will be needed to provide further insights on how BAP1/ASXL1/ASXL2 coordinate H2A deubiquitination on chromatin, our data strongly emphasize the existence of an important regulatory network governing this epigenetic modification.

Another important result is the requirement of multiple domains in BAP1, in addition to the catalytic site, to generate an ASXM-inducible composite ubiquitin binding interface (CUBI). Whether ASXM also directly contacts ubiquitin remains to be determined. We note that low affinity interaction between ASXM and ubiquitin in the absence of BAP1 might not be observed in our ubiquitin pulldown conditions. Nonetheless, our data support a model whereby ASXM constitutes a versatile module that uses several determinants for interaction with BAP1 to stimulate ubiquitin binding and/or H2A deubiquitination. Moreover, the ASXM is embedded in ASXL1 and ASXL2 which are large proteins containing other conserved domains, e.g., ASXN and PHD, thus providing a more extensive platform for regulation of the complex by interacting partners and post-translational modifications.

We also investigated the role of ASXL1/ASXL2/BAP1 in cell cycle progression. Using RNAi, we showed that ASXL1 negatively regulates cell cycle, while in contrast ASXL2 promotes cell cycle. Consistently, ASXL2 positively regulates CDC6 protein levels, whereas ASXL1 exerts a negative effect on CDC6 expression. Thus, although ASXL1/2 are paralogs, interact in a similar manner with BAP1 and promote its DUB activity, these factors nonetheless appear to exert different roles and even opposite functions in coordinating BAP1 function. Of note, CDC6 is a critical DNA replication factor, possesses proto-oncogenic functions and its deregulated expression is associated with several cancers (42, 43). *CDC6*

was previously shown to be regulated by HCF-1 which activates or represses the expression of a subset of E2F targets including *CDC6* (36). Moreover YY1, also endowed with dual transcription activating and repressive functions, interacts with HCF-1 and BAP1 and was also shown to regulate *CDC6* (12, 37). Thus, BAP1 might assemble ASXL2 co-activator or ASXL1 co-repressor complexes to regulate *CDC6* expression. Consistent with this assumption, it was shown that ASXL1 and ASXL2 act as a repressor and activator respectively (21, 25). Moreover, although the prevalent view is that deubiquitination of H2A activates transcription (2), The PR-DUB complex can repress transcription in a catalytic activity-dependent manner (16). Thus, it would be very interesting to further understand how BAP1-mediated deubiquitination of H2A by ASXL1 or ASXL2 might produce two opposite transcriptional outcomes.

Knockdown of ASXL2, and to a lesser extent BAP1, also induced the p53/p21 DNA damage response and subsequent cell cycle attenuation. This effect might be caused by transcriptional deregulation of components of the replication machinery, which in turn could induce replication fork collapse and DNA double strand breaks. On the other hand, production of reactive oxygen species (ROS) that might also result from transcription deregulation of metabolic pathways could also generate DNA damage and activate the p53/p21 pathway. In support of this view, depletion of BMI1, a component of the H2A E3 ligase complex PRC1, was shown to induce ROS, DNA damage and the p53 response (44, 45). We also found that enforced expression of ASXL2, but not ASXL1, induced cell senescence in a BAP1-dependent manner, indicating that the proper balance of BAP1 complexes and proper coordination of H2A deubiquitination is required for normal cell proliferation. Consistent with this view, overexpression of BAP1 or its catalytic dead form also induced cell

senescence in ASXL1/2-dependent manner. Interestingly, the cell cycle inhibitor $p16^{INK4a}$ does not appear to be a major determinant of BAP1-induced senescence. Thus, aside from the PcG factors implication in controlling the expression of the $p16^{INK4a}$/ARF tumor suppressor pathway (38, 46), we observed here an upregulation of the p53/p21 tumor suppressor pathway concomitant with a decreased phosphorylation of pRB. Clearly, our studies provide impetus for further studies to delineate the exact roles of BAP1 complexes in coordinating pRB/E2F and p53 tumor suppressor pathways.

Our study also shed light on the role of H2Aub deregulation in tumorigenesis. Indeed (i) several cancer mutations of BAP1 target the UCH/CC1/CTD/ASXM interface, critical for ubiquitin binding and H2A deubiquitination, indicating the importance of this modification for tumor suppression (Fig. 7D), (ii) BAP1 null cancer cells display high H2Aub levels and reintroduction of BAP1, but not ASXL1/2 interaction-deficient mutants, in these cells reduced its abundance, and (iii) both PcG proteins Ring1B and BMI1, two critical components of the PRC1 complex that catalyze H2A ubiquitination are overexpressed in cancer (47-50). Furthermore, BMI1 also promotes the bypass of cellular senescence and extends replicative lifespan (51). It is worth mentioning that although several DUBs have been proposed to counteract H2Aub catalyzed by the PRC1 E3 ligase PcG complex, the BAP1 complex is the only known DUB whose subunits YY1, OGT and ASXL1/2 as well as BAP1 itself are PcG proteins (2), and we showed here that among all members of the DUB repertoire, BAP1 is a major DUB for H2A. Our study also adds to an emerging notion that PcG proteins regulate cell proliferation more dynamically than previously recognized.

In conclusion, we demonstrated that ASXL1/2 coordinates the DUB activity of BAP1 toward H2A, and that this activity is abolished as a consequence of cancer mutations that involve multiple mechanisms that target the DUB activity of the BAP1/ASXL1/2 complexes. These findings have major implications not only for understanding cell cycle control, but also in defining the mechanisms of cancer pathogenesis and suppression.

Materials and Methods

Cell culture, cell cycle synchronization and senescence studies

Cell lines were cultured according to standard protocols. Primary skin fibroblasts (LF1) were synchronized in G0 by contact inhibition and U2OS cells were synchronized at the G1/S border using thymidine double block or nocodazole methods as described (52). pMSCV retroviral vectors were used to produce viruses and infect IMR90 cells. After infection and selection, cells were harvested for cell count or evaluated for by senescence-associated-β-galactosidase (SA-β-gal) activity assay as described (53).

siRNA DUB screen

HeLa cells were transfected with individual siRNA pool targeting DUBs (~100 genes) using Lipofectamine 2000 as described (13). Three days post-transfection, cells were fixed and used for immunostaining with H2Aub antibody.

Tandem Immuno-affinity Purification, Immunodepletion and immunoprecipitation

The protein complex purification was done on total cell extracts from cell lines stably expressing Flag-HA-BAP1 or mutant forms. For immunodepletion experiments of endogenous proteins, HeLa nuclear extracts were incubated overnight with either anti-BAP1, anti-ASXL2 or control IgG. The immuno-complexes were recovered with protein G Sepharose beads, eluted with Laemmli buffer and subjected to immunoblotting. Co-

immunoprecipitation (coIP) from purified complexes or cell extracts was conducted essentially as previously described (12).

GST-pull down assays

GST-pulldown studies were conducted using either in vitro translated S35-labeled ASXL1 or ASXL2 fragments incubated with GST-fused full length or deletion fragments of BAP1. GST-ASXM1, GST-ASXM2 (and its mutants). MBP-ASXM2 (and its mutants) were used for pulldown with purified His-BAP1.

In vitro Deubiquitination assay

For the purification of nucleosomes and in vitro histone DUB assay, 293T cells were transfected with pCDNA-Flag-H2A and harvested three days post-transfection. Chromatin fraction was digested with Micrococcal nuclease (MNase). The purified nucleosomes were used for the in vitro DUB assay with Flag-HA purified BAP1 complexes or recombinant BAP1 and ASXM2.

Ubiquitin pull down interaction assays

GST-ubiquitin-agarose or ubiquitin-agarose beads and corresponding mutants were incubated with His-BAP1 or its different mutants along with either GST-ASXM1, GST-ASXM2, MBP-ASXM2 and the corresponding mutant forms at 4 ºC for 3 hours. Following washing, the associated proteins were eluted in Laemmli buffer and subjected to western blotting.

Immunofluorescence

The immunostaining procedure was carried essentially as previously described (54). Briefly, cells were fixed in PFA and permeabilized using PBS 0.1% NP-40. Following blocking, the coverslips were incubated with mouse monoclonal and/or rabbit polyclonal for three hours. Alexa Fluor® 594 and Alexa Fluor® 488-labeled secondary antibodies were used (Life Technologies). Nuclei were stained with 4',6-diamidino-2-phenylindole (DAPI).

Acknowledgements

We thank Yang Shi for his support during the initial stage of this project, Haider Dar, Sarah, Hadj-Mimoune, Diana Adjaoud and Marie-Anne Germain for technical assistance. This work was supported by grants from the Canadian Institutes of Health Research (CIHR) to E.B.A. from (MOP-115132), and to F.A.M from CIHR (MOP-133442). E.B.A. is a scholar of the Fonds de la Recherche du Québec - Santé (FRQS) and the CIHR. F.A.M. is a Scholar of the FRQS. S.D. had a PhD scholarship from the Islamic Bank for Development. H.Y. had a PhD scholarship from the CIHR. H.B has a PhD scholarship from the Ministry of Higher Education and Scientific Research of Tunisia. A.M. obtained a Ph.D. studentship from the Cole Foundation.

REFERENCES

1.Komander D & Rape M (2012) The ubiquitin code. Annual review of biochemistry 81:203-229.

2.Hammond-Martel I, Yu H, & Affar el B (2012) Roles of ubiquitin signaling in transcription regulation. Cell Signal 24(2):410-421.

3.Jackson SP & Durocher D (2013) Regulation of DNA damage responses by ubiquitin and SUMO. Molecular cell 49(5):795-807.

4.Reyes-Turcu FE, Ventii KH, & Wilkinson KD (2009) Regulation and cellular roles of ubiquitin-specific deubiquitinating enzymes. Annual review of biochemistry 78:363-397.

5.Eletr ZM & Wilkinson KD (2014) Regulation of proteolysis by human deubiquitinating enzymes. Biochimica et biophysica acta 1843(1):114-128.

6.Murali R, Wiesner T, & Scolyer RA (2013) Tumours associated with BAP1 mutations. Pathology 45(2):116-126.

7.Carbone M, et al. (2013) BAP1 and cancer. Nature reviews. Cancer 13(3):153-159.

8.Dey A, et al. (2012) Loss of the tumor suppressor BAP1 causes myeloid transformation. Science 337(6101):1541-1546.

9.Xu J, et al. (2014) Germline Mutation of Bap1 Accelerates Development of Asbestos-Induced Malignant Mesothelioma. Cancer research.

10.Machida YJ, Machida Y, Vashisht AA, Wohlschlegel JA, & Dutta A (2009) The deubiquitinating enzyme BAP1 regulates cell growth via interaction with HCF-1. The Journal of biological chemistry.

11.Sowa ME, Bennett EJ, Gygi SP, & Harper JW (2009) Defining the human deubiquitinating enzyme interaction landscape. Cell 138(2):389-403.

12.Yu H, et al. (2010) The Ubiquitin Carboxyl Hydrolase BAP1 Forms a Ternary Complex with YY1 and HCF-1 and is a Critical Regulator of Gene Expression. Molecular and cellular biology.

13.Yu H, et al. (2014) Tumor suppressor and deubiquitinase BAP1 promotes DNA double-strand break repair. Proceedings of the National Academy of Sciences of the United States of America 111(1):285-290.

14.Ismail IH, et al. (2014) Germ-line Mutations in BAP1 Impair its Function in DNA Double-Strand break Repair. Cancer research.

15.Mashtalir N, et al. (2014) Autodeubiquitination protects the tumor suppressor BAP1 from cytoplasmic sequestration mediated by the atypical ubiquitin ligase UBE2O. Molecular cell 54(3):392-406.

16.Scheuermann JC, et al. (2010) Histone H2A deubiquitinase activity of the Polycomb repressive complex PR-DUB. Nature 465(7295):243-247.

17.Milne TA, Sinclair DA, & Brock HW (1999) The Additional sex combs gene of Drosophila is required for activation and repression of homeotic loci, and interacts specifically with Polycomb and super sex combs. Mol Gen Genet 261(4-5):753-761.

18.Gildea JJ, Lopez R, & Shearn A (2000) A screen for new trithorax group genes identified little imaginal discs, the Drosophila melanogaster homologue of human retinoblastoma binding protein 2. Genetics 156(2):645-663.

19.Cho YS, Kim EJ, Park UH, Sin HS, & Um SJ (2006) Additional sex comb-like 1 (ASXL1), in cooperation with SRC-1, acts as a ligand-dependent coactivator for retinoic acid receptor. The Journal of biological chemistry 281(26):17588-17598.

20.Lee SW, et al. (2010) ASXL1 represses retinoic acid receptor-mediated transcription through associating with HP1 and LSD1. The Journal of biological chemistry 285(1):18-29.

21.Park UH, Yoon SK, Park T, Kim EJ, & Um SJ (2011) Additional sex comb-like (ASXL) proteins 1 and 2 play opposite roles in adipogenesis via reciprocal regulation of peroxisome proliferator-activated receptor gamma. The Journal of biological chemistry 286(2):1354-1363.

22.Abdel-Wahab O, et al. (2012) ASXL1 mutations promote myeloid transformation through loss of PRC2-mediated gene repression. Cancer cell 22(2):180-193.

23.Lai HL, et al. (2012) Maintenance of adult cardiac function requires the chromatin factor Asxl2. Journal of molecular and cellular cardiology 53(5):734-741.

24.Abdel-Wahab O, et al. (2013) Deletion of Asxl1 results in myelodysplasia and severe developmental defects in vivo. The Journal of experimental medicine 210(12):2641-2659.

25.Park UH, et al. (2014) Reciprocal regulation of LXRalpha activity by ASXL1 and ASXL2 in lipogenesis. Biochemical and biophysical research communications 443(2):489-494.

26.Wang J, et al. (2014) Loss of Asxl1 leads to myelodysplastic syndrome-like disease in mice. Blood 123(4):541-553.

27.Katoh M (2013) Functional and cancer genomics of ASXL family members. British journal of cancer.

28.Micol JB, et al. (2014) Frequent ASXL2 mutations in acute myeloid leukemia patients with t(8;21)/RUNX1-RUNX1T1 chromosomal translocations. Blood.

29.Huether R, et al. (2014) The landscape of somatic mutations in epigenetic regulators across 1,000 paediatric cancer genomes. Nature communications 5:3630.

30.Ventii KH, et al. (2008) BRCA1-associated protein-1 is a tumor suppressor that requires deubiquitinating activity and nuclear localization. Cancer research 68(17):6953-6962.

31.Belle JI & Nijnik A (2014) H2A-DUBbing the mammalian epigenome: expanding frontiers for histone H2A deubiquitinating enzymes in cell biology and physiology. The international journal of biochemistry & cell biology 50:161-174.

32.Mattiroli F, et al. (2012) RNF168 ubiquitinates K13-15 on H2A/H2AX to drive DNA damage signaling. Cell 150(6):1182-1195.

33.Morrow ME, et al. (2013) Stabilization of an unusual salt bridge in ubiquitin by the extra C-terminal domain of the proteasome-associated deubiquitinase UCH37 as a mechanism of its exo specificity. Biochemistry 52(20):3564-3578.

34.Sauvageau M & Sauvageau G (2010) Polycomb group proteins: multi-faceted regulators of somatic stem cells and cancer. Cell stem cell 7(3):299-313.

35.Crea F, Paolicchi E, Marquez VE, & Danesi R (2012) Polycomb genes and cancer: time for clinical application? Critical reviews in oncology/hematology 83(2):184-193.

36.Tyagi S, Chabes AL, Wysocka J, & Herr W (2007) E2F activation of S phase promoters via association with HCF-1 and the MLL family of histone H3K4 methyltransferases. Molecular cell 27(1):107-119.

37.Schlisio S, Halperin T, Vidal M, & Nevins JR (2002) Interaction of YY1 with E2Fs, mediated by RYBP, provides a mechanism for specificity of E2F function. The EMBO journal 21(21):5775-5786.

38.Jacobs JJ, Kieboom K, Marino S, DePinho RA, & van Lohuizen M (1999) The oncogene and Polycomb-group gene bmi-1 regulates cell proliferation and senescence through the ink4a locus. Nature 397(6715):164-168.

39.Dietrich N, et al. (2007) Bypass of senescence by the polycomb group protein CBX8 through direct binding to the INK4A-ARF locus. The EMBO journal 26(6):1637-1648.

40.Luis NM, et al. (2011) Regulation of human epidermal stem cell proliferation and senescence requires polycomb- dependent and -independent functions of Cbx4. Cell stem cell 9(3):233-246.

41.Misaghi S, et al. (2009) Association of C-terminal ubiquitin hydrolase BRCA1-associated protein 1 with cell cycle regulator host cell factor 1. Molecular and cellular biology 29(8):2181-2192.

42.Gonzalez S, et al. (2006) Oncogenic activity of Cdc6 through repression of the INK4/ARF locus. Nature 440(7084):702-706.

43.Liontos M, et al. (2007) Deregulated overexpression of hCdt1 and hCdc6 promotes malignant behavior. Cancer research 67(22):10899-10909.

44.Chatoo W, et al. (2009) The polycomb group gene Bmi1 regulates antioxidant defenses in neurons by repressing p53 pro-oxidant activity. The Journal of neuroscience : the official journal of the Society for Neuroscience 29(2):529-542.

45.Liu J, et al. (2009) Bmi1 regulates mitochondrial function and the DNA damage response pathway. Nature 459(7245):387-392.

46.Kotake Y, et al. (2007) pRB family proteins are required for H3K27 trimethylation and Polycomb repression complexes binding to and silencing p16INK4alpha tumor suppressor gene. Genes & development 21(1):49-54.

47.Leung C, et al. (2004) Bmi1 is essential for cerebellar development and is overexpressed in human medulloblastomas. Nature 428(6980):337-341.

48.Xu F, et al. (2011) Overexpression of the EZH2, RING1 and BMI1 genes is common in myelodysplastic syndromes: relation to adverse epigenetic alteration and poor prognostic scoring. Annals of hematology 90(6):643-653.

49.Bosch A, et al. (2014) The Polycomb group protein RING1B is overexpressed in ductal breast carcinoma and is required to sustain FAK steady state levels in breast cancer epithelial cells. Oncotarget 5(8):2065-2076.

50.Zhou Y, et al. (2014) Polycomb Group Oncogene RING1 is Over-expressed in Non-Small Cell Lung Cancer. Pathology oncology research : POR 20(3):549-556.

51.Itahana K, et al. (2003) Control of the replicative life span of human fibroblasts by p16 and the polycomb protein Bmi-1. Molecular and cellular biology 23(1):389-401.

52.Hammond-Martel I, et al. (2010) PI 3 kinase related kinases-independent proteolysis of BRCA1 regulates Rad51 recruitment during genotoxic stress in human cells. PloS one 5(11):e14027.

53.Mallette FA & Richard S (2012) JMJD2A promotes cellular transformation by blocking cellular senescence through transcriptional repression of the tumor suppressor CHD5. Cell reports 2(5):1233-1243.

54.Daou S, et al. (2011) Crosstalk between O-GlcNAcylation and proteolytic cleavage regulates the host cell factor-1 maturation pathway. Proceedings of the National Academy of Sciences of the United States of America 108(7):2747-2752.

FIGURE LEGENDS

Figure 1. BAP1 assembles mutually exclusive multi-subunit complexes with ASXL1 or ASXL2.

A) Schematic representation and conservation of the major domains of ASXL1/2. The N-terminal domains, ASXN and ASXM, and a C-terminal Plant Homeo Domain (PHD) finger are indicated. B) Reciprocal immunoprecipitation (Re-IP) of ASXL2 from the immuno-purified Flag-HA-BAP1 protein complexes. C) 293T cells were transfected with 6 μg of Myc-ASXL2 with or without 4 μg of Flag-ASXL1 expression vectors. Three days after transfection, cells were harvested for IP of Myc (ASXL2) and subjected to immunoblot analysis as indicated. D) GST-pulldown interaction assay using full length GST-BAP1 and methionine S^{35}-labeled ASXL1 or ASXL2 N-terminal fragments. The arrows indicate the full length form of each *in vitro* translated fragments. E) Immunoprecipitation of Myc-ASXL1, Myc-ASXL1$^{\Delta ASXM}$, Myc-ASXL2, Myc-ASXL2$^{\Delta ASXM}$. 293T cells were transfected with 4 μg of Myc-ASXL1, 4 μg of Myc-ASXL1 ΔASXM, 4 μg of Myc-ASXL2 or 6 μg of Myc-ASXL2 ΔASXM expression vectors along with 1 μg of BAP1 expression vector. Three days post-transfection, cells were harvested for IP with anti-Myc antibody and subjected to immunoblot analysis with the indicated antibodies. F) Schematic representation of the BAP1 fragments used (left panel). The main domains and motifs of BAP1 are shown. UCH, Ubiquitin Carboxyl Hydrolase catalytic domain; CC1, Coiled-Coil 1; HBM, HCF-1-Binding Motif; CTD, C-Terminal Domain; CC2 Coiled-Coil 2. Note that the CC2 motif is contained within the CTD. GST-pulldown interaction assay using GST-BAP1 fragments and methionine S^{35}-labeled ASXM domains of ASXL1 or ASXL2 (right panel). The arrows indicate the full

length forms of each BAP1 fragments. G) Left panel, silver stain of the immunopurified Flag-HA-BAP1 and Flag-HA-BAP1$^{\Delta CTD1}$ complexes (see Fig. S2A for description of the mutant). HeLa cells stably expressing BAP1 and BAP1$^{\Delta CTD1}$ were generated by retroviral infection. BAP1 complexes were purified with Flag and HA beads from total cell extracts. Right panel, western blot detection of components of the BAP1 complexes. H) 293T cells were transfected with Flag-BAP1 and Myc-ASXL2 expression constructs in the presence of increasing amounts of Myc-ASXL1 expression construct. Cells were harvested three days post-transfection for IP of BAP1 using anti-Flag, and proteins were detected by immunoblotting. Overexpressed Myc-ASXL2 was detected with anti-ASXL2 and anti-Myc antibodies. ASXL1 was detected with anti-Myc antibody. The difference in M.W. allows discrimination between ASXL1 and ASXL2 bands. The dot and the star indicate a modified form of BAP1 and a non-specific band respectively (panels B, C, E).

Figure 2. BAP1 and ASXL1/2 are co-regulated and loss of BAP1 in cancer is concomitant with ASXL2 depletion.

A) Overexpression of BAP1 with increasing amounts of Myc-ASXL1 or Myc-ASXL2 in 293T cells. Cells were transfected as indicated and harvested three days post-transfection for immunoblotting on total cell extracts. Detection of YY1 was used as a loading control. B) Overexpression of Myc-ASXL1 or Myc-ASXL2 with increasing amounts of BAP1 in 293T cells. Cells were transfected and harvested as described in panel A. C) Protein expression following siRNA depletion of BAP1 and/or ASXL1/2 in U2OS cells. The cells were harvested four days post-transfection for Immunoblotting. β-Actin is used as a loading

control. Quantification of band intensity was conducted relative to the non-target siRNA control (siNT). D) Immunodepletion of BAP1 or ASXL2 from HeLa nuclear extracts. PARP1 was used as a control, which mostly remained in the flow through fraction. E) Reconstitution of H28 mesothelioma and H226 non-small lung carcinoma BAP1-deficient cells with BAP1 or $BAP1^{C91S}$. Cells stably expressing BAP1 were generated by retroviral infection. F) mRNA of ASXL2 in reconstituted H226 cells with empty vector or BAP1 was quantitated by qPCR. The data represent two independent experiments. The dot and stars indicate a monoubiquitinated form of BAP1 and non-specific bands respectively (panels, A, B, C, E).

Figure 3. ASXM of ASXL1/2 stimulates BAP1 DUB activity and promotes BAP1 binding to ubiquitin.

A) siRNA screen for DUBs that coordinate H2Aub levels. Following transfection with siRNA DUB library, cells were fixed and immunostained for H2Aub. The fluorescence signal was determined with a plate reader and the values were used to derive the Z-cores. B) 293T cells were transfected as indicated using 0.2 μg of Flag H2A, 1 μg of BAP1, 4 μg of Myc-ASXL1 or 4 μg of Myc-ASXL1 ΔASXM expression vectors (left panel); 4 μg of Myc-ASXL2 or 6 μg of Myc-ASXL2 ΔASXM expression vectors (right panel). Three days post-transfection, cells were harvested for Immunoblotting. YY1 is used as the loading control. C) In vitro deubiquitination assay of histone H2A using bacterial purified His-BAP1 in presence of increasing amounts of purified GST-CTD, GST-ASXM1 or GST-ASXM2. Monoubiquitinated nucleosomal Flag-H2A was purified by IP using anti-Flag beads and used as a substrate for the *in vitro* DUB reaction. The reaction was stopped at different times as

indicated and analysed by western blotting. D) Bacterially purified His-BAP1 and GST-ASXM1/2 were incubated with ubiquitin-agarose beads and the pull down was analysed by western blotting as indicated. E) Schematic representation of the different deletion fragments of ASXM2 generated for the pull down experiments. F) GST pull down interaction assay and *in vitro* DUB reactions of H2Aub using purified His-BAP1 and the bacteria-purified GST fragments of ASXM2. The DUB reactions were done as in (C) (left panel). Purified His-BAP1 and the different fragments of ASXM2 were subjected to ubiquitin pull down assay followed by western blotting (right panel). G) Schematic representation of ASXM2 showing the second set of mutants generated for the *in vitro* assays. H) MBP-pull down interaction assay using bacteria-purified MBP-ASXM2 (full length and various mutant forms) and His-BAP1. I) GST-ubiquitin pull down interaction assay and DUB reaction of nucleosomal H2Aub using ASXM2 fragments with His-BAP1. The dot indicates a monoubiquitinated form of BAP1 (panel B).

Figure 4. Intramolecular interface in BAP1 is required with ASXM2 to create a composite ubiquitin binding interface and to stimulate DUB activity.

A) Schematic representation of the different BAP1 mutants generated for *in vitro* experiments. B) *in vitro* DUB reaction of H2Aub using His-BAP1 mutants and GST-ASXM2. GST was used as a control. C) His-BAP1 mutants and GST-ASXM2 were subjected to ubiquitin pull down assays followed by western blotting. D) Ubiquitin pull down interaction assays using GST-Ubiquitin or its mutants and His-BAP1 with and without MBP-ASXM2 followed by western blotting.

Figure 5. Multiple mechanisms of disruption of BAP1 DUB activity by cancer – associated mutations of BAP1 and ASXL2.

A) Schematic representation of BAP1 showing the cancer-associated mutations (Top panel). 6 µg of Myc-ASXL2 expression construct was co-transfected in 293T with either 1 µg of Flag-BAP1, Flag-BAP1 C91S or Flag-BAP1 mutants expression constructs. Three days post-transfection, cells were harvested for Flag IP of BAP1 followed by western blotting with the indicated antibodies. B) Ubiquitin pull down interaction assays and DUB assay of H2A using GST-ASXM2 and bacterial His-BAP1 or its mutants presented in panel A. The DUB reactions and the pull down were analysed by immunoblotting as indicated. C) BAP1 complexes were Flag-HA purified from total cell extracts of HeLa cells stably expressing Flag-HA-BAP1 or Flag-HA-BAP1$^{R666\text{-}H669}$ (see Fig. S2A for description of the mutant). Left panel, Silver stain shows the profiles of the complexes. Right panel, western blot detection of the major components of BAP1 complexes. The high and low arrows indicate the position of ASXL2 and BAP1 respectively. D) In vitro deubiquitination assay of H2A (left panel) and ubiquitin pull down interaction assay (right panel) using purified BAP1 or BAP1$^{R666\text{-}H669}$ complexes. E) H226 BAP1-null cells stably expressing BAP1, BAP1^{C91S} or BAP1$^{R666\text{-}H669}$ was analyzed by western blot as indicated. F) Schematic representation of ASXM2 showing the cancer-associated mutants generated for the *in vitro* assays. G) Bacteria-purified His-BAP1 and MBP-cancer associated mutants forms of ASXM2 were subjected to MBP pull down interaction assays. H) His-BAP1 and MBP-ASXM2 fragments were subjected to GST-ubiquitin pull down as well as in vitro DUB activity of H2A. The dot indicates a monoubiquitinated form of BAP1 (panels C, E).

Figure 6. BAP1/ASXL1/ASXL2 tightly regulate cell cycle progression.

A) LF1 cells stably expressing empty vector or Flag-HA-BAP1 were synchronized in G0 by contact inhibition. IP using Flag beads was performed on total cell extracts and the elutions were analyzed by western blot for the indicated proteins. B) Protein expression following siRNA depletion of BAP1, ASXL1 and ASXL2 in U2OS cells. The cells were harvested four days post-transfection for Immunoblotting to analyze endogenous proteins. Tubulin was used as a loading control. Quantification of band intensity was conducted relative to the non-target siRNA control (siNT). C) U2OS cells were transfected with siRNA of BAP1, ASXL1 or ASXL2 and synchronized at the G1/S boundary following thymidine double block and released for 7 hours to progress through S phase (top panel). siRNA transfected U2OS cells were also treated with nocodazole to block the cells in M to follow the progression of the cells from G1 to G2/M (bottom panel). Following release, cells were harvested at different times for FACS analysis. D) Protein expression levels after depletion of endogenous BAP1 using siRNA in U2OS cells stably expressing empty vector, siRNA-resistant BAP1, BAP1C91S or $BAP1^{R666\text{-}H669}$. E) Following siRNA for endogenous BAP1, U2OS cells stably expressing siRNA-resistant BAP1, $BAP1^{C91S}$ or $BAP1^{R666\text{-}H669}$ were arrested at the G1/S boundary and released for 7 hours to progress through S phase and were then subjected to FACS analysis. The dot and star indicate a monoubiquitinated form of BAP1 and non-specific bands respectively (panels A, D).

Figure 7. ASXL2 and BAP1 overexpression induces senescence respectively in an ASXM- and CTD-dependent manner.

A-B) IMR90 cells were transduced using retroviral expression vectors for BAP1, ASXL1, ASXL2 and their respective mutant forms. Eight days post-selection the cells were fixed for staining of senescence-associated β-galactosidase activity (SA-β-gal) (panel A) and cells were also counted every three days after selection to follow cell proliferation (panel B). Note that data from the SA-β-Gal assays were quantified from 100 cells counts in triplicate and presented as the mean percent of positive cells ± SD. C) BAP1 overexpression triggers cellular senescence via p53/p21 DNA damage response in ASXL1/2 dependent manner. Eight days post-selection the senescent cells were harvested for western blot to detect proteins levels as indicated. Quantification of band intensity was conducted relative to the empty vector transduced cells. D) Model for regulation of BAP1-mediated H2A deubiquitination by ASXM. An intramolecular interaction involving UCH/CC1 and CTD creates an ASXM-inducible Composite Ubiquitin Binding Interface (CUBI) that facilitates ubiquitin binding and catalysis. The red stars indicate cancer-associated mutations of BAP1 or ASXM. The dot indicates a monoubiquitinated form of BAP1 (panel C).

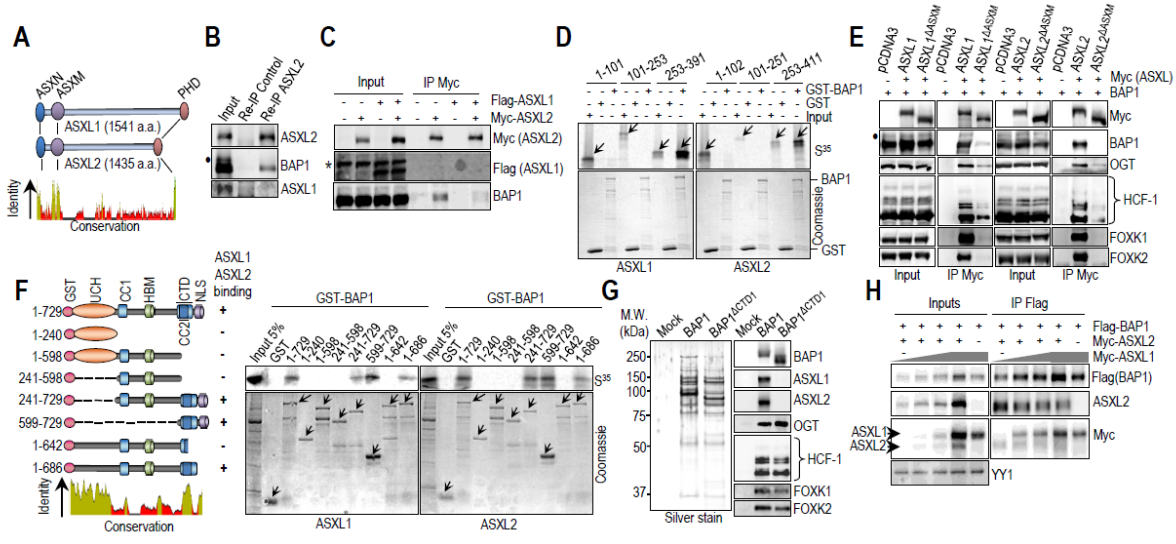
A
ASXN
ASXM
PHD
ASXL1 (1541 a.a.)
ASXL2 (1435 a.a.)
Identity
Conservation
B
Input
Re-IP Control
Re-IP ASXL2
ASXL2
BAP1
ASXL1
C
Input
IP Myc
Flag-ASXL1
Myc-ASXL2
Myc (ASXL2)
Flag (ASXL1)
BAP1
D
1-101
101-253
253-391
1-102
101-251
253-411
GST-BAP1
GST
Input
S35
BAP1
Coomassie
GST
ASXL1
ASXL2
E
pCDNA3
ASXL1
ASXL1ΔASXM
ASXL2
ASXL2ΔASXM
Myc (ASXL)
BAP1
Myc
BAP1
OGT
HCF-1
FOXK1
FOXK2
Input
IP Myc
F
GST
UCH
CC1
HBM
CTD
NLS
CC2
ASXL1
ASXL2
binding
1-729
1-240
1-598
241-598
241-729
599-729
1-642
1-686
Identity
Conservation
GST-BAP1
Input 5%
GST
ASXL1
ASXL2
G
M.W. (kDa)
Mock
BAP1
BAP1ΔCTD1
250
150
100
75
50
37
Silver stain
BAP1
ASXL1
ASXL2
OGT
HCF-1
FOXK1
FOXK2
H
Inputs
IP Flag
Flag-BAP1
Myc-ASXL2
Myc-ASXL1
Flag(BAP1)
ASXL2
Myc
ASXL1
ASXL2
YY1

Figure 1

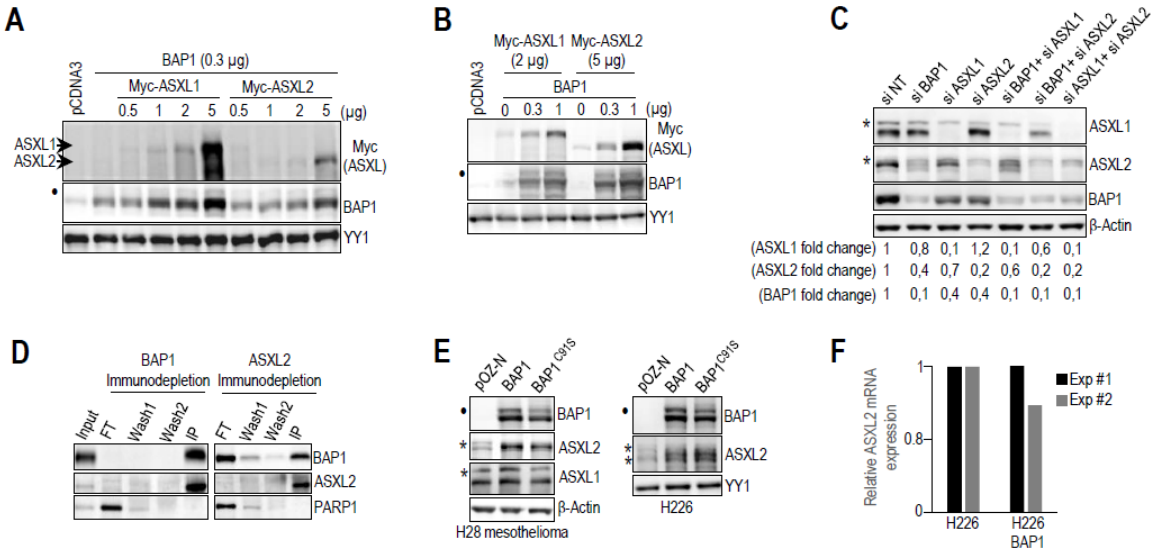
A
pCDNA3
BAP1 (0.3 µg)
Myc-ASXL1
Myc-ASXL2
0.5 1 2 5 0.5 1 2 5 (µg)
ASXL1
ASXL2
Myc (ASXL)
BAP1
YY1
B
Myc-ASXL1 (2 µg)
Myc-ASXL2 (5 µg)
pCDNA3
BAP1
0 0.3 1 0 0.3 1 (µg)
Myc (ASXL)
BAP1
YY1
C
si NT
si BAP1
si ASXL1
si ASXL2
si BAP1+ si ASXL1
si BAP1+ si ASXL2
si ASXL1+ si ASXL2
ASXL1
ASXL2
BAP1
β-Actin
(ASXL1 fold change) 1 0,8 0,1 1,2 0,1 0,6 0,1
(ASXL2 fold change) 1 0,4 0,7 0,2 0,6 0,2 0,2
(BAP1 fold change) 1 0,1 0,4 0,4 0,1 0,1 0,1
D
BAP1 Immunodepletion
ASXL2 Immunodepletion
Input
FT
Wash1
Wash2
IP
FT
Wash1
Wash2
IP
BAP1
ASXL2
PARP1
E
pOZ-N
BAP1
BAP1 C91S
BAP1
ASXL2
ASXL1
β-Actin
H28 mesothelioma
pOZ-N
BAP1
BAP1 C91S
BAP1
ASXL2
YY1
H226
F
Relative ASXL2 mRNA expression
1
0.8
0
Exp #1
Exp #2
H226
H226 BAP1

Figure 2

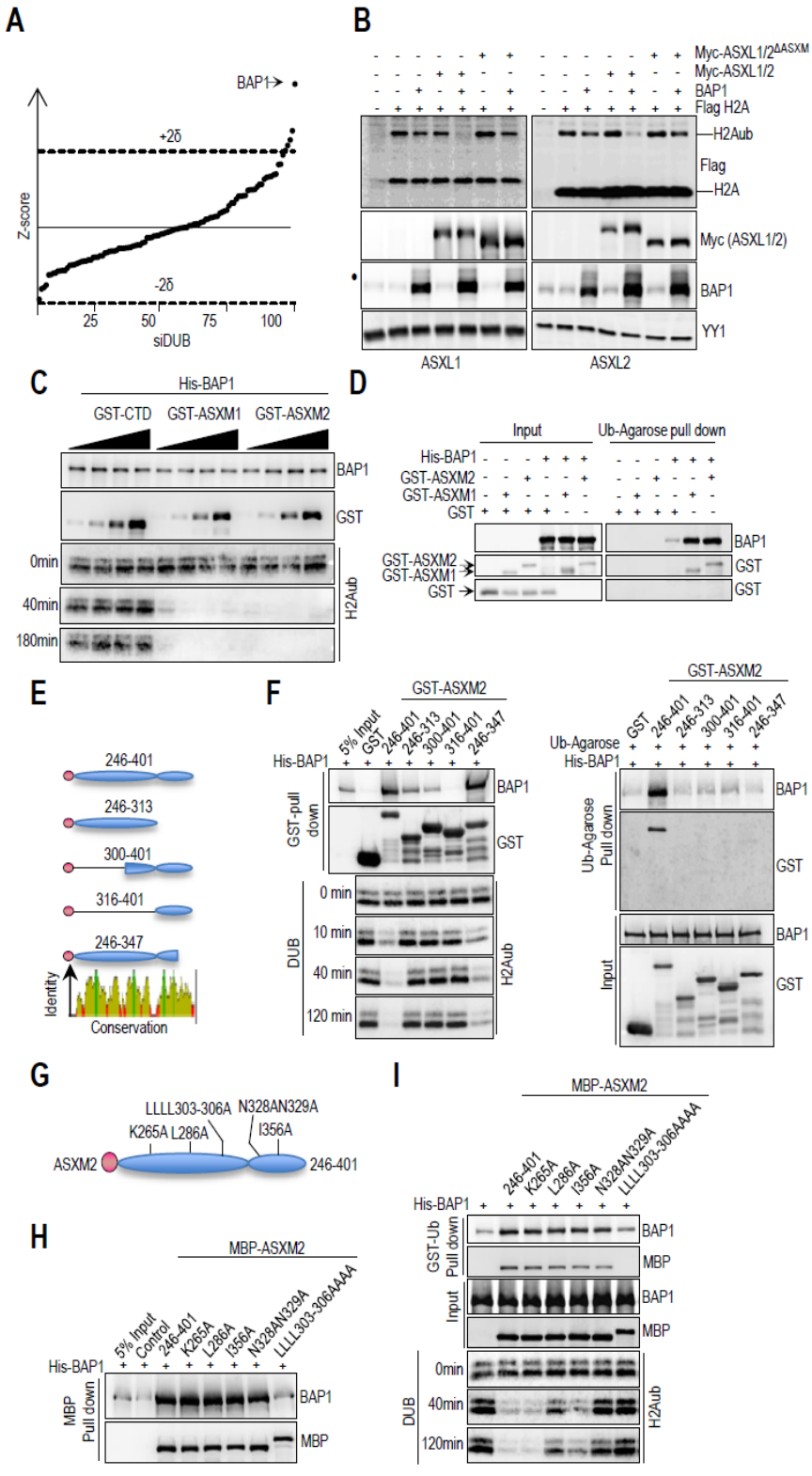
A
BAP1
+2δ
-2δ
Z-score
25
50
75
100
siDUB
B
Myc-ASXL1/2ΔASXM
Myc-ASXL1/2
BAP1
Flag H2A
H2Aub
Flag
H2A
Myc (ASXL1/2)
BAP1
YY1
ASXL1
ASXL2
C
His-BAP1
GST-CTD
GST-ASXM1
GST-ASXM2
BAP1
GST
0min
40min
180min
H2Aub
D
Input
Ub-Agarose pull down
His-BAP1
GST-ASXM2
GST-ASXM1
GST
BAP1
GST
GST
E
246-401
246-313
300-401
316-401
246-347
Identity
Conservation
F
GST-ASXM2
5% Input
GST
246-401
246-313
300-401
316-401
246-347
His-BAP1
GST-pull down
BAP1
GST
DUB
0 min
10 min
40 min
120 min
H2Aub
Ub-Agarose
Ub-Agarose Pull down
Input
G
LLLL303-306A
N328AN329A
K265A L286A
I356A
ASXM2
246-401
H
MBP-ASXM2
5% Input
Control
246-401
K265A
L286A
I356A
N328AN329A
LLLL303-306AAAA
His-BAP1
MBP Pull down
BAP1
MBP
I
MBP-ASXM2
246-401
K265A
L286A
I356A
N328AN329A
LLLL303-306AAAA
His-BAP1
GST-Ub Pull down
BAP1
MBP
Input
BAP1
MBP
DUB
0min
40min
120min
H2Aub

Figure 3

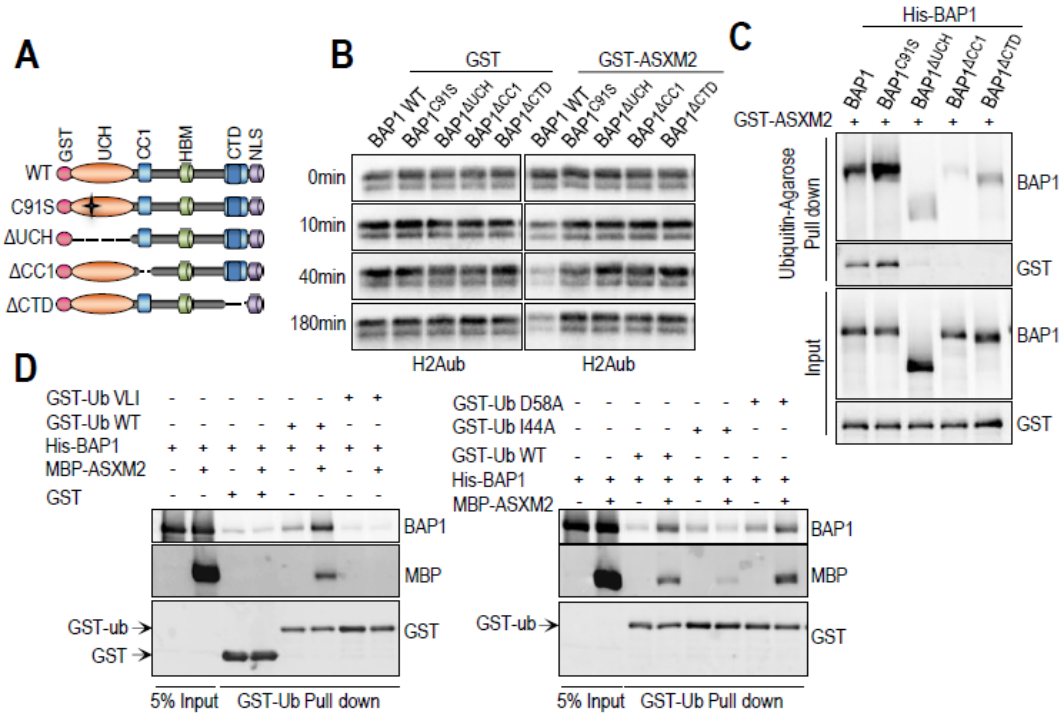
A
GST
UCH
CC1
HBM
CTD
NLS
WT
C91S
ΔUCH
ΔCC1
ΔCTD
B
GST
GST-ASXM2
BAP1 WT
BAP1C91S
BAP1ΔUCH
BAP1ΔCC1
BAP1ΔCTD
0min
10min
40min
180min
H2Aub
C
His-BAP1
GST-ASXM2
Ubiquitin-Agarose Pull down
Input
BAP1
GST
D
GST-Ub VLI
GST-Ub WT
His-BAP1
MBP-ASXM2
GST
GST-Ub D58A
GST-Ub I44A
MBP
GST-ub
5% Input
GST-Ub Pull down

Figure 4

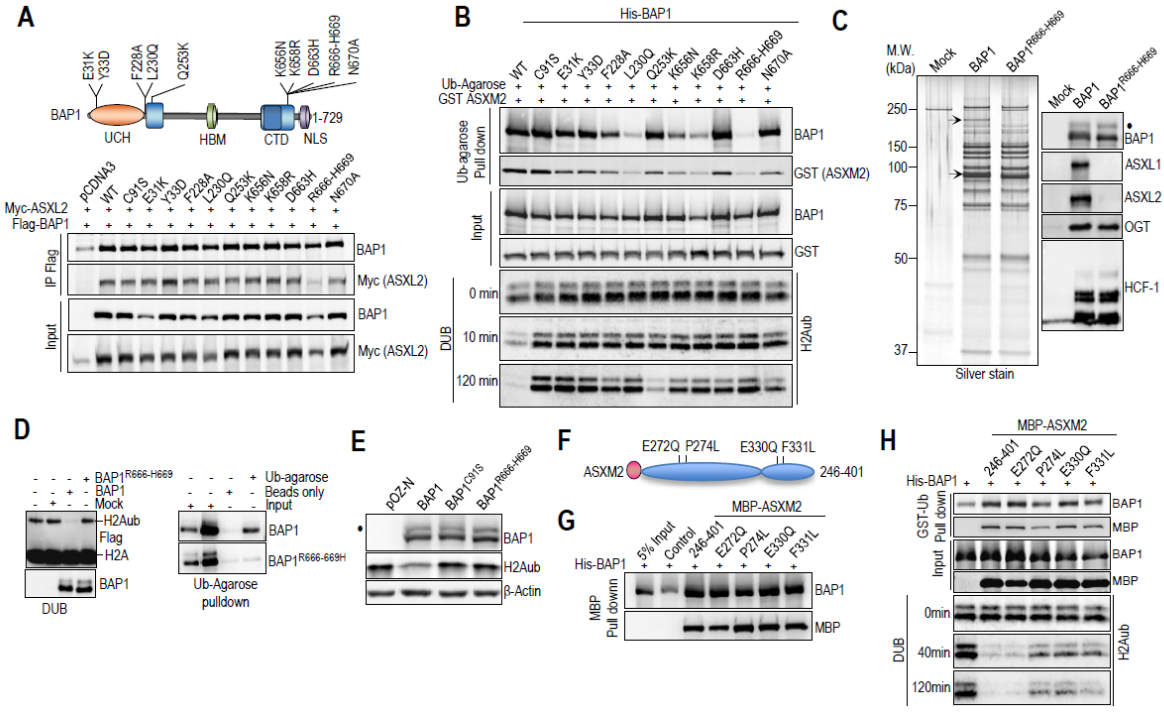
A
B
C
D
E
F
G
H
BAP1
UCH
HBM
CTD
NLS
1-729
Myc-ASXL2
Flag-BAP1
IP Flag
Input
DUB
His-BAP1
Ub-Agarose
GST ASXM2
Ub-agarose Pull down
GST (ASXM2)
GST
0 min
10 min
120 min
H2Aub
M.W. (kDa)
Mock
Silver stain
ASXL1
ASXL2
OGT
HCF-1
Flag
H2A
Ub-Agarose pulldown
Beads only
Input
pCDNA3
pCZ-N
β-Actin
ASXM2
246-401
MBP-ASXM2
5% Input
Control
MBP
MBP Pull down
GST-Ub Pull down
0min
40min
120min

Figure 5

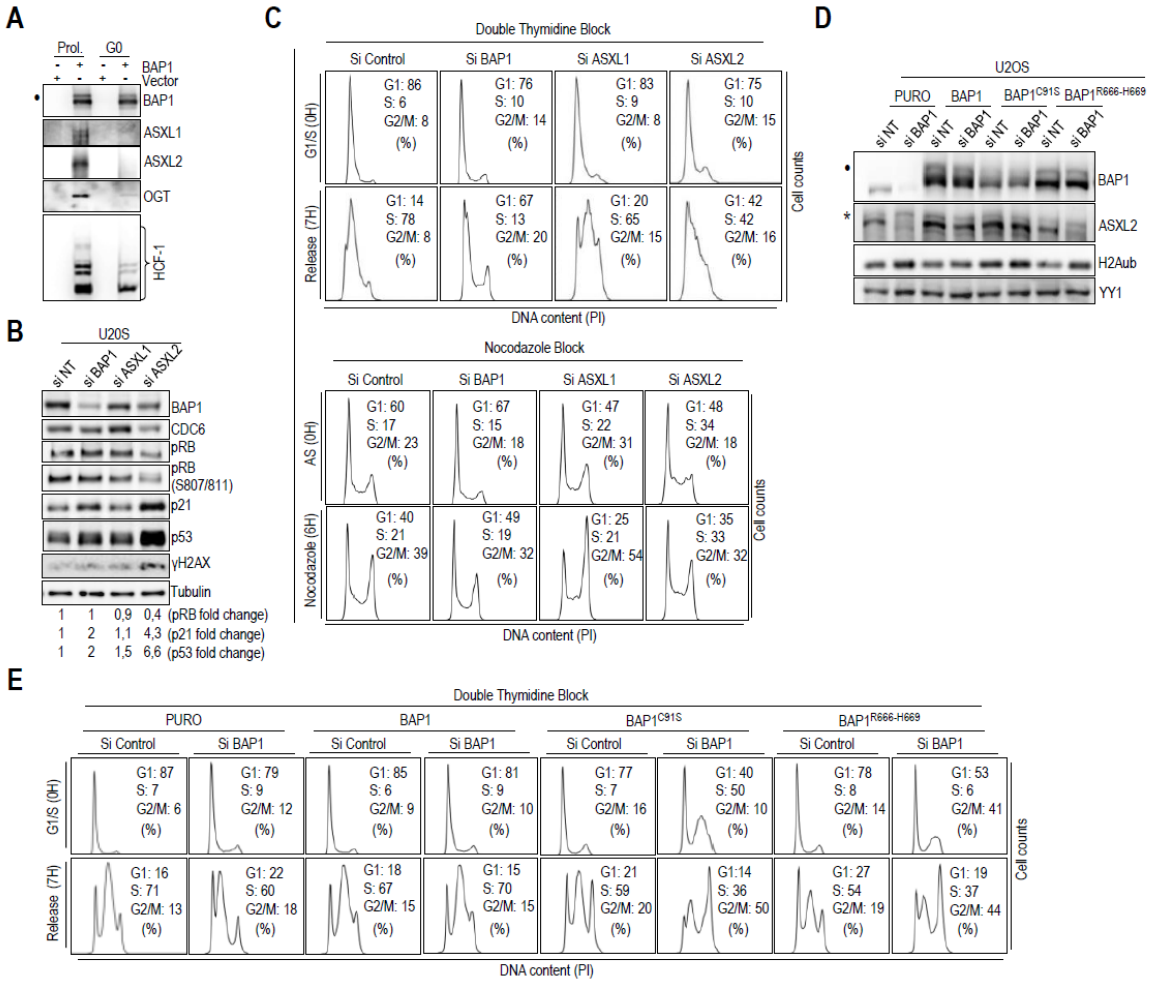
A
Prol.
G0
BAP1 Vector
BAP1
ASXL1
ASXL2
OGT
HCF-1
B
U20S
si NT
si BAP1
si ASXL1
si ASXL2
BAP1
CDC6
pRB
pRB (S807/811)
p21
p53
γH2AX
Tubulin
1 1 0,9 0,4 (pRB fold change)
1 2 1,1 4,3 (p21 fold change)
1 2 1,5 6,6 (p53 fold change)
C
Double Thymidine Block
Si Control
Si BAP1
Si ASXL1
Si ASXL2
G1/S (0H)
Release (7H)
G1: 86 S: 6 G2/M: 8 (%)
G1: 76 S: 10 G2/M: 14 (%)
G1: 83 S: 9 G2/M: 8 (%)
G1: 75 S: 10 G2/M: 15 (%)
G1: 14 S: 78 G2/M: 8 (%)
G1: 67 S: 13 G2/M: 20 (%)
G1: 20 S: 65 G2/M: 15 (%)
G1: 42 S: 42 G2/M: 16 (%)
Cell counts
DNA content (PI)
Nocodazole Block
AS (0H)
Nocodazole (6H)
G1: 60 S: 17 G2/M: 23 (%)
G1: 67 S: 15 G2/M: 18 (%)
G1: 47 S: 22 G2/M: 31 (%)
G1: 48 S: 34 G2/M: 18 (%)
G1: 40 S: 21 G2/M: 39 (%)
G1: 49 S: 19 G2/M: 32 (%)
G1: 25 S: 21 G2/M: 54 (%)
G1: 35 S: 33 G2/M: 32 (%)
D
U2OS
PURO
BAP1
BAP1C91S
BAP1R666-H669
si NT
si BAP1
BAP1
ASXL2
H2Aub
YY1
E
Double Thymidine Block
PURO
BAP1
BAP1C91S
BAP1R666-H669
Si Control
Si BAP1
G1/S (0H)
Release (7H)
G1: 87 S: 7 G2/M: 6 (%)
G1: 79 S: 9 G2/M: 12 (%)
G1: 85 S: 6 G2/M: 9 (%)
G1: 81 S: 9 G2/M: 10 (%)
G1: 77 S: 7 G2/M: 16 (%)
G1: 40 S: 50 G2/M: 10 (%)
G1: 78 S: 8 G2/M: 14 (%)
G1: 53 S: 6 G2/M: 41 (%)
G1: 16 S: 71 G2/M: 13 (%)
G1: 22 S: 60 G2/M: 18 (%)
G1: 18 S: 67 G2/M: 15 (%)
G1: 15 S: 70 G2/M: 15 (%)
G1: 21 S: 59 G2/M: 20 (%)
G1:14 S: 36 G2/M: 50 (%)
G1: 27 S: 54 G2/M: 19 (%)
G1: 19 S: 37 G2/M: 44 (%)
Cell counts
DNA content (PI)

Figure 6

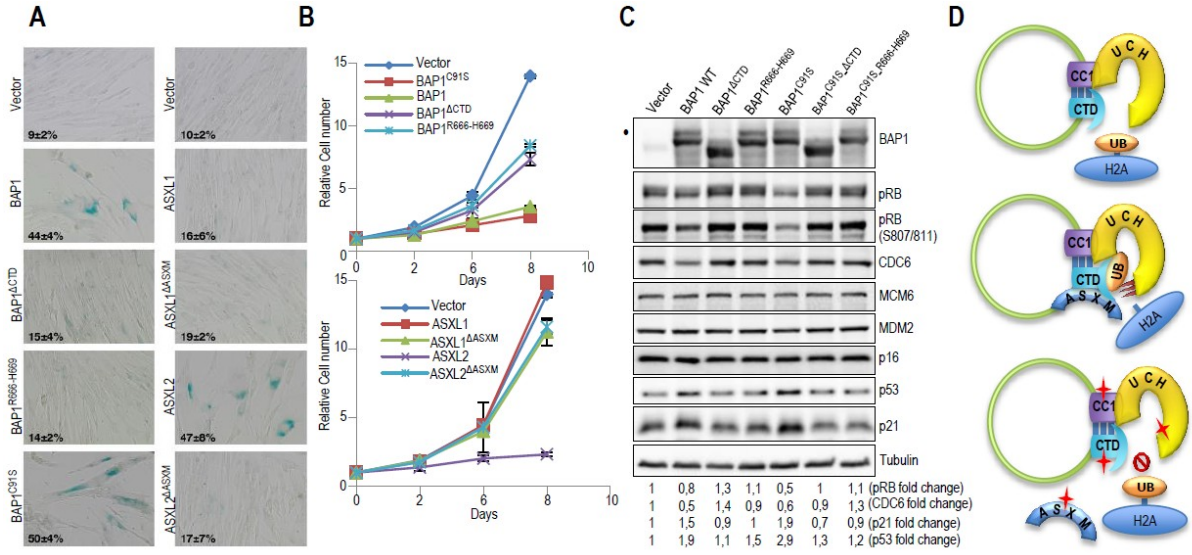
A
B
C
D
Vector
BAP1
BAP1ΔCTD
BAP1R666-H669
BAP1C91S
ASXL1
ASXL1ΔASXM
ASXL2
ASXL2ΔASXM
9±2%
44±4%
15±4%
14±2%
50±4%
10±2%
16±6%
19±2%
47±8%
17±7%
Relative Cell number
Days
Vector
BAP1C91S
BAP1
BAP1ΔCTD
BAP1R666-H669
ASXL1
ASXL1ΔASXM
ASXL2
ASXL2ΔASXM
Vector
BAP1 WT
BAP1ΔCTD
BAP1R666-H669
BAP1C91S
BAP1C91S_ΔCTD
BAP1C91S_R666-H669
BAP1
pRB
pRB (S807/811)
CDC6
MCM6
MDM2
p16
p53
p21
Tubulin
1 0,8 1,3 1,1 0,5 1 1,1 (pRB fold change)
1 0,5 1,4 0,9 0,6 0,9 1,3 (CDC6 fold change)
1 1,5 0,9 1 1,9 0,7 0,9 (p21 fold change)
1 1,9 1,1 1,5 2,9 1,3 1,2 (p53 fold change)
UCH
CC1
CTD
UB
H2A
ASXM

Figure 7

Supporting Information

SI Materials and Methods

Plasmids.

Retroviral constructs pOZ-N-Flag-HA-BAP1, pOZ-N-Flag-HA-BAP1 C91S (catalytic dead) and pOZ-N-Flag-HA-BAP1ΔHBM (BAP1 mutant deleted in the NHNY sequence corresponding to the HCF-1 binding motif); constructs to produce recombinant full-length GST-BAP1 and various deleted forms; pET30a+ BAP1 for production of His-tagged BAP1 were previously described (1). pCDNA3-Flag-H2A was obtained from Moshe Oren (2). pOZ-N-Flag-HA-BAP1 ΔCTD1 and pOZ-N-Flag-HA-BAP1 ΔCC2 were generated by PCR-based subcloning. Non-tagged pCDNA3-BAP1 and pCDNA3-BAP1-C91S were generated by subcloning the cDNAs from pOZ-N-Flag-HA-BAP1 and pOZ-N-Flag-HA-BAP1-C91S respectively. siRNA resistant constructs for BAP1, BAP1-C91S, BAP1 ΔCTD, BAP1R666-H669 and expression constructs for H2A, H2AK118R, H2AK119R, H2AK118R/K119R, H2AK13R/K15R were generated using gene synthesis (BioBasic) and then subcloned into modified pENTR D-Topo plasmid (Life Technologies). Histones H2AX and H2AZ were cloned from U2OS total RNA by reverse transcription and inserted into pENTR D-Topo plasmid. Expression constructs of siRNA resistant BAP1, BAP1 C91S, BAP1 ΔCTD and BAP1 ΔR666-H669 were generated by recombination using LR clonase kit (Life Technologies) into pMSCV-Flag-HA-IRES-Puro or pDEST-Myc constructs (3). Expression constructs of H2AX, H2AZ, H2A and corresponding mutant forms were generated by recombination into pDEST-Flag. BAP1ΔUCH, BAP1ΔCC1 and BAP1ΔCTD were previously described (4), and were sub-cloned by PCR into pENTR. Ubiquitin constructs flanked by att-

B and att-P recombination sites were generated by gene synthesis (Life technologies) directly into pMK-Rq plasmid and expression constructs were generated by recombination into pDEST-GST. Human ASXL1 and ASXL2 were cloned from HeLa total RNA by reverse transcription and inserted into pENTR D-Topo plasmid. BAP1 point mutations constructs were generated by site direct mutagenesis in pENTR D-Topo BAP1 using PfuUltra High-Fidelity DNA Polymerase. Human Myc-ASXL1 ΔASXM and ASXL2 ΔASXM constructs were generated by PCR-based subcloning of 2 fragments each ligated in frame into pENTR D-Topo. Expression constructs of ASXL1, ASXL2 and corresponding vectors with deletions of ASXM were generated using LR clonase in pDEST-Myc, pDEST-Flag and pMSCV-Flag-HA-IRES-Puro based constructs. Other expression constructs for BAP1 and corresponding mutants forms, were generated using LR clonase in pDEST-Myc, pDEST-Flag and bacterial pDEST-His. Full length ASXM1 and ASXM2 and deletions mutants forms of ASXM2 (ASXM2 246-313, ASXM2 300-401, ASXM2 316-401, ASXM2 246-347) were sub-cloned by PCR and inserted into pENTR D-Topo plasmid. ASXM2 point mutations constructs were generated by site direct mutagenesis in pENTR D-Topo ASXM2 using PfuUltra High-Fidelity DNA Polymerase. Expression vectors of ASXM1, ASXM2 and respective mutant forms were generated using LR clonase in pDEST-GST and pDEST-MBP.

Cell culture and cell transfection.

Primary skin fibroblasts (LF1), BAP1-deficient human lung squamous carcinoma NCI-H226, BAP1-deficient human mesothelioma NCI-H28, U2OS osteosarcoma, human embryonic kidney HEK293T (293T), HeLa, normal Human Lung Fibroblasts (IMR90), phoenix ampho

and 293-GPG packaging cells were cultured in Dulbecco's modified Eagle's medium (DMEM) supplemented with foetal bovine serum (FBS), L-glutamine and penicillin/streptomycin. Cervical cancer HeLa S3 cells were cultured in Minimum Essential Media (MEM) supplemented with FBS, L-glutamine and penicillin/streptomycin. 293T cells were transfected with the mammalian expressing vectors using polyethylenimine (PEI) (Sigma-Aldrich). Three days post-transfection, cells were harvested for immunoblotting, immunoprecipitation or immunostaining. U2OS or LF1 cells were transfected using Lipofectamine 2000 (Life technologies) with 200 pmol of either ON-TARGET plus Non-targeting pool (D-001810) or ON-TARGET plus SMARTpool BAP1 (L-005791) (Thermo Scientific, Dharmacon) or with a pool of siRNA sequences purchased from Sigma-Aldrich targeting ASXL1 (pool of 4 oligonucleotides, SASI_Hs02_00347642, SASI_Hs01_00200507, SASI_Hs01_00200508, SASI_Hs01_00200509) and ASXL2 (2 pools of 4 oligonucleotides, SASI_Hs01_00202197, SASI_Hs01_00202198, SASI_Hs01_00202199, SASI_Hs01_00202200 and SASI_Hs01_00202197, SASI_Hs01_00202200, SASI_Hs01_00202203, SASI_Hs01_00202201). Four days post-transfection, cells were harvested for immunoblotting or immunostaining.

siRNA DUB screen.

HeLa cells were transfected with individual siRNA pool targeting DUBs (ON-TARGETplus® SMARTpool® siRNA Library-Human Deubiquitinating Enzymes) using Lipofectamine 2000 (Life Technologies). Three days post-transfection, cells were fixed and used for immunostaining with H2Aub antibody and the fluorescence signals were detected

with a Fluoroskan Ascent™ Microplate Fluorometer (Thermo Scientific), and the obtained values were used to derive the Z-scores. The screen was done in duplicate and the values of H2Aub signals were normalized to DAPI staining.

qRT-PCR analysis of mRNA expression.

Total RNA was extracted using Trizol reagent (Life technologies) followed by the RNeasy kit (QIAGEN). Total mRNA was used for reverse transcription using the Superscript III reverse transcriptase and oligo-dT primers (Life Technologies). The cDNAs were analyzed by Real time PCR using SYBR Green detection DNA quantification kit (Life technologies) to determine levels of gene mRNAs. PCR was conducted on an Applied Biosystems® 7500 Real-Time PCR Systems (Life Technologies). To ensure accurate quantification of mRNA, similar amounts of total RNA were spiked with an in vitro synthesized GAL4 mRNA, which was performed following the manufacturer procedure (MAXIscript Kit Procedure, Life Technologies). The transcript was synthesized from pcDNA.3-GAL4 construct with T7 promoter. The primers used are listed below.

ASXL2: hASXL2-F: GAATCCAGGTGCGAAAAGTAC

hASXL2-R: GATGGAGACTGGAAAACGAGC

p21: hp21-F: AGCATGACAGATTTCTACCA

hp21-R: CCAGGGTATGTACATGAGGA

GAL4: GAL4-F: CAACTGGGAGTGTCGCTACT

GAL4-R: AATCATGTCAAGGTCTTCTCGA

Immunoblotting and antibodies.

Total cell extracts were prepared by lysing cells with buffer containing 25 mM Tris pH 7.3 and 1% sodium dodecyl sulfate (SDS). Cell extracts were boiled at 95 °C for 10 min and then sonicated. Quantification of total proteins was conducted using the bicinchoninic acid (BCA) assay, and samples were diluted in Laemmli buffer. SDS-PAGE and immunoblotting were done according to standard procedures. The band signals were acquired with a LAS-3000 LCD camera coupled to MultiGauge software (Fuji, Stamford, CT, USA). Anti-FOXK2 rabbit polyclonal antibody was previously described (4). The Anti-ASXL1 was generated using bacteria-expressed fragment (700-950 amino acids of the human protein) with Pacific Immunology. Mouse monoclonal anti-BAP1 (C4, sc-28383), polyclonal anti-BAP1 (H300, sc-28236), rabbit polyclonal anti-YY1 (H414, sc-1703), rabbit polyclonal anti-OGT (H300, sc-32921), mouse monoclonal anti-CDC6 (180.2, sc-9964), mouse monoclonal anti-MCM6, mouse monoclonal anti-tubulin (B-5-1-2, sc-SC-23948), mouse monoclonal anti-p53 (DO-1, sc-126), mouse monoclonal anti-p16 (JC8, sc-56330), mouse monoclonal anti-MDM2 (SMP14, sc-965), rabbit polyclonal anti-FOXK1 (H-140, sc-134550), and mouse monoclonal anti-PARP1 (F2, sc-8007) were from Santa Cruz. Rabbit polyclonal anti-HCF-1 (A301-400A) and rabbit polyclonal anti-ASXL2 (A302-037A) were from Bethyl Laboratories. Mouse monoclonal anti-p21 (55643) was from BD PHARMIGEN. Mouse monoclonal anti-Flag (M2) and rabbit polyclonal anti-GST (G7781) were from Sigma-Aldrich. Mouse monoclonal anti-MYC (9E10) was from Covance. Rabbit polyclonal anti-H2Aub (D27C4) rabbit polyclonal anti-H2Bub (Lysine 120) (D11 XP), mouse monoclonal anti-RB (4H1), rabbit polyclonal anti-pRB (S807/811) and mouse monoclonal (HRP conjugated) anti-MBP were from Cell Signaling. Mouse monoclonal anti-H2Bub antibody (NRO3) was from

MEDIMABS. Mouse monoclonal anti-Phospho-H2AX (ser139) (clone JBW301, 05-636), Mouse monoclonal anti-H2Bub antibody clone 56 (05-1312), Mouse monoclonal anti-H2Aub antibody clone E6C5 (05-678) and mouse monoclonal anti-β-Actin (MAB1501, clone C4) were from Millipore.

Immunodepletion and Immunoprecipitation.

For immunodepletion experiments of endogenous proteins, ~100 µg of HeLa nuclear extracts was incubated overnight at 4 ºC with either 2 µg of anti-BAP1 (C4), 2 µg of anti-ASXL2 (Bethyl) or control IgG in IP buffer (50 mM Tris, pH 7.3; 150 mM NaCl; 5 mM EDTA; 10 mM NaF; 1% Triton X-100; 0.1 % BSA, 1 mM phenylmethylsulfonyl fluoride (PMSF) and protease inhibitors cocktail (Sigma-Aldrich). The immuno-complexes were incubated next day for 6 hours at 4 ºC with protein G sepharose beads which were saturated with 1% BSA in IP buffer. Immuno-depleted complexes were then washed 2 times with the IP buffer supplemented with 0.1% BSA. Bound proteins were eluted with Laemmli buffer and subjected, along with the flow through fractions, to immunoblotting. Reciprocal immunoprecipitation from the purified BAP1 complexes was conducted essentially as described above. Briefly, the purified BAP1 complexes were incubated with the indicated antibodies overnight at 4 ºC. The immuno-depleted complexes were recovered next day with protein G sepharose beads saturated with 1% BSA. Co-immunoprecipitation following overexpression in 293T cells was conducted using total cell lysates. Cells were resuspended in 50 mM Tris, pH 7.3; 150 mM NaCl; 5 mM EDTA; 10 mM NaF; 1% Triton X-100; 1 mM PMSF, protease inhibitors cocktail (Sigma-Aldrich), and the lysates were clarified by

centrifugation at 21,000 g for 30 min. The supernatants were incubated with indicated antibodies overnight along with protein-G sepharose beads. Bound proteins were washed extensively with the same lysis buffer and eluted in Laemmli buffer for western blot analysis.

Stable cell lines and protein complex purification.

HeLa S3 cell lines stably expressing Flag-HA-BAP1, Flag-HA-BAP1$^{\Delta CTD1}$, or Flag-HA-BAP1$^{R666\text{-}H669}$, H28 cell lines stably expressing Flag-HA-BAP1 and Flag-HA-BAP1^{C91S}, as well as H226 cell lines stably expressing Flag-HA-BAP1, Flag-HA-BAP1^{C91S} and Flag-HA-BAP1$^{R666\text{-}H669}$ were generated following retroviral infection using pOZ-N-Flag-HA-IRES-IL2R retroviral constructs and selection using anti-IL2 magnetic beads (Life Technologies) (1). U2OS expressing siRNA resistant Flag-HA-BAP1, Flag-HA-BAP1^{C91S}, Flag-HA-BAP1 $^{\Delta CTD}$ and Flag-HA-BAP1$^{R666\text{-}H669}$ were generated following retroviral infection using pMSCV-Flag-HA-IRES-Puro based constructs and selection with 3 μg/ml of puromycin. Around 3 X 10^9 of HeLa S3 cells were used for the immunoaffinity purification of the different BAP1 complexes. Total cell extracts obtained after resuspending cells in 50 mM Tris-HCl pH 7.5, 150 mM NaCl, 0,5% NP-40, 50 mM NaF, 10 mM β-glycerophosphate, 1 mM Na3VO4, 1 mM DTT, 1 mM EDTA, 1 mM PMSF and protease inhibitors cocktail (Sigma-Aldrich) were used for the immunopurification. The extracts were first clarified by centrifugation at 30,000 g for 1 hour, followed by filtration through a 0,45 μm pore filter. The lysates were then incubated with the anti-Flag M2 resin (Sigma-Aldrich) overnight and extensively washed with the lysis buffer. The resin was eluted three times with 200 μg/ml of Flag peptide. The eluted fractions were incubated with anti-HA resin (Sigma-Aldrich) overnight, and the procedure

was repeated as for the previous column. The HA eluted fractions were used for silver stain, western blot and in vitro DUB assay.

***In vitro* interaction assays.**

Protein interaction pull down assays were conducted essentially as previously described (1). Recombinant His-BAP1 fusion proteins were purified using Ni-NTA Agarose Resins (Life technologies). The eluted purified His proteins were obtained using 200 mM of imidazole elution buffer. GST-BAP1, GST-ASXM1/2 and respective deletion mutant forms and GST-CTD were purified using glutathione agarose beads (Sigma-Aldrich). GST eluted proteins were obtained using 25 mM glutathione in the wash buffer. MBP-ASXM2 and corresponding mutant forms were purified using Amylose resin (New England Biolabs). MBP eluted proteins were obtained using the elution buffer (10 mM maltose, 50 mM Tris-HCl pH 7.4, 150 mM NaCl, 5 mM EDTA, 2 mM DTT). For the GST pull down interaction assays of BAP1 with in vitro translated ASXL1/2, full length GST-BAP1 or its deletion fragments (2 to 3 µg) immobilized beads were incubated with 10 µl of in vitro translated methionine-S35 labeled (TNT® T7 Quick Coupled Transcription/Translation System, Promega) ASXL1 or ASXL2 fragments for 6 to 8 hours at 4 ºC in 50 mM Tris, pH 7.5; 50 mM NaCl; 0.02% Tween 20; 1 mM PMSF and 500 µM DTT). The beads were extensively washed with the same buffer, and associated proteins were eluted in Laemmli buffer and subjected to SDS-PAGE followed by autoradiography or coomassie blue staining. For the in vitro interaction assays of BAP1 with purified ASXM2, around 2 µg of purified His-BAP1 was incubated with GST-ASXM2 or MBP-ASXM2 or its mutant forms (2 to 3 µg each) immobilized on GSH-

agarose or Maltose-agarose beads respectively for 3 hours at 4 ºC in 50 mM Tris, pH 7.5; 150 mM NaCl; 1% Triton; 1 mM PMSF, protease inhibitors cocktail and 2mM DTT (Buffer A). The beads were pre-blocked for 1 hour in the same buffer containing 1% BSA and were washed 6 to 8 times after pull down with the buffer cited above. The associated proteins were eluted in Laemmli buffer and subjected to immunoblotting.

Ubiquitin pull down interaction assays.

GST-ubiquitin immobilized beads and its corresponding mutant forms were purified using glutathione agarose beads. For the ubiquitin-agarose pull down interaction assays, His-BAP1 or its different mutant forms were pre-incubated for 30 min to 1 hour with GST-ASM1 or GST-ASXM2 at 4 ºC in the buffer A. The mix was incubated for 3 hours with ubiquitin-agarose beads which were then washed 6 times with the same buffer. The associated proteins were eluted in Laemmli buffer and subjected to western blotting. For the GST-ubiquitin (GST-Ub) pull down interaction assays, His-BAP1 was pre-incubated for 30 min to 1 hour with either MBP-ASM2 or its mutant forms. The mix was then incubated for 3 hours with either GST-Ubiquitin immobilized beads or mutant forms. The beads were washed 6 times with the same buffer and the associated proteins were subjected to western blotting.

Purification of the nucleosomes and *in vitro* DUB assay.

293T cells were transfected with 7 µg of pCDNA-Flag-H2A using PEI in serum free media. Three days post-transfection, cells were harvested and chromatin fraction extraction and nucleosomes digestion with Micrococcal nuclease (MNase, Sigma-Aldrich) were conducted

as previously described with some modifications (5). Cell pellets were resuspended in 50 mM Tris-HCl pH 7.3, 420 mM NaCl, 1% NP-40, 1 mM MgCl2, 10 mM β-mercapto ethanol, 1 mM PMSF, protease inhibitor cocktail (Sigma-Aldrich), and 20 mM of N-ethylmaleimide (NEM). The lysate was incubated on ice for 20 min. After centrifugation at 2000 g for 5 min, the chromatin pellet was washed twice with the same buffer followed with two washes using MNase buffer (20 mM Tris-HCl pH 7.5, 100 mM KCl, 2 mM MgCl2, 1 mM CaCl2, 0.3 M sucrose, 0.1% NP-40, 1 mM PMSF and protease inhibitor cocktail). After MNase treatment (3 U/ml for 10 min at room temperature), the reaction was stopped with 5 mM EDTA. Following centrifugation at 20,000g for 10 min at 4°C, the soluble chromatin fraction was incubated overnight at 4°C with anti-Flag M2 beads. The beads were washed several times with 50 mM Tris-HCl, pH 7.3; 5 mM EDTA; 300 mM NaCl; 10 mM NaF; 1% NP-40; 1 mM PMSF; 1 mM DTT; protease inhibitors cocktail. Bound nucleosomes were then eluted with 200 µg/ml of Flag peptides (Biobasic Inc.). 2 µg of pDEST-Flag-H2AK118R/K119R and pDEST-Flag-H2AK13R/K15R were transfected in 293T cells. Three days post-transfection, cells were harvested and chromatin fraction extraction and purified nucleosomal H2A were obtained as described above. The purified nucleosomes were used for the *in vitro* deubiquitination assay using either Flag-HA purified BAP1 complexes or bacteria-purified His-BAP1 with or without bacteria purified GST-ASXM1/2 or MBP-ASXM2. The deubiquitination reaction was carried out in the reaction buffer (50 mM Tris-HCl, pH 7.3; 1 mM MgCl2; 50 mM NaCl; 1 mM DTT) for the indicated times at 37°C. The *in vitro* reaction was stopped by adding Laemmli buffer and analyzed by immunoblotting. Nucleososomes were pre-treated with benzonase (0.64 U/µl) in the DUB reaction for 30 min prior to the addition of the BAP1 complexes.

Cellular senescence.

5 x 106 Phoenix Ampho packaging cells were plated into a 10 cm petri dish, incubated 24 hours, and then transiently transfected using Lipofectamine 2000 with 10 μg of pMSCV-Flag-HA-IRES-Puro based constructs expressing ASXL1/2, BAP1 and corresponding deletions mutant form along with 1 μg of a helper plasmid containing env of 4070A MuMLV virus (Helper ampho). The medium was changed 24 hours after incubation. Viral soups were collected 48 hours and 60 hours after transfection, filtered through a 0.45 μm filter, supplemented with 8 μg/ml polybrene and 10% of FBS and then added twice on IMR90 cells at 8-12 hour intervals. Twelve hours after the last infection, cells were selected for two days with 2 μg/ml of puromycin (Wisent). Eight days after selection, cells were either collected in the buffer (25 mM Tris pH 7.3 and 1% sodium dodecyl sulfate (SDS)) for western blot analysis or evaluated for cellular senescence by performing senescence-associated-β-galactosidase (SA-β-gal) activity. Briefly, at day 7 post-selection, IMR90 cells were plated at representative confluency overnight, and fixed in 0.5% glutaraldehyde in PBS. Washes were performed in PBS + 1mM MgCl2 in pH 6. Cells were then incubated with X-gal (1mg/ml) solution at 37^{o}C for 3-6h. Percentages of senescent cells from the SA-β-Gal assays were quantified from 100 cells counts in triplicate and presented as the mean percent of positive cells ± SD.

Synchronization and cell cycle analysis.

LF1 primary skin fibroblasts stably expressing BAP1 were synchronized in G0 by contact inhibition as previously described (6). U2OS cells were synchronized at the G1/S border

using the method of thymidine (2 mM) double block as described previously (6). Cells were then released into new media to follow the progression during S phase. To study the progression of the cells through the cell cycle, cells were treated with 200 ng/ml of Nocodazole and followed at different times point. Cell cycle analysis was carried out as described (6). Briefly, cells were harvested by trypsinization and fixed with 70 % ethanol. Following centrifugation and resuspention in PBS, cells were treated with 100 µg/ml RNase A for 30 min at 37 °C and stained with 50 µg/ml propidium iodide. DNA content of cells was analyzed using a FACScan flow cytometer fitted with CellQuestPro software (BD Biosciences).

Immunofluorescence.

The immunostaining procedure was carried essentially as previously described (7). Briefly, cells were fixed in 3% PFA-PBS and permeabilized using PBS 0.1% NP-40. Following blocking with 10% FBS in PBS 0.1% NP-40, the coverslips were incubated with mouse monoclonal and/or rabbit polyclonal for three hours. Anti-mouse Alexa Fluor® 594, anti-mouse Alexa Fluor® 488, Anti-rabbit Alexa Fluor® 488 or anti-rabbit Alexa Fluor® 594 (Life Technologies) were used as secondary antibodies. Nuclei were stained with 4',6-diamidino-2-phenylindole (DAPI). Images were acquired using BX53 OLYMPUS microscope U-HGLGPS, XM10 digital monochrome camera and UPlan SApo 60X/1.35 Oil objective. Images were processed using WCIF-ImageJ program (NIH).

Supplemental References

1.Yu H, et al. (2010) The Ubiquitin Carboxyl Hydrolase BAP1 Forms a Ternary Complex with YY1 and HCF-1 and is a Critical Regulator of Gene Expression. Molecular and cellular biology.

2.Minsky N & Oren M (2004) The RING domain of Mdm2 mediates histone ubiquitylation and transcriptional repression. Molecular cell 16(4):631-639.

3.Sowa ME, Bennett EJ, Gygi SP, & Harper JW (2009) Defining the human deubiquitinating enzyme interaction landscape. Cell 138(2):389-403.

4.Mashtalir N, et al. (2014) Autodeubiquitination protects the tumor suppressor BAP1 from cytoplasmic sequestration mediated by the atypical ubiquitin ligase UBE2O. Molecular cell 54(3):392-406.

5.Groisman R, et al. (2003) The ubiquitin ligase activity in the DDB2 and CSA complexes is differentially regulated by the COP9 signalosome in response to DNA damage. Cell 113(3):357-367.

6.Hammond-Martel I, et al. (2010) PI 3 kinase related kinases-independent proteolysis of BRCA1 regulates Rad51 recruitment during genotoxic stress in human cells. PloS one 5(11):e14027.

7.Daou S, et al. (2011) Crosstalk between O-GlcNAcylation and proteolytic cleavage regulates the host cell factor-1 maturation pathway. Proceedings of the National Academy of Sciences of the United States of America 108(7):2747-2752.

8.Ventii KH, et al. (2008) BRCA1-associated protein-1 is a tumor suppressor that requires deubiquitinating activity and nuclear localization. Cancer research 68(17):6953-6962.

9.Morrow ME, et al. (2013) Stabilization of an unusual salt bridge in ubiquitin by the extra C-terminal domain of the proteasome-associated deubiquitinase UCH37 as a mechanism of its exo specificity. Biochemistry 52(20):3564-3578.

Supplemental Figure Legends

Figure S1. ASXM of ASXL1 and ASXL2 is critical for interaction with BAP1.

A) BAP1 complexes contain relatively similar amounts of ASXL1/2 peptides. ASXL1/2 peptides identified by mass spectrometry following the purification of BAP1 complexes from HeLa S3 cells. The amino acid positions of the peptides are indicated. B) ASXM domain of ASXL1/2 is highly conserved. Multiple sequence alignment between human ASXL1/2 and drosophila ASX showing the conservation of the ASXL family protein sequences. The mutants of ASXM2 used are shown. C) ASXM is required for ASXL2, but not ASXL1, stability. Flag-ASXL1/2 and their respective Flag-ASXL1/2 $^{\Delta ASXM}$ mutants (3 μg each) were transfected in 293T cells which were harvested three days post-transfection for immunoblotting. A duplicate of transfection is shown for Flag-ASXL1/2 $^{\Delta ASXM}$ mutants.

Figure S2. Intact interaction of ASXL1/2 with the CTD domain is required for BAP1 stability.

A) BAP1 sequence conservation. Multiple sequence alignment of BAP1 orthologs showing the conservation of BAP1 among different species. The main functional domains of BAP1 (UCH, CTD and NLS) are indicated (top Panel). Schema of the different deletions in the CTD domain used to generate BAP1 mutants (bottom panel). BAP1$^{\Delta CTD1}$ represents a deletion of the CTD from 635 up to 693 amino acids. Except the KRKKFK motif which is suggested to function as an NLS (8). However, we later realized that this motif is dispensable for BAP1 localization in the nucleus (4). Therefore, we generated a BAP1$^{\Delta CTD}$ which represents a mutant with a deletion of the CTD domain (Δ632-692 amino acids). Of note BAP1$^{\Delta CTD}$ and

$BAP1^{\Delta CTD1}$ acted essentially in a similar manner in respect to the functional assays conducted. $BAP1^{\Delta CC2}$ represents a mutant with a smaller deletion within the CTD domain (Δ635-655 amino acids). $BAP1^{R666\text{-}H669}$ is a cancer mutant with a deletion of the R666 to H669 amino acids. Bottom, comparison between BAP1 and UCH37. tsUCH37 of the worm Trichinella spiralis whose crystal structure was recently reported (9), was aligned with human UCH37 and BAP1. The alignment show conserved motifs and residues in the UCH, CC1 and CTD domains. The mutants of BAP1 used are shown. B) HCF-1 is not required to maintain the interaction between BAP1 and ASXL1/2. Purification of BAP1 or $BAP1^{\Delta HBM}$ (lacking the HCF-1-binding motif) complexes and detection of ASXL1/2 and BAP1 by immunoblotting (Left panel). The immunopurifed proteins were also analyzed by immunoblotting to detect the two major components of the BAP1 complexes, HCF-1 and OGT (right panel). Note that OGT is greatly reduced in the $BAP1^{\Delta HBM}$ complexes due to the absence of HCF-1. The dot indicates a monoubiquitinated form of BAP1 (4), C) A functional CTD is required for proper protein stability of BAP1. Myc-BAP1, Myc-$BAP1^{\Delta CTD}$ or Myc-$BAP1^{R666\text{-}H669}$ expression constructs (3 μg each) were transfected in 293T cells, which were harvested three days post-transfection for immunoblotting.

Fig S3. ASXL1/2 promote deubiquitination of H2AubK119 in vivo.

A) Concomitant Knockdown of ASXL1 and ASXL2 induces a significant increase of the global level of H2AubK119. U2OS cells were transfected with siRNA as indicated and harvested four days post-transfection for immunoblotting using the indicated antibodies. Quantification of band intensity for H2Aub was conducted relative to the non-target siRNA

control (siNT). B) ASXL1/2 promotes BAP1 DUB activity toward H2Aub *in vivo*. U2OS cells (top panel) or 293T cells (bottom panel) were transfected with either 0.5 μg of Myc-BAP1 or Myc-BAP1 C91S expression constructs in the presence or absence of 4 μg of Flag-ASXL1/2 expression constructs. Three days post-transfection, cells were harvested for Immunostaining using the indicated antibodies. The cells overexpressing BAP1 and BAP1ΔC91S were encircled. Note that the transfections were conducted with plasmid ratios optimized to ensure that most BAP1 transfected cells also express ASXL1 or ASXL2. Cells overexpressing BAP1 were counted for change in H2Aub signal. The percentages at the right of the panel represent the number of cells showing very low signal of H2Aub versus the total number of BAP1 expressing cells.

Figure S4. Characterization of BAP1 mediated-H2A deubiquitination.

A) BAP1 deubiquitinates H2Aub K118 and K119 and its variant H2AX and H2AZ. Top, Experimental design; Bottom, 293T cells were co-transfected as indicated using 0.2 μg of Flag H2A wild type or the corresponding mutants (K118R, K119R, K118R/K119R, and K13R/K15R) or H2AX or H2AZ along with 1 μg of Flag-BAP1 and 4 μg of Myc-ASXL2. Three days post-transfection, cells were harvested for Immunoblotting. Tubulin is used as the loading control. B-C) BAP1 deubiquitinates H2A independently of the structure of the nucleosome. B) Flag-H2A-purified nucleosomes were treated with Benzonase for 30 min to digest DNA, and histones were then incubated with the Flag-HA purified BAP1 complexes for indicated times (left panel). DNA was extracted from the nucleosomes (+ and – Benzonase) with phenol-chloroform and analyzed by agarose gel/ethidium bromide staining

(right panel). C) Native or pre-denatured monoubiquitinated nucleosomal Flag-H2A preparations were subjected to DUB activity assay using Flag-HA BAP1 complexes for the indicated times (left panel). Flag preparations of nucleosomes and denatured histones were subjected to silver stain or western blot (right panel). D) Top, Experimental design; Bottom, BAP1 does not deubiquitinate H2AubK13/K15. *In vitro* deubiquitination assay of either purified ubiquitinated nucleosomal H2A K13R/K15R or H2A K118R/K119R using Flag-HA BAP1 complexes. The reactions were carried out for the indicated times and subjected to immunoblotting. Note that Flag-H2A K13R/K15R or Flag-H2A K118R/K119R were co-transfected with RNF168 in 293T cells before the purification of nucleosomes. For the Flag-H2A K13R/K15R, only K118/K119 are available for ubiquitination. For the Flag-H2A K118R/K119R, only K13/K15 are available for ubiquitination. E) BAP1 does not deubiquitinate H2BubK120 *in vivo*. U2OS cells were transfected using a NT or BAP1 siRNA and harvested four days post-transfection for immunoblotting. The three commercially available antibodies against H2BubK120 were used. Quantification of bands intensity for H2Aub to determine fold changes was done relative to the siNT (left panel). Reconstitution of H28 mesothelioma BAP1-deficient cell line with the Flag-HA-BAP1 or Flag-HA-BAPC91S. Cells were subjected to western blot analysis with the indicated antibodies. Quantification of bands intensity was done relative to the signal obtained with cells expressing the empty vector (pOZ-N) (right panel). F) BAP1 does not deubiquitinate H2BubK120 *in vitro*. Purified monoubiquitinated nucleosomal Flag-H2A was subjected to *in vitro* DUB assay using BAP1 and BAP1C91S complexes. The reactions were stopped at different times as indicated and analyzed by western blotting using H2Aub and two different antibodies for H2BubK120. The dot indicates a monoubiquitinated form of BAP1 (panels A, B, C, D, E).

Figure S5. Intact CTD and CC2 domains of BAP1 are required for its proper DUB activity in vivo and in vitro.

A) DUB activity of BAP1$^{\Delta CTD}$ is abolished due to the lack of interaction with ASXL1/2. 0.2 µg of Flag-H2A expression construct was co-expressed in 293T cells with either 1 µg of Myc-BAP1 or 1 µg of Myc-BAP1$^{\Delta CTD}$ with or without 4 µg of Myc-ASXL1 or 6 µg of Myc-ASXL2 expression constructs. Three days post-transfection, cells were harvested for immunoblotting. B) CC2 domain of BAP1 is required for H2A DUB activity. In vitro deubiquitination assay of histone H2A using purified Flag-HA BAP1, BAP1$^{\Delta CTD1}$ or BAP1$^{\Delta CC2}$ complexes. C) HCF-1 is not required to promote BAP1 DUB activity. In vitro deubiquitination assay of histone H2A using purified Flag-HA BAP1 or BAP1$^{\Delta HBM}$ complexes. D) R666-H669 cancer mutation of BAP1, results in the abrogation of its DUB activity in vivo. 0.2 µg of Flag-H2A construct was co-expressed in 293T cells with either 1 µg of Myc-BAP1 or 1 µg of Myc-BAP1$^{R666\text{-}H669}$ with or without 4 µg of Myc-ASXL1 or 6 µg of Myc-ASXL2 expression constructs. Three days post-transfection, cells were harvested for immunoblotting. The dot indicates monoubiquitinated band of BAP1.

Figure S6. The BAP1/ASXL1/ASXL2 axis exerts positive and negative effects on cell proliferation.

A) Primary skin fibroblasts (LF1) stably expressing Flag-HA-BAP1or the empty vector were synchronized in G0 by contact inhibition. Western blot for the replication licensing factor CDC6 was done to ensure that contact-inhibited cells have exited the cell cycle. Cells were collected every day for four days after reaching confluence. B) Proliferation and state of

U2OS following depletion of BAP1, ASXL1 and ASXL2. Phase contrast pictures were taken 4 days following siRNA transfection. Note the significant effect of ASXL2 on cell proliferation. C) Protein expression following siRNA depletion of BAP1, ASXL1 and ASXL2 in primary skin fibroblasts (LF1). The cells were harvested four days post-transfection for Immunoblotting as indicated. β-Actin is used as a loading control. Quantification of band intensity was conducted relative to the non-target siRNA control (siNT). The star indicates a non-specific band. D) Depletion of ASXL1 in LF1 cells results in culture medium (acidic pH) color change. Decrease of medium pH reflects active proliferation and metabolism. E) BAP1 and ASXL2 regulate p21 expression. mRNA was isolated from U2OS cells following siRNA depletion of BAP1, ASXL1 and ASXL2. cDNAs were quantitated by qRT-PCR. The mRNA levels were normalized to Gal4 that was transcribed in vitro and combined with total RNA as an internal control.

Figure S7. Regulation of cell cycle by BAP1 is disrupted following deletion of its CTD.

A) Protein expression levels after depletion of endogenous BAP1 using siRNA in U2OS cells stably expressing empty vector, siRNA-resistant BAP1 or BAP1$^{\Delta CTD}$. B) ΔCTD mutation disrupts BAP1 function in regulating cell proliferation. Following siRNA knockdown of endogenous BAP1, U2OS cells stably expressing BAP1 or its mutant forms were arrested at the G1/S boundary and released for 7 hours to progress through S phase and were then subjected to FACS analysis.

Figure S8. BAP1C91S induces cellular senescence in an ASXL1/2 dependent manner.

A-B) IMR90 cells were infected with retroviral expression vectors for BAP1, BAP1^{C91S} and its respective mutant forms. Eight days post-selection the cells were fixed for staining of senescence-associated β-galactosidase activity assay (SA-β-gal) (A), and cells were also counted every three days after selection to follow cell proliferation (B). Note that data from the SA-β-Gal assays were quantified from 100 cells counts in triplicate and presented as the mean percent of positive cells ± SD.

A

ASXL1

Peptide sequence	AA start	AA stop
RLVLENYSDAPMTPKQ	18	33
KQILQVIEAEGLKEMRF	32	47
RGGEGLFYKLPGRI	65	78
RISLFTLKKD	77	86
RGQAEVTQDPAPLLRG	218	233
RNRGEEIDFETPGSILVNTNLRA	244	266
RLADGEFTHEMQVRI	323	337
KLGLTKEESLQQNVGQEEAEIKS	362	384
KTDPAGLSSPHLPGTSSAAPDLEGPEFPVESVASRI	455	490
RIQAEPDNLARA	489	500
RAMSQDSNSNAAPGKSPGDLTTSRT	1247	1271
RFSSPNVISFGPEQTGRA	1273	1290
KLGPSTNSMSGGVQTPRE	1337	1354
KGLSEPLEPSSLPSQLSIKQ	1419	1438
KLQLSSTSFNYSSSSPTFPKG	1446	1466

ASXL2

Peptide sequence	AA start	AA stop
KEILQVIQRE	32	41
KVENTLLGLGKK	237	248
RLLLLLPEVDRQ	302	313
RLSEGEFTPEMQVRI	342	356
KSMPVSEASLIRI	410	422
RARFPVSITSPNRT	639	652
RGGSPGSDRVSETGKGPTLELAGTGSRG	711	738
KTVPLTAKEERG	978	989
RGMGALIATNTTENSTRE	988	1005
KATQDQILQTLIQRV	1060	1074
RETLSTSDCLASKN	1217	1230
KTLARDLIQAAQKQ	1259	1272
KLYGSPTQIGPSYRG	1315	1329
KLCVSCLVVR	1426	1435

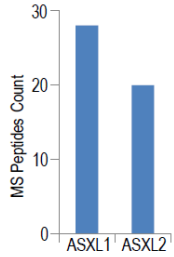

B

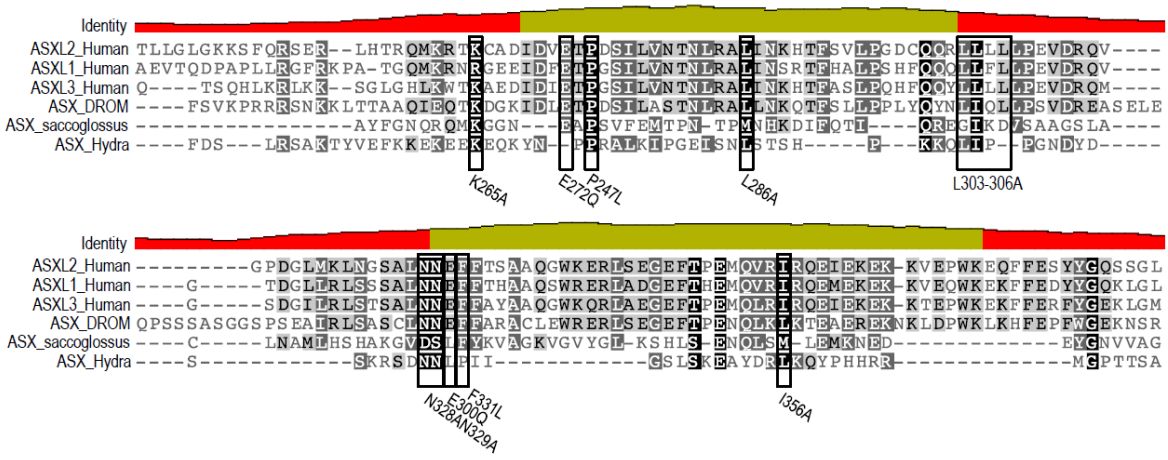

C

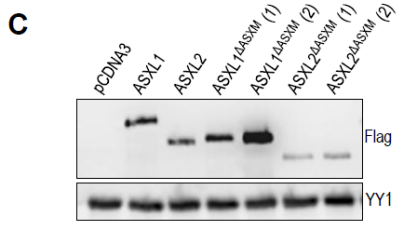

Figure S1

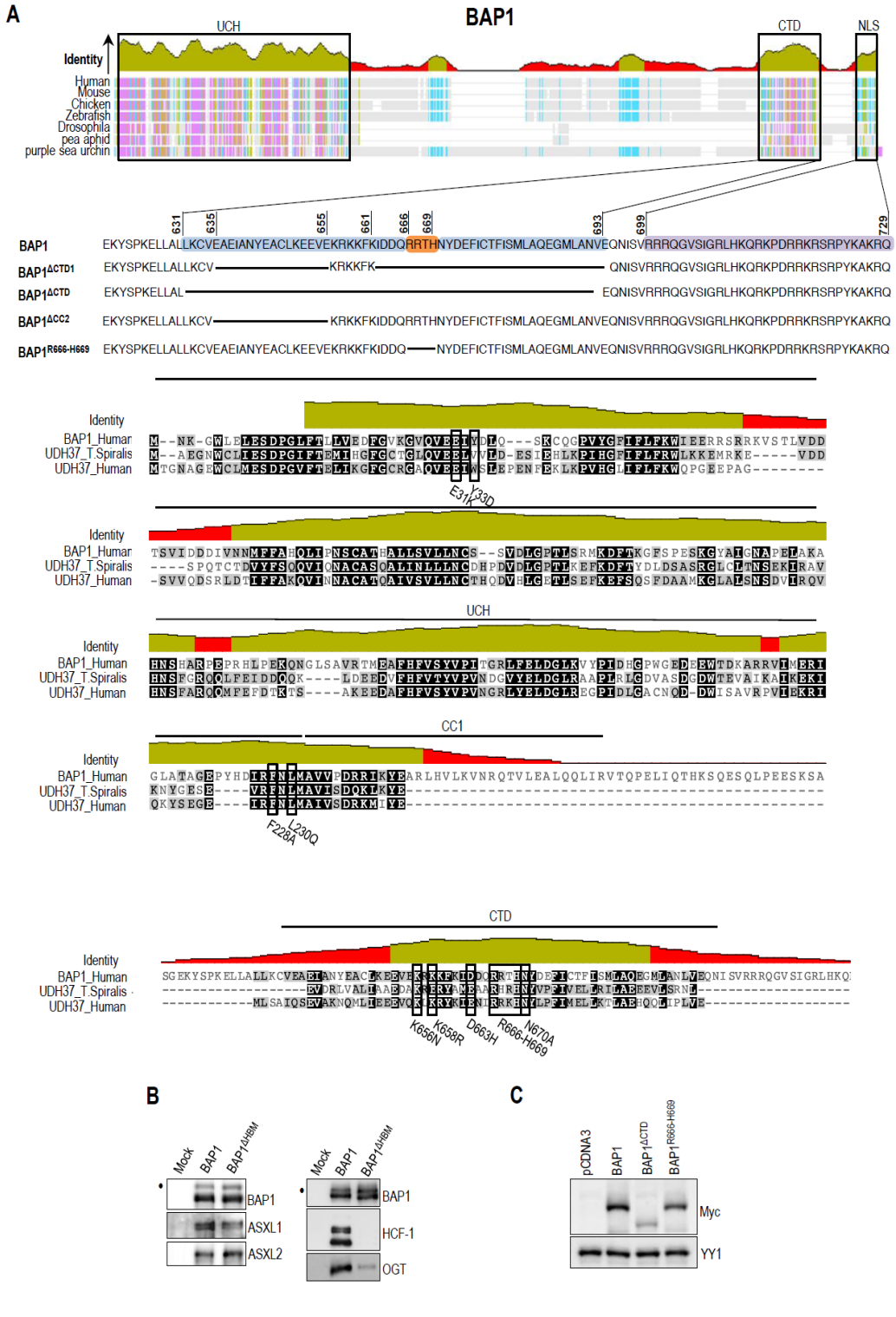
A
BAP1
UCH
CTD
NLS
Identity
Human
Mouse
Chicken
Zebrafish
Drosophila
pea aphid
purple sea urchin
631
635
655
661
666
669
693
699
729
BAP1
BAP1ΔCTD1
BAP1ΔCTD
BAP1ΔCC2
BAP1R666-H669
EKYSPKELLALLKCVEAEIANYEACLKEEVEKRKKFKIDDQRRTHNYDEFICTFISMLAQEGMLANVEQNISVRRRQGVSIGRLHKQRKPDRRKRSRPYKAKRQ
EKYSPKELLALLKCV
KRKKFK
QNISVRRRQGVSIGRLHKQRKPDRRKRSRPYKAKRQ
EKYSPKELLAL
EQNISVRRRQGVSIGRLHKQRKPDRRKRSRPYKAKRQ
EKYSPKELLALLKCV
KRKKFKIDDQRRTHNYDEFICTFISMLAQEGMLANVEQNISVRRRQGVSIGRLHKQRKPDRRKRSRPYKAKRQ
EKYSPKELLALLKCVEAEIANYEACLKEEVEKRKKFKIDDQ
NYDEFICTFISMLAQEGMLANVEQNISVRRRQGVSIGRLHKQRKPDRRKRSRPYKAKRQ
BAP1_Humar
UDH37_T.Spiralis
UDH37_Human
E311K
Y330D
UCH
CC1
F228A
L230Q
CTD
K656N
K658R
D663H
R666-H669
N670A
B
Mock
BAP1
BAP1ΔHBM
BAP1
ASXL1
ASXL2
HCF-1
OGT
C
pCDNA3
BAP1
BAP1ΔCTD
BAP1R666-H669
Myc
YY1

Figure S2

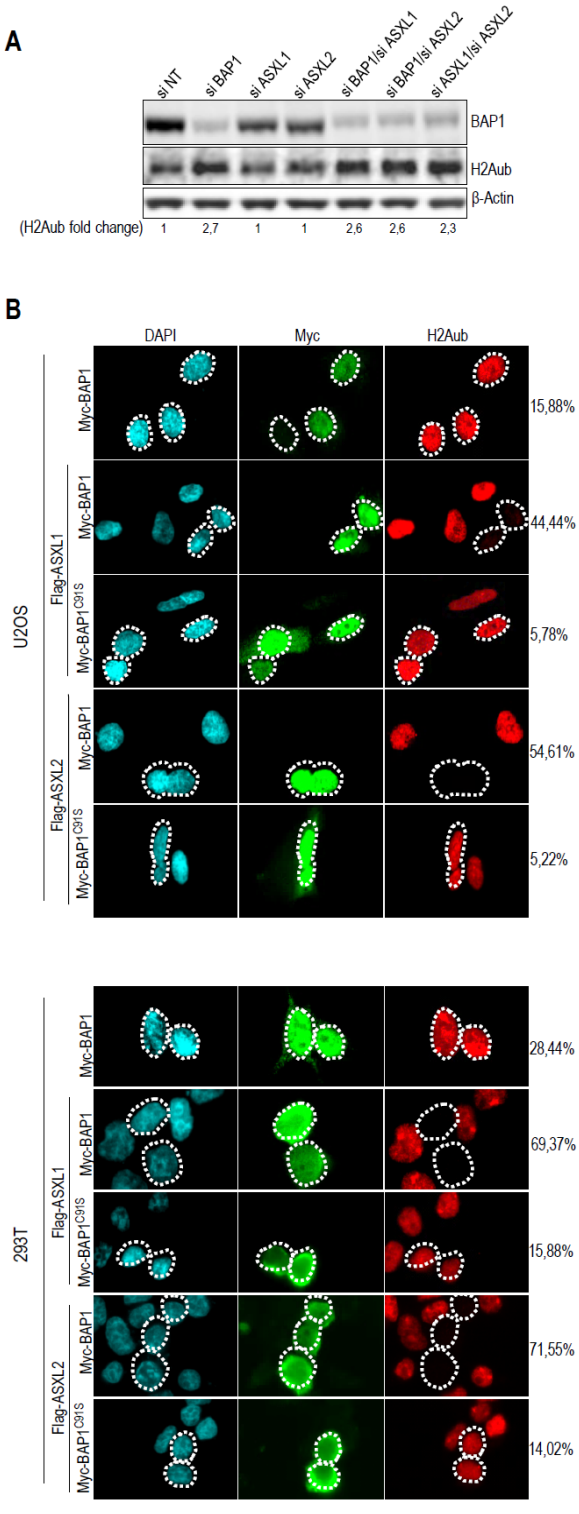
A
si NT
si BAP1
si ASXL1
si ASXL2
si BAP1/si ASXL1
si BAP1/si ASXL2
si ASXL1/si ASXL2
BAP1
H2Aub
β-Actin
(H2Aub fold change) 1 2,7 1 1 2,6 2,6 2,3
B
DAPI
Myc
H2Aub
U2OS
Flag-ASXL1
Flag-ASXL2
Myc-BAP1
Myc-BAP1C91S
15,88%
44,44%
5,78%
54,61%
5,22%
293T
28,44%
69,37%
15,88%
71,55%
14,02%

Figure S3

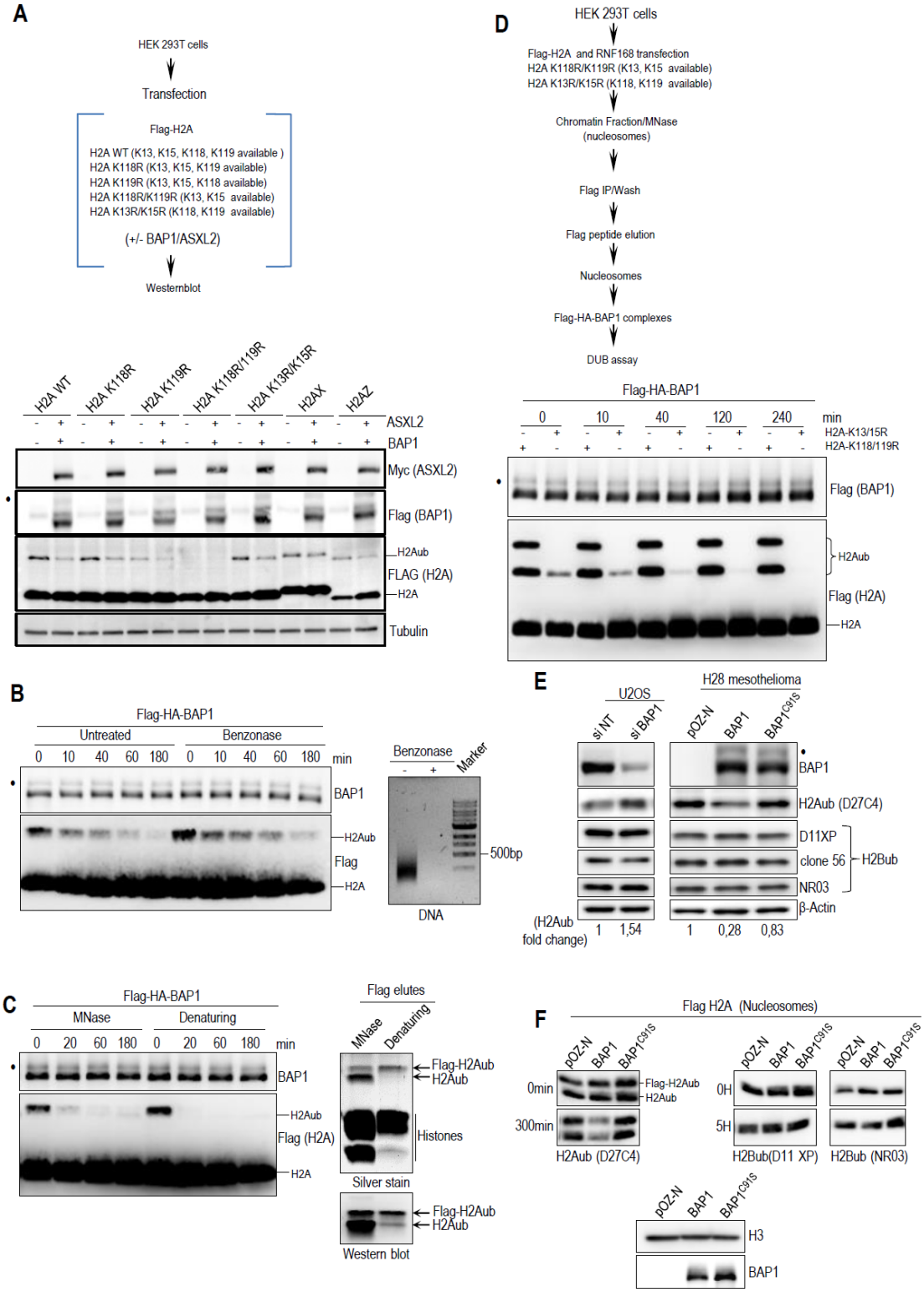
A
HEK 293T cells
Transfection
Flag-H2A
H2A WT (K13, K15, K118, K119 available)
H2A K118R (K13, K15, K119 available)
H2A K119R (K13, K15, K118 available)
H2A K118R/K119R (K13, K15 available)
H2A K13R/K15R (K118, K119 available)
(+/- BAP1/ASXL2)
Westernblot
H2A WT
H2A K118R
H2A K119R
H2A K118R/119R
H2A K13R/K15R
H2AX
H2AZ
ASXL2
BAP1
Myc (ASXL2)
Flag (BAP1)
H2Aub
FLAG (H2A)
H2A
Tubulin
D
HEK 293T cells
Flag-H2A and RNF168 transfection
H2A K118R/K119R (K13, K15 available)
H2A K13R/K15R (K118, K119 available)
Chromatin Fraction/MNase (nucleosomes)
Flag IP/Wash
Flag peptide elution
Nucleosomes
Flag-HA-BAP1 complexes
DUB assay
Flag-HA-BAP1
0
10
40
120
240
min
H2A-K13/15R
H2A-K118/119R
Flag (BAP1)
H2Aub
Flag (H2A)
H2A
B
Flag-HA-BAP1
Untreated
Benzonase
0 10 40 60 180 0 10 40 60 180 min
BAP1
H2Aub
Flag
H2A
Benzonase
Marker
500bp
DNA
E
U2OS
H28 mesothelioma
si NT
si BAP1
pOZ-N
BAP1
BAP1C91S
BAP1
H2Aub (D27C4)
D11XP
clone 56
NR03
H2Bub
β-Actin
(H2Aub fold change)
1
1,54
1
0,28
0,83
C
Flag-HA-BAP1
MNase
Denaturing
0 20 60 180 0 20 60 180 min
BAP1
H2Aub
Flag (H2A)
H2A
Flag elutes
MNase
Denaturing
Flag-H2Aub
H2Aub
Histones
Silver stain
Flag-H2Aub
H2Aub
Western blot
F
Flag H2A (Nucleosomes)
pOZ-N
BAP1
BAP1C91S
0min
300min
Flag-H2Aub
H2Aub
H2Aub (D27C4)
0H
5H
H2Bub(D11 XP)
H2Bub (NR03)
H3
BAP1

Figure S4

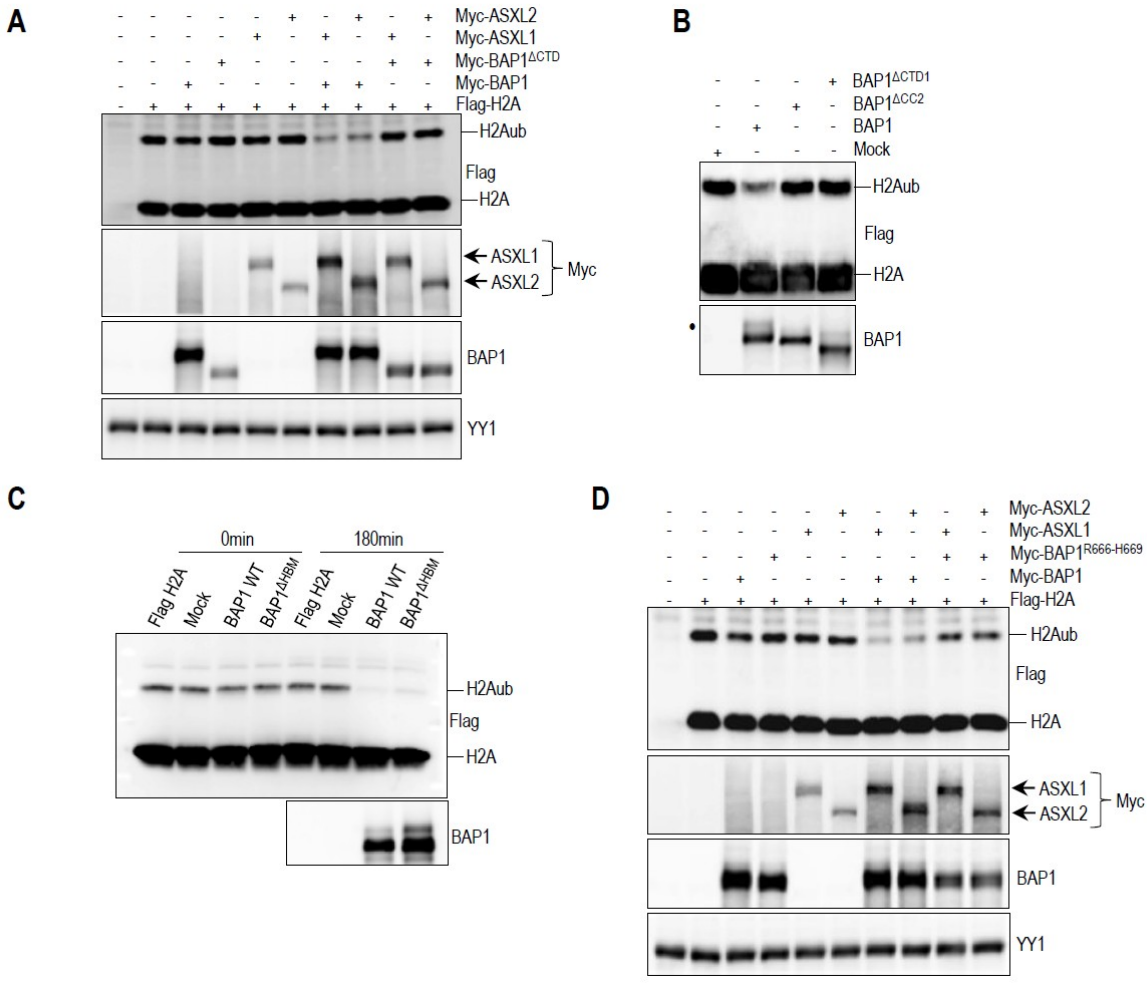
A
Myc-ASXL2
Myc-ASXL1
Myc-BAP1ΔCTD
Myc-BAP1
Flag-H2A
H2Aub
Flag
H2A
ASXL1
ASXL2
Myc
BAP1
YY1
B
BAP1ΔCTD1
BAP1ΔCC2
BAP1
Mock
H2Aub
Flag
H2A
BAP1
C
0min
180min
Flag H2A
Mock
BAP1 WT
BAP1ΔHBM
H2Aub
Flag
H2A
BAP1
D
Myc-ASXL2
Myc-ASXL1
Myc-BAP1R666-H669
Myc-BAP1
Flag-H2A
H2Aub
Flag
H2A
ASXL1
ASXL2
Myc
BAP1
YY1

Figure S5

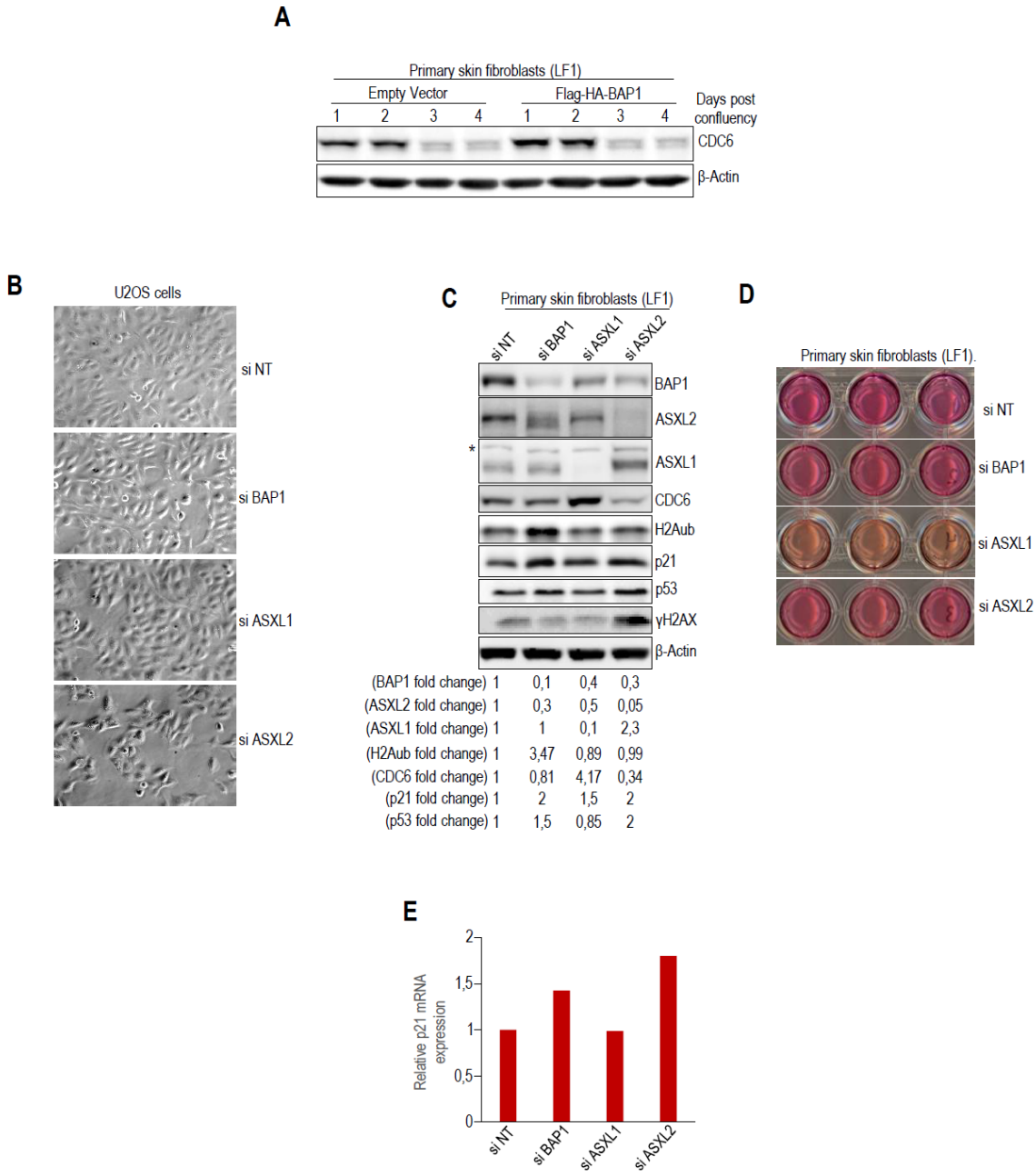
A
Primary skin fibroblasts (LF1)
Empty Vector
Flag-HA-BAP1
1 2 3 4 1 2 3 4
Days post confluency
CDC6
β-Actin
B
U2OS cells
si NT
si BAP1
si ASXL1
si ASXL2
C
Primary skin fibroblasts (LF1)
si NT
si BAP1
si ASXL1
si ASXL2
BAP1
ASXL2
*
ASXL1
CDC6
H2Aub
p21
p53
γH2AX
β-Actin
(BAP1 fold change) 1 0,1 0,4 0,3
(ASXL2 fold change) 1 0,3 0,5 0,05
(ASXL1 fold change) 1 1 0,1 2,3
(H2Aub fold change) 1 3,47 0,89 0,99
(CDC6 fold change) 1 0,81 4,17 0,34
(p21 fold change) 1 2 1,5 2
(p53 fold change) 1 1,5 0,85 2
D
Primary skin fibroblasts (LF1).
si NT
si BAP1
si ASXL1
si ASXL2
E
Relative p21 mRNA expression
2
1,5
1
0,5
0
si NT
si BAP1
si ASXL1
si ASXL2

Figure S6

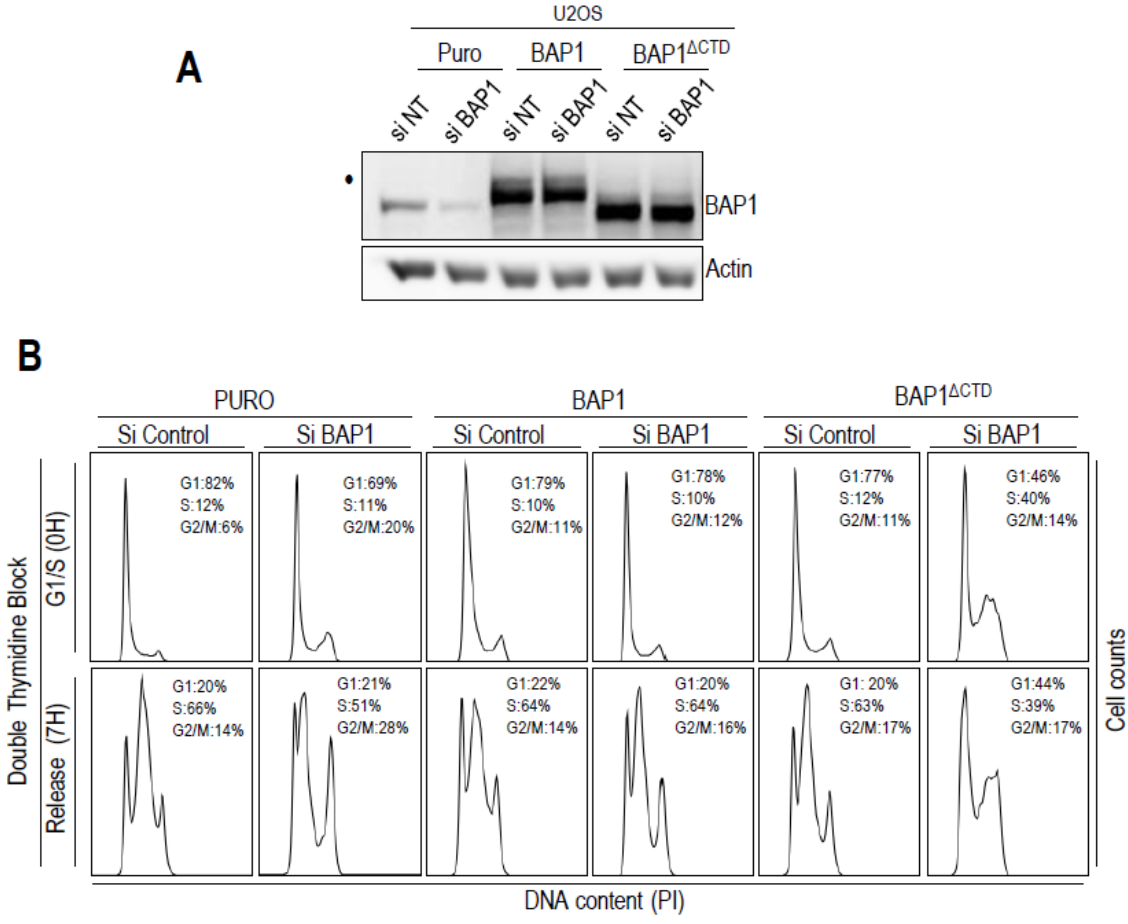
A
U2OS
Puro
BAP1
BAP1ΔCTD
si NT
si BAP1
si NT
si BAP1
si NT
si BAP1
BAP1
Actin
B
PURO
BAP1
BAP1ΔCTD
Si Control
Si BAP1
Si Control
Si BAP1
Si Control
Si BAP1
Double Thymidine Block
G1/S (0H)
Release (7H)
G1:82%
S:12%
G2/M:6%
G1:69%
S:11%
G2/M:20%
G1:79%
S:10%
G2/M:11%
G1:78%
S:10%
G2/M:12%
G1:77%
S:12%
G2/M:11%
G1:46%
S:40%
G2/M:14%
G1:20%
S:66%
G2/M:14%
G1:21%
S:51%
G2/M:28%
G1:22%
S:64%
G2/M:14%
G1:20%
S:64%
G2/M:16%
G1: 20%
S:63%
G2/M:17%
G1:44%
S:39%
G2/M:17%
Cell counts
DNA content (PI)

Figure S7

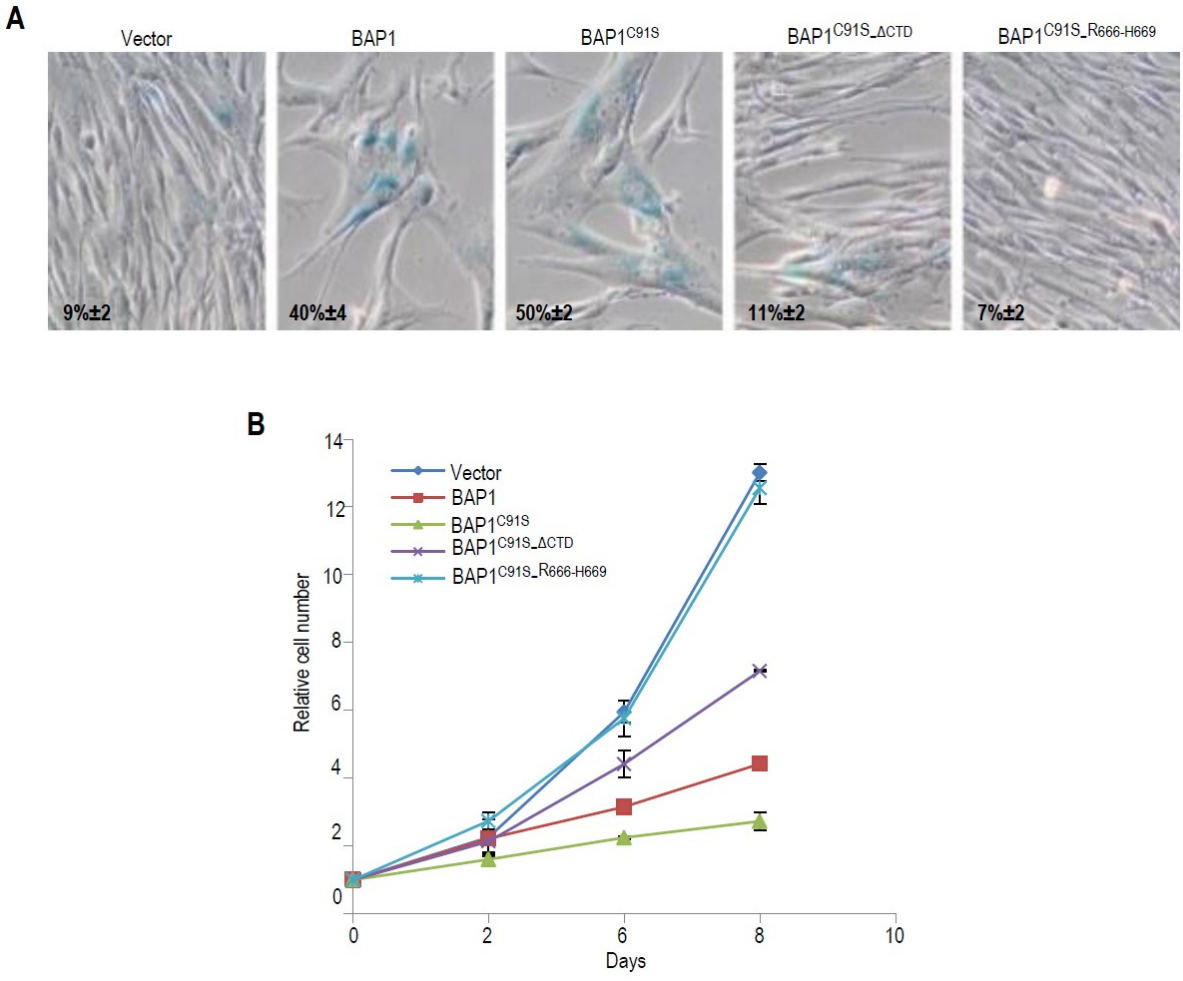
A
Vector
BAP1
BAP1C91S
BAP1C91S_ΔCTD
BAP1C91S_R666-H669
9%±2
40%±4
50%±2
11%±2
7%±2
B
Relative cell number
Days
Vector
BAP1
BAP1C91S
BAP1C91S_ΔCTD
BAP1C91S_R666-H669
0
2
4
6
8
10
12
14
0
2
6
8
10

Figure S8

Chapter 4: Discussion

4.1 Understanding the mechanism and importance of BRCA1 degradation following genotoxic stress

In Chapter 2, we showed that BRCA1 is downregulated, through proteasomal degradation, following exposure to the DNA helix distorting agent UV or the DNA alkylating agent Methyl Methanesulfonate (MMS), two DNA damaging agents that do not directly generate DSBs. This downregulation is reversible and is independent of major kinases involved in the DDR, ATM, ATR or DNA-PK. Furthermore, our model proposes that BRCA1 downregulation prevents the untimely recruitment of BRCA1 and associated factors to DNA damage sites that are not DSBs, thus coordinating the DNA damage/repair response. However, many questions were left still unanswered about the mechanism and importance of BRCA1 degradation following genotoxic stress.

4.1.1 What post-translational modifications (PTMs) of BRCA1 are required for its timely downregulation?

We clearly showed that phosphorylation through the PI3 kinase related kinases, is not involved in BRCA1 degradation. But we cannot rule out other phosphorylation events, since BRCA1 is also known to be phosphorylated by cyclin-dependent kinases, Akt and Aurora-A[191]. In fact, Aurora-A was shown to interact directly with BRCA1 through the a.a. 1314-1863 region to phosphorylate BRCA1 on S308 for proper G2 to M cell cycle transition[192]. This is interesting since we showed that BRCA1 ΔBRCT (a.a. 1527-1863) is not downregulated following exposure to MMS compared to endogenous BRCA1 (Chapter 2,

Figure 5). A conundrum to a potential involvement of Aurora-A in mediating BRCA1 degradation is that the BRCA1 ΔMid1 (a.a. 305-770), containing the S308 phosphorylation site, is properly degraded after MMS treatment. However, Aurora-A (in a phosphorylation-independent manner) and/or other kinases could potentially be involved in BRCA1 downregulation directly or indirectly through phosphorylation of BRCA1 interacting proteins. Therefore, the role of BRCA1 phosphorylation in mediating its degradation requires additional investigations.

Another post-translational modification known to affect BRCA1 and that could be involved in its degradation is sumoylation. Small ubiquitin-like modifier (SUMO) proteins are analogous to ubiquitin, as they are attached to target proteins through a similar enzymatic cascade and are involved in numerous cellular processes, including the DNA damage response[193,194]. The protein inhibitor of activated signal transducer and activator of transcription (PIAS) family of SUMO E3 ligases are involved in BRCA1 (as well as 53BP1) sumoylation, which increases ligase activity and is required for BRCA1 recruitment downstream of RNF8 to DNA DSB sites[195,196]. In addition, RNF4, a SUMO-targeted ubiquitin ligase, has also been shown to play a role in DNA DSB repair and signaling[197]. The RNF4 protein has four N-terminal SUMO-interacting motifs (SIMs) and a C-terminal RING domain which promotes ubiquitination of previously sumoylated proteins[198]. While sumoylation is not known for signalling for proteasomal degradation, RNF4 has been shown to target sumoylated PML to the proteasome following arsenic exposure[198,199]. Furthermore, it was shown that RNF4-deficiency leads to sustained IR-induced DNA damage signaling. In fact, lentiviral knockdown of RNF4 led to an increase in sumoylated BRCA1 levels. Therefore, it was

suggested that sumoylation targets BRCA1 for proteasome degradation[197]. Interestingly, BRCA1 was found in a screen for ubiquitin/SUMO conjugates affected by proteasome inhibition[200]. Hence, it is possible that following treatment with UV or MMS, BRCA1 is sumoylated which signals for its ubiquitination and proteasomal degradation. This hypothesis would also required further elucidation of the possible crosstalk between ubiquitination and sumoylation in BRCA1 downregulation after genotoxic stress.

In a more general perspective, it would be very interesting and informative to search and map for novel BRCA1 PTMs, with or without treatment of various genotoxic agents, by mass spectrometry (MS). Progress in MS-based proteomics over the last decade now allow for a more comprehensive study of PTMs[201]. While phosphorylation and ubiquitination are the most studied BRCA1 PTMs, less is known about BRCA1 acetylation, methylation and sumoylation. In fact, BRCA1 has been shown to be methylated by PRMT1 at arginine residues[202]. Moreover, the BRCA1 504-802 region was found to be highly methylated. Furthermore, while no direct link between BRCA1 and acetylation has been found, BACH1 was shown to be acetylated, which was required for its role in the DNA damage response[203]. Elucidating BRCA1 PTMs will lead to a better understanding of the different signaling pathways that regulate this tumor suppressor. In addition, it would then be possible to mutate residues affected by PTMs and study how they modulate BRCA1 function in different cellular processes.

4.1.2 Identification of the ubiquitin ligase responsible for BRCA1 downregulation

We showed that BRCA1 is reversibly ubiquitinated and degraded by the proteasome following MMS treatment (Chapter 2, Figure 7). However, as our model illustrates (Chapter 2, Figure 10), the identity of the E3 ligase(s) and/or DUB(s) regulating BRCA1 degradation are still unknown. We did some preliminary experiments that have not been fully validated yet to identify these proteins.

First, we wanted to elucidate the ubiquitin ligase(s) involved in BRCA1 degradation. It is important to keep in mind that we showed that BRCA1 lacking its RING domain is still degraded following genotoxic stress, meaning that BRCA1 ligase activity is not required for its degradation. Since we did not have access to a high throughput screening system and that E3 ligases are very abundants (more than 600), we decided to utilize the protein complex purification technique that is widely used in our lab[152], with the aim of isolating potential E3 ligases that target BRCA1. We generated a Flag-HA tagged BRCA1 expressed in the pcDNA vector, which allows for constitutive high-level expression. Since BRCA1 is known to be significantly more stable when bound to BARD1, we co-transfected 293T kidney cells with both Flag-HA BRCA1 and an untagged BARD1 to stabilize BRCA1. We initially used untreated transfected cells to purify the BRCA1 complexes. After conducting sequential anti-Flag and anti-HA columns, we loaded the final elutions for silver stain to validate that very low or non-specific binding of proteins is observed for the non-transfected cells (compare mock and Flag-HA BRCA1 lanes in Figure 11A). We also validated our purification by western blotting for known BRCA1-interacting proteins such as Abraxas, RAP80, BACH1 and NBS1 (Figure 11B). We then purified the BRCA1 protein complex from cells treated with 200 μM MMS for 1 hour and analysed the eluted proteins by mass spectrometry in order

to determine whether we could isolate novel BRCA1 interacting proteins including ubiquitin ligases (and also DUBs). The mass spectrometry analysis revealed the presence of ubiquitin ligases in our MMS-treated BRCA1 protein. The interaction between BRCA1 and these potential interacting proteins was not further validated by immunoprecipitation experiments.

One of the ubiquitin ligases found in our BRCA1 complex was DDB1 (DNA-damage binding protein 1), which functions as an adaptor protein in the CUL4 (cullin 4) ubiquitin ligase complex along with DDB2. Importantly, the CUL4-DDB1-DDB2 complex is known to act in the DNA damage response to UV[26,204]. Interestingly, DDB1 has been shown to link CUL4 to the replication licensing factor CDT1 following UV irradiation, which leads to CDT1 polyubquitination signaling and its proteasomal degradation[205]. Furthermore, the CUL4 ligase has also been shown to be responsible for polyubiquitination of the p53 tumor suppressor following UV exposure leading to its proteasomal degradation[206,207]. Since we observed BRCA1 proteasomal degradation following exposure to genotoxic agents such as UV and MMS, it would be really interesting to further explore the involvement of DDB1 and CUL4 in mediating BRCA1 ubiquitination. In addition, CUL4 has been shown to be overexpressed in primary breast cancers[208].

While purification of the BRCA1 protein complex did identify a few potential E3 ligases that might regulate BRCA1 following genotoxic stress, it would be informative to perform an RNAi screen of E3 ubiquitin ligases affecting BRCA1 protein levels. Since ubiquitination is often a transient modification, our BRCA1 complex purification could have missed some very interesting interacting partners. Clearly much more work still needs to be

done to elucidate the ubiquitin ligase(s) required for BRCA1 degradation following genotoxic stress.

4.1.3 Identification of the DUB(s) required for BRCA1 recovery following MMS exposure

We then wanted to identify the DUB(s) regulating BRCA1 recovery from MMS exposure. We conducted a DUB RNAi screen, similar to the screen already done by our lab (Annex 1, Figure 1)[147] to identify regulators of BRCA1 stability following treatment with MMS. Briefly, U2OS cells were transfected with siRNA pools targeting known human DUBs. Three days after transfection, we treated cells with 200 μM MMS for 6 hours followed by recovery in MMS-free media for another 20 hours (similar experiment as in Chapter 2, Figure 2A). We then observed BRCA1 foci formation after recovery from MMS exposure. The depletion of a DUB positively affecting BRCA1 recovery following MMS exposure would result in a reduced formation of BRCA1 foci during the recovery phase. The depletion of a negative regulator would lead to more pronounced BRCA1 foci formation after MMS exposure. This experiment was insightful as we did find a significant number of regulators of BRCA1 stability, but we still haven't confirmed the results of the screen. However, BAP1 is one DUB that would clearly be interesting to test as a BRCA1 regulator following MMS exposure since we have already shown that BAP1 affects BRCA1 function[147].

The importance of elucidating the ligase(s) and DUB(s) regulating BRCA1 degradation following genotoxic is evident since these enzymes could represent novel breast and ovarian cancer biomarkers. While cancers associated with BRCA1 usually involves mutations in BRCA1 that renders the protein absent or functionally inactive, it is not

impossible to hypothesize that in some cancers BRCA1 is not mutated but that the proteins regulating it are mutated thereby leading to abnormal BRCA1 protein levels and/or localization resulting in genomic instability and cancer.

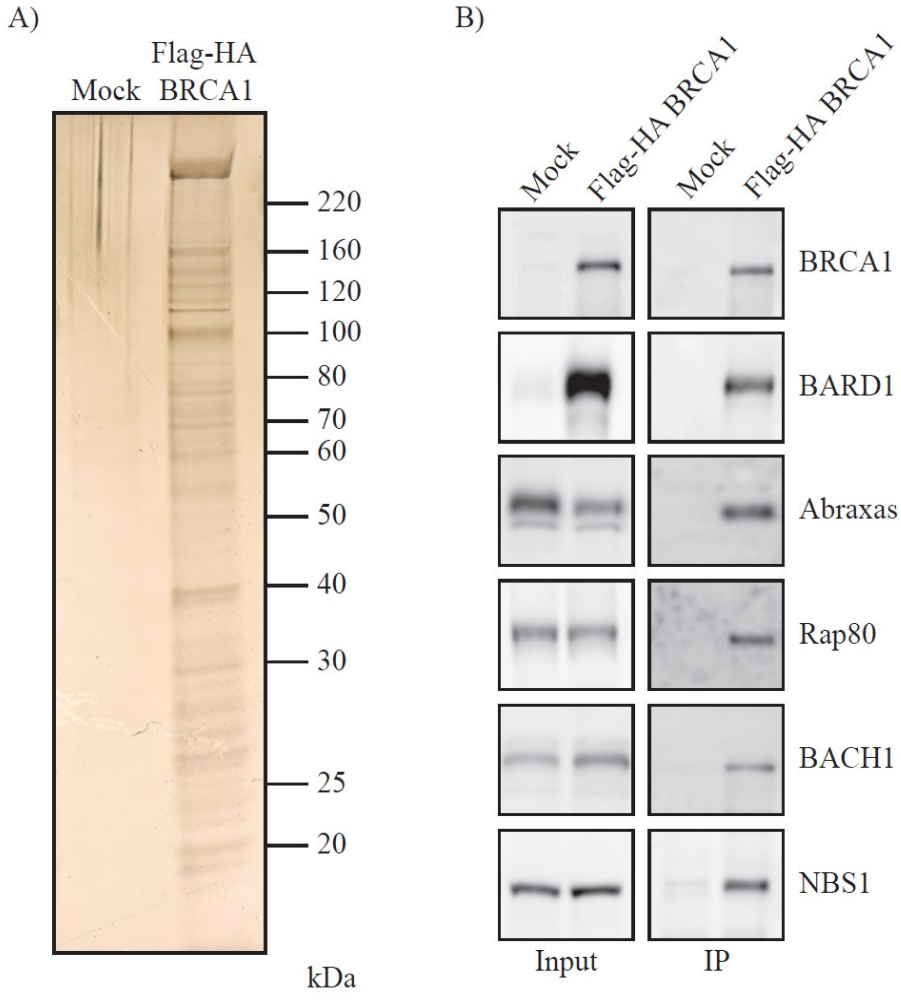

Figure 11. Purification of the BRCA1 protein complex. A) BRCA1 protein complex from non-treated cells. 293T were transfected with a mock plasmid or a plasmid for Flag-HA BRCA1 expression in combination with a plasmid expressing non-tagged BARD1. Following sequencial Flag and HA purification steps, final elutions were loaded for Silver stain. B) Western blotting of known BRCA1 interacting proteins to validate BRCA1 protein complex from elutions used in A. BRCA1-A complex (Abraxas, Rap80), BRCA1-B (BACH1) and MRN complex (NBS1) are specifically present in the BRCA1 protein complex.

4.2 How does the BAP1/ASXL1/ASXL2 axis control gene expression?

In Chapter 3, we showed that BAP1 tumor suppressor function requires interaction with ASXL1/2. BAP1 forms mutually exclusive complexes with ASXL1 and ASXL2. Interestingly, both factors were able to promote BAP1 DUB activity towards H2Aub. Furthermore, both were absent in the protein complex from BAP1$^{R666\text{-}H669}$, a cancer mutation that inhibits BAP1 binding Ub and H2Aub DUB activity. However, ASXL1 and ASXL2 had opposite affects on cell cycle progression. In addition, knockdown of ASXL1 and ASLX2 respectively increased or decreased the protein levels of the replication-promoting factor CDC6. Moreover, only ASXL2 overexpression had an affect on cellular senescence. In sum, the proper coordination of the BAP1/ASXL1/ASXL2 axis is required for histone H2A deubiquitination and disuption of this interaction leads to cell cycle progression defects and cancer development. But it still remains unclear how BAP1 and ASXL1/2 control gene expression through regulation of H2A ubiquitination. Our lab showed that BAP1 depletion both negatively and positively affected the expression of genes including cell cycle associated genes[152]. But how BAP1 could act as both an activator and repressor is still unknown. A possible explanation would be that BAP1 forms multiple sub-complexes and that the composition of these complexes determines the switch between gene activation and repression through modulation of H2A ubiquitination. This hypothesis is supported by the fact that BAP1 interacts in a mutually exclusive manner with ASXL1 and ASXL2, transcription co-factors that have been suggested to play opposing roles in gene expression[174].

ASXL1 is known to act as a corepressor of gene transcription and occupies promoter regions in association with the repressive mark methylated H3K9. Furthermore, ASXL1 has

been shown to directly interact with the H3 demethylase LSD1[173], which is capable of both activating[209] and repressing[210] transcription by respectively removing methyl groups from H3K9 and H3K4. ASXL2, on the other hand, is associated with transcriptional coactivation where it is found on promoter regions with the methyltransferase MLL1 and the histone marks H3K9ac and H3K4me[174]. Interestingly, HCF-1, the major stoichiometric interacting protein found in the BAP1 complex, has been shown to recruit MLL1 to E2F gene promoters during the G1-to-S transition[158]. In addition, HCF-1, contrary to ASXL1, has been shown to recruit LSD1 to activate gene expresion[211]. Moreover, HCF-1 and another transcription factor in the BAP1 complex, YY1, can both act as activators or repressors of gene expression. Therefore, in the BAP1 complex there are many proteins that can act as repressors and/or activators of transcription. What determines with which proteins BAP1 will interact with in a given biological context is still unknown, but ASXL1 and ASXL2 could play a major role in this decision. It would interesting and necessary to further study through ChIP and ChIP-seq experiments: **1)** Which promoters BAP1 occupies with ASXL1 and ASXL2. **2)** Determine the presence or absence of H2Aub at promoters occupied by BAP1. **3)** Determine the global landscape of transcription factors and co-factors found at a BAP1 target gene promoter. This would give insight into which BAP1 sub-complexes are formed at specific promoters and if they act as activitors or repressors of gene expression.

We performed some preliminary ChIP experiments to answer the questions involving BAP1 sub-complexes at gene promoter regions, which suggest that ASXL1 and ASXL2 might indeed act as opposing co-factors interacting with BAP1. Much more research must be done to fully elucidate how BAP1 forms different sub-complexes and how these complexes

control gene expression. How BAP1 functions as a DUB during transcription is of major importance to better understanding how this factor acts as a tumor suppressor.

4.3 Involvement of post-translational modifications in regulating BAP1 interaction with ASXL1/2

BAP1 has been shown to be phosphorylated following ionizing radiation[147,148]. However, not much is known about other post-translational modifications regulating BAP1, ASXL1 or ASXL2. Our lab showed that BAP1 interacts with the O-linked *N*-acetylglucosamine transferase (OGT) protein[152]. OGT is a highly conserved enzyme that regulates protein function by attaching a single N-acetylglucosamine (O-GlcNAc) to serine/threonine (S/T) residues[212,213]. Furthermore, our lab[214] and others[215,216] have shown that OGT regulates HCF-1 proteolytic cleavage and function in gene expression. In addition, it has been suggested that a crosstalk between phosphorylation and glycosylation exists to regulate transcription following cellular stress[212]. Therefore, it would be important to study how phosphorylation and glycosylation (and/or their crosstalk) might regulate the BAP1 protein complex and its role in gene expression.

Our lab has also showed that BAP1 interacts with and is multi-monoubiquitinated by the ubiquitin-conjugating enzyme UBE2O[152,217]. Moreover, BAP1 possesses autodeubiquitination capacity that counteracts UBE2O activity, which is required for its tumor suppression function. Interestingly, during adipogenesis UBE2O was shown to ubiquitinate BAP1 promoting the cytoplasmic localization of BAP1 and differentiation. Since

ASXL1 and ASXL2 are suggested to play opposing roles in adipogenesis[174], it would be interesting to study the effect of BAP1 ubiquitination/autodeubiquitination in regulating its interactions with ASXL1 and ASXL2, and how this modification could impact BAP1 target gene expression.

In addition, as already discussed for BRCA1, it would also be interesting to search for novel BAP1, ASXL1 and ASXL2 PTMs by MS and how they affect the BAP1 protein complex. Furthermore, purification of the ASXL1 and ASXL2 protein complexes could lead to a better understanding of the composition of different BAP1 sub-complexes, by determining novel interacting partners for ASXL1 and ASXL2. Moreover, there are many other proteins found in the BAP1 complex, such as the forkhead transcription factors FOXK1 and FOXK2 and the histone H3K4 demethylase KDM1B, which could have an impact on the interaction between BAP1 and ASXL1/2. It is clear that we have only begun to scratch the surface of BAP1 and its interacting partners. Elucidating how BAP1 is regulated will lead to a better understanding of its role as a tumor suppressor and this will in turn help establish improved diagnostic and therapeutic strategies to treat cancer.

Conclusion

In this thesis we discussed the biochemical and functional characterization of two related tumor suppressors, BRCA1 and BAP1. We showed that BRCA1 is downregulated in a ubiquitin-mediated manner following genotoxic stress to coordinate the DNA damage response. In addition, we showed that BAP1 forms mutually exclusive complexes with the PcG proteins ASXL1 and ASXL2, which are required for its histone H2A DUB and tumor suppression activities. However, much is still unknown about the roles of BRCA1 and BAP1 in tumorigenesis.

While cancer was long thought as being a genetic-based disease, recently it has been shown that mutations in epigenetic regulators occur at high frequency in cancer cells[218]. Therefore it is now accepted that both genetic and epigenetic mechanisms play a role in establishing hallmarks of cancer[219,220]. In fact, mutation of epigenetic control genes, such as *BAP1*, are widespread[187,220]. Furthermore, epigenetic silencing of DNA repair genes, such as *BRCA1*, lead to increased mutation rate and concomitant loss of genomic stability[221]. It will be interesting to further study how BRCA1 and BAP1 influence the relationship between the cancer genome and epigenome, and how this could translate into better diagnostic, prognostic and treatment of cancer patients.

Bibliography

1 **Schlesinger, D. H., Goldstein, G. & Niall, H. D. The complete amino acid sequence of ubiquitin, an adenylate cyclase stimulating polypeptide probably universal in living cells. *Biochemistry* 14, 2214-2218 (1975).**

2 **Hershko, A. Lessons from the discovery of the ubiquitin system. *Trends in biochemical sciences* 21, 445-449 (1996).**

3 **Hershko, A. & Ciechanover, A. The ubiquitin system. *Annual review of biochemistry* 67, 425-479, doi:10.1146/annurev.biochem.67.1.425 (1998).**

4 **Hershko, A., Ciechanover, A. & Rose, I. A. Identification of the active amino acid residue of the polypeptide of ATP-dependent protein breakdown. *The Journal of biological chemistry* 256, 1525-1528 (1981).**

5 **Hershko, A., Heller, H., Elias, S. & Ciechanover, A. Components of ubiquitin-protein ligase system. Resolution, affinity purification, and role in protein breakdown. *The Journal of biological chemistry* 258, 8206-8214 (1983).**

6 **Chau, V. *et al.* A multiubiquitin chain is confined to specific lysine in a targeted short-lived protein. *Science* 243, 1576-1583 (1989).**

7 **Ciechanover, A. The ubiquitin-proteasome pathway: on protein death and cell life. *The EMBO journal* 17, 7151-7160, doi:10.1093/emboj/17.24.7151 (1998).**

8 **Komander, D., Clague, M. J. & Urbe, S. Breaking the chains: structure and function of the deubiquitinases. *Nature reviews. Molecular cell biology* 10, 550-563, doi:10.1038/nrm2731 (2009).**

9 **Wilkinson, K. D. *et al.* Metabolism of the polyubiquitin degradation signal: structure, mechanism, and role of isopeptidase T. *Biochemistry* 34, 14535-14546 (1995).**

10 **Komander, D. The emerging complexity of protein ubiquitination. *Biochemical Society transactions* 37, 937-953, doi:10.1042/BST0370937 (2009).**

11 **Woelk, T., Sigismund, S., Penengo, L. & Polo, S. The ubiquitination code: a signalling problem. *Cell division* 2, 11, doi:10.1186/1747-1028-2-11 (2007).**

12 **Borden, K. L. & Freemont, P. S. The RING finger domain: a recent example of a sequence-structure family. *Current opinion in structural biology* 6, 395-401 (1996).**

13 **Huibregtse, J. M., Scheffner, M., Beaudenon, S. & Howley, P. M. A family of proteins structurally and functionally related to the E6-AP ubiquitin-protein ligase. *Proceedings of the National Academy of Sciences of the United States of America* 92, 2563-2567 (1995).**

14 **Wu, W. *et al.* HERC2 is an E3 ligase that targets BRCA1 for degradation. *Cancer research* 70, 6384-6392, doi:10.1158/0008-5472.CAN-10-1304 (2010).**

15 **Nijman, S. M. *et al.* A genomic and functional inventory of deubiquitinating enzymes. *Cell* 123, 773-786, doi:10.1016/j.cell.2005.11.007 (2005).**

16 **Reyes-Turcu, F. E., Ventii, K. H. & Wilkinson, K. D. Regulation and cellular roles of ubiquitin-specific deubiquitinating enzymes. *Annual review of biochemistry* 78, 363-397, doi:10.1146/annurev.biochem.78.082307.091526 (2009).**

17 **Johnston, S. C., Larsen, C. N., Cook, W. J., Wilkinson, K. D. & Hill, C. P. Crystal structure of a deubiquitinating enzyme (human UCH-L3) at 1.8 A resolution. *The EMBO journal* 16, 3787-3796, doi:10.1093/emboj/16.13.3787 (1997).**

18 **Johnston, S. C., Riddle, S. M., Cohen, R. E. & Hill, C. P. Structural basis for the specificity of ubiquitin C-terminal hydrolases. *The EMBO journal* 18, 3877-3887, doi:10.1093/emboj/18.14.3877 (1999).**

19 **Yao, T. *et al.* Proteasome recruitment and activation of the Uch37 deubiquitinating enzyme by Adrm1. *Nature cell biology* 8, 994-1002, doi:10.1038/ncb1460 (2006).**

20 **Jensen, D. E. *et al.* BAP1: a novel ubiquitin hydrolase which binds to the BRCA1 RING finger and enhances BRCA1-mediated cell growth suppression. *Oncogene* 16, 1097-1112 (1998).**

21 **Jackson, S. P. & Bartek, J. The DNA-damage response in human biology and disease. *Nature* 461, 1071-1078, doi:10.1038/nature08467 (2009).**

22 **Jackson, S. P. & Durocher, D. Regulation of DNA damage responses by ubiquitin and SUMO. *Molecular cell* 49, 795-807, doi:10.1016/j.molcel.2013.01.017 (2013).**

23 **Sugasawa, K. Regulation of damage recognition in mammalian global genomic nucleotide excision repair. *Mutation research* 685, 29-37, doi:10.1016/j.mrfmmm.2009.08.004 (2010).**

24 **Scrima, A. *et al.* Detecting UV-lesions in the genome: The modular CRL4 ubiquitin ligase does it best! *FEBS letters* 585, 2818-2825, doi:10.1016/j.febslet.2011.04.064 (2011).**

25 **Groisman, R. *et al.* The ubiquitin ligase activity in the DDB2 and CSA complexes is differentially regulated by the COP9 signalosome in response to DNA damage. *Cell* 113, 357-367 (2003).**

26 **Wang, H. *et al.* Histone H3 and H4 ubiquitylation by the CUL4-DDB-ROC1 ubiquitin ligase facilitates cellular response to DNA damage. *Molecular cell* 22, 383-394, doi:10.1016/j.molcel.2006.03.035 (2006).**

27 **Sugasawa, K. *et al.* UV-induced ubiquitylation of XPC protein mediated by UV-DDB-ubiquitin ligase complex. *Cell* 121, 387-400, doi:10.1016/j.cell.2005.02.035 (2005).**

28 **Gaillard, H. & Aguilera, A. Transcription coupled repair at the interface between transcription elongation and mRNP biogenesis. *Biochimica et biophysica acta* 1829, 141-150, doi:10.1016/j.bbagrm.2012.09.008 (2013).**

29 **Groisman, R. *et al.* CSA-dependent degradation of CSB by the ubiquitin-proteasome pathway establishes a link between complementation factors of the Cockayne syndrome. *Genes & development* 20, 1429-1434, doi:10.1101/gad.378206 (2006).**

30 **Cleaver, J. E. Photosensitivity syndrome brings to light a new transcription-coupled DNA repair cofactor. *Nature genetics* 44, 477-478, doi:10.1038/ng.2255 (2012).**

31 **Nakazawa, Y. *et al.* Mutations in UVSSA cause UV-sensitive syndrome and impair RNA polymerase IIo processing in transcription-coupled nucleotide-excision repair. *Nature genetics* 44, 586-592, doi:10.1038/ng.2229 (2012).**

32 **Schwertman, P. *et al.* UV-sensitive syndrome protein UVSSA recruits USP7 to regulate transcription-coupled repair. *Nature genetics* 44, 598-602, doi:10.1038/ng.2230 (2012).**

33 **Ulrich, H. D. Timing and spacing of ubiquitin-dependent DNA damage bypass. *FEBS letters* 585, 2861-2867, doi:10.1016/j.febslet.2011.05.028 (2011).**

34 **Sale, J. E., Lehmann, A. R. & Woodgate, R. Y-family DNA polymerases and their role in tolerance of cellular DNA damage. *Nature reviews. Molecular cell biology* 13, 141-152, doi:10.1038/nrm3289 (2012).**

35 **Jentsch, S., McGrath, J. P. & Varshavsky, A. The yeast DNA repair gene RAD6 encodes a ubiquitin-conjugating enzyme. *Nature* 329, 131-134, doi:10.1038/329131a0 (1987).**

36 **Stelter, P. & Ulrich, H. D. Control of spontaneous and damage-induced mutagenesis by SUMO and ubiquitin conjugation. *Nature* 425, 188-191, doi:10.1038/nature01965 (2003).**

37 **Hoege, C., Pfander, B., Moldovan, G. L., Pyrowolakis, G. & Jentsch, S. RAD6-dependent DNA repair is linked to modification of PCNA by ubiquitin and SUMO. *Nature* 419, 135-141, doi:10.1038/nature00991 (2002).**

38 **Lehmann, A. R. Ubiquitin-family modifications in the replication of DNA damage. *FEBS letters* 585, 2772-2779, doi:10.1016/j.febslet.2011.06.005 (2011).**

39 **Huang, T. T. *et al.* Regulation of monoubiquitinated PCNA by DUB autocleavage. *Nature cell biology* 8, 339-347, doi:10.1038/ncb1378 (2006).**

40 **Nathanson, K. L., Wooster, R. & Weber, B. L. Breast cancer genetics: what we know and what we need. *Nature medicine* 7, 552-556, doi:10.1038/87876 (2001).**

41 **Venkitaraman, A. R. Cancer susceptibility and the functions of BRCA1 and BRCA2. *Cell* 108, 171-182 (2002).**

42 **Honrado, E., Benitez, J. & Palacios, J. The molecular pathology of hereditary breast cancer: genetic testing and therapeutic implications. *Modern pathology : an official journal of the United States and Canadian Academy of Pathology, Inc* 18, 1305-1320, doi:10.1038/modpathol.3800453 (2005).**

43 **Rahman, N. & Scott, R. H. Cancer genes associated with phenotypes in monoallelic and biallelic mutation carriers: new lessons from old players. *Human molecular genetics* 16 Spec No 1, R60-66, doi:10.1093/hmg/ddm026 (2007).**

44 **Miki, Y. *et al.* A strong candidate for the breast and ovarian cancer susceptibility gene BRCA1. *Science* 266, 66-71 (1994).**

45 **Peto, J. *et al.* Prevalence of BRCA1 and BRCA2 gene mutations in patients with early-onset breast cancer. *Journal of the National Cancer Institute* 91, 943-949 (1999).**

46 **King, M. C., Marks, J. H., Mandell, J. B. & New York Breast Cancer Study, G. Breast and ovarian cancer risks due to inherited mutations in BRCA1 and BRCA2. *Science* 302, 643-646, doi:10.1126/science.1088759 (2003).**

47 **Chapman, J. R., Taylor, M. R. & Boulton, S. J. Playing the end game: DNA double-strand break repair pathway choice. *Molecular cell* 47, 497-510, doi:10.1016/j.molcel.2012.07.029 (2012).**

48 **Symington, L. S. & Gautier, J. Double-strand break end resection and repair pathway choice. *Annual review of genetics* 45, 247-271, doi:10.1146/annurev-genet-110410-132435 (2011).**

49 **Ciccia, A. & Elledge, S. J. The DNA damage response: making it safe to play with knives. *Molecular cell* 40, 179-204, doi:10.1016/j.molcel.2010.09.019 (2010).**

50 **Hakem, R. DNA-damage repair; the good, the bad, and the ugly. *The EMBO journal* 27, 589-605, doi:10.1038/emboj.2008.15 (2008).**

51 **Hoeijmakers, J. H. Genome maintenance mechanisms for preventing cancer. *Nature* 411, 366-374, doi:10.1038/35077232 (2001).**

52 **Sartori, A. A. *et al.* Human CtIP promotes DNA end resection. *Nature* 450, 509-514, doi:10.1038/nature06337 (2007).**

53 **Mazon, G., Mimitou, E. P. & Symington, L. S. SnapShot: Homologous recombination in DNA double-strand break repair. *Cell* 142, 646, 646 e641, doi:10.1016/j.cell.2010.08.006 (2010).**

54 **Yang, H., Li, Q., Fan, J., Holloman, W. K. & Pavletich, N. P. The BRCA2 homologue Brh2 nucleates RAD51 filament formation at a dsDNA-ssDNA junction. *Nature* 433, 653-657, doi:10.1038/nature03234 (2005).**

55 **Jensen, R. B., Carreira, A. & Kowalczykowski, S. C. Purified human BRCA2 stimulates RAD51-mediated recombination. *Nature* 467, 678-683, doi:10.1038/nature09399 (2010).**

56 **Sy, S. M., Huen, M. S. & Chen, J. PALB2 is an integral component of the BRCA complex required for homologous recombination repair. *Proceedings of the National Academy of Sciences of the United States of America* 106, 7155-7160, doi:10.1073/pnas.0811159106 (2009).**

57 **Dray, E. *et al.* Enhancement of RAD51 recombinase activity by the tumor suppressor PALB2. *Nature structural & molecular biology* 17, 1255-1259, doi:10.1038/nsmb.1916 (2010).**

58 **Weterings, E. & Chen, D. J. The endless tale of non-homologous end-joining. *Cell research* 18, 114-124, doi:10.1038/cr.2008.3 (2008).**

59 **Grawunder, U., Zimmer, D., Kulesza, P. & Lieber, M. R. Requirement for an interaction of XRCC4 with DNA ligase IV for wild-type V(D)J recombination and DNA double-strand break repair in vivo. *The Journal of biological chemistry* 273, 24708-24714 (1998).**

60 **Ma, Y., Pannicke, U., Schwarz, K. & Lieber, M. R. Hairpin opening and overhang processing by an Artemis/DNA-dependent protein kinase complex in nonhomologous end joining and V(D)J recombination. *Cell* 108, 781-794 (2002).**

61 **Caestecker, K. W. & Van de Walle, G. R. The role of BRCA1 in DNA double-strand repair: past and present. *Experimental cell research* 319, 575-587, doi:10.1016/j.yexcr.2012.11.013 (2013).**

62 **Smith, J., Tho, L. M., Xu, N. & Gillespie, D. A. The ATM-Chk2 and ATR-Chk1 pathways in DNA damage signaling and cancer. *Advances in cancer research* 108, 73-112, doi:10.1016/B978-0-12-380888-2.00003-0 (2010).**

63 **McGowan, C. H. Checking in on Cds1 (Chk2): A checkpoint kinase and tumor suppressor. *BioEssays : news and reviews in molecular, cellular and developmental biology* 24, 502-511, doi:10.1002/bies.10101 (2002).**

64 **Lee, J. S., Collins, K. M., Brown, A. L., Lee, C. H. & Chung, J. H. hCds1-mediated phosphorylation of BRCA1 regulates the DNA damage response. *Nature* 404, 201-204, doi:10.1038/35004614 (2000).**

65 **Joughin, B. A., Tidor, B. & Yaffe, M. B. A computational method for the analysis and prediction of protein:phosphopeptide-binding sites. *Protein science : a publication of the Protein Society* 14, 131-139, doi:10.1110/ps.04964705 (2005).**

66 **Yarden, R. I., Pardo-Reoyo, S., Sgagias, M., Cowan, K. H. & Brody, L. C. BRCA1 regulates the G2/M checkpoint by activating Chk1 kinase upon DNA damage. *Nature genetics* 30, 285-289, doi:10.1038/ng837 (2002).**

67 **Thakur, S. *et al.* Localization of BRCA1 and a splice variant identifies the nuclear localization signal. *Molecular and cellular biology* 17, 444-452 (1997).**

68 **Wu, L. C. *et al.* Identification of a RING protein that can interact in vivo with the BRCA1 gene product. *Nature genetics* 14, 430-440, doi:10.1038/ng1296-430 (1996).**

69 **Joukov, V., Chen, J., Fox, E. A., Green, J. B. & Livingston, D. M. Functional communication between endogenous BRCA1 and its partner, BARD1, during Xenopus laevis development. *Proceedings of the National Academy of Sciences of the United States of America* 98, 12078-12083, doi:10.1073/pnas.211427098 (2001).**

70 **Wu-Baer, F., Lagrazon, K., Yuan, W. & Baer, R. The BRCA1/BARD1 heterodimer assembles polyubiquitin chains through an unconventional linkage involving lysine residue K6 of ubiquitin. *The Journal of biological chemistry* 278, 34743-34746, doi:10.1074/jbc.C300249200 (2003).**

71 **Nishikawa, H. *et al.* Mass spectrometric and mutational analyses reveal Lys-6-linked polyubiquitin chains catalyzed by BRCA1-BARD1 ubiquitin ligase. *The Journal of biological chemistry* 279, 3916-3924, doi:10.1074/jbc.M308540200 (2004).**

72 **Morris, J. R. & Solomon, E. BRCA1 : BARD1 induces the formation of conjugated ubiquitin structures, dependent on K6 of ubiquitin, in cells during DNA replication and repair. *Human molecular genetics* 13, 807-817, doi:10.1093/hmg/ddh095 (2004).**

73 **Yu, X., Fu, S., Lai, M., Baer, R. & Chen, J. BRCA1 ubiquitinates its phosphorylation-dependent binding partner CtIP. *Genes & development* 20, 1721-1726, doi:10.1101/gad.1431006 (2006).**

74 **Thakar, A., Parvin, J. & Zlatanova, J. BRCA1/BARD1 E3 ubiquitin ligase can modify histones H2A and H2B in the nucleosome particle. *Journal of biomolecular structure & dynamics* 27, 399-406, doi:10.1080/07391102.2010.10507326 (2010).**

75 **Li, M. L. & Greenberg, R. A. Links between genome integrity and BRCA1 tumor suppression. *Trends in biochemical sciences* 37, 418-424, doi:10.1016/j.tibs.2012.06.007 (2012).**

76 **Hakem, R. *et al.* The tumor suppressor gene Brca1 is required for embryonic cellular proliferation in the mouse. *Cell* 85, 1009-1023 (1996).**

77 **Liu, C. Y., Flesken-Nikitin, A., Li, S., Zeng, Y. & Lee, W. H. Inactivation of the mouse Brca1 gene leads to failure in the morphogenesis of the egg cylinder in early postimplantation development. *Genes & development* 10, 1835-1843 (1996).**

78 **Ludwig, T., Chapman, D. L., Papaioannou, V. E. & Efstratiadis, A. Targeted mutations of breast cancer susceptibility gene homologs in mice: lethal phenotypes of Brca1, Brca2, Brca1/Brca2, Brca1/p53, and Brca2/p53 nullizygous embryos. *Genes & development* 11, 1226-1241 (1997).**

79 **Reid, L. J. *et al.* E3 ligase activity of BRCA1 is not essential for mammalian cell viability or homology-directed repair of double-strand DNA breaks. *Proceedings of the National Academy of Sciences of the United States of America* 105, 20876-20881, doi:10.1073/pnas.0811203106 (2008).**

80 **Shakya, R. *et al.* BRCA1 tumor suppression depends on BRCT phosphoprotein binding, but not its E3 ligase activity. *Science* 334, 525-528, doi:10.1126/science.1209909 (2011).**

81 **Drost, R. *et al.* BRCA1 RING function is essential for tumor suppression but dispensable for therapy resistance. *Cancer cell* 20, 797-809, doi:10.1016/j.ccr.2011.11.014 (2011).**

82 **Manke, I. A., Lowery, D. M., Nguyen, A. & Yaffe, M. B. BRCT repeats as phosphopeptide-binding modules involved in protein targeting. *Science* 302, 636-639, doi:10.1126/science.1088877 (2003).**

83 **Yu, X., Chini, C. C., He, M., Mer, G. & Chen, J. The BRCT domain is a phospho-protein binding domain. *Science* 302, 639-642, doi:10.1126/science.1088753 (2003).**

84 **Harper, J. W. & Elledge, S. J. The DNA damage response: ten years after. *Molecular cell* 28, 739-745, doi:10.1016/j.molcel.2007.11.015 (2007).**

85 **Stewart, G. S., Wang, B., Bignell, C. R., Taylor, A. M. & Elledge, S. J. MDC1 is a mediator of the mammalian DNA damage checkpoint. *Nature* 421, 961-966, doi:10.1038/nature01446 (2003).**

86 **Stucki, M. *et al.* MDC1 directly binds phosphorylated histone H2AX to regulate cellular responses to DNA double-strand breaks. *Cell* 123, 1213-1226, doi:10.1016/j.cell.2005.09.038 (2005).**

87 **Huen, M. S. *et al.* RNF8 transduces the DNA-damage signal via histone ubiquitylation and checkpoint protein assembly. *Cell* 131, 901-914, doi:10.1016/j.cell.2007.09.041 (2007).**

88 **Kolas, N. K. *et al.* Orchestration of the DNA-damage response by the RNF8 ubiquitin ligase. *Science* 318, 1637-1640, doi:10.1126/science.1150034 (2007).**

89 **Mailand, N. *et al.* RNF8 ubiquitylates histones at DNA double-strand breaks and promotes assembly of repair proteins. *Cell* 131, 887-900, doi:10.1016/j.cell.2007.09.040 (2007).**

90 **Messick, T. E. & Greenberg, R. A. The ubiquitin landscape at DNA double-strand breaks. *The Journal of cell biology* 187, 319-326, doi:10.1083/jcb.200908074 (2009).**

91 **Doil, C. *et al.* RNF168 binds and amplifies ubiquitin conjugates on damaged chromosomes to allow accumulation of repair proteins. *Cell* 136, 435-446, doi:10.1016/j.cell.2008.12.041 (2009).**

92 **Stewart, G. S. *et al.* The RIDDLE syndrome protein mediates a ubiquitin-dependent signaling cascade at sites of DNA damage. *Cell* 136, 420-434, doi:10.1016/j.cell.2008.12.042 (2009).**

93 Sy, S. M., Jiang, J., O, W. S., Deng, Y. & Huen, M. S. The ubiquitin specific protease USP34 promotes ubiquitin signaling at DNA double-strand breaks. *Nucleic acids research* 41, 8572-8580, doi:10.1093/nar/gkt622 (2013).

94 Juang, Y. C. *et al.* OTUB1 co-opts Lys48-linked ubiquitin recognition to suppress E2 enzyme function. *Molecular cell* 45, 384-397, doi:10.1016/j.molcel.2012.01.011 (2012).

95 Nakada, S. *et al.* Non-canonical inhibition of DNA damage-dependent ubiquitination by OTUB1. *Nature* 466, 941-946, doi:10.1038/nature09297 (2010).

96 Wu, J. *et al.* Histone ubiquitination associates with BRCA1-dependent DNA damage response. *Molecular and cellular biology* 29, 849-860, doi:10.1128/MCB.01302-08 (2009).

97 Yan, J. *et al.* The ubiquitin-interacting motif containing protein RAP80 interacts with BRCA1 and functions in DNA damage repair response. *Cancer research* 67, 6647-6656, doi:10.1158/0008-5472.CAN-07-0924 (2007).

98 Kim, H., Chen, J. & Yu, X. Ubiquitin-binding protein RAP80 mediates BRCA1-dependent DNA damage response. *Science* 316, 1202-1205, doi:10.1126/science.1139621 (2007).

99 Sobhian, B. *et al.* RAP80 targets BRCA1 to specific ubiquitin structures at DNA damage sites. *Science* 316, 1198-1202, doi:10.1126/science.1139516 (2007).

100 Wang, B. *et al.* Abraxas and RAP80 form a BRCA1 protein complex required for the DNA damage response. *Science* 316, 1194-1198, doi:10.1126/science.1139476 (2007).

101 Shao, G. *et al.* The Rap80-BRCC36 de-ubiquitinating enzyme complex antagonizes RNF8-Ubc13-dependent ubiquitination events at DNA double strand breaks. *Proceedings of the National Academy of Sciences of the United States of America* 106, 3166-3171, doi:10.1073/pnas.0807485106 (2009).

102 Feng, L., Huang, J. & Chen, J. MERIT40 facilitates BRCA1 localization and DNA damage repair. *Genes & development* 23, 719-728, doi:10.1101/gad.1770609 (2009).

103 Shao, G. *et al.* MERIT40 controls BRCA1-Rap80 complex integrity and recruitment to DNA double-strand breaks. *Genes & development* 23, 740-754, doi:10.1101/gad.1739609 (2009).

104 Moyal, L. *et al.* Requirement of ATM-dependent monoubiquitylation of histone H2B for timely repair of DNA double-strand breaks. *Molecular cell* 41, 529-542, doi:10.1016/j.molcel.2011.02.015 (2011).

105 Nakamura, K. *et al.* Regulation of homologous recombination by RNF20-dependent H2B ubiquitination. *Molecular cell* 41, 515-528, doi:10.1016/j.molcel.2011.02.002 (2011).

106 Peng, M., Litman, R., Jin, Z., Fong, G. & Cantor, S. B. BACH1 is a DNA repair protein supporting BRCA1 damage response. *Oncogene* 25, 2245-2253, doi:10.1038/sj.onc.1209257 (2006).

107 Cantor, S. B. & Andreassen, P. R. Assessing the link between BACH1 and BRCA1 in the FA pathway. *Cell cycle* 5, 164-167 (2006).

108 Greenberg, R. A. *et al.* Multifactorial contributions to an acute DNA damage response by BRCA1/BARD1-containing complexes. *Genes & development* 20, 34-46, doi:10.1101/gad.1381306 (2006).
109 Nam, E. A. & Cortez, D. ATR signalling: more than meeting at the fork. *The Biochemical journal* 436, 527-536, doi:10.1042/BJ20102162 (2011).
110 Morishima, K. *et al.* TopBP1 associates with NBS1 and is involved in homologous recombination repair. *Biochemical and biophysical research communications* 362, 872-879, doi:10.1016/j.bbrc.2007.08.086 (2007).
111 Yu, X. & Chen, J. DNA damage-induced cell cycle checkpoint control requires CtIP, a phosphorylation-dependent binding partner of BRCA1 C-terminal domains. *Molecular and cellular biology* 24, 9478-9486, doi:10.1128/MCB.24.21.9478-9486.2004 (2004).
112 Wu, X. *et al.* ATM phosphorylation of Nijmegen breakage syndrome protein is required in a DNA damage response. *Nature* 405, 477-482, doi:10.1038/35013089 (2000).
113 Haber, J. E. The many interfaces of Mre11. *Cell* 95, 583-586 (1998).
114 Yuan, J. & Chen, J. MRE11-RAD50-NBS1 complex dictates DNA repair independent of H2AX. *The Journal of biological chemistry* 285, 1097-1104, doi:10.1074/jbc.M109.078436 (2010).
115 Zhang, F., Fan, Q., Ren, K. & Andreassen, P. R. PALB2 functionally connects the breast cancer susceptibility proteins BRCA1 and BRCA2. *Molecular cancer research : MCR* 7, 1110-1118, doi:10.1158/1541-7786.MCR-09-0123 (2009).
116 Xia, B. *et al.* Control of BRCA2 cellular and clinical functions by a nuclear partner, PALB2. *Molecular cell* 22, 719-729, doi:10.1016/j.molcel.2006.05.022 (2006).
117 Zimmermann, M., Lottersberger, F., Buonomo, S. B., Sfeir, A. & de Lange, T. 53BP1 regulates DSB repair using Rif1 to control 5' end resection. *Science* 339, 700-704, doi:10.1126/science.1231573 (2013).
118 Feng, L., Fong, K. W., Wang, J., Wang, W. & Chen, J. RIF1 counteracts BRCA1-mediated end resection during DNA repair. *The Journal of biological chemistry* 288, 11135-11143, doi:10.1074/jbc.M113.457440 (2013).
119 Escribano-Diaz, C. *et al.* A cell cycle-dependent regulatory circuit composed of 53BP1-RIF1 and BRCA1-CtIP controls DNA repair pathway choice. *Molecular cell* 49, 872-883, doi:10.1016/j.molcel.2013.01.001 (2013).
120 Chapman, J. R. *et al.* RIF1 is essential for 53BP1-dependent nonhomologous end joining and suppression of DNA double-strand break resection. *Molecular cell* 49, 858-871, doi:10.1016/j.molcel.2013.01.002 (2013).
121 Al-Hakim, A. *et al.* The ubiquitous role of ubiquitin in the DNA damage response. *DNA repair* 9, 1229-1240, doi:10.1016/j.dnarep.2010.09.011 (2010).
122 Bohgaki, M. *et al.* RNF168 ubiquitylates 53BP1 and controls its response to DNA double-strand breaks. *Proceedings of the National Academy of Sciences of the United States of America* 110, 20982-20987, doi:10.1073/pnas.1320302111 (2013).
123 Nakamura, K. *et al.* Genetic dissection of vertebrate 53BP1: a major role in non-homologous end joining of DNA double strand breaks. *DNA repair* 5, 741-749, doi:10.1016/j.dnarep.2006.03.008 (2006).

124 **Hakem, R., de la Pompa, J. L., Elia, A., Potter, J. & Mak, T. W. Partial rescue of Brca1 (5-6) early embryonic lethality by p53 or p21 null mutation. *Nature genetics* 16, 298-302, doi:10.1038/ng0797-298 (1997).**

125 **Bouwman, P. *et al.* 53BP1 loss rescues BRCA1 deficiency and is associated with triple-negative and BRCA-mutated breast cancers. *Nature structural & molecular biology* 17, 688-695, doi:10.1038/nsmb.1831 (2010).**

126 **Bunting, S. F. *et al.* 53BP1 inhibits homologous recombination in Brca1-deficient cells by blocking resection of DNA breaks. *Cell* 141, 243-254, doi:10.1016/j.cell.2010.03.012 (2010).**

127 **Cao, L. *et al.* A selective requirement for 53BP1 in the biological response to genomic instability induced by Brca1 deficiency. *Molecular cell* 35, 534-541, doi:10.1016/j.molcel.2009.06.037 (2009).**

128 **Farmer, H. *et al.* Targeting the DNA repair defect in BRCA mutant cells as a therapeutic strategy. *Nature* 434, 917-921, doi:10.1038/nature03445 (2005).**

129 **Helleday, T., Bryant, H. E. & Schultz, N. Poly(ADP-ribose) polymerase (PARP-1) in homologous recombination and as a target for cancer therapy. *Cell cycle* 4, 1176-1178 (2005).**

130 **Tutt, A. *et al.* Oral poly(ADP-ribose) polymerase inhibitor olaparib in patients with BRCA1 or BRCA2 mutations and advanced breast cancer: a proof-of-concept trial. *Lancet* 376, 235-244, doi:10.1016/S0140-6736(10)60892-6 (2010).**

131 **El-Khamisy, S. F., Masutani, M., Suzuki, H. & Caldecott, K. W. A requirement for PARP-1 for the assembly or stability of XRCC1 nuclear foci at sites of oxidative DNA damage. *Nucleic acids research* 31, 5526-5533 (2003).**

132 **Sanderson, R. J. & Lindahl, T. Down-regulation of DNA repair synthesis at DNA single-strand interruptions in poly(ADP-ribose) polymerase-1 deficient murine cell extracts. *DNA repair* 1, 547-558 (2002).**

133 **Woodhouse, B. C. & Dianov, G. L. Poly ADP-ribose polymerase-1: an international molecule of mystery. *DNA repair* 7, 1077-1086, doi:10.1016/j.dnarep.2008.03.009 (2008).**

134 **Wang, Z. Q. *et al.* PARP is important for genomic stability but dispensable in apoptosis. *Genes & development* 11, 2347-2358 (1997).**

135 **Simbulan-Rosenthal, C. M. *et al.* Chromosomal aberrations in PARP(-/-) mice: genome stabilization in immortalized cells by reintroduction of poly(ADP-ribose) polymerase cDNA. *Proceedings of the National Academy of Sciences of the United States of America* 96, 13191-13196 (1999).**

136 **Ashworth, A. A synthetic lethal therapeutic approach: poly(ADP) ribose polymerase inhibitors for the treatment of cancers deficient in DNA double-strand break repair. *Journal of clinical oncology : official journal of the American Society of Clinical Oncology* 26, 3785-3790, doi:10.1200/JCO.2008.16.0812 (2008).**

137 **Aly, A. & Ganesan, S. BRCA1, PARP, and 53BP1: conditional synthetic lethality and synthetic viability. *Journal of molecular cell biology* 3, 66-74, doi:10.1093/jmcb/mjq055 (2011).**

138 **Ashworth, A. Drug resistance caused by reversion mutation. *Cancer research* 68, 10021-10023, doi:10.1158/0008-5472.CAN-08-2287 (2008).**

139 Fong, P. C. *et al.* Poly(ADP)-ribose polymerase inhibition: frequent durable responses in BRCA carrier ovarian cancer correlating with platinum-free interval. *Journal of clinical oncology : official journal of the American Society of Clinical Oncology* 28, 2512-2519, doi:10.1200/JCO.2009.26.9589 (2010).

140 Sakai, W. *et al.* Secondary mutations as a mechanism of cisplatin resistance in BRCA2-mutated cancers. *Nature* 451, 1116-1120, doi:10.1038/nature06633 (2008).

141 Swisher, E. M. *et al.* Secondary BRCA1 mutations in BRCA1-mutated ovarian carcinomas with platinum resistance. *Cancer research* 68, 2581-2586, doi:10.1158/0008-5472.CAN-08-0088 (2008).

142 Wang, W. & Figg, W. D. Secondary BRCA1 and BRCA2 alterations and acquired chemoresistance. *Cancer biology & therapy* 7, 1004-1005 (2008).

143 de Laat, W. L., Jaspers, N. G. & Hoeijmakers, J. H. Molecular mechanism of nucleotide excision repair. *Genes & development* 13, 768-785 (1999).

144 Pathania, S. *et al.* BRCA1 is required for postreplication repair after UV-induced DNA damage. *Molecular cell* 44, 235-251, doi:10.1016/j.molcel.2011.09.002 (2011).

145 Mallery, D. L., Vandenberg, C. J. & Hiom, K. Activation of the E3 ligase function of the BRCA1/BARD1 complex by polyubiquitin chains. *The EMBO journal* 21, 6755-6762 (2002).

146 Nishikawa, H. *et al.* BRCA1-associated protein 1 interferes with BRCA1/BARD1 RING heterodimer activity. *Cancer research* 69, 111-119, doi:10.1158/0008-5472.CAN-08-3355 (2009).

147 Yu, H. *et al.* Tumor suppressor and deubiquitinase BAP1 promotes DNA double-strand break repair. *Proceedings of the National Academy of Sciences of the United States of America* 111, 285-290, doi:10.1073/pnas.1309085110 (2014).

148 Ismail, I. H. *et al.* Germline mutations in BAP1 impair its function in DNA double-strand break repair. *Cancer research* 74, 4282-4294, doi:10.1158/0008-5472.CAN-13-3109 (2014).

149 Ventii, K. H. *et al.* BRCA1-associated protein-1 is a tumor suppressor that requires deubiquitinating activity and nuclear localization. *Cancer research* 68, 6953-6962, doi:10.1158/0008-5472.CAN-08-0365 (2008).

150 Jensen, D. E. & Rauscher, F. J., 3rd. BAP1, a candidate tumor suppressor protein that interacts with BRCA1. *Annals of the New York Academy of Sciences* 886, 191-194 (1999).

151 Jensen, D. E. & Rauscher, F. J., 3rd. Defining biochemical functions for the BRCA1 tumor suppressor protein: analysis of the BRCA1 binding protein BAP1. *Cancer letters* 143 Suppl 1, S13-17 (1999).

152 Yu, H. *et al.* The ubiquitin carboxyl hydrolase BAP1 forms a ternary complex with YY1 and HCF-1 and is a critical regulator of gene expression. *Molecular and cellular biology* 30, 5071-5085, doi:10.1128/MCB.00396-10 (2010).

153 Machida, Y. J., Machida, Y., Vashisht, A. A., Wohlschlegel, J. A. & Dutta, A. The deubiquitinating enzyme BAP1 regulates cell growth via interaction with HCF-1. *The Journal of biological chemistry* 284, 34179-34188, doi:10.1074/jbc.M109.046755 (2009).

154 **Narayanan, A., Ruyechan, W. T. & Kristie, T. M. The coactivator host cell factor-1 mediates Set1 and MLL1 H3K4 trimethylation at herpesvirus immediate early promoters for initiation of infection.** ***Proceedings of the National Academy of Sciences of the United States of America*** **104, 10835-10840, doi:10.1073/pnas.0704351104 (2007).**

155 **Wysocka, J. & Herr, W. The herpes simplex virus VP16-induced complex: the makings of a regulatory switch.** ***Trends in biochemical sciences*** **28, 294-304, doi:10.1016/S0968-0004(03)00088-4 (2003).**

156 **Kristie, T. M., Liang, Y. & Vogel, J. L. Control of alpha-herpesvirus IE gene expression by HCF-1 coupled chromatin modification activities.** ***Biochimica et biophysica acta*** **1799, 257-265, doi:10.1016/j.bbagrm.2009.08.003 (2010).**

157 **Vogel, J. L. & Kristie, T. M. The dynamics of HCF-1 modulation of herpes simplex virus chromatin during initiation of infection.** ***Viruses*** **5, 1272-1291, doi:10.3390/v5051272 (2013).**

158 **Tyagi, S., Chabes, A. L., Wysocka, J. & Herr, W. E2F activation of S phase promoters via association with HCF-1 and the MLL family of histone H3K4 methyltransferases.** ***Molecular cell*** **27, 107-119, doi:10.1016/j.molcel.2007.05.030 (2007).**

159 **Kristie, T. M., Pomerantz, J. L., Twomey, T. C., Parent, S. A. & Sharp, P. A. The cellular C1 factor of the herpes simplex virus enhancer complex is a family of polypeptides.** ***The Journal of biological chemistry*** **270, 4387-4394 (1995).**

160 **Wilson, A. C., Peterson, M. G. & Herr, W. The HCF repeat is an unusual proteolytic cleavage signal.** ***Genes & development*** **9, 2445-2458 (1995).**

161 **Julien, E. & Herr, W. Proteolytic processing is necessary to separate and ensure proper cell growth and cytokinesis functions of HCF-1.** ***The EMBO journal*** **22, 2360-2369, doi:10.1093/emboj/cdg242 (2003).**

162 **Eletr, Z. M. & Wilkinson, K. D. An emerging model for BAP1's role in regulating cell cycle progression.** ***Cell biochemistry and biophysics*** **60, 3-11, doi:10.1007/s12013-011-9184-6 (2011).**

163 **Misaghi, S.** ***et al.*** **Association of C-terminal ubiquitin hydrolase BRCA1-associated protein 1 with cell cycle regulator host cell factor 1.** ***Molecular and cellular biology*** **29, 2181-2192, doi:10.1128/MCB.01517-08 (2009).**

164 **Freiman, R. N. & Herr, W. Viral mimicry: common mode of association with HCF by VP16 and the cellular protein LZIP.** ***Genes & development*** **11, 3122-3127 (1997).**

165 **Lu, R., Yang, P., Padmakumar, S. & Misra, V. The herpesvirus transactivator VP16 mimics a human basic domain leucine zipper protein, luman, in its interaction with HCF.** ***Journal of virology*** **72, 6291-6297 (1998).**

166 **Wilson, A. C., Freiman, R. N., Goto, H., Nishimoto, T. & Herr, W. VP16 targets an amino-terminal domain of HCF involved in cell cycle progression.** ***Molecular and cellular biology*** **17, 6139-6146 (1997).**

167 **Gordon, S., Akopyan, G., Garban, H. & Bonavida, B. Transcription factor YY1: structure, function, and therapeutic implications in cancer biology.** ***Oncogene*** **25, 1125-1142, doi:10.1038/sj.onc.1209080 (2006).**

168 **Shi, Y., Lee, J. S. & Galvin, K. M. Everything you have ever wanted to know about Yin Yang 1. *Biochimica et biophysica acta* 1332, F49-66 (1997).**

169 **Yang, W. M., Inouye, C., Zeng, Y., Bearss, D. & Seto, E. Transcriptional repression by YY1 is mediated by interaction with a mammalian homolog of the yeast global regulator RPD3. *Proceedings of the National Academy of Sciences of the United States of America* 93, 12845-12850 (1996).**

170 **Seelan, R. S. & Grossman, L. I. Structural organization and promoter analysis of the bovine cytochrome c oxidase subunit VIIc gene. A functional role for YY1. *The Journal of biological chemistry* 272, 10175-10181 (1997).**

171 **Scheuermann, J. C. *et al.* Histone H2A deubiquitinase activity of the Polycomb repressive complex PR-DUB. *Nature* 465, 243-247, doi:10.1038/nature08966 (2010).**

172 **Sinclair, D. A. *et al.* The Additional sex combs gene of Drosophila encodes a chromatin protein that binds to shared and unique Polycomb group sites on polytene chromosomes. *Development* 125, 1207-1216 (1998).**

173 **Lee, S. W. *et al.* ASXL1 represses retinoic acid receptor-mediated transcription through associating with HP1 and LSD1. *The Journal of biological chemistry* 285, 18-29, doi:10.1074/jbc.M109.065862 (2010).**

174 **Park, U. H., Yoon, S. K., Park, T., Kim, E. J. & Um, S. J. Additional sex comb-like (ASXL) proteins 1 and 2 play opposite roles in adipogenesis via reciprocal regulation of peroxisome proliferator-activated receptor {gamma}. *The Journal of biological chemistry* 286, 1354-1363, doi:10.1074/jbc.M110.177816 (2011).**

175 **Park, U. H. *et al.* Reciprocal regulation of LXRalpha activity by ASXL1 and ASXL2 in lipogenesis. *Biochemical and biophysical research communications* 443, 489-494, doi:10.1016/j.bbrc.2013.11.124 (2014).**

176 **Abdel-Wahab, O. *et al.* ASXL1 mutations promote myeloid transformation through loss of PRC2-mediated gene repression. *Cancer cell* 22, 180-193, doi:10.1016/j.ccr.2012.06.032 (2012).**

177 **Abdel-Wahab, O. & Dey, A. The ASXL-BAP1 axis: new factors in myelopoiesis, cancer and epigenetics. *Leukemia* 27, 10-15, doi:10.1038/leu.2012.288 (2013).**

178 **Abdel-Wahab, O. *et al.* Concomitant analysis of EZH2 and ASXL1 mutations in myelofibrosis, chronic myelomonocytic leukemia and blast-phase myeloproliferative neoplasms. *Leukemia* 25, 1200-1202, doi:10.1038/leu.2011.58 (2011).**

179 **Fisher, C. L. *et al.* Loss-of-function Additional sex combs like 1 mutations disrupt hematopoiesis but do not cause severe myelodysplasia or leukemia. *Blood* 115, 38-46, doi:10.1182/blood-2009-07-230698 (2010).**

180 **Dey, A. *et al.* Loss of the tumor suppressor BAP1 causes myeloid transformation. *Science* 337, 1541-1546, doi:10.1126/science.1221711 (2012).**

181 **Micol, J. B. *et al.* Frequent ASXL2 mutations in acute myeloid leukemia patients with t(8;21)/RUNX1-RUNX1T1 chromosomal translocations. *Blood* 124, 1445-1449, doi:10.1182/blood-2014-04-571018 (2014).**

182 **Carbone, M. *et al.* BAP1 and cancer. *Nature reviews. Cancer* 13, 153-159 (2013).**

183 **Harbour, J. W. *et al.* Frequent mutation of BAP1 in metastasizing uveal melanomas. *Science* 330, 1410-1413, doi:10.1126/science.1194472 (2010).**

184 **Landreville, S., Agapova, O. A. & Harbour, J. W. Emerging insights into the molecular pathogenesis of uveal melanoma.** ***Future oncology*** **4, 629-636, doi:10.2217/14796694.4.5.629 (2008).**

185 **Kamp, D. W. Asbestos-induced lung diseases: an update.** ***Translational research : the journal of laboratory and clinical medicine*** **153, 143-152, doi:10.1016/j.trsl.2009.01.004 (2009).**

186 **Bott, M.** ***et al.*** **The nuclear deubiquitinase BAP1 is commonly inactivated by somatic mutations and 3p21.1 losses in malignant pleural mesothelioma.** ***Nature genetics*** **43, 668-672, doi:10.1038/ng.855 (2011).**

187 **Testa, J. R.** ***et al.*** **Germline BAP1 mutations predispose to malignant mesothelioma.** ***Nature genetics*** **43, 1022-1025, doi:10.1038/ng.912 (2011).**

188 **Carbone, M.** ***et al.*** **Malignant mesothelioma: facts, myths, and hypotheses.** ***Journal of cellular physiology*** **227, 44-58, doi:10.1002/jcp.22724 (2012).**

189 **Xu, J.** ***et al.*** **Germline mutation of Bap1 accelerates development of asbestos-induced malignant mesothelioma.** ***Cancer research*** **74, 4388-4397, doi:10.1158/0008-5472.CAN-14-1328 (2014).**

190 **Harbour, J. W. & Dean, D. C. The Rb/E2F pathway: expanding roles and emerging paradigms.** ***Genes & development*** **14, 2393-2409 (2000).**

191 **Ouchi, T. BRCA1 phosphorylation: biological consequences.** ***Cancer biology & therapy*** **5, 470-475 (2006).**

192 **Ouchi, M.** ***et al.*** **BRCA1 phosphorylation by Aurora-A in the regulation of G2 to M transition.** ***The Journal of biological chemistry*** **279, 19643-19648, doi:10.1074/jbc.M311780200 (2004).**

193 **Hochstrasser, M. Origin and function of ubiquitin-like proteins.** ***Nature*** **458, 422-429, doi:10.1038/nature07958 (2009).**

194 **Bergink, S. & Jentsch, S. Principles of ubiquitin and SUMO modifications in DNA repair.** ***Nature*** **458, 461-467, doi:10.1038/nature07963 (2009).**

195 **Galanty, Y.** ***et al.*** **Mammalian SUMO E3-ligases PIAS1 and PIAS4 promote responses to DNA double-strand breaks.** ***Nature*** **462, 935-939, doi:10.1038/nature08657 (2009).**

196 **Morris, J. R.** ***et al.*** **The SUMO modification pathway is involved in the BRCA1 response to genotoxic stress.** ***Nature*** **462, 886-890, doi:10.1038/nature08593 (2009).**

197 **Vyas, R.** ***et al.*** **RNF4 is required for DNA double-strand break repair in vivo.** ***Cell death and differentiation*** **20, 490-502, doi:10.1038/cdd.2012.145 (2013).**

198 **Tatham, M. H.** ***et al.*** **RNF4 is a poly-SUMO-specific E3 ubiquitin ligase required for arsenic-induced PML degradation.** ***Nature cell biology*** **10, 538-546, doi:10.1038/ncb1716 (2008).**

199 **Lallemand-Breitenbach, V.** ***et al.*** **Arsenic degrades PML or PML-RARalpha through a SUMO-triggered RNF4/ubiquitin-mediated pathway.** ***Nature cell biology*** **10, 547-555, doi:10.1038/ncb1717 (2008).**

200 **Schimmel, J.** ***et al.*** **The ubiquitin-proteasome system is a key component of the SUMO-2/3 cycle.** ***Molecular & cellular proteomics : MCP*** **7, 2107-2122, doi:10.1074/mcp.M800025-MCP200 (2008).**

201 **Olsen, J. V. & Mann, M. Status of large-scale analysis of post-translational modifications by mass spectrometry. *Molecular & cellular proteomics : MCP* 12, 3444-3452, doi:10.1074/mcp.O113.034181 (2013).**

202 **Guendel, I. *et al.* Methylation of the tumor suppressor protein, BRCA1, influences its transcriptional cofactor function. *PloS one* 5, e11379, doi:10.1371/journal.pone.0011379 (2010).**

203 **Xie, J. *et al.* FANCJ/BACH1 acetylation at lysine 1249 regulates the DNA damage response. *PLoS genetics* 8, e1002786, doi:10.1371/journal.pgen.1002786 (2012).**

204 **Li, J. *et al.* DNA damage binding protein component DDB1 participates in nucleotide excision repair through DDB2 DNA-binding and cullin 4A ubiquitin ligase activity. *Cancer research* 66, 8590-8597, doi:10.1158/0008-5472.CAN-06-1115 (2006).**

205 **Hu, J., McCall, C. M., Ohta, T. & Xiong, Y. Targeted ubiquitination of CDT1 by the DDB1-CUL4A-ROC1 ligase in response to DNA damage. *Nature cell biology* 6, 1003-1009, doi:10.1038/ncb1172 (2004).**

206 **Nag, A., Bagchi, S. & Raychaudhuri, P. Cul4A physically associates with MDM2 and participates in the proteolysis of p53. *Cancer research* 64, 8152-8155, doi:10.1158/0008-5472.CAN-04-2598 (2004).**

207 **Thirunavukarasou, A., Singh, P., Govindarajalu, G., Bandi, V. & Baluchamy, S. E3 ubiquitin ligase Cullin4B mediated polyubiquitination of p53 for its degradation. *Molecular and cellular biochemistry* 390, 93-100, doi:10.1007/s11010-014-1960-3 (2014).**

208 **Chen, L. C. *et al.* The human homologue for the Caenorhabditis elegans cul-4 gene is amplified and overexpressed in primary breast cancers. *Cancer research* 58, 3677-3683 (1998).**

209 **Metzger, E. *et al.* LSD1 demethylates repressive histone marks to promote androgen-receptor-dependent transcription. *Nature* 437, 436-439, doi:10.1038/nature04020 (2005).**

210 **Shi, Y. *et al.* Histone demethylation mediated by the nuclear amine oxidase homolog LSD1. *Cell* 119, 941-953, doi:10.1016/j.cell.2004.12.012 (2004).**

211 **Liang, Y., Vogel, J. L., Narayanan, A., Peng, H. & Kristie, T. M. Inhibition of the histone demethylase LSD1 blocks alpha-herpesvirus lytic replication and reactivation from latency. *Nature medicine* 15, 1312-1317, doi:10.1038/nm.2051 (2009).**

212 **Butkinaree, C., Park, K. & Hart, G. W. O-linked beta-N-acetylglucosamine (O-GlcNAc): Extensive crosstalk with phosphorylation to regulate signaling and transcription in response to nutrients and stress. *Biochimica et biophysica acta* 1800, 96-106, doi:10.1016/j.bbagen.2009.07.018 (2010).**

213 **Slawson, C., Copeland, R. J. & Hart, G. W. O-GlcNAc signaling: a metabolic link between diabetes and cancer? *Trends in biochemical sciences* 35, 547-555, doi:10.1016/j.tibs.2010.04.005 (2010).**

214 **Daou, S. *et al.* Crosstalk between O-GlcNAcylation and proteolytic cleavage regulates the host cell factor-1 maturation pathway. *Proceedings of the National Academy of Sciences of the United States of America* 108, 2747-2752, doi:10.1073/pnas.1013822108 (2011).**

215 Capotosti, F. *et al.* O-GlcNAc transferase catalyzes site-specific proteolysis of HCF-1. *Cell* 144, 376-388, doi:10.1016/j.cell.2010.12.030 (2011).

216 Lazarus, M. B. *et al.* HCF-1 is cleaved in the active site of O-GlcNAc transferase. *Science* 342, 1235-1239, doi:10.1126/science.1243990 (2013).

217 Mashtalir, N. *et al.* Autodeubiquitination protects the tumor suppressor BAP1 from cytoplasmic sequestration mediated by the atypical ubiquitin ligase UBE2O. *Molecular cell* 54, 392-406, doi:10.1016/j.molcel.2014.03.002 (2014).

218 You, J. S. & Jones, P. A. Cancer genetics and epigenetics: two sides of the same coin? *Cancer cell* 22, 9-20, doi:10.1016/j.ccr.2012.06.008 (2012).

219 Hanahan, D. & Weinberg, R. A. Hallmarks of cancer: the next generation. *Cell* 144, 646-674, doi:10.1016/j.cell.2011.02.013 (2011).

220 Shen, H. & Laird, P. W. Interplay between the cancer genome and epigenome. *Cell* 153, 38-55, doi:10.1016/j.cell.2013.03.008 (2013).

221 Toyota, M. & Suzuki, H. Epigenetic drivers of genetic alterations. *Advances in genetics* 70, 309-323, doi:10.1016/B978-0-12-380866-0.60011-3 (2010).

Annex 1

The Ubiquitin Carboxyl Hydrolase BAP1 Forms a Ternary Complex with YY1 and HCF-1 and is a Critical Regulator of Gene Expression.

Helen Yu[1], Nazar Mashtalir[1], Salima Daou[1], Ian Hammond-Martel[1], Julie Ross[1], Guangchao Sui[2], Gerald W. Hart[3], Frank J. Rauscher III[4], Elliot Drobetsky[1], Eric Milot[1], Yang Shi[5] and El Bachir Affar[1,6]

[1]Maisonneuve-Rosemont Hospital Research Center, Department of Medicine and Department of Biochemistry, University of Montréal, Montréal, Canada
[2]Wake Forest University School of Medicine, Winston-Salem, NC, USA.
[3]John Hopkins University School of Medicine, Baltimore, MD, USA
[4]The Wistar Institute, Philadelphia, PA, USA
[5]Department of Pathology, Harvard Medical School and Division of New Born Medicine, Department of Medicine, Children's Hospital Boston, MA, USA

Running title: BAP1 is a transcription co-activator

[6]Correspondence
El Bachir Affar
Universitity of Montréal, Centre de Recherche, Hôpital Maisonneuve-Rosemont
5415 boul. de l'Assomption, Montréal, Québec, H1T 2M4, CANADA
Tel: 514 252-3400 (Ext: 3343)
Fax: 514 252-3430

ABSTRACT

The candidate tumor suppressor BAP1 is a deubiquitinating enzyme (DUB) involved in the regulation of cell proliferation, although the molecular mechanisms governing its function remain poorly defined. BAP1 was recently shown to interact with, and deubiquitinate the transcriptional regulator Host Cell Factor-1 (HCF-1). Here, we show that BAP1 assembles multi-protein complexes containing numerous transcription factors and cofactors including HCF-1 and the transcription factor Yin Yang 1 (YY1). Through its coiled coil motif, BAP1 directly interacts with the zinc fingers of YY1. Moreover, HCF-1 interacts with the middle region of YY1 encompassing the glycine-lysine-rich domain and is essential for the formation of a ternary complex with YY1 and BAP1 in vivo. BAP1 activates transcription in an enzymatic activity-dependent manner and regulates the expression of a variety of genes involved in numerous cellular processes. We further show that BAP1 and HCF-1 are recruited by YY1 to the promoter of cox7c gene, which encodes a mitochondrial protein used here as a model of BAP1-activated gene expression. Our findings (i) establish a direct link between BAP1 and transcriptional control of genes regulating cell growth and proliferation and (ii) shed light on a novel mechanism of transcription regulation involving ubiquitin signaling.

INTRODUCTION

Post-translational modification of proteins with ubiquitin plays a central role in a wide variety of biological processes in eukaryotic cells (44, 64). Depending on the nature of the modification (e.g. poly- vs. mono-ubiquitination), modified substrates can be either degraded by the proteasome or regulated at the level of their activity and function (4, 45). Ubiquitination is reversible and a significant repertoire of proteases, termed deubiquitinating enzymes (DUBs), are emerging as critical regulators of ubiquitin signaling (40, 46).

BAP1 (BRCA1-Associated Protein1) was originally isolated as a nuclear DUB that interacts with, and enhances the growth suppressive effect of, the tumor suppressor BRCA1 (19). BAP1 also acts in a BRCA1-independent manner, as its overexpression in cells lacking BRCA1 was shown to inhibit cell proliferation and tumor growth (60). Interestingly, recent studies indicate that RNAi-mediated depletion of BAP1 can also exert an inhibitory effect on cell proliferation (31, 36, 41). Although the exact molecular mechanisms are largely unknown, the above data suggest that BAP1 controls cell cycle progression. In further support of this notion, homozygous inactivating mutations in BAP1 have been found in subsets of lung carcinoma and breast cancer cell lines suggesting that this DUB is a tumor suppressor (19, 67).

BAP1 is a member of the UCH family including UCH-L1, UCH-L3 and UCH-L5 (UCH37), all of which possess a conserved catalytic domain containing an invariant histidine, cysteine, and aspartic acid catalytic triad (20). Although UCH family members were initially associated with the maturation and turnover of ubiquitin, these enzymes possess isopeptidase activity and thus might selectively regulate protein stability or activity (32, 35, 41). Remarkably BAP1 possesses a large C-terminal domain, not present in other UCH members, which is predicted to play an important role in regulating and coordinating its DUB activity through selective association with potential substrates or regulatory components.

Host cell factor 1 (HCF-1) is a chromatin-associated protein initially identified as part of a multi-protein complex comprising the viral co-activator VP16 and the POU domain

transcription factor Oct-1 (23). During herpes simplex virus infection, this complex is recruited to the enhancer/promoter of the immediate early gene to activate viral gene expression (23). HCF-1 was further shown to interact, often through a tetrapeptide sequence termed the HCF-1 binding motif (HBM), with specific members of diverse classes of transcription factors including E2F1, Krox20, Sp1, and GABP. This suggests a crucial role for HCF-1 in regulating the expression of a plethora of genes involved in diverse cellular processes (7, 10, 16, 22, 28-30, 34, 58, 62). HCF-1 also associates with chromatin modifying enzymes, most notably methyltransferases (Set1, MLL1, MLL5), acetyltransferases (hMOF) and deacetylases (HDAC1, HDAC2) (8, 11, 39, 58, 68, 72). Most recently HCF-1 was shown to recruit LSD1 to demethylate the repressive mark histone H3 lysine 9, and to promote the trimethylation of histone H3 lysine 4 by Set1, a mark associated with active genes (26). Although HCF-1 has been mostly associated with transcription activation, this regulator is also involved in transcription repression (6, 58, 68). It is thought that sequence-specific DNA-binding transcription factors are responsible for the differential recruitment of distinct HCF-1 complexes to either positively or negatively regulate target gene expression. For instance HCF-1 was shown to regulate the G1/S transition of cell cycle through specific interaction with either E2F4 or E2F1 which, respectively, represses or activates E2F target genes (58). Despite the above findings, the manner in which HCF-1 is selectively recruited to coordinate the assembly of diverse chromatin modifying complexes that tightly regulate gene expression remains an area of active investigation.

BAP1 was recently shown to interact, through a NHNY sequence (HBM) located in its middle region, with the kelch motif of HCF-1; moreover this interaction appears to be required for cell proliferation (31, 36). Ectopic expression studies indicate that BAP1 can deubiquitinate HCF-1 (31, 36), although the significance of this event remains to be elucidated. Additional proteins identified by virtue of their co-purification with BAP1 have also been recently reported, most of which are involved in regulation of chromatin-associated processes particularly transcription (31, 54). These include the forkhead transcription factors FOXK1 and FOXK2, the histone acetyltransferase HAT1, the human homolog of additional sex combs ASXL1 and ASXL2, the histone lysine demethylase KDM1B (LSD2), and the

ubiquitin conjugating E2 enzyme UBE20. Interestingly, very recently, the drosophila polycomb group protein Calypso was found to be the orthologue of BAP1. Calypso associates with ASX to form the transcription complex PR-DUB that in turn deubiquitinates histone H2A and regulates hox gene expression (47). However it should be noted that the association of human BAP1 with several additional partners as described above suggests a substantially more complex network of functional interactions.

Here, we establish that mammalian BAP1 is assembled into high molecular weight multi-protein complexes containing transcription factors and cofactors including HCF-1. We reveal novel BAP1-interacting partners including the transcription factor Yin Yang 1 (YY1), a zinc finger protein that possesses dual functionality by either activating or repressing gene expression depending upon its association with specific transcription co-activators or co-repressors at specific target gene promoters (see reviews (13, 51)). We show that BAP1 directly interacts with YY1, and HCF-1 is required for this interaction in vivo. Finally, in providing a model for BAP1-mediated control of gene expression, we demonstrate that this DUB is a direct co-activator of *cox7c*, a nuclear gene encoding a component of the mitochondrial respiratory chain. Our data provide novel molecular insight into the involvement of deubiquitination in the control of gene expression.

MATERIALS AND METHODS

Plasmids and Antibodies

Retroviral constructs that express N-terminal Flag-HA-tagged wildtype or mutant forms of human BAP1 were generated by subcloning the cDNA into the POZ-N plasmid provided by Y. Nakatani (38). The catalytically inactive BAP1, POZ-BAP1 (C91S) was generated by site-directed mutagenesis. The BAP1 mutant deleted in the NHNY sequence corresponding the HCF-1 binding domain (ΔHBD) was generated by PCR-based subcloning of 2 fragments ligated in frame into POZ-N. The Gal4-BAP1 and Gal4-BAP1 catalytically inactive (C91S) constructs were generated by PCR amplification of the Gal4 DNA binding sequence and ligation in frame into pCDNA.3 BAP1. The Gal4-BAP1 ΔHBM was generated by subcloning BAP1 ΔHBM in frame into pCDNA.3 containing Gal4 DNA binding sequence. shRNAs for hBAP1 (#1 and #2) and hHCF-1 were generated as previously described (57). The targeted sequences of these shRNAs are listed in the supplemental information. The constructs used to produce recombinant full length GST-YY1 and various deletion fragments have been described (25). Constructs to produce recombinant full length GST-BAP1 and various deleted forms were obtained by PCR-amplification of various fragments, which were cloned into pGEX4T1. The construct for producing recombinant human His-tagged YY1 has been described (56). A construct to produce recombinant human His-tagged BAP1 was generated by subcloning BAP1 cDNA into pET30a+. The shRNA construct for YY1 and non-target sequence have been described (56). The pCGN-HCF-1 vector (65) was used for subcloning HCF-1 into the pcDNA.3/HA vector.

Monoclonal anti-BAP1 (C4) and anti-YY1 (H10), polyclonal anti-BAP1 (H300) and anti-TFIID (N12) were from Santa Cruz. Monoclonal anti-HCF-1 (M2) (66) and polyclonal anti-HCF-1 (N18) (14) have been used. Polyclonal anti-HCF-1 (A301-400A) was from Bethyl laboratories. Monoclonal anti-RNA Polymerase II (H14) was from Covance. Polyclonal anti-Histone H3 (06-755), polyclonal anti-Histone H3 trimethylated at lysine 27 (H3 K27 me3) (17-622) and monoclonal anti-βactin (MAB1501) were from Millipore. The antibodies used as controls for IP and ChIP were the polyclonal anti-GFP (FL), anti-HA (Y-11) and rabbit IgG (sc-2027), and were from Santa Cruz.

Cell culture, RNAi and immunoblotting

HeLa cervical cancer, U2OS osteosarcoma and PhenixA virus-producing cells were cultured in Dulbecco's modified Eagle's medium (DMEM) supplemented with 10% fetal bovine serum and penicillin/streptomycin. Cells were transfected with either a non-targeting control or BAP1 RNA interference (RNAi) plasmid using Lipofectamine 2000 (Invitrogen). For transient RNAi experiments, shRNA vectors were mixed with the pBABE puromycin resistance-encoding vector, and transfected cells were selected by adding 2 μg/ml of puromycin for 2 days as described (1). U2OS cells with stable depletion of BAP1 were generated by co-transfection of RNAi vectors with pCDNA.3 neomycin resistance-encoding vector, and independent clones were isolated following G418 selection (1.5 mg/ml) and tested for BAP1 knockdown by western blotting. The siRNA smart pools for human HCF-1, BAP1 and a non-target control were from Dharmacon (Thermo Scientific) and were transfected into HeLa or U2OS cells using Lipofectamine 2000.

Total cell extracts were prepared in lysis buffer (50 mM Tris-HCl, pH 7.3; 5 mM EDTA; 50 mM KCl; 0.1% NP-40; 1 mM phenylmethylsulfonyl fluoride (PMSF); 1 mM dithiothreitol and protease inhibitors cocktail (Sigma)), and protein concentration determined by Bradford assay. SDS-PAGE and western blotting were conducted according to standard procedures.

Purification of BAP1-associated proteins and co-immunoprecipitation

HeLa and U2OS cell lines stably expressing Flag-HA-BAP1 (WT, C91S or ΔHBD) were generated following retroviral transduction and 4 rounds of selection using magnetic beads coupled to IL2 receptor antibody as previously described (38). HeLa (~9 X 10^9 cells) or U2OS (~0.5 X 10^9 cells) were used for purification of BAP1-associated proteins, essentially as previously described (38). Standard co-immunoprecipitations using appropriate antibodies were conducted as previously described (56).

Immunodepletion was conducted on HeLa nuclear extracts (~100 μg of proteins) by overnight incubation at 4 ºC with 2 μg of anti-HCF-1 or anti-BAP1 polyclonal antibody in IP

buffer (50 mM Tris, pH 7.3; 150 mM NaCl; 5 mM EDTA; 10 mM NaF; 1% Triton X-100; 1 mM PMSF and protease inhibitors cocktail (Sigma)). The anti-HA (Y-11) polyclonal antibody was used as control. The immuno-complexes were incubated for 7 hours at 4 ºC with protein G agarose beads (Sigma) which were saturated with 1% BSA in IP buffer. After centrifugation, the flow through and bead fractions were collected. The immuno-complexes were washed once with the IP buffer supplemented with 1% BSA. Bound proteins were eluted from the beads with Laemmli buffer and subjected, along with the flow through fractions, to western blotting.

Preparation of chromatin fractions and digestion with Micrococcal nuclease (MNase) were conducted as previously described (15). Briefly, the nuclear pellet was resuspended in 20 mM Tris-HCl (pH 7.5), 100 mM KCl, 2 mM MgCl2, 1 mM CaCl2, 0.3 M sucrose, 0.1% Triton X-100, and protease inhibitor cocktail. Following MNase treatment (3 U/ml for 10 min), the reaction was ended with 5 mM each EGTA and EDTA. The samples were then centrifuged at 13,000 g for 10 min at 4°C to obtain the soluble chromatin fraction.

Glycerol gradient and gel filtration analysis

Molecular mass separation of native BAP1 complexes from nuclear extract was conduced using a 10-40 % glycerol gradient prepared in 20 mM Tris-HCl, pH 7.9; 100 mM KCl; 5 mM MgCl2; 1 mM PMSF; 0.1% NP40 and 10 mM 2-mercaptoethanol. The samples were centrifuged for 12 h at 50,000 RPM (SW55Ti rotor, Beckman,) at 4 ºC. Individual fractions were then collected from top to bottom and analyzed by western blotting. The CtBP co-repressor complex estimated to have a molecular mass of 1.3-1.5 MDa was used as reference (52).

Gel filtration analysis of purified BAP1 complexes was conducted using a Superose6 HR gel exclusion chromatography column. Eluted fractions were analysed by silver staining and western blotting. The native molecular weight markers used for column calibration were thyroglobulin (669 KDa), ferritin (440 KDa), catalase (232 KDa), lactate dehydrogenase (140 KDa) and albumin (66 KDa) (obtained from GE Healthcare).

Deubiquitination assay on Ub-AMC

Deubiquitination assay on Ub-AMC was conducted as previously described (32) with the following modifications. Purified BAP1 complexes (WT, C91S and ΔHBM) and recombinant His-BAP1 were adjusted to the same amount of BAP1 protein (125 ng; 1.5 pmol) and incubated individually with 37.5 pmol of Ub-AMC (Boston Biochem) in 100 µl of assay buffer (50 mM Tris pH 7.3, 0.25 mM EDTA, 10% DMSO and 1 mM DTT) for 1200 sec. Fluorescence was measured using a fluorimeter (Cytofluor, PerSeptive Biosystems) at excitation and emission wavelengths of 380 nm and 460 nm, respectively.

In vitro interaction assays

Recombinant GST fusion proteins were purified using glutathione agarose beads (Sigma) and 2 to 3 µg of beads containing bound proteins were incubated with 10 µl of in vitro translated methionine-S35 labeled HCF-1 (TNT® T7 Quick Coupled Transcription/Translation System, Promega), 1 µg His-YY1, or 1 µg His-BAP1 for 6 to 8 hours at 4 ºC in 50 mM Tris, pH 7.5; 50 mM NaCl; 0.02% Tween 20; 1 mM PMSF and 500 µM dithiothreitol). The beads were extensively washed with the same buffer, and bound proteins eluted in Laemmli buffer and subjected to autoradiography or western blotting.

Immunofluorescence

Cells were fixed for 20 min using 3 % paraformaldehyde prepared in phosphate-buffered saline (PBS). Cells were then permeabilized with 0.5% NP-40 in PBS for 20 min and washed with PBS containing 0.1% NP-40. Cells were further incubated in blocking solution (PBS containing 0.1% NP-40 and 10% FBS) and stained with a monoclonal anti-BAP1 antibody. Anti-mouse Alexa Fluor® 594 (Invitrogen) was used as secondary antibody. Nuclei were stained with 4',6-diamidino-2-phenylindole (DAPI). Z-stacks were acquired using Leica DMRE microscope, HCX PL APO 63X/ 1.32-0.6 OIL CS objective and Retiga Ex (Qimaging) camera and deconvoluted with the Openlab 3.1.1 program. RGB profiles were generated by WCIF-ImageJ program (NIH).

Cell synchronization and cell cycle analysis

U2OS cells were synchronized at the G1/S border using a thymidine double block protocol (17). The DNA content of cells was analyzed essentially as described (1). Briefly, cells were harvested by trypsinization and fixed with 70 % ethanol. After one wash with PBS, cells were treated with 100 µg/ml RNase A (Sigma-Aldrich) for 30 min at 37°C, stained with 50 µg/ml propidium iodide (Sigma-Aldrich), and analyzed using a FACScan flow cytometer equipped with Cellquest software (Becton Dickinson).

Genome-wide gene expression analysis and qRT-PCR analysis of individual mRNAs

U2OS cells, transfected with a non-target control shRNA or shRNAs targeting BAP1, were selected with puromycin containing medium and then synchronized at the G1/S border to allow comparative analysis of gene expression. RNA was prepared using Trizol reagent (Invitrogen) and the RNeasy kit (QIAGEN). The generation of cDNA and biotinylated cRNA and hybridization to Human genome Hu133 plus 2.0 arrays (Affymetrix; containing 47,000 transcripts and transcripts variants) were conducted following the One-Cycle target Labeling Protocol of the GeneChip ® Expression Analysis Technical Manual from Affymetrix (Genome Québec Innovation Centre, Montréal, Canada). Gene expression levels from shControl and shRNAs were subjected to comparative analysis using the expression analysis software Flex Array V1.1. A functional analysis of genes deregulated following BAP1 depletion was conducted using Ingenuity Pathways Analysis Version 8.5 (3). The gene expression data for both shRNAs are deposited in the Gene Expression Omnibus (GEO) NCBI database.

Levels of individual mRNAs in BAP1 depleted cells were determined by RT-PCR. Total mRNA (prepared as described above) was used for reverse transcription using the Superscript III reverse transcriptase and oligo(dT)12-18 primers (Invitrogen). The obtained cDNAs were subjected to PCR amplification with the primer sets described in Supplemental Information. The mRNA levels were normalized to GAPDH expression.

Chromatin immunoprecipitation analysis

Chromatin immunoprecipitation (ChIP) experiments were conducted essentially as previously described (2) with the following modifications. U2OS cells (5 X 10^6) were cross-linked with 1% formaldehyde in PBS at room temperature for 10 min with prior incubation in 1.5 mM EGS (ethylene glycolbis [succnimidyl succinate]; Sigma-Aldrich) in PBS for 30 min at room temperature as described (42, 73). Following quenching with glycine (125 mM) for 5 min, cells were scraped in cold PBS. The cells were first washed with buffer A (50 mM Tris-HCl, pH 8.0; 0.1% NP40; 2 mM EDTA; 10% glycerol; 1 mM PMSF and protease inhibitors cocktail (Sigma)) and then sonicated in Buffer B (50 mM Tris-HCL, pH 8.0; 1% SDS; 10 mM EDTA; 1 mM PMSF and protease inhibitors cocktail) to generate 300-600 bp fragments. After centrifugation and pre-clearing for 1 hour, the suspension was incubated overnight with polyclonal anti-HCF-1, anti-BAP1, anti-YY1 or a non-relevant antibody used as control. Immunocomplexes were recovered with protein A agarose beads (Millipore) and the DNA was purified after decrosslinking with phenol-chloroform extraction. Real time PCR was conducted using SYBR green reaction and detection kit (Invitrogen) on an iCycler iQ apparatus (Bio-Rad). Quantification was conducted using the 2– CT method, where CT is calculated as follows: (ChIP CT– input CT of the control antibody) – (ChIP CT – input CT of the target antibody). The results are shown as a ratio of target gene promoter versus reference gene promoter. The amplification efficiency of all primer sets was verified before qPCR analysis. All experiments were done at least 3 times and the data shown are results of a representative experiment. The primer sets used are described in the Supplemental Information.

Luciferase reporter assays

HeLa cells were transfected with various amounts of Gal4-BAP1, Gal4-BAP (C91S), BAP1 or Gal4 expression plasmids along with 500 ng Gal4-TK-Luciferase or 500 ng TK-luciferase reporter plasmids. pEGFP-N2 construct (10 ng) was also included to ensure equal transfection efficiency between the different conditions. Luciferase activity was measured 2 days post-transfection using a luciferase assay (Promega).

RESULTS

BAP1 is assembled into high molecular weight multi-protein complexes and interacts with the transcription factor YY1.

HeLa nuclear extracts were prepared wherein nearly all nuclear BAP1 protein was recovered (Figure 1A, top panel). Glycerol density gradient fractionation of these extracts showed that most of the endogenous protein is detected as a peak in the high molecular weight fractions (~ 1.3 to1.8 MDa), suggesting that BAP1 is assembled into multi-protein complexes (Figure 1A, bottom panel). To identify these potential complexes, we generated a stable HeLa cell line expressing Flag-HA-BAP1 and conducted a large-scale double immunopurification of the protein using anti-Flag and anti-HA columns. Silver stain of the eluted material revealed that several polypeptides co-purify with BAP1 (Figure 1B). These proteins are specific since no apparent protein bands were detected in the HA elution from the mock purification. Of note, most of the proteins co-purifying with BAP1 were readily detectable following the anti-Flag purification step. Nonetheless, to ensure high specificity, the HA-eluted material was used for mass spectrometry analysis to identify BAP1-interacting partners. Several recently reported as well as novel BAP1-interacting proteins were recovered (Figure 1B). As reflected by the protein sequence coverage and the number of identified peptides for each protein, the most abundant polypeptides identified include the transcriptional regulator HCF-1, the forkhead transcription factors FOXK1 and FOXK2, the O-linked N-acetyl glucosamine transferase (OGT), the human homolog of additional sex combs ASXL1 and ASXL2, the ETS-related transcription factors ELF-1 and ELF-2, and the E2 enzyme UBE20. Less abundant BAP1-interacting proteins comprise specific transcription factors and cofactors such as YY1, ZNF131, PRDM10, and the histone H3 K4 demethylase KDM1B. To validate these results, we also established a U2OS osteosarcoma cell line stably expressing Flag-HA-BAP1. Using this model cell type, we found that, although a small-scale cell preparation was used, most of the major BAP1-associated proteins were recovered following purification. These include HCF-1, OGT, ASXL1/ASXL2, FOXK1/FOXK2, and KDM1B.

Stoichiometric amounts of HCF-1 co-purify with BAP1, as a large number of peptides were obtained following mass spectrometry analysis and the intensities of the silver stained bands were similar for the two proteins (Figure 1B). Since the majority of endogenous BAP1 protein migrates within a high molecular weight fraction (Figure 1A), we reasoned that all of the cellular BAP1 might be complexed with HCF-1. In fact, nearly all BAP1 protein could be immunodepleted from nuclear extracts using an excess of HCF-1 antibody (Figure 1C, top panel). As expected, virtually all HCF-1 protein was recovered in the bead fraction. As negative control, the nuclear protein PARP1 was shown to remain in the extracts. Next, we immunodepleted BAP1 using a specific antibody and observed that although nearly all BAP1 was recovered, only a minor fraction of HCF-1 was depleted (Figure 1C, bottom panel). This indicates that (i) HCF-1 is highly abundant relative to BAP1, and (ii) essentially all cellular BAP1 is complexed with HCF-1. Thus, HCF-1 could be a major scaffold protein for BAP1 and might play a critical role in coordinating the association of this DUB with other partners to form specific transcription regulatory complexes.

To provide insight into the potential role of BAP1 as a gene-specific transcription regulator, we focused in this study on characterizing the interaction of BAP1/HCF-1 with YY1. The anti-HA eluted material was fractionated using size exclusion chromatography, which revealed that BAP1 is assembled into ~1.3-1.8 MDa multi-protein complexes (Figure 1D). These complexes contain the transcription factor YY1 and HCF-1, and very likely additional components. Next, the anti-Flag purified BAP1 material was used as input for immunoprecipitation using anti-HCF-1 antibody, and both YY1 and BAP1 were co-immunoprecipitated (Figure 1E). These results strongly suggest the existence of at least one complex simultaneously containing BAP1, HCF-1 and YY1. Moreover, the interactions of endogenous YY1 with HCF-1 and BAP1 were also confirmed (Figure 1F).

The DUB activity is not required for BAP1 complexes formation.

It was recently shown that BAP1 can disassemble K48 ubiquitin chains on HCF-1 suggesting that this DUB might regulate the stability of HCF-1 and possibly other substrates

(31, 36). In addition, ubiquitin peptides were detected following mass spectrometry analysis of BAP1-associated proteins suggesting that some polypeptides were ubiquitinated (data not shown). Thus, we first tested whether loss of BAP1 function affects the stability of YY1. Knockdown of BAP1 using two shRNAs resulted in its substantial depletion, whereas no significant changes were observed in steady state levels of YY1 or HCF-1 (Figure 2A, left panel). These results were confirmed using a pool of 4 different siRNAs targeting BAP1 (Figure 2A, right panel). Next, we sought to determine whether DUB activity is required for assembly of BAP1 complexes. For this purpose, a stable cell line expressing BAP1 mutated in the catalytic cysteine (C91S) was generated. As BAP1 wildtype or C91S are not highly expressed, we did not observe a significant difference in cell proliferation between these two conditions (data not shown). Importantly, the purified complexes containing either BAP1, or its catalytically inactive form, are essentially indistinguishable (Figure 2B, left panel). These results were confirmed by immunoblotting for some of the associated components i.e., YY1 and HCF-1 (Figure 2B, right panel).

BAP1 directly interacts with YY1 in vitro and HCF-1 is required for complex formation in vivo.

To provide further insight into YY1 interaction with HCF-1/BAP1, we generated recombinant proteins including various deletion mutants and conducted in vitro GST pulldown assays. We found that BAP1 directly interacts with YY1. The C-terminus region of BAP1 (aa 599-729), encompassing the coiled coil domain, is necessary and sufficient for this interaction (Figure 3A, top right panel). We used smaller GST-BAP1 deletion fragments within the 599-729 aa region and identified the coiled coil domain as the interacting motif (Figure 3A, bottom right panel). Thus, BAP1 could simultaneously bind YY1 and HCF-1. Next, we demonstrated that in vitro translated full length 35S Met-HCF-1 interacts directly with YY1 and the central region of the latter (aa 142-260), which contains the GA/GK rich domain, is required for this interaction (Figure 3B, bottom left panel). Finally, we determined that the zinc fingers region of YY1 (aa 313-414) is necessary and sufficient for interaction with BAP1 (Figure 3B, bottom right panel). Taken together the above data indicate that

BAP1, HCF-1 and YY1 interact using non-overlapping domains, and thus can form a ternary complex involving binary binding for each protein.

To further characterize these interactions in vivo, a stable cell line expressing BAP1 lacking the HBM was generated and used for the double immunopurification of BAP1-associated proteins. Silver staining of the eluted proteins reveals that while some polypeptide bands appear similar between wildtype and mutant, several other bands were absent or substantially reduced in the elution of the mutant BAP1 (Figure 4A, left panel). As expected, HCF-1 was not detected in the elution of the mutant BAP1 (31, 36) (Figure 4A, right panel). Significantly, BAP1 interaction with YY1 was dramatically reduced between the wildtype and the mutant lacking HBM, suggesting that HCF-1 is required for optimal interaction between YY1 and BAP1 in vivo. Of note neither YY1 nor HCF-1 levels were changed upon expression of BAP1 lacking HBM. Next, we depleted HCF-1 using shRNA and immunopurified BAP1. As expected, substantially reduced levels of HCF-1 were observed following the BAP1 purification (Figure 4B), and the interaction of BAP1 with YY1 was again reduced. Altogether, these data indicate that BAP1, HCF-1, and YY1 form a ternary complex in vivo, strongly suggesting a functional link between these proteins. We then sought to determine whether the DUB activity of BAP1 is modulated by its interacting partners using similar amounts of BAP1, either recombinant or assembled into complexes, i.e., WT, ΔHBM and C91S (Figure 4C, left panel). Deubiquitination assays toward the substrate ubiquitin-AMC (Figure 4C, right panel) were conducted. As expected, no activity could be detected for the catalytic inactive BAP1 used as control. However recombinant BAP1 and BAP1 complexes (wildype or ΔHBM) exhibited similar DUB activities.

BAP1 is associated with transcriptionally active chromatin.

Most of the BAP1-interacting proteins are known to be involved in chromatin-associated processes suggesting a role for BAP1 in regulating gene expression. BAP1 was shown to associate with chromatin (31). In our study, we found that this protein is mostly excluded from heterochromatic regions as indicated by the nearly mutually exclusive staining between BAP1 and the highly packed chromatin, i.e., regions strongly stained with DAPI

(Figure 5A). Thus, we set out to determine whether BAP1 is associated with transcriptionally active regions by isolating the chromatin fraction and conducting short-term incubations with micrococcal nuclease (MNase) to release accessible nucleosomes. Nearly all BAP1 was recovered in the soluble fraction (Figure 5B). As expected, the basal transcription factor TFIID and RNA pol II were also recovered predominantly in the soluble fraction. HCF-1 and YY1 were found in this fraction as well, but to a lesser extent than BAP1 or RNA pol II. Histone H3 was only partially recovered indicating that a fraction less accessible to MNase, the heterochromatin, remained in the pellet. Consistent with this, histone H3 trimethylated at lysine 27, which is associated with transcriptional repression and compacted chromatin (49), was found predominantly in the pellet. These results suggest that BAP1 is associated with actively transcribed regions where it might form complexes with HCF-1, YY1 and other regulators to control gene expression. Although, BAP1/HCF-1 and YY1 were found on chromatin, the possibility remained that these proteins coexist in different complexes. To determine whether BAP1/HCF-1/YY1 indeed form a complex on chromatin, we immunopurified BAP1 from the chromatin fraction following digestion with MNase. We found that BAP1 immunoprecipitated both HCF-1 and YY1 from this fraction (Figure 5C, right panel). Of note, MNase digestion was nearly complete as indicated by the release of mononucleosomes (Figure 5C, left panel).

BAP1 is a transcriptional co-activator and regulates the expression of genes involved in numerous cellular processes.

To elucidate the role of BAP1 in transcription regulation, a well-established transcription reporter assay was used (24). This consists of targeting a protein of interest, fused in frame with the GAL4 DNA binding domain, to the luciferase reporter driven by a promoter containing GAL4 binding sites and the thymidine kinase promoter (Figure 6A). A fusion between the DNA binding domain of Gal4 (1-147aa) and BAP1 was generated and expressed in HeLa cells by transient transfection (Figure 6B, bottom panel). Gal4-BAP1 activated transcription of the reporter gene by 3 to 4 fold (Figure 6B, top panel). This effect was not observed following expression of BAP1 alone, the Gal4 domain alone, or Gal4-BAP1

along with a thymidine kinase reporter lacking Gal4 binding sites. Altogether, these results suggest that transcription activation by Gal4-BAP1 requires DNA binding and is not an indirect effect. A Gal4-BAP1 mutant lacking the HBM, expressed at the same levels as the wildtype (Figure 6C, right panel), also activated transcription although less efficiently than the wildtype form (Figure 6C, left panel). Importantly, a Gal4-BAP1 catalytic inactive mutant (C91S) was unable to activate transcription suggesting that BAP1 regulates gene expression in a DUB activity-dependent manner (Figure 6D, top panel). We note that although BAP1 C91S was expressed at lower levels than the wildtype for the same quantity of transfected DNA (Figure 6D, bottom panel), no reporter activation was observed with C91S over a wide range of plasmid concentrations.

In order to identify potential BAP1 target genes, global mRNA expression profiling using microarrays was conducted following BAP1 depletion in U2OS cells using two shRNA constructs and a non-targeting shRNA as a control. The gene expression data for both shRNAs are deposited in the Gene Expression Omnibus (GEO) NCBI database. Using the cut-off of two-fold difference relative to the control, we found that BAP1 depletion resulted in significantly elevated or decreased expression of about 249 genes (137 up-regulated and 112 down-regulated). Among these genes, several are associated with cell cycle progression, DNA damage signaling/repair, as well as survival and metabolism, suggesting that BAP1 participates in a diverse cellular processes (Figure 7A and Table 1). Interestingly, several E2F target genes including skp2, p107, cdc2, cdc25a were downregulated. The effect of BAP1 knockdown on the expression of some of these genes and others was further validated by RT-PCR (Figure 7B).

BAP1 is recruited by YY1 to regulate cox7c gene expression.

It is not known whether BAP1 assembles complexes that can be recruited to specific promoters to activate transcription. In light of our data, we reasoned that BAP1 might be recruited by YY1 to regulate gene expression. To investigate this possibility, we selected *cox7c*, one of the most downregulated genes based on our microarrays data. *cox7c* encodes a subunit of the holoenzyme that mediates the terminal step of the mitochondrial electron

transport chain. The bovine *cox7c* promoter has been shown to contain two YY1 binding sites, mutations in which abrogate most of the promoter activity (50). These sites are highly conserved in mouse and human (Figure 8A). First, we confirmed that COX7C protein levels were also downregulated following BAP1 depletion in U2OS and HeLa cells (Figures 8B). Moreover, similar results were obtained following knockdown of HCF-1 (Figures 8B). Interestingly, depletion of YY1 induces a significant increase of COX7C expression in both HeLa and U2OS cells (Figure 8B). To determine whether BAP1 regulates *cox7c* expression in a DUB activity-dependent manner, we transducded U2OS cells with retroviral particles to overexpress either BAP1 or C91S mutant (Figure 8C). BAP1 C91S significantly inhibited the expression of COX7C protein, an effect not observed with the wildtype form. Of note, BAP1 C91S is a bona fide dominant negative mutant since it competes with wildtype BAP1 for assembly of the same multi-protein complexes (Figure 2B). To further characterize the role of the BAP1/HCF-1/YY1 complex in regulating gene expression, we conducted ChIP assays and found that these proteins are all enriched on the promoter region of *cox7c*, but not on the α-globin promoter (Figure 8D, left panel). Moreover, YY1 depletion by shRNA significantly decreased the enrichment of BAP1 and HCF-1 on the *cox7c* promoter indicating an essential role of YY1 in targeting BAP1/HCF-1 to specific gene regulatory regions (Figure 8D, left panel). Of note, shRNA-mediated depletion of YY1 did not affect either HCF-1 or BAP1 levels (Figure 8D, right panel).

DISCUSSION

In this study, we identified novel BAP1-interacting proteins and showed that nearly all cellular BAP1 forms high molecular weight multi-protein complexes with several transcription factors and cofactors. The associated partners are likely to play critical roles in targeting BAP1 to potential substrates, thereby regulating its function. Based on the relative abundance of BAP1-associated proteins purified from HeLa or U2OS cells, and on data from other studies (31, 36, 54), it appears that HCF-1, ASXL1 and/or ASXL2, OGT, FOXK1 and/or FOXK2 might form a BAP1 core complex. This minimal complex may selectively associate with additional regulators or transcription factors to form specific functional complexes in a cell type- and/or promoter-dependent manner. Indeed. sub-stoichiometric levels of several transcription factors co-purified with BAP1. These factors are involved in a wide range of cellular processes, suggesting that BAP1 might exert a much broader role in regulating cell function than previously appreciated. Consistent with this notion, BAP1 depletion by RNAi induced profound changes in the expression of genes mediating and/or controlling numerous cellular pathways. Further studies will be needed to investigate how BAP1, via selective interactions with specific transcription factors and cofactors, regulates specific biological responses.

We provided strong evidence that BAP1 is a transcriptional co-activator: i) BAP1 associates with transcriptionally active chromatin. ii) BAP1 acts as an activator, in a DUB activity-dependent manner when targeted to a promoter using the Gal4 system. iii) Genome wide expression analysis reveals a considerable number of genes downregulated following BAP1 depletion. iv) BAP1 directly occupies the *cox7c* promoter, and depletion of BAP1 results in downregulation of this gene. It is also possible that BAP1 possesses dual co-activator/co-repressor functions, depending upon its association with specific transcription factors and cofactors on the regulatory elements of target genes. In agreement with this latter hypothesis, some BAP1-interacting proteins including HCF-1, YY1, OGT and ASXL are known to interact with both co-activators and co-repressors (5, 9, 12, 43, 53, 68, 70, 71). In addition, a significant number of genes were up-regulated following depletion of BAP1. This suggests that BAP1 might exert a repressive effect on their promoters although these genes

could constitute indirect targets, i.e., their up-regulation results from secondary changes induced by BAP1 depletion.

Using YY1 as a model for sequence-specific transcription factors that interact with BAP1/HCF-1, we demonstrated that these three proteins form a ternary complex in vivo which can associate with chromatin. Moreover, we found that BAP1 and HCF-1 are recruited by YY1 to co-activate *cox7c*, a gene previously reported to depend on YY1 binding sites for transcriptional activation (50). While depletion of BAP1 or HCF-1 reduces expression of *cox7c*, in contrast depletion of YY1 induces an increase in expression of this gene. These results suggest that YY1 possesses a dual function of both repressor and activator of *cox7c*, depending on its association with the HCF-1/BAP1 co-activator complex. A similar repression/activation mechanism by YY1 has been previously shown for the murine beta interferon promoter (37, 63). Consistent with this model, YY1 interacts with HCF-1 through the central region containing a GA/GK rich domain, previously shown to be involved in interactions with HDACs (70). This suggests that the association of YY1 with HCF-1/BAP1 is mutually exclusive with respect to its interaction with HDAC co-repressive complexes. With respect to cox7c expression, it is well-known that nuclear-encoded mitochondrial genes including components of the cytochrome C oxidase complex are not constitutively expressed, but rather subject to tight regulation by several transcription factors and cofactors depending on the state of cell growth, energy balance and other tissues-specific needs (18). Therefore, such genes are expected to oscillate between activation and repression states.

It is not clear at the present time whether BAP1 might regulate all YY1 target genes. It is possible that it might regulate only a subset of these targets, perhaps those on which YY1 acts as an activator only or on which it might exert dual activator/repressor function. Other transcription factors might dictate the specificity via interaction with YY1. Indeed YY1 is well known to interact with numerous transcription factors such as SP1, C-myc, and E2Fs (25, 48, 74). HCF-1, via additional interactions, might also contribute to the selectivity of recruitment of BAP1 to specific YY1-target genes. In this respect it is not surprising that Gal4-BAP1 lacking HBM is only slightly impaired in transcription activation, suggesting that

the interaction between HCF-1 and BAP1 might be mostly involved in recruitment of the latter to specific promoters.

Precisely how the assembled BAP1/HCF-1/YY1 complex acts to induce activation of *cox7c* or other target genes remains to be established. Nonetheless, the data suggest that the molecular mechanism involves ubiquitin signaling and deubiquitination of specific substrates on target promoters. BAP1 might be continuously needed to prevent degradation of HCF-1 (31, 36). Although the stability of the total cellular pool of HCF-1 is not significantly affected by BAP1 depletion, it is nonetheless possible that BAP1 stabilizes HCF-1 only on specific promoters following recruitment by YY1 or other transcription factors. Consistent with this, a BAP1 catalytic inactive mutant exerts a dominant negative effect on *cox7c* expression. It is also plausible that HCF-1 association with BAP1 and YY1 targets the DUB activity to deubiquitinate histones, specific transcription factors, or components of the general transcription machinery. Consistent with this, the drosophila BAP1 Calyposo deubiquitinates H2A, a histone mark associated with gene repression (47). However, Calyposo does not possess HBM and thus the mammalian BAP1 appears to selectively associate with HCF-1 and numerous other proteins not found with Calypso. In addition, in contrast to Calypso whose activity on ubiquitin AMC is very low when not associated with ASX, the recombinant mammalian BAP1 appears to have the same activity as complexed BAP1. We note that although BAP1 partners do not affect its DUB activity on ubiquitin-AMC, this does not exclude the possibility of their effect in the context of a physiological substrate in vivo.

Our results also shed light on the biological function of BAP1. This DUB was previously shown to be required for proper cell cycle progression, particularly the G1/S transition (31, 41), Moreover we observed similar effects in U2OS (data not shown), the cell type used here for global gene expression analysis. We also provided molecular insight linking BAP1 to the control of cell cycle genes including subsets of E2F targets. In addition HCF-1 is known to be required for normal G1/S transition, and was recently shown to play a major role in regulating the expression of E2F target genes by promoting histone H3 K4 trimethylation (21, 58). Thus, BAP1 might play a pivotal role in regulating the G1/S transition

under normal and possibly stress conditions. Supporting this view, BAP1 is phosphorylated on an ATM/ATR consensus motif in response to DNA damage (33, 55), suggesting that these critical DNA damage-responsive checkpoint kinases might regulate BAP1 DUB activity and thus its function in controlling expression of cell cycle genes.

BAP1 might also participate in transcriptional regulatory programs that coordinate cell growth with cell cycle. For instance, in addition to *cox7c*, the expression of several mitochondrial and general metabolism genes are shown here to be deregulated upon BAP1 knockdown. Interestingly, recent bioinformatics and genome-wide promoter occupancy studies indicated that YY1 binding sites are enriched in the promoter regions of nuclear genes that encode mitochondrial proteins (59, 69). Moreover, NRF1, a major regulator of mitochondrial respiration, co-purifies with BAP1 (Figure 1B); and both YY1 and NRF1 binding sites are frequently found in close proximity in a large number of promoters of genes encoding mitochondrial proteins (59, 69). Furthermore HCF-1 has been found to interact with, and increase the transcriptional activity of, peroxisome proliferator-activated receptor gamma co-activator-1 (PGC-1), a major transcriptional regulator of mitochondrial biogenesis (27, 61). Thus BAP1 might play an important role in dynamically controlling transcriptional responses that coordinate mitochondrial function. Such responses in turn could constitute targets of stress signaling pathways (e.g., induced by DNA damage) that orchestrate adaptative metabolic responses.

In summary, our work indicates that BAP1 associates with several transcription factors and co-factors and is a gene-specific transcription regulator. As such, our findings establish a framework for further studies to (i) delineate the exact role of BAP1 in regulating the expression of genes involved in cell cycle progression, and (ii) define how deregulation of BAP1 function contributes to tumorigenesis.

Acknowledgements

This work was supported by grants to E.B.A. from the Terry Fox Foundation (grant#018144) and to Y.S from NIH (grant#GM053874). E.B.A. is a scholar of Le Fonds de la Recherche en Santé du Québec (FRSQ). H.Y. is a scholar of the Cole Foundation. We are grateful to Winship Herr for his generous gift of HCF-1 construct and antibodies.

REFERENCES

1. Affar, E. B., F. Gay, Y. Shi, H. Liu, M. Huarte, S. Wu, C. Tucker, E. Li, and Y. Shi. 2006. Essential dosage-dependent functions of the transcription factor Yin Yang 1 in late embryonic development and cell cycle progression. Mol. Cell Biol. 26:3565-3581.

2. Bottardi, S., J. Ross, V. Bourgoin, N. Fotouhi-Ardakani, B. Affar el, M. Trudel, and E. Milot. 2009. Ikaros and GATA-1 combinatorial effect is required for silencing of human gamma-globin genes. Mol Cell Biol 29:1526-37.

3. Calvano, S. E., W. Xiao, D. R. Richards, R. M. Felciano, H. V. Baker, R. J. Cho, R. O. Chen, B. H. Brownstein, J. P. Cobb, S. K. Tschoeke, C. Miller-Graziano, L. L. Moldawer, M. N. Mindrinos, R. W. Davis, R. G. Tompkins, and S. F. Lowry. 2005. A network-based analysis of systemic inflammation in humans. Nature 437:1032-7.

4. Chen, Z. J., and L. J. Sun. 2009. Nonproteolytic functions of ubiquitin in cell signaling. Mol Cell 33:275-86.

5. Cho, Y. S., E. J. Kim, U. H. Park, H. S. Sin, and S. J. Um. 2006. Additional sex comb-like 1 (ASXL1), in cooperation with SRC-1, acts as a ligand-dependent coactivator for retinoic acid receptor. J Biol Chem 281:17588-98.

6. Dejosez, M., J. S. Krumenacker, L. J. Zitur, M. Passeri, L. F. Chu, Z. Songyang, J. A. Thomson, and T. P. Zwaka. 2008. Ronin is essential for embryogenesis and the pluripotency of mouse embryonic stem cells. Cell 133:1162-74.

7. Delehouzee, S., T. Yoshikawa, C. Sawa, J. Sawada, T. Ito, M. Omori, T. Wada, Y. Yamaguchi, Y. Kabe, and H. Handa. 2005. GABP, HCF-1 and YY1 are involved in Rb gene expression during myogenesis. Genes Cells 10:717-31.

8. Dou, Y., T. A. Milne, A. J. Tackett, E. R. Smith, A. Fukuda, J. Wysocka, C. D. Allis, B. T. Chait, J. L. Hess, and R. G. Roeder. 2005. Physical association and coordinate function of the H3 K4 methyltransferase MLL1 and the H4 K16 acetyltransferase MOF. Cell 121:873-85.

9. Fisher, C. L., I. Lee, S. Bloyer, S. Bozza, J. Chevalier, A. Dahl, C. Bodner, C. D. Helgason, J. L. Hess, R. K. Humphries, and H. W. Brock. 2010. Additional sex combs-like 1 belongs to the enhancer of trithorax and polycomb group and genetically interacts with Cbx2 in mice. Dev Biol 337:9-15.

10. Freiman, R. N., and W. Herr. 1997. Viral mimicry: common mode of association with HCF by VP16 and the cellular protein LZIP. Genes Dev 11:3122-7.

11. Fujiki, R., T. Chikanishi, W. Hashiba, H. Ito, I. Takada, R. G. Roeder, H. Kitagawa, and S. Kato. 2009. GlcNAcylation of a histone methyltransferase in retinoic-acid-induced granulopoiesis. Nature 459:455-9.

12. Gambetta, M. C., K. Oktaba, and J. Muller. 2009. Essential role of the glycosyltransferase sxc/Ogt in polycomb repression. Science 325:93-6.

13. Gordon, S., G. Akopyan, H. Garban, and B. Bonavida. 2006. Transcription factor YY1: structure, function, and therapeutic implications in cancer biology. Oncogene 25:1125-42.

14. Goto, H., S. Motomura, A. C. Wilson, R. N. Freiman, Y. Nakabeppu, K. Fukushima, M. Fujishima, W. Herr, and T. Nishimoto. 1997. A single-point mutation in HCF causes temperature-sensitive cell-cycle arrest and disrupts VP16 function. Genes Dev 11:726-37.

15. Groisman, R., J. Polanowska, I. Kuraoka, J. Sawada, M. Saijo, R. Drapkin, A. F. Kisselev, K. Tanaka, and Y. Nakatani. 2003. The ubiquitin ligase activity in the DDB2 and CSA complexes is differentially regulated by the COP9 signalosome in response to DNA damage. Cell 113:357-67.

16. Gunther, M., M. Laithier, and O. Brison. 2000. A set of proteins interacting with transcription factor Sp1 identified in a two-hybrid screening. Mol Cell Biochem 210:131-42.

17. Harper, J. V. 2005. Synchronization of cell populations in G1/S and G2/M phases of the cell cycle. Methods Mol Biol 296:157-66.

18. Hock, M. B., and A. Kralli. 2009. Transcriptional control of mitochondrial biogenesis and function. Annu Rev Physiol 71:177-203.

19. Jensen, D. E., M. Proctor, S. T. Marquis, H. P. Gardner, S. I. Ha, L. A. Chodosh, A. M. Ishov, N. Tommerup, H. Vissing, Y. Sekido, J. Minna, A. Borodovsky, D. C. Schultz, K. D. Wilkinson, G. G. Maul, N. Barlev, S. L. Berger, G. C. Prendergast, and F. J. Rauscher, 3rd. 1998. BAP1: a novel ubiquitin hydrolase which binds to the BRCA1 RING finger and enhances BRCA1-mediated cell growth suppression. Oncogene 16:1097-1112.

20. Johnston, S. C., C. N. Larsen, W. J. Cook, K. D. Wilkinson, and C. P. Hill. 1997. Crystal structure of a deubiquitinating enzyme (human UCH-L3) at 1.8 A resolution. Embo J 16:3787-96.

21. Julien, E., and W. Herr. 2003. Proteolytic processing is necessary to separate and ensure proper cell growth and cytokinesis functions of HCF-1. Embo J 22:2360-9.

22. Knez, J., D. Piluso, P. Bilan, and J. P. Capone. 2006. Host cell factor-1 and E2F4 interact via multiple determinants in each protein. Mol Cell Biochem 288:79-90.

23. Kristie, T. M., Y. Liang, and J. L. Vogel. 2009. Control of alpha-herpesvirus IE gene expression by HCF-1 coupled chromatin modification activities. Biochim Biophys Acta 1799:257-65.

24. Lee, J. S., K. M. Galvin, R. H. See, R. Eckner, D. Livingston, E. Moran, and Y. Shi. 1995. Relief of YY1 transcriptional repression by adenovirus E1A is mediated by E1A-associated protein p300. Genes Dev 9:1188-98.

25. Lee, J. S., K. M. Galvin, and Y. Shi. 1993. Evidence for physical interaction between the zinc-finger transcription factors YY1 and Sp1. Proc Natl Acad Sci U S A 90:6145-9.

26. Liang, Y., J. L. Vogel, A. Narayanan, H. Peng, and T. M. Kristie. 2009. Inhibition of the histone demethylase LSD1 blocks alpha-herpesvirus lytic replication and reactivation from latency. Nat Med 15:1312-7.

27. Lin, J., P. Puigserver, J. Donovan, P. Tarr, and B. M. Spiegelman. 2002. Peroxisome proliferator-activated receptor gamma coactivator 1beta (PGC-1beta), a novel PGC-1-related transcription coactivator associated with host cell factor. J Biol Chem 277:1645-8.

28. Lu, R., P. Yang, S. Padmakumar, and V. Misra. 1998. The herpesvirus transactivator VP16 mimics a human basic domain leucine zipper protein, luman, in its interaction with HCF. J Virol 72:6291-7.

29. Luciano, R. L., and A. C. Wilson. 2003. HCF-1 functions as a coactivator for the zinc finger protein Krox20. J Biol Chem 278:51116-24.

30. Luciano, R. L., and A. C. Wilson. 2000. N-terminal transcriptional activation domain of LZIP comprises two LxxLL motifs and the host cell factor-1 binding motif. Proc Natl Acad Sci U S A 97:10757-62.

31. Machida, Y. J., Y. Machida, A. A. Vashisht, J. A. Wohlschlegel, and A. Dutta. 2009. The deubiquitinating enzyme BAP1 regulates cell growth via interaction with HCF-1. J Biol Chem.

32. Mason, D. E., J. Ek, E. C. Peters, and J. L. Harris. 2004. Substrate profiling of deubiquitin hydrolases with a positional scanning library and mass spectrometry. Biochemistry 43:6535-44.

33. Matsuoka, S., B. A. Ballif, A. Smogorzewska, E. R. McDonald, 3rd, K. E. Hurov, J. Luo, C. E. Bakalarski, Z. Zhao, N. Solimini, Y. Lerenthal, Y. Shiloh, S. P. Gygi, and S. J. Elledge. 2007. ATM and ATR substrate analysis reveals extensive protein networks responsive to DNA damage. Science 316:1160-6.

34. Mazars, R., A. Gonzalez-de-Peredo, C. Cayrol, A. C. Lavigne, J. L. Vogel, N. Ortega, C. Lacroix, V. Gautier, G. Huet, A. Ray, B. Monsarrat, T. M. Kristie, and J. P. Girard. 2010. The thap-zinc finger protein thap1 associates with coactivator HCF-1 and O-GLcNAc transferase: A link between DYT6 and DYT3 dystonias. J Biol Chem.

35. Misaghi, S., P. J. Galardy, W. J. Meester, H. Ovaa, H. L. Ploegh, and R. Gaudet. 2005. Structure of the ubiquitin hydrolase UCH-L3 complexed with a suicide substrate. J Biol Chem 280:1512-20.

36. Misaghi, S., S. Ottosen, A. Izrael-Tomasevic, D. Arnott, M. Lamkanfi, J. Lee, J. Liu, K. O'Rourke, V. M. Dixit, and A. C. Wilson. 2009. Association of C-terminal ubiquitin hydrolase BRCA1-associated protein 1 with cell cycle regulator host cell factor 1. Mol Cell Biol 29:2181-92.

37. Mokrani, H., O. Sharaf el Dein, Z. Mansuroglu, and E. Bonnefoy. 2006. Binding of YY1 to the proximal region of the murine beta interferon promoter is essential to allow CBP recruitment and K8H4/K14H3 acetylation on the promoter region after virus infection. Mol Cell Biol 26:8551-61.

38. Nakatani, Y., and V. Ogryzko. 2003. Immunoaffinity purification of mammalian protein complexes. Methods Enzymol 370:430-44.

39. Narayanan, A., W. T. Ruyechan, and T. M. Kristie. 2007. The coactivator host cell factor-1 mediates Set1 and MLL1 H3K4 trimethylation at herpesvirus immediate early promoters for initiation of infection. Proc Natl Acad Sci U S A 104:10835-40.

40. Nijman, S. M., M. P. Luna-Vargas, A. Velds, T. R. Brummelkamp, A. M. Dirac, T. K. Sixma, and R. Bernards. 2005. A genomic and functional inventory of deubiquitinating enzymes. Cell 123:773-786.

41. Nishikawa, H., W. Wu, A. Koike, R. Kojima, H. Gomi, M. Fukuda, and T. Ohta. 2009. BRCA1-associated protein 1 interferes with BRCA1/BARD1 RING heterodimer activity. Cancer Res 69:111-9.

42. Nowak, D. E., B. Tian, and A. R. Brasier. 2005. Two-step cross-linking method for identification of NF-kappaB gene network by chromatin immunoprecipitation. Biotechniques 39:715-25.

43. Ozcan, S., S. S. Andrali, and J. E. Cantrell. 2010. Modulation of transcription factor function by O-GlcNAc modification. Biochim Biophys Acta.

44. Pickart, C. M., and M. J. Eddins. 2004. Ubiquitin: structures, functions, mechanisms. Biochim. Biophys. Acta 1695:55-72.

45. Pickart, C. M., and D. Fushman. 2004. Polyubiquitin chains: polymeric protein signals. Curr Opin Chem Biol 8:610-6.

46. Reyes-Turcu, F. E., K. H. Ventii, and K. D. Wilkinson. 2009. Regulation and cellular roles of ubiquitin-specific deubiquitinating enzymes. Annu Rev Biochem 78:363-97.

47. Scheuermann, J. C., A. G. de Ayala Alonso, K. Oktaba, N. Ly-Hartig, R. K. McGinty, S. Fraterman, M. Wilm, T. W. Muir, and J. Muller. 2010. Histone H2A deubiquitinase activity of the Polycomb repressive complex PR-DUB. Nature 465:243-7.

48. Schlisio, S., T. Halperin, M. Vidal, and J. R. Nevins. 2002. Interaction of YY1 with E2Fs, mediated by RYBP, provides a mechanism for specificity of E2F function. Embo J 21:5775-86.

49. Schuettengruber, B., D. Chourrout, M. Vervoort, B. Leblanc, and G. Cavalli. 2007. Genome regulation by polycomb and trithorax proteins. Cell 128:735-45.

50. Seelan, R. S., and L. I. Grossman. 1997. Structural organization and promoter analysis of the bovine cytochrome c oxidase subunit VIIc gene. A functional role for YY1. J Biol Chem 272:10175-81.

51. Shi, Y., J. S. Lee, and K. M. Galvin. 1997. Everything you have ever wanted to know about Yin Yang 1. Biochim Biophys Acta 1332:F49-66.

52. Shi, Y., J. Sawada, G. Sui, B. Affar el, J. R. Whetstine, F. Lan, H. Ogawa, M. P. Luke, and Y. Nakatani. 2003. Coordinated histone modifications mediated by a CtBP co-repressor complex. Nature 422:735-8.

53. Sinclair, D. A., M. Syrzycka, M. S. Macauley, T. Rastgardani, I. Komljenovic, D. J. Vocadlo, H. W. Brock, and B. M. Honda. 2009. Drosophila O-GlcNAc transferase (OGT) is encoded by the Polycomb group (PcG) gene, super sex combs (sxc). Proc Natl Acad Sci U S A 106:13427-32.

54. Sowa, M. E., E. J. Bennett, S. P. Gygi, and J. W. Harper. 2009. Defining the human deubiquitinating enzyme interaction landscape. Cell 138:389-403.

55. Stokes, M. P., J. Rush, J. Macneill, J. M. Ren, K. Sprott, J. Nardone, V. Yang, S. A. Beausoleil, S. P. Gygi, M. Livingstone, H. Zhang, R. D. Polakiewicz, and M. J. Comb. 2007. Profiling of UV-induced ATM/ATR signaling pathways. Proc Natl Acad Sci U S A 104:19855-60.

56. Sui, G., B. Affar el, Y. Shi, C. Brignone, N. R. Wall, P. Yin, M. Donohoe, M. P. Luke, D. Calvo, S. R. Grossman, and Y. Shi. 2004. Yin Yang 1 is a negative regulator of p53. Cell 117:859-872.

57. Sui, G., C. Soohoo, B. Affar el, F. Gay, Y. Shi, W. C. Forrester, and Y. Shi. 2002. A DNA vector-based RNAi technology to suppress gene expression in mammalian cells. Proc. Natl. Acad. Sci. U. S. A. 99:5515-5520.

58. Tyagi, S., A. L. Chabes, J. Wysocka, and W. Herr. 2007. E2F activation of S phase promoters via association with HCF-1 and the MLL family of histone H3K4 methyltransferases. Mol Cell 27:107-19.

59. van Waveren, C., and C. T. Moraes. 2008. Transcriptional co-expression and co-regulation of genes coding for components of the oxidative phosphorylation system. BMC Genomics 9:18.

60. Ventii, K. H., N. S. Devi, K. L. Friedrich, T. A. Chernova, M. Tighiouart, E. G. Van Meir, and K. D. Wilkinson. 2008. BRCA1-associated protein-1 is a tumor suppressor that requires deubiquitinating activity and nuclear localization. Cancer Res 68:6953-62.

61. Vercauteren, K., N. Gleyzer, and R. C. Scarpulla. 2008. PGC-1-related coactivator complexes with HCF-1 and NRF-2beta in mediating NRF-2(GABP)-dependent respiratory gene expression. J Biol Chem 283:12102-11.

62. Vogel, J. L., and T. M. Kristie. 2000. The novel coactivator C1 (HCF) coordinates multiprotein enhancer formation and mediates transcription activation by GABP. Embo J 19:683-90.

63. Weill, L., E. Shestakova, and E. Bonnefoy. 2003. Transcription factor YY1 binds to the murine beta interferon promoter and regulates its transcriptional capacity with a dual activator/repressor role. J Virol 77:2903-14.

64. Welchman, R. L., C. Gordon, and R. J. Mayer. 2005. Ubiquitin and ubiquitin-like proteins as multifunctional signals. Nat. Rev. Mol. Cell Biol. 6:599-609.

65. Wilson, A. C., K. LaMarco, M. G. Peterson, and W. Herr. 1993. The VP16 accessory protein HCF is a family of polypeptides processed from a large precursor protein. Cell 74:115-25.

66. Wilson, A. C., J. E. Parrish, H. F. Massa, D. L. Nelson, B. J. Trask, and W. Herr. 1995. The gene encoding the VP16-accessory protein HCF (HCFC1) resides in human Xq28 and is highly expressed in fetal tissues and the adult kidney. Genomics 25:462-8.

67. Wood, L. D., D. W. Parsons, S. Jones, J. Lin, T. Sjoblom, R. J. Leary, D. Shen, S. M. Boca, T. Barber, J. Ptak, N. Silliman, S. Szabo, Z. Dezso, V. Ustyanksky, T. Nikolskaya, Y. Nikolsky, R. Karchin, P. A. Wilson, J. S. Kaminker, Z. Zhang, R. Croshaw, J. Willis, D. Dawson, M. Shipitsin, J. K. Willson, S. Sukumar, K. Polyak, B. H. Park, C. L. Pethiyagoda,

P. V. Pant, D. G. Ballinger, A. B. Sparks, J. Hartigan, D. R. Smith, E. Suh, N. Papadopoulos, P. Buckhaults, S. D. Markowitz, G. Parmigiani, K. W. Kinzler, V. E. Velculescu, and B. Vogelstein. 2007. The genomic landscapes of human breast and colorectal cancers. Science 318:1108-13.

68. Wysocka, J., M. P. Myers, C. D. Laherty, R. N. Eisenman, and W. Herr. 2003. Human Sin3 deacetylase and trithorax-related Set1/Ash2 histone H3-K4 methyltransferase are tethered together selectively by the cell-proliferation factor HCF-1. Genes Dev 17:896-911.

69. Xi, H., Y. Yu, Y. Fu, J. Foley, A. Halees, and Z. Weng. 2007. Analysis of overrepresented motifs in human core promoters reveals dual regulatory roles of YY1. Genome Res 17:798-806.

70. Yang, W. M., C. Inouye, Y. Zeng, D. Bearss, and E. Seto. 1996. Transcriptional repression by YY1 is mediated by interaction with a mammalian homolog of the yeast global regulator RPD3. Proc Natl Acad Sci U S A 93:12845-50.

71. Yang, X., F. Zhang, and J. E. Kudlow. 2002. Recruitment of O-GlcNAc transferase to promoters by corepressor mSin3A: coupling protein O-GlcNAcylation to transcriptional repression. Cell 110:69-80.

72. Yokoyama, A., Z. Wang, J. Wysocka, M. Sanyal, D. J. Aufiero, I. Kitabayashi, W. Herr, and M. L. Cleary. 2004. Leukemia proto-oncoprotein MLL forms a SET1-like histone methyltransferase complex with menin to regulate Hox gene expression. Mol Cell Biol 24:5639-49.

73. Zeng, P. Y., C. R. Vakoc, Z. C. Chen, G. A. Blobel, and S. L. Berger. 2006. In vivo dual cross-linking for identification of indirect DNA-associated proteins by chromatin immunoprecipitation. Biotechniques 41:694, 696, 698.

74. Zhao, J. H., T. Inoue, W. Shoji, Y. Nemoto, and M. Obinata. 1998. Direct association of YY-1 with c-Myc and the E-box binding protein in regulation of glycophorin gene expression. Oncogene 17:1009-17.

FIGURE LEGENDS

Figure 1. BAP1 assembles high molecular weight multi-protein complexes containing YY1 transcription factor.

(A) Top panel, extraction of cellular BAP1 protein. HeLa nuclei isolated with hypotonic buffer were extracted with 300 mM of KCl for 30 min to obtain the nuclear extract and the chromatin/nuclear matrix pellet fractions. The nuclear pellet was washed once. All fractions were resuspended in the same volume and used for to the immunodetection of BAP1. TFIID was detected as a marker for the transcriptional machinery and Histone H3 as a marker for chromatin.WCE, whole cell extract. Bottom panel, endogenous BAP1 migrates in high molecular weight fractions. HeLa nuclear extract was fractionated using glycerol density gradient ultracentrifugation. Fractions collected from the top to the bottom were subsequently used for immunodetection of BAP1. The gradient was calibrated with the previously purified CtBP complex whose estimated molecular weight is ~1.3-1.5 MDa. (B) Purification of BAP1-associated proteins. A HeLa cell line stably expressing Flag-HA-BAP1 was used for sequential double immunopurification using anti-Flag antibody and anti-HA antibody columns. The Flag- or HA-eluted proteins were separated by SDS-PAGE and detected by silver staining. The mock purification was conducted using a stable cell line generated with the empty vector. Several regions were cut from the gel and the polypeptides were identified by mass spectrometry. (C) Immunodepletion of HCF-1 (top panel) or BAP1 (bottom panel) from nuclear extracts using an excess of anti-HCF-1 or anti-BAP1 polyclonal antibodies. A non-relevant anti-HA polyclonal antibody was used as a control IgG. BAP1 and HCF-1 were immunodetected in the beads and the flow through fractions. The nuclear protein PARP1 was detected as a negative control. (D) BAP1 forms high molecular weight multi-protein complexes. Fractionation of the BAP1 purified material using a Superose6 HR gel filtration column. The eluted complexes were detected with silver stain. BAP1, HCF-1 and YY1 were detected by immunoblotting. (E) Reciprocal immunoprecipitation. The Flag purified BAP1 material was used as input for additional immunoprecipitations using a polyclonal antibody against HCF-1 or a non-relevant anti-GFP antibody (IgG control). The immunocomplexes were extensively washed and YY1, HCF-1 and BAP1 were detected by immunoblotting. (F) Interaction of endogenous HCF-1, BAP1 and YY1. HeLa nuclear extract was used for

immunoprecipitation using a polyclonal antibody against YY1 (top panel), a polyclonal antibody against HCF-1 (bottom panel) or a non-relevant anti-GFP antibody (IgG control). The immunocomplexes were washed and YY1, HCF-1 and BAP1 were detected by immunoblotting.

Figure 2. The DUB activity is not required for the assembly of BAP1 complexes or YY1 stability.

(A) Depletion of BAP1 does not affect the steady-state levels of YY1 and HCF-1. Left panel, HeLa cells were transfected with either non-targeting control or BAP1 shRNA plasmids along with the pBABE puromycin resistance-encoding vector, and transfected cells were selected by adding puromycin for 2 days prior to harvesting for western blotting using the indicated antibodies. Right panel, the siRNA smart pools for human BAP1, or a non-target control, were transfected into U2OS cells and expressed for 3 days prior to harvesting for western blotting using the indicated antibodies. (B) BAP1 catalytic activity is not required for BAP1 complexes formation. A HeLa cell line stably expressing Flag-HA-BAP1 catalytic inactive mutant (C91S) was used along with the wildtype control cells for double immuno-purification of BAP1 complexes. Silver staining was conducted on fractions from two elutions (E1 and E2) with HA peptide (left panel). Immunoblotting was conducted for YY1, HCF-1 and BAP1 (right panel).

Figure 3. HCF-1 is required for ternary complex formation with YY1 and BAP1.

(A) Interaction in vitro between YY1 and BAP1 mutants. Various GST deletion fragments of BAP1 bound to GSH beads were incubated with His-YY1 for 8 hours and, following extensive washes, the bead-associated complexes were analyzed by coomassie blue staining for GST-BAP1 fragments and western blotting for YY1. HBM, HCF-1 Binding Motif; CC, coiled-coil domain. (B) Interaction in vitro between HCF-1 or BAP1 and various YY1 mutants. Bottom left panel, interaction in vitro between YY1 and HCF-1. Various GST deletion fragments of YY1 bound to GSH beads were incubated with in vitro translated 35S labeled-HCF-1 for 8 hours and following purification, HCF-1 was analyzed by autoradiography. Bottom right panel, identification of the YY1 domain required for

interaction with BAP1. Various GST deletion fragments of YY1 were incubated with His-BAP1 for 8 hours and the bead-associated complexes were analyzed by coomassie blue staining and western blotting for BAP1.

Figure 4. HCF-1 is required for ternary complex formation with BAP1 and YY1 in vivo.
(A) HCF-1 is required for proper assembly of BAP1 complexes. A HeLa cell line stably expressing Flag-HA-BAP1 lacking the HBM was used for immunopurification using anti-Flag and anti-HA antibodies. The eluted material was used for SDS-PAGE and silver stain (left panel). Immunoblotting detection of BAP1, HCF-1 and YY1 (right panel). The BAP1 wildtype (WT) was used as a control. (B) Depletion of HCF-1 destabilizes BAP1 interaction with YY1. A HeLa cell line stably expressing Flag-HA-BAP1 was transfected with either a non-targeting control or HCF-1 shRNA plasmid along with the pBABE puromycin resistance-encoding vector, and transfected cells were selected by adding puromycin for 2 days prior harvesting for double immunopurification of BAP1. The eluted proteins were detected by western blotting using the indicated antibodies. (C) Cleavage of Ub-AMC by various BAP1 complexes (WT, C91S and ΔHBM) and recombinant BAP1. Left panel, equal quantities of BAP1 were used for deubiquitination reactions with 37.5 pmol of Ub-AMC. Right panel, release of AMC was monitored by fluorescence spectroscopy (Excitation: 380 nm and Emission: 460 nm). All experiments were repeated at least 3 times and the data are presented as mean ± SD. a.u., arbitrary units.

Figure 5. A BAP1/HCF-1/YY1 complex is associated with euchromatin regions.
(A) Immunolocalization of BAP1 in U2OS cells, indicating that this DUB is mostly excluded from heterochromatic regions. To ensure the specificity of immunostaining, U2OS cells were transiently transfected with siRNA against BAP1 and at three days post-transfection cells were used for immunostaining employing a BAP1 monoclonal antibody. Following Z-stacks image acquisition, RGB profiles were generated by WCIF-ImageJ program (NIH). Although most of the cells are depeleted of BAP1, some were not transfected and show normal BAP1 expression. In the image shown, the cell delimited with the discontinuous line has been RNAi-depleted for BAP1. The other cell shown in the image presumably did not receive the

siRNA and expresses normal levels of BAP1. The intensity of fluorescence signals for BAP1 (red) and DNA (blue) at the indicated bars are shown in relative units (bottom right panel). (B) BAP1 as well as other components of the BAP1 complexes are associated with euchromatin. The chromatin/nuclear matrix fraction was treated with micrococcal nuclease (MNase) to release nucleosomes. Proteins were detected in the soluble and pellet fractions by immunoblotting or coomassie blue staining. (C) Purification of BAP1/HCF-1/YY1 from chromatin fraction. Chromatin fraction of HeLa cells stably expressing Flag-HA-BAP1 was digested with MNase (3U/ml) for 10 min. Following centrifugation at 13,000 g/10 min, an aliquot was used for phenol-chloroform extraction of DNA and agarose gel analysis (left panel). Immunopurification of BAP1 was conducted with the prepared chromatin fraction. The eluted proteins were detected using BAP1, YY1 and HCF-1 antibodies (right panel).

Figure 6. BAP1 activates transcription in a DUB-activity dependent manner.

(A) Schematic representation of the Gal4 transcription system. A transcription reporter assay was conducted by targeting BAP1 to the Gal4-TK-luciferase using Gal4-BAP1 fusion protein. This consists of targeting a protein of interest, fused in frame to the GAL4 DNA binding domain, to the luciferase reporter driven by a promoter containing GAL4 binding sites and the thymidine kinase proximal promoter. (B) Gal4-BAP1 activates transcription. HeLa cells were transfected with 100 ng of Gal4-BAP1, BAP1 or Gal4 expression plasmids along with 500 ng Gal4-TK-Luciferase or 500 ng TK-Luciferase reporter plasmids. Equal expression of various BAP1 constructs was confirmed by western blotting using anti-BAP1 (bottom panel) and luciferase activity was measured (top panel) at 2 days post-transfection. (C) HCF-1 is essentially dispensable for Gal4-BAP1 transcriptional activity. The Gal4 reporter assay was conducted using 500 ng Gal4-TK-Luciferase and equal amount of Gal4-BAP1 WT and Gal4-BAP1 ΔHBM. The expression of BAP1 constructs was monitored by western blotting (right panel) and luciferase activity was measured (left panel) at 2 days post-transfection. (D) The BAP1 catalytic activity is required for transcription activation. The Gal4 reporter assay was conducted using 500 ng Gal4-TK-Luciferase and various amounts of Gal4-BAP1 WT or the catalytic inactive mutant (C91S). The expression of BAP1 constructs was monitored by western blotting (bottom panel) and luciferase activity was measured (top panel) at 2 days

post-transfection. All experiments were repeated at least 3 times and the results shown are from a representative experiment. Data are presented as mean ± SD.

Figure 7. BAP1 regulates the expression of genes involved in numerous cellular processes.

(A) Functional analysis of genes deregulated following BAP1 depletion. The bar chart was generated by Ingenuity Pathways Analysis Version 8.5 using 1244 genes deregulated for both shBAP1s (Fold change: less than 0.7 and more than 1.5). The p value is calculated using the Fisher Exact Test. The smaller the p-value the less likely that the association is random. The line denotes the cutoff for significance (p value of 0.05). (B) RT-PCR analysis of selected genes. U2OS cells were transfected with either a non-targeting control or BAP1 shRNA plasmids along with the pBABE puromycin resistance-encoding vector, and transfected cells were selected by adding puromycin for 24 hours prior to synchronization at the G1/S border by the method of double thymidine block. mRNA quantification was conducted by real time RT-PCR analysis. All experiments were repeated at least 3 times and the data are presented as mean ± SD.

Figure 8. YY1 recruits BAP1 to co-activate cox7c expression.

(A) Alignment of cox7c promoter sequences from various mammalian species, Homo Sapiens, NC000005.9; Bos Taurus, NC007305.3; Mus Musculus NC000079.5. The YY1 binding sites are framed. The TSS is underlined. (B) Expression of COX7C following depletion of BAP1, HCF-1 or YY1. COX7C protein levels following transfection with BAP1 (left panel), HCF-1 (middle panel), YY1 (right panel) or non-target control shRNAs in U2OS or HeLa cells. Following transfection and selection with puromycin for 2 days, cells were harvested for immunoblotting. (C) Downregulation of COX7C following expression of catalytic inactive BAP1. U2OS cells were transduced with retroviral particles to overexpress either BAP1 or its catalytic inactive form (C91S). Following 3 days, cells were harvested for western blotting using the indicated antibodies. (D) cox7c promoter occupancy by YY1, BAP1, and HCF-1. YY1 shRNA was expressed in U2OS cells by transfection and selection with puromycin for 2 days before harvesting for ChIP (left panel) or western blotting (right

panel). ChIP was conducted using polyclonal antibodies against BAP1, HCF-1 or YY1. An IgG was used as control. The enrichment of factors was calculated versus β-globin promoter used as a control. All experiments were repeated at least 3 times and the results shown are from a representative experiment. Data are presented as mean ± SD. (E) Model representing the recruitment of BAP1 and HCF-1 to the cox7c promoter by the transcription factor YY1.

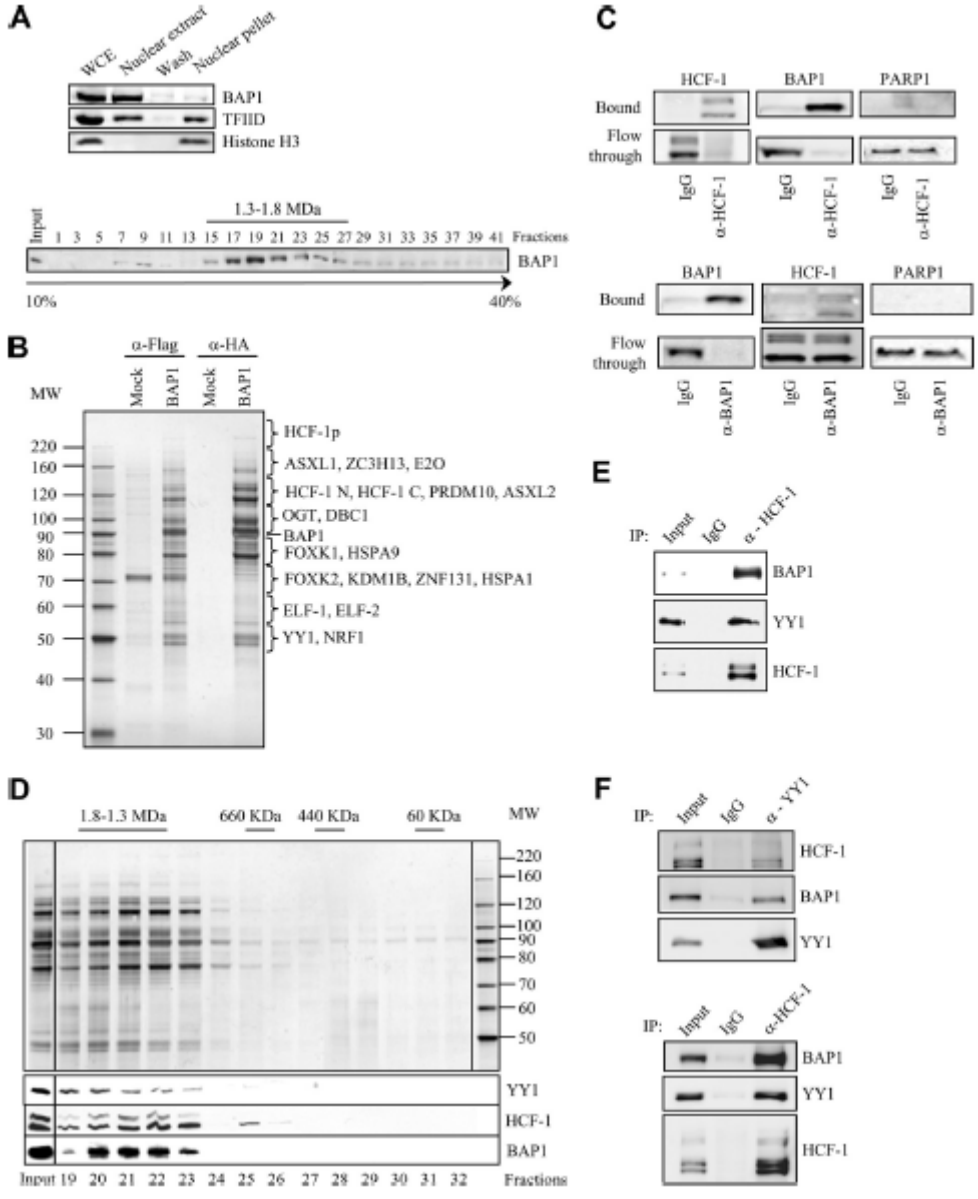
A
WCE
Nuclear extract
Wash
Nuclear pellet
BAP1
TFIID
Histone H3
1.3-1.8 MDa
Input
1 3 5 7 9 11 13 15 17 19 21 23 25 27 29 31 33 35 37 39 41 Fractions
BAP1
10%
40%
B
α-Flag
α-HA
MW
Mock
BAP1
Mock
BAP1
220
160
120
100
90
80
70
60
50
40
30
HCF-1p
ASXL1, ZC3H13, E2O
HCF-1 N, HCF-1 C, PRDM10, ASXL2
OGT, DBC1
BAP1
FOXK1, HSPA9
FOXK2, KDM1B, ZNF131, HSPA1
ELF-1, ELF-2
YY1, NRF1
C
HCF-1
BAP1
PARP1
Bound
Flow through
IgG
α-HCF-1
IgG
α-HCF-1
IgG
α-HCF-1
BAP1
HCF-1
PARP1
Bound
Flow through
IgG
α-BAP1
IgG
α-BAP1
IgG
α-BAP1
D
1.8-1.3 MDa
660 KDa
440 KDa
60 KDa
MW
220
160
120
100
90
80
70
60
50
YY1
HCF-1
BAP1
Input 19 20 21 22 23 24 25 26 27 28 29 30 31 32 Fractions
E
IP:
Input
IgG
α - HCF-1
BAP1
YY1
HCF-1
F
IP:
Input
IgG
α - YY1
HCF-1
BAP1
YY1
IP:
Input
IgG
α-HCF-1
BAP1
YY1
HCF-1

Figure 1

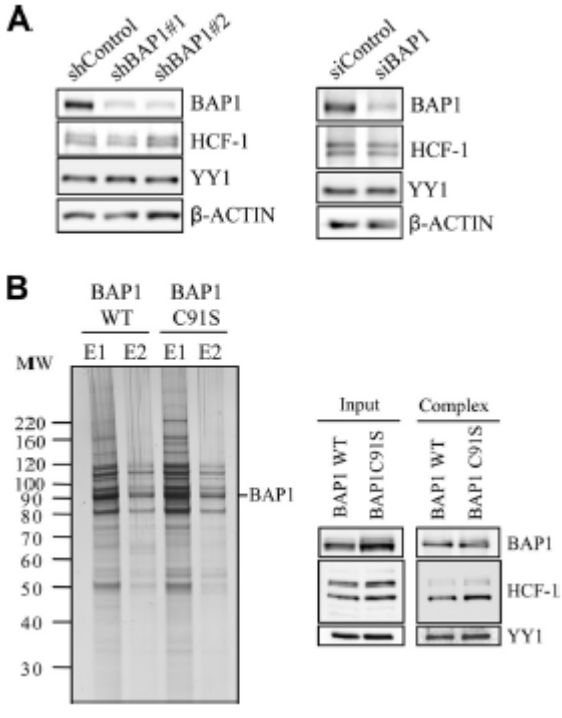
A
shControl
shBAP1#1
shBAP1#2
BAP1
HCF-1
YY1
β-ACTIN
siControl
siBAP1
BAP1
HCF-1
YY1
β-ACTIN
B
BAP1 WT
BAP1 C91S
E1 E2 E1 E2
MW
220
160
120
100
90
80
70
60
50
40
30
BAP1
Input
Complex
BAP1 WT
BAP1C91S
BAP1 WT
BAP1 C91S
BAP1
HCF-1
YY1

Figure 2

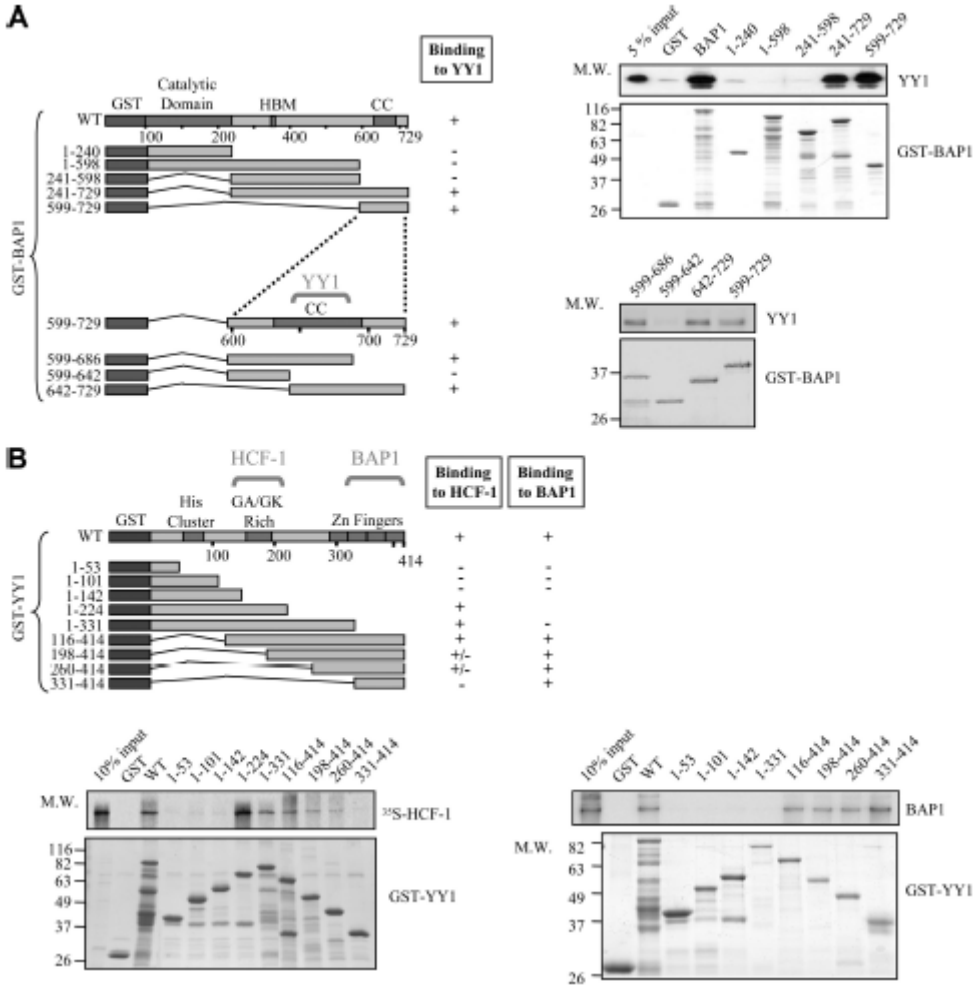
A
Binding to YY1
GST
Catalytic Domain
HBM
CC
WT
100
200
400
600
729
1-240
1-598
241-598
241-729
599-729
GST-BAP1
YY1
CC
600
700
729
599-686
599-642
642-729
5 % input
GST
BAP1
1-240
1-598
241-598
241-729
599-729
M.W.
YY1
116
82
63
49
37
26
GST-BAP1
599-686
599-642
642-729
599-729
B
HCF-1
BAP1
Binding to HCF-1
Binding to BAP1
His Cluster
GA/GK Rich
Zn Fingers
100
200
300
414
1-53
1-101
1-142
1-224
1-331
116-414
198-414
260-414
331-414
GST-YY1
10% input
35S-HCF-1
BAP1

Figure 3

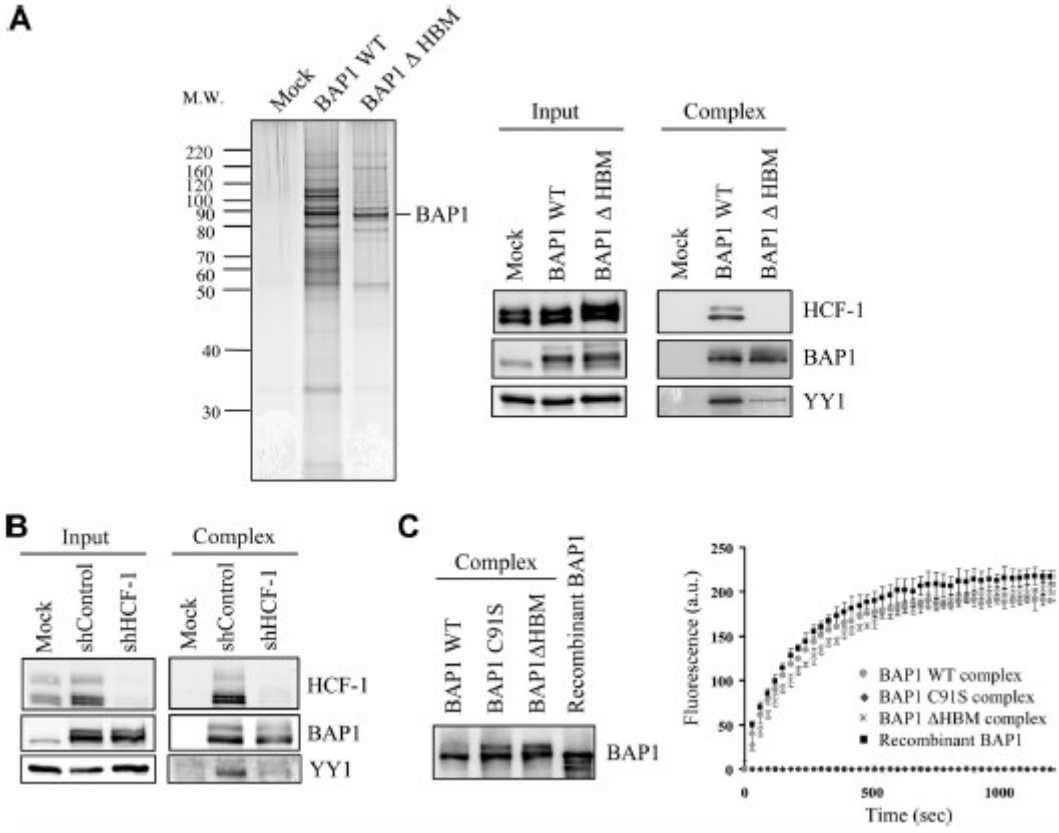
A
M.W.
Mock
BAP1 WT
BAP1 Δ HBM
220
160
120
100
90
80
70
60
50
40
30
BAP1
Input
Complex
Mock
BAP1 WT
BAP1 Δ HBM
HCF-1
BAP1
YY1
B
Input
Complex
Mock
shControl
shHCF-1
HCF-1
BAP1
YY1
C
Complex
BAP1 WT
BAP1 C91S
BAP1ΔHBM
Recombinant BAP1
BAP1
Fluorescence (a.u.)
250
200
150
100
50
0
0
500
1000
Time (sec)
BAP1 WT complex
BAP1 C91S complex
BAP1 ΔHBM complex
Recombinant BAP1

Figure 4

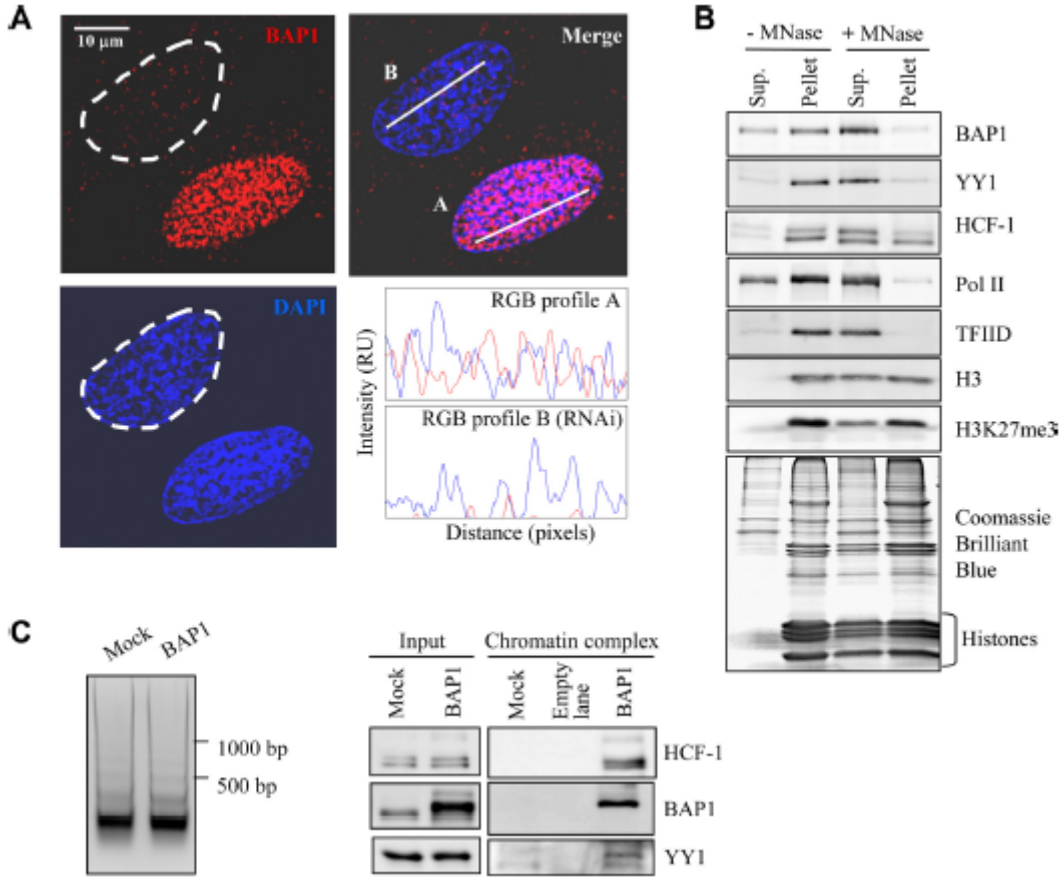
A
10 µm
BAP1
Merge
B
A
DAPI
RGB profile A
RGB profile B (RNAi)
Intensity (RU)
Distance (pixels)
B
- MNase
+ MNase
Sup.
Pellet
Sup.
Pellet
BAP1
YY1
HCF-1
Pol II
TFIID
H3
H3K27me3
Coomassie Brilliant Blue
Histones
C
Mock
BAP1
1000 bp
500 bp
Input
Chromatin complex
Mock
BAP1
Mock
Empty lane
BAP1
HCF-1
BAP1
YY1

Figure 5

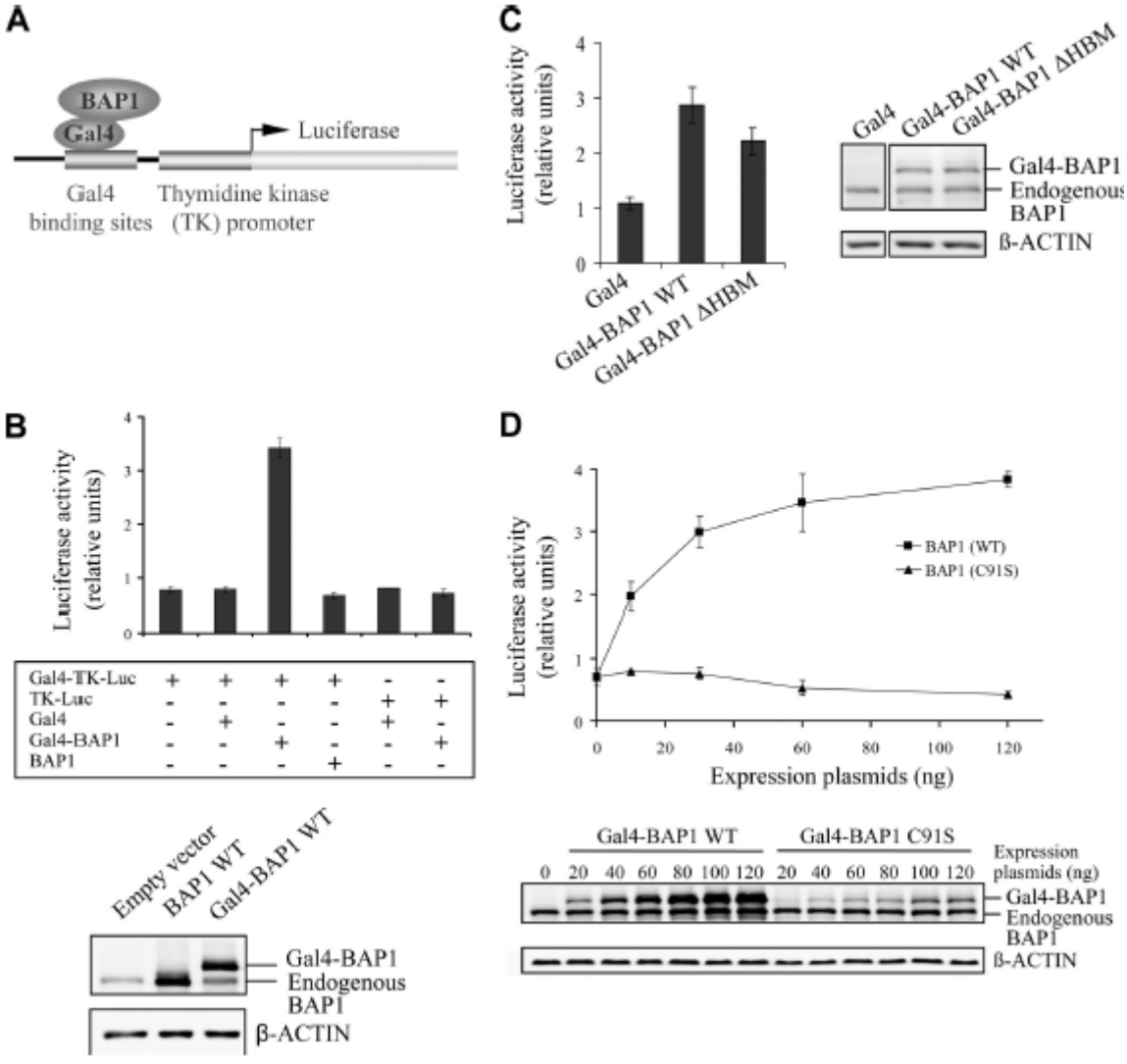
A
BAP1
Gal4
Luciferase
Gal4 binding sites
Thymidine kinase (TK) promoter
B
Luciferase activity (relative units)
Gal4-TK-Luc
TK-Luc
Gal4
Gal4-BAP1
BAP1
Empty vector
BAP1 WT
Gal4-BAP1 WT
Gal4-BAP1
Endogenous BAP1
β-ACTIN
C
Luciferase activity (relative units)
Gal4
Gal4-BAP1 WT
Gal4-BAP1 ΔHBM
Gal4-BAP1
Endogenous BAP1
ß-ACTIN
D
Luciferase activity (relative units)
BAP1 (WT)
BAP1 (C91S)
Expression plasmids (ng)
Gal4-BAP1 WT
Gal4-BAP1 C91S
Expression plasmids (ng)
Gal4-BAP1
Endogenous BAP1
ß-ACTIN

Figure 6

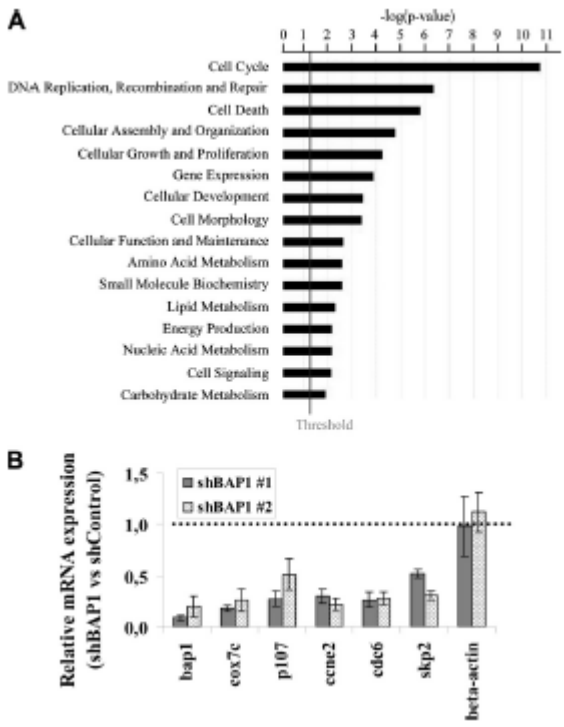
A
-log(p-value)
0 1 2 3 4 5 6 7 8 9 10 11
Cell Cycle
DNA Replication, Recombination and Repair
Cell Death
Cellular Assembly and Organization
Cellular Growth and Proliferation
Gene Expression
Cellular Development
Cell Morphology
Cellular Function and Maintenance
Amino Acid Metabolism
Small Molecule Biochemistry
Lipid Metabolism
Energy Production
Nucleic Acid Metabolism
Cell Signaling
Carbohydrate Metabolism
Threshold
B
Relative mRNA expression (shBAP1 vs shControl)
1,5
1,0
0,5
0,0
shBAP1 #1
shBAP1 #2
bap1
cox7c
p107
ccne2
cdc6
skp2
beta-actin

Figure 7

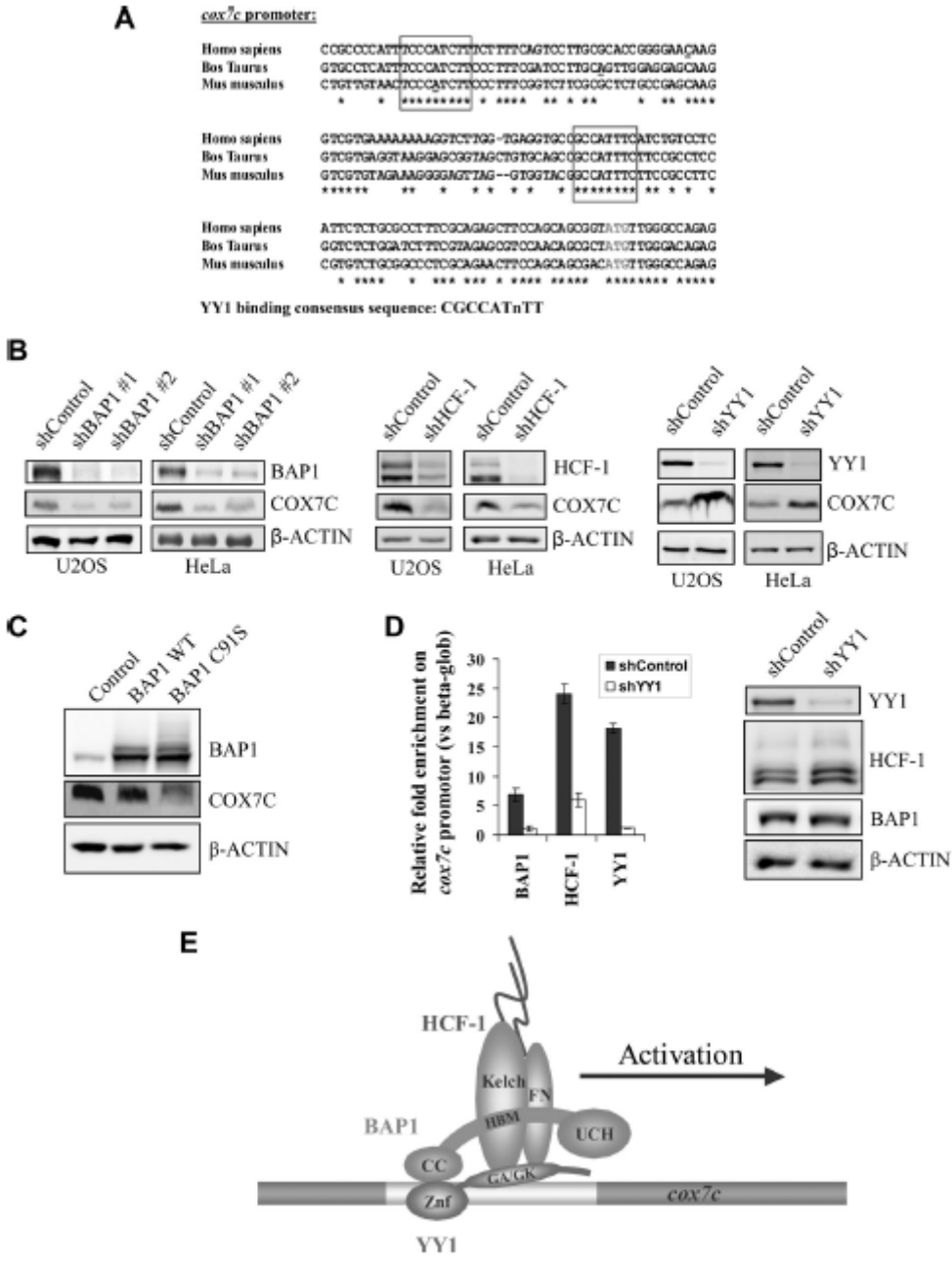
A
cox7c promoter:
Homo sapiens
Bos Taurus
Mus musculus
YY1 binding consensus sequence: CGCCATnTT
B
shControl
shBAP1 #1
shBAP1 #2
shHCF-1
shYY1
BAP1
HCF-1
YY1
COX7C
β-ACTIN
U2OS
HeLa
C
Control
BAP1 WT
BAP1 C91S
D
Relative fold enrichment on cox7c promotor (vs beta-glob)
shControl
shYY1
E
HCF-1
Activation
Kelch
FN
HBM
UCH
BAP1
CC
GAGK
Znf
cox7c
YY1

Figure 8

TABLE 1. Genes deregulated following BAP1 depletion are associated with different cellular functions

Gene function and name[a]	Gene designation	shBAP1 #1		shBAP1 #2	
		Fold change[b]	*P*	Fold change[b]	*P*
Cell cycle					
Cyclin E2	CCNE2	0.18	5.15E−07	0.18	6.05E−06
CDC5 cell division cycle 5-like (*Schizosaccharomyces pombe*)	CDC5L	0.30	1.23E−06	0.65	1.02E−05
S-phase kinase-associated protein 2 (p45)	SKP2	0.39	2.07E−05	0.28	1.84E−05
Cell division cycle 2	CDC2	0.39	1.38E−05	0.33	3.55E−05
Cell division cycle 25A	CDC25A	0.42	2.41E−04	0.40	1.85E−07
Retinoblastoma-like 1 (p107)	p107	0.44	2.11E−05	0.53	6.88E−04
E2F transcription factor 5	E2F5	2.10	9.17E−05	4.00	3.74E−07
Cyclin D2	CCND2	2.32	8.10E−07	3.01	6.18E−08
DNA replication					
Replication factor C (activator 1) 3	RFC3	0.42	7.01E−06	0.29	5.79E−05
CDC6 cell division cycle 6 homolog (*Saccharomyces cerevisiae*)	CDC6	0.46	1.58E−05	0.34	5.78E−06
CDC45 cell division cycle 45-like (*S. cerevisiae*)	CDC45L	0.47	1.91E−04	0.31	6.95E−05
Geminin	GMNN	0.48	2.41E−05	0.56	1.97E−05
DNA repair					
CHK1 checkpoint homolog (*S. pombe*)	CHEK1	0.38	9.19E−07	0.51	5.31E−07
RAD51-like 1 (*S. cerevisiae*)	RAD51L1	0.44	2.24E−04	0.47	5.41E−06
Ubiquitin-specific peptidase 1	USP1	0.48	1.06E−05	0.40	3.67E−05
Breast cancer 1, early onset	BRCA1	0.48	5.43E−05	0.44	2.19E−04
BRCA1-interacting protein C-terminal helicase 1	BRIP1	0.49	1.19E−04	0.37	5.13E−05
Survival/apoptosis					
Platelet-derived growth factor receptor, alpha polypeptide	PDGFRA	0.20	6.26E−05	0.18	1.05E−05
Baculoviral IAP repeat-containing 5 (survivin)	BIRC5	0.41	4.92E−06	0.44	1.73E−04
Transcriptional adaptor 3 (NGG1 homolog, yeast)-like	TADA3L	0.43	2.33E−06	0.51	5.14E−04
Tumor necrosis factor receptor superfamily, member 10b	TNFRSF10B	2.13	1.25E−07	2.93	4.56E−08
BCL2-related protein A1	BCL2A1	3.72	1.14E−05	5.81	4.48E−07
Metabolism					
Carbonic anhydrase II	CA2	0.22	8.99E−06	0.45	4.26E−06
Cytochrome *c* oxidase subunit VIIc	COX7C	0.23	7.85E−07	0.57	1.48E−05
UDP-glucuronate decarboxylase 1	UXS1	0.30	8.45E−06	0.27	7.60E−07
ELOVL family member 6	ELOVL6	0.32	2.79E−06	0.52	1.32E−05
N-Acetylneuraminate pyruvate lyase (dihydrodipicolinate synthase)	NPL	0.41	3.38E−06	0.65	9.79E−05
Cytochrome b_5 reductase 1	CYB5R1	0.45	5.21E−07	0.63	3.34E−05
BRCA1-associated protein 1	BAP1	0.33	4.59E−05	0.33	7.46E−07

[a] Genes are selected as representative examples of different cellular functions.
[b] Values are shBAP1/shControl ratios.

Annex 2

The Tumor Suppressor and Deubiquitinase BAP1 Promotes DNA Double-Strand Breaks Repair

Helen Yu[a,1], Helen Pak[a,1], Ian Hammond-Martel[a], Mehdi Ghram[a], Amélie Rodrigue[b], Salima Daou[a], Haithem Barbour[a], Luc Corbeil[a], Josée Hébert[a], Elliot Drobetsky[a], Jean Yves Masson[b], Javier M Di Noia[c] and El Bachir Affar[a,2]

[a]Maisonneuve-Rosemont Hospital Research Center, Department of Medicine, Université de Montréal, Montréal, PQ, H1T 2M4, Canada.
[b]Genome Stability Laboratory, Laval University Cancer Research Center, Hôtel-Dieu de Québec (Centre Hospitalier Universitaire de Québec), Québec, PQ, G1R 2J6, Canada.
[c]Research Unit in Mechanisms of Genetic Diversity, Institut de Recherches Cliniques de Montréal, Department of Medicine, Université de Montréal, Montréal, PQ, H2W 1R7, Canada.

Running title: BAP1 promotes homologous recombination repair.

[1]Equal contribution

[2]Correspondence

SUMMARY

The cellular response to highly genotoxic DNA double-strand breaks (DSBs) involves the exquisite coordination of multiple signaling and repair factors. Here, we conducted a functional RNAi screen and identified BAP1 as a DUB required for efficient assembly of the homologous recombination (HR) factors BRCA1 and RAD51 at ionizing radiation (IR)-induced foci (IRIF). BAP1 is a chromatin-associated protein frequently inactivated in cancers of various tissues. To further investigate the role of BAP1 in DSB repair, we used a gene targeting approach to knock out this DUB in chicken DT40 cells. We demonstrate that BAP1-deficient cells are (i) sensitive to IR and other agents that induce DSBs, (ii) defective in HR-mediated immunoglobulin gene conversion and (iii) exhibit an increased frequency of chromosomal breaks following IR treatment. We also show that BAP1 is recruited to chromatin in the proximity of a single site-specific I-SceI-induced DSB. Finally, we identified six IR-induced phosphorylation sites in BAP1 and demonstrated that mutation of these residues inhibits BAP1 recruitment to DSB site. We also found that both BAP1 catalytic activity and its phosphorylation are critical for promoting DNA repair and cellular recovery from DNA damage. Our data reveal a novel role for BAP1 in DSB repair by HR, thereby providing a possible molecular basis for its tumor suppressor function.

Significance Statement

BAP1 is a deubiquitinase of histone H2A involved in chromatin remodeling. Several studies identified BAP1 as major tumor suppressor inactivated in various cancers. Nonetheless, the manner in which BAP1 protects against cancer development remains enigmatic. We now demonstrate that BAP1 is recruited to double strand DNA break sites and promotes error-free repair of these lesions. We also provide the first evidence that phosphorylation coordinates the function of BAP1 in promoting cellular recovery from DNA damage. Thus, our study represents a significant advance in the field of ubiquitin signaling in the context of cancer development.

INTRODUCTION

Following induction of DSBs, a convoluted ubiquitin-mediated signaling cascade culminates in the assembly of multiple repair proteins at the site of DNA damage (1). These early ubiquitin signaling events involve, most notably, the recruitment of the RING finger E3 ligases RNF8/RNF168. RNF168 catalyzes K63-linked ubiquitin chains formation on histones H2A/H2AX, which is required for the recruitment of key downstream factors including 53BP1, BRCA1, and RAD51 (2). 53BP1 and BRCA1/RAD51 promote, in a cell cycle-dependent manner, DSB repair via non-homologous end joining (NHEJ) and homologous recombination (HR) respectively (3). In parallel, another ubiquitin signaling pathway, involving the Polycomb group complex PRC1, also contributes to coordinate the DSB response. PRC1 catalyzes the monoubiquitination of H2A on K119 residue (H2Aub), a critical chromatin modification involved in regulating gene expression and DNA damage/repair responses (4). It was proposed that H2Aub promotes silencing of transcription in chromatin regions flanking the DSBs, thus facilitating DNA repair (5, 6).

Several deubiquitinases (DUBs) have also been linked to DSB signaling and growing evidence suggests that deubiquitination might exert an extensive control on the recruitment and/or disassembly of proteins at the site of DNA damage. For instance, BRCC36, a K63 chain-specific DUB, regulates the recruitment of repair proteins by modulating the level of ubiquitin chains (7, 8). POH1/rpn11/PSMD14, a regulatory subunit of the 19S proteasome, deconjugates ubiquitin chains at DSB sites and promotes the recruitment of RAD51 (9). USP3 and OTUB1 have also been reported to be important for DSB signaling and repair (10, 11).

The DUB BAP1 is a tumor suppressor inactivated in various types of cancer (12). BAP1 forms multi-protein complexes with several chromatin associated-proteins notably the host cell factor 1 (HCF-1) and regulates transcription (13). The Drosophila BAP1, Calypso was shown to deubiquitinate H2Aub (14). Thus BAP1 might be involved in the DNA damage response by coordinating H2A ubiquitination. Notably, proteomic studies revealed BAP1 among phosphorylated proteins during DNA damage (15). Nonetheless, the role of BAP1 in DNA damage response, and more generally the mechanism of tumor suppression exerted by

this DUB, remains unclear. In the current study, we identify BAP1 as a novel regulator of DSB repair, which in turn may elucidate the molecular underpinnings of its to date poorly understood tumor suppressor function.

RESULTS

A DUB RNAi screen reveals novel regulators of HR proteins assembly at IRIF.

We sought to identify novel DUBs required for the recruitment or the dispersion of repair proteins at IRIF. A human DUB RNAi library was used to screen for DUBs whose depletion affect the number of RAD51 or BRCA1 foci at DSB sites (Fig. 1A). A twenty-four hours time point post-IR was selected for our studies, time at which 50-60 % of cells still exhibit DSB foci, thus facilitating detection of any potential increase or decrease of foci formation (Fig. 1B). Several DUBs were identified in this manner as associated with either increased, or more often decreased, RAD51 and/or BRCA1 foci (Fig. 1C, Table S1). As a proof of validity, we also identified BRCC36, USP3 and PSMD14, which have been previously reported to regulate DSB signaling by impacting RAD51 and/or BRCA1 foci formation (9, 10, 16). The novel DUB candidates whose knockdown induced a decrease in BRCA1/RAD51 foci formation include BAP1, DUB3, STAMBP, STAMBPL1 and COPS5 (Fig. 1C). We also identified candidate DUBs whose knockdown result in increased BRCA1/RAD51 foci formation, notably ZRANB1 (Fig. 1C). Immunostainings of BRCA1 and RAD51 foci following depletion of the known DSB regulator PSMD14 and the novel candidate BAP1 are shown (Fig. 1D).

BAP1 promotes the recruitment of HR proteins at IRIF.

We focused on further characterization of BAP1 in the DNA damage signaling/repair processes. We used two additional shRNA constructs targeting BAP1 and found that in each case both BRCA1 and RAD51 foci were significantly reduced (Fig. S1A). Next, we monitored the dynamics of IRIF formation for several key proteins in BAP1-depleted cells. Primary human fibroblasts (LF1) were transfected either with control or BAP1 siRNA constructs, irradiated and analyzed at different time points post-damage (Fig. 2A,B and Fig. S1B). Relative to control cells, the majority of BAP1-depleted cells exhibited less than 10 BRCA1 and RAD51 foci per cell at all time points, although γH2AX focus formation was similar. It is known that 53BP1 inhibits BRCA1-mediated HR and promotes NHEJ during the G1 phase (17). However, cell cycle analysis did not reveal any substantial accumulation of cells in the G1 phase (Fig. S2A). In addition, we did not observe any significant increase in

53BP1 foci either prior to, or post, IR treatment (Fig. 2A,B). Consistent with these results, staining for foci containing auto-phosphorylated DNA-PK, a kinase required for NHEJ (18), did not reveal significant differences between BAP1-depleted and control cells (Fig. 2A,B). Interestingly, constitutive BRCA1 foci, that are distinct from IRIF, were also reduced in BAP1-depleted cells indicating that this DUB might be involved in coordinating BRCA1 association with chromatin under normal growth conditions. Of note, BRCA1/RAD51 protein expression were not significantly different following BAP1 depletion (Fig. 2C). We note that IR-induced accumulation of the p53 tumor suppressor was essentially similar in control vs. BAP1-depleted cells (Fig. S2B). As expected, BAP1-depleted cells manifested a global increase of H2Aub (Fig. 2C and Fig. S2C).

BAP1 does not distinctly accumulate at IRIF (Fig. S1A), but might be transiently and dynamically recruited to DSBs. To assess the potential recruitment of BAP1 to DNA breaks, we fractionated cellular extracts from untreated vs. IR-treated cells and observed a consistent increase of BAP1 in the chromatin fraction in response to IR (Fig. 2D). As expected, accumulation of RAD51 and BRCA1 on chromatin was readily observed. Of note, no obvious change of global H2Aub was observed in the chromatin fractions suggesting that DNA damage-induced H2A ubiquitination marginally contribute to the global H2Aub signal. We further probed whether BAP1 is indeed recruited to DSB sites by chromatin immunoprecipitation (ChIP) (Fig. 2E). Real-time PCR quantification of immunoprecipitated chromatin by BAP1 in the vicinity of a unique DSB created by I-SceI in vivo indicated that BAP1 is enriched near the DSB site. Importantly, at the break site, H2Aub levels were inversely correlated with BAP1 recruitment. In contrast, no recruitment of BAP1 was detected distal to the break, where high levels of H2Aub were observed.

BAP1 KO DT40 cells are sensitive to DSB-inducing agents and defective in HR-mediated sIgM gene conversion.

To further investigate the function of BAP1 in HR, we generated a conditional BAP1 KO chicken B lymphoma DT40 cells (Fig. 3A). BAP1 is highly conserved between human and chicken (Fig. S3A). Southern blot analysis indicated that both alleles were ablated (Fig.

3B). Targeting of one allele included an expression cassette with the human BAP1 cDNA flanked by two loxP sites allowing Cre-mediated excision. The DT40 Cre-1 cell line used for the KO generation stably expresses a tamoxifen inducible Cre recombinase (19). Thus, following tamoxifen treatment, >95% of the cells lose BAP1 expression (Fig. S3B). To obtain cell populations that are completely BAP1-deficient, we isolated two single cell KO clones with complete absence of BAP1 expression (Fig. 3C). BAP1-deficient DT40 cells show, as expected, a global increase of H2Aub (Fig. 3C). Cell proliferation was also delayed in BAP1 KO cells (Fig. S4).

To assess the role of BAP1 in DSB repair, we conducted survival assays with BAP1 KO DT40 cells treated with DNA damaging agents that induce DSBs. Since BAP1 KO cells proliferate slower than WT cells (Fig. S4), cell numbers were adjusted before treatment to compensate for any potential bias that could be introduced as a consequence of unequal cell proliferation. We observed that the BAP1-/- cells are more sensitive to IR than WT cells (Fig. 3D). BAP1 KO sensitivity to IR is accompanied by an elevated level of chromosome aberrations (Fig. 3E, S5). HR-deficient cells, such as cancer cells harboring inactivating mutations in BRCA1 or BRCA2, are hypersensitive to poly (ADP-ribose) polymerase (PARP) inhibition (20). We analyzed the response of BAP1 -/- cells to the PARP inhibitor, Olaparib. Indeed, BAP1 -/- cells are strikingly sensitive to PARP inhibition relative to BAP1 +/+ and +/- cells (Fig. 3D). The high sensitivity of BAP1 KO cells to IR and Olaparib is consistent with the recently reported sensitivity of renal carcinoma-derived BAP1-deficient cells to DSB-inducing agents (21).

In order to confirm a role for BAP1 in HR, we took advantage of the fact that DT40 cells constitutively diversify their immunoglobulin loci by gene conversion (22). The DT40 Cre-1 cell line harbors a frameshift in the rearranged V segment of the Ig light chain gene (IgL), which results in a surface IgM negative (sIgM-) phenotype. This frameshift can be repaired by HR-based gene conversion in a fraction of the cells, leading to the re-expression of sIgM (Fig. 3F). Thus, the proportion of sIgM+ revertants in the population can be used to quantify gene conversion efficiency. sIgM- cells were sorted and expanded to allow gene

reversion for the same number of population doublings. While approximately 8 % of BAP1 +/+ cells reverted, both BAP1 -/- clones were relatively defective (1 % and 0.5 %) whereas BAP1 +/- cells showed an intermediate phenotype (5 %) (Fig. 3F).

Phosphorylation of BAP1 following IR treatment promotes DNA repair and cellular recovery from DNA damage.

In global proteomics studies, BAP1 was reported to be phosphorylated on S592 (ATM/ATR SQ motif) following IR treatment (15). We conducted a large-scale immunopurification of BAP1 post-IR from HeLa cells followed by mass spectrometry analysis. We identified another SQ phosphosite (S276) and novel IR-induced phosphorylation sites two of which are conserved between human and chicken (Fig 4A. Fig. S6A-C).

Using an anti-pSQ(G) antibody, expected to recognize S592, we found that mutation of S592, indeed abolished the phosphorylation of BAP1 on this site (Fig S7A). Next, using this antibody, we found that inhibition of ATM with caffeine or KU-55933 resulted in decreased phosphorylation of BAP1 S592 (Fig 4B). However, ATR inhibition only resulted in a slight decrease of the S592 phosphorylation signal, while ATR-mediated CHK1 phosphorylation was abrogated (Fig. S7B). Using DNA-PK-deficient cells, we found that this kinase is not responsible for phosphorylation of BAP1 S592 following IR (Fig. S7C). Of note, HCF-1 is not required for BAP1 phosphorylation by ATM since the S592 phosphorylation signal on BAP1 lacking HBM is not decreased following IR treatment (Fig. S7D). CDKs are involved in DSB repair (23, 24), and might in concert with ATM, phosphorylate BAP1 in order to coordinate its function. Using chemical inhibitors in conjunction with the anti-pSQ(G) antibody, we did not observe a requirement of CDKs for BAP1 phosphorylation by ATM (Fig.S7E). Using the PRO-Q phosphostain, we found that the global phosphorylation state of BAP1 did not significantly change following IR treatment or CDK inhibition (Fig. S7E), likely due to the high level of constitutive phosphorylation of BAP1.

Next, we found that the stable components of the BAP1 complexes are unaffected by IR treatment (Fig. 4C and Fig. S6D). We then used an activity-directed ubiquitin probe that

binds to the catalytic site of cysteine protease DUBs, and found that the probe labeled purified BAP1 from untreated and IR-treated cells with similar efficiency (Fig. 4D, top panel). Similar results were observed for endogenous BAP1 in HeLa or U2OS cells (Fig. S6E). Next, we evaluated BAP1 DUB activity toward H2A using purified nucleosomes incubated with BAP1 complexes isolated from untreated vs. IR-treated cells (Fig. 4D, bottom panel) and no significant difference was observed. Therefore, we sought to determine the importance of the IR-specific phosphosites of BAP1 for its DNA damage function in vivo. We generated a set of BAP1 phospho-mutants including the conserved residues S/T273/A and S276A, the SQ sites (S276A/S592A, SQ-MUT), and all IR-phosphorylated residues of BAP1 (6 phosphosites converted to alanines, P-MUT). These mutants were used, along with the BAP1 ΔHBM, and the BAP1 catalytically dead (C91S), to stably reconstitute the BAP1-deficient lung carcinoma cell line H226 (Fig. 5A). As previously shown (25), expression of BAP1 WT, but not the catalytic dead mutant, induced a delay in H226 cell proliferation (Fig. 5B). BAP1-deficient in interaction with HCF-1 did not affect cell proliferation. Interestingly, the BAP1 P-MUT also failed to reduce cell proliferation. To further determine the sensitivity of these cells to IR, clonogenic survival assay was performed. To exclude any potential bias that can be introduced by the unequal cell proliferation of the BAP1 stable cell lines, survival rates were normalized to untreated cells. Thus, although H226 cells expressing BAP1 WT proliferate relatively slowly, they were more resistant to IR compared to H226 cells expressing the empty vector. The BAP1 C91S, BAP1 ΔHBM and BAP1 P-MUT were the most sensitive to IR (Fig. 5C). Based on the above, we concluded that phosphorylation of BAP1 on multiple sites as well as catalytic activity are required for promoting cell survival following IR. Of note, no overt apoptosis is induced following IR treatment of H226 expressing the WT or mutant forms of BAP1 (Fig. S8B). Next, we conducted ChIP analysis and found that while the recruitment of BAP1 SQ-MUT to the site of DSB was partially decreased, the recruitment BAP1 P-MUT, was totally abolished (Fig. 5D). Of note, similar to the WT BAP1, the P-MUT assembled protein complexes (Fig S7F, G) and efficiently deubiquitinated nucleosomal H2A in vitro (Fig S7H). To directly analyze DSB repair, we determined the levels of γH2AX in H226 stably expressing BAP1 WT or mutants following IR treatment (Fig. 5E). We found that the WT BAP1, but not the C91S or the P-MUT reduced both the constitutive and IR-

induced accumulation γH2AX. BAP1, but not the C91S mutant, promoted a strong deubiquitination of H2A. Interestingly, while expression of BAP1 P-MUT also significantly promoted deubiquitination of H2A, the remaining levels of H2Aub were consistently twice higher in cells expressing the BAP1 P-MUT than the cells expressing the WT form (Fig. 5E).

DISCUSSION

We report the identification of DUB candidates that might play important roles in the cellular response to DSBs. Notably, STAMBP and COPS5 appear to be interesting candidates. These DUBs are zinc-dependent metalloproteases of the JAMM/MPN+ family which have intrinsic specificity toward K63-linked ubiquitin chains (26). Since K63 chains are highly involved in the DSB response, it is possible that these DUBs regulate DSB repair. Notably, we also identify BAP1 as a novel regulator of HR. Consistently, BAP1 KO phenocopies BRCA1 KO and RAD51 KO in DT40 cells, being both hypersensitive to DSB-inducing agents accompanied with high levels of chromosome breaks (27, 28). We emphasize that BAP1 heterozygous clones also exhibit chromosomal defects and decreased HR-mediated sIgM reversion. This suggests that BAP1 dosage is critical, which may reflect the fact that all nuclear BAP1 is contained within multi-protein complexes (13). Indeed, BAP1 heterozygous mutations are found in human tumors (29).

Several mechanisms, not necessarily mutually exclusive, might explain how BAP1 regulates HR proteins. First BAP1 depletion decreases the assembly of constitutive BRCA1 foci, which are associated with replication of heterochromatin (30). Thus, it is plausible that BAP1 depletion affects the expression of genes involved in BRCA1 recruitment on chromatin. It is also possible that the effects of BAP1 on the recruitment of HR proteins might be directly linked to its previously reported interaction with BRCA1/BARD1 (31, 32). Although our studies failed to reveal BRCA1/BARD1 as stable components of the BAP1 complexes (13), and BAP1 exerts BRCA1-independent effects on cell proliferation (25), it is possible that BRCA1 interaction with BAP1 is transient and associated with DNA damage-dependent and -independent events. Thus, the implication of BAP1 in HR revealed herein provides impetus for future studies to determine the exact significance of the interaction between BAP1 and BRCA1/BARD1.

On the other hand, to facilitate DNA repair, transcription appears to be blocked at DSB by PRC1-mediated H2A ubiquitination (5). Accordingly, DUBs that remove H2Aub at DSBs are expected to inhibit HR. However, we observed the opposite effect, i.e., the H2A

DUB BAP1 promotes HR. In fact, the BAP1 complex might act in concert with the PRC1 complex to promote dynamic ubiquitination/deubiquitination of H2A thereby ensuring the proper dosage of this modification at the site of DSB. Based on our ChIP analysis for BAP1 and H2Aub near the DSB site, it is possible that BAP1 deubiquitinates H2A in the proximity of the DSB site to increase chromatin accessibility at this specific region to allow, e.g., DNA resection during HR. Thus, BAP1 depletion causing an increase of H2Aub might interfere with specific chromatin and/or histone modifications events at DSBs, which might explain the observed defect in HR. Moreover, it is possible that more than one H2A DUB is involved in the signaling at DSBs. Some DUBs might assist in chromatin organization to promote DNA repair, whereas others could play a role in foci resolution. Consistent with this model, it was reported that another H2A DUB, USP16, regulates the level of this histone modification to control the derepression of transcription at DSB sites (6).

In support of BAP1 function in the cellular response to DSBs, we showed that its phosphorylation is required for promoting survival after IR. Since BAP1 phosphorylation does not directly impact intrinsic BAP1 DUB activity, it is possible that it rather promotes BAP1 interaction with other factors to facilitate the recruitment to DSBs where it regulates H2Aub levels. Indeed, the residual levels of H2Aub are consistently higher in H226 cells expressing the BAP1 P-MUT than the WT form, probably reflecting an inability of the mutant to deubiquitinate the small pool of H2Aub associated with DSBs. We also note that several sites of BAP1 are phosphorylated following IR treatment, including SQ and non-SQ sites indicating that BAP1 is phosphorylated by multiple DNA damage-responsive kinases. Thus, BAP1 involvement in the DNA damage response might be more complex than anticipated. Indeed, the use of BAP1 P-MUT to reconstitute BAP1-deficient H226 cells indicated that the decrease of cell proliferation following re-introduction of WT BAP1 depends on its phosphorylation, even in the absence of exogenously inflicted DNA damage. The effect of BAP1 phosphorylation on cell proliferation likely reflects a role of this DUB in DNA damage-induced checkpoint responses. In fact, normally growing H226 cells have elevated levels of γH2AX and a severe genomic instability (Fig. S8C,D), indicative of high rates of spontaneous DNA damage in these BAP1-deficient cells. These cancer cells must necessarily

harbor defects in DNA damage checkpoints that allow them to proliferate under such genomic instability. Therefore, the expression of BAP1 WT in H226 cells might re-activate certain DNA damage checkpoints thus causing decreased cell proliferation.

In summary, we provide strong evidence indicating that BAP1 is a DNA damage signaling and repair enzyme (Fig. 5F). Loss of BAP1 is expected to decrease HR, an error free repair mechanism. Under such conditions, cells might become much more reliant on NHEJ, an error-prone repair mechanism, resulting in the net accumulation of mutations and chromosomal aberrations that cause genomic instability. Moreover, as a consequence of BAP1 inactivation, defects in checkpoint(s) signaling could promote the survival of cells harboring damaged DNA, thus driving neoplastic transformation.

MATERIALS AND METHODS

RNAi, gene targeting and phenotypic analysis.

Cells were transfected with siRNA or shRNA targeting DUBs or non-target control and harvested as indicated. The DT40 Cre-1 cell line was used to generate the BAP1 KO. Clonogenic survival assay, cytogenetic analysis, sIgM gene conversion assay, preparation of cell extracts and chromatin fraction for western blotting were done as described in the SI text.

Immunofluorescence and flow cytometry analysis.

Cells were immunostained as previously described (33). Flow cytometry determination of DNA content, BAP1, phospho histone H3 serine 10, and BrdU incorporation were conducted using LSRII flow cytometer and data were processed with FlowJo V887 software.

Chromatin immunoprecipitation on I-SceI-induced double strand break (DSB).

Induction of a single DSB following I-SceI expression, ChIP experiments and real-time PCR were done as described in the SI text.

Purification of BAP1 complexes and identification of phosphorylation sites.

HeLa S3 cells expressing stably Flag-HA-BAP1 or the empty vector were treated with IR and used for immunopurification and Mass spectrometry. Additional details are provided in the SI text.

Deubiquitination assays.

Ubiquitin-Vinyl Methyl Ester (Ub-VME) probe labeling and In vitro H2Aub deubiquitination assay were done as described in the SI text.

Acknowledgements. This work was supported by grants from the Cancer Research Society to EBA, the Canadian Institutes of Health Research (CIHR) to JYM, the Canadian Cancer Society Research Institute (grant #700348) to JMDN, and the Natural Sciences and Engineering Research Council of Canada to ED. EBA is a scholar of the CIHR and Le Fonds de la Recherche en Santé du Québec (FRSQ). JYM is a FRSQ National investigator. JMDN is supported by a Canada research chair tier 2. HY was supported by a PhD scholarship from the Cole foundation and the CIHR. We want to thank Huib Ovaa for kindly providing us the DUB probe and Sylvie Lavallée for cytogenetic analysis.

REFERENCES

1. HARPER JW & ELLEDGE SJ (2007) THE DNA DAMAGE RESPONSE: TEN YEARS AFTER. MOL CELL 28(5):739-745.
2. PRICE BD & D'ANDREA AD (2013) CHROMATIN REMODELING AT DNA DOUBLE-STRAND BREAKS. CELL 152(6):1344-1354.
3. CHAPMAN JR, TAYLOR MR, & BOULTON SJ (2012) PLAYING THE END GAME: DNA DOUBLE-STRAND BREAK REPAIR PATHWAY CHOICE. MOL CELL 47(4):497-510.
4. ZHOU W, WANG X, & ROSENFELD MG (2009) HISTONE H2A UBIQUITINATION IN TRANSCRIPTIONAL REGULATION AND DNA DAMAGE REPAIR. INT J BIOCHEM CELL BIOL 41(1):12-15.
5. CHAGRAOUI J, HEBERT J, GIRARD S, & SAUVAGEAU G (2011) AN ANTICLASTOGENIC FUNCTION FOR THE POLYCOMB GROUP GENE BMI1. PROC NATL ACAD SCI U S A 108(13):5284-5289.
6. SHANBHAG NM, RAFALSKA-METCALF IU, BALANE-BOLIVAR C, JANICKI SM, & GREENBERG RA (2010) ATM-DEPENDENT CHROMATIN CHANGES SILENCE TRANSCRIPTION IN CIS TO DNA DOUBLE-STRAND BREAKS. CELL 141(6):970-981.
7. SHAO G, ET AL. (2009) THE RAP80-BRCC36 DE-UBIQUITINATING ENZYME COMPLEX ANTAGONIZES RNF8-UBC13-DEPENDENT UBIQUITINATION EVENTS AT DNA DOUBLE STRAND BREAKS. PROC NATL ACAD SCI U S A 106(9):3166-3171.
8. COOPER EM, ET AL. (2009) K63-SPECIFIC DEUBIQUITINATION BY TWO JAMM/MPN+ COMPLEXES: BRISC-ASSOCIATED BRCC36 AND PROTEASOMAL POH1. EMBO J.
9. BUTLER LR, ET AL. (2012) THE PROTEASOMAL DE-UBIQUITINATING ENZYME POH1 PROMOTES THE DOUBLE-STRAND DNA BREAK RESPONSE. EMBO J 31(19):3918-3934.

10. NICASSIO F, ET AL. (2007) HUMAN USP3 IS A CHROMATIN MODIFIER REQUIRED FOR S PHASE PROGRESSION AND GENOME STABILITY. CURR BIOL 17(22):1972-1977.

11. NAKADA S, ET AL. (2010) NON-CANONICAL INHIBITION OF DNA DAMAGE-DEPENDENT UBIQUITINATION BY OTUB1. NATURE 466(7309):941-946.

12. CARBONE M, ET AL. (2013) BAP1 AND CANCER. NAT REV CANCER 13(3):153-159.

13. YU H, ET AL. (2010) THE UBIQUITIN CARBOXYL HYDROLASE BAP1 FORMS A TERNARY COMPLEX WITH YY1 AND HCF-1 AND IS A CRITICAL REGULATOR OF GENE EXPRESSION. MOL CELL BIOL. 30, 5071-5085.

14. SCHEUERMANN JC, ET AL. (2010) HISTONE H2A DEUBIQUITINASE ACTIVITY OF THE POLYCOMB REPRESSIVE COMPLEX PR-DUB. NATURE 465(7295):243-247.

15. STOKES MP, ET AL. (2007) PROFILING OF UV-INDUCED ATM/ATR SIGNALING PATHWAYS. PROC NATL ACAD SCI U S A 104(50):19855-19860.

16. CHEN X, ARCIERO CA, WANG C, BROCCOLI D, & GODWIN AK (2006) BRCC36 IS ESSENTIAL FOR IONIZING RADIATION-INDUCED BRCA1 PHOSPHORYLATION AND NUCLEAR FOCI FORMATION. CANCER RES 66(10):5039-5046.

17. ESCRIBANO-DIAZ C, ET AL. (2013) A CELL CYCLE-DEPENDENT REGULATORY CIRCUIT COMPOSED OF 53BP1-RIF1 AND BRCA1-CTIP CONTROLS DNA REPAIR PATHWAY CHOICE. MOL CELL 49(5):872-883.

18. CHEN BP, ET AL. (2005) CELL CYCLE DEPENDENCE OF DNA-DEPENDENT PROTEIN KINASE PHOSPHORYLATION IN RESPONSE TO DNA DOUBLE STRAND BREAKS. J BIOL CHEM 280(15):14709-14715.

19. ARAKAWA H, LODYGIN D, & BUERSTEDDE JM (2001) MUTANT LOXP VECTORS FOR SELECTABLE MARKER RECYCLE AND CONDITIONAL KNOCK-OUTS. BMC BIOTECHNOL 1:7.

20. BRYANT HE, ET AL. (2005) SPECIFIC KILLING OF BRCA2-DEFICIENT TUMOURS WITH INHIBITORS OF POLY(ADP-RIBOSE) POLYMERASE. NATURE 434(7035):913-917.

21. PENA-LLOPIS S, ET AL. (2012) BAP1 LOSS DEFINES A NEW CLASS OF RENAL CELL CARCINOMA. NAT GENET 44(7):751-759.

22. WINDING P & BERCHTOLD MW (2001) THE CHICKEN B CELL LINE DT40: A NOVEL TOOL FOR GENE DISRUPTION EXPERIMENTS. J IMMUNOL METHODS 249(1-2):1-16.

23. HUERTAS P, CORTES-LEDESMA F, SARTORI AA, AGUILERA A, & JACKSON SP (2008) CDK TARGETS SAE2 TO CONTROL DNA-END RESECTION AND HOMOLOGOUS RECOMBINATION. NATURE 455(7213):689-692.

24. JOHNSON N, ET AL. (2009) CDK1 PARTICIPATES IN BRCA1-DEPENDENT S PHASE CHECKPOINT CONTROL IN RESPONSE TO DNA DAMAGE. MOL CELL 35(3):327-339.

25. VENTII KH, ET AL. (2008) BRCA1-ASSOCIATED PROTEIN-1 IS A TUMOR SUPPRESSOR THAT REQUIRES DEUBIQUITINATING ACTIVITY AND NUCLEAR LOCALIZATION. CANCER RES 68(17):6953-6962.

26. KOMANDER D, CLAGUE MJ, & URBE S (2009) BREAKING THE CHAINS: STRUCTURE AND FUNCTION OF THE DEUBIQUITINASES. NAT REV MOL CELL BIOL 10(8):550-563.

27. VANDENBERG CJ, ET AL. (2003) BRCA1-INDEPENDENT UBIQUITINATION OF FANCD2. MOL CELL 12(1):247-254.

28. SONODA E, ET AL. (1998) RAD51-DEFICIENT VERTEBRATE CELLS ACCUMULATE CHROMOSOMAL BREAKS PRIOR TO CELL DEATH. EMBO J 17(2):598-608.

29. DEY A, ET AL. (2012) LOSS OF THE TUMOR SUPPRESSOR BAP1 CAUSES MYELOID TRANSFORMATION. SCIENCE 337(6101):1541-1546.

30. PAGEAU GJ & LAWRENCE JB (2006) BRCA1 FOCI IN NORMAL S-PHASE NUCLEI ARE LINKED TO INTERPHASE CENTROMERES AND REPLICATION OF PERICENTRIC HETEROCHROMATIN. J CELL BIOL 175(5):693-701.

31. JENSEN DE, ET AL. (1998) BAP1: A NOVEL UBIQUITIN HYDROLASE WHICH BINDS TO THE BRCA1 RING FINGER AND ENHANCES BRCA1-MEDIATED CELL GROWTH SUPPRESSION. ONCOGENE 16(9):1097-1112.
32. NISHIKAWA H, ET AL. (2009) BRCA1-ASSOCIATED PROTEIN 1 INTERFERES WITH BRCA1/BARD1 RING HETERODIMER ACTIVITY. CANCER RES 69(1):111-119.
33. HAMMOND-MARTEL I, ET AL. (2010) PI 3 KINASE RELATED KINASES-INDEPENDENT PROTEOLYSIS OF BRCA1 REGULATES RAD51 RECRUITMENT DURING GENOTOXIC STRESS IN HUMAN CELLS. PLOS ONE 5(11):E14027.

FIGURE LEGENDS

Figure 1. DUB screen identifies novel regulators of HR protein assembly at IRIF.

A) Schematic representation of DUB loss-of-function screen for IRIF regulators. U2OS cells were transfected with individual siRNA pool targeting DUBs, exposed to IR and collected for staining. B) Graphs represent the percentage of cells with more than 10 foci of BRCA1 or RAD51. Dashed red line shows the percentage of cells with protein foci for the control sample. C) Venn diagrams showing DUBs associated with reduced or increased percentage of cells with foci. DUBs having the same phenotype with both BRCA1 and RAD51 foci are indicated. D) Representative staining of BRCA1 and RAD51 foci in PSMD14- and BAP1-depleted cells.

Figure 2. BAP1 promotes IRIF formation and is recruited to the site of double strand breaks (DSBs).

LF1 cells were transfected with either control or BAP1 siRNA. Three days following transfection, control and BAP1 RNAi cells were combined (1:1) and treated with IR (7.5 Gy). Cells were fixed and stained for IRIF proteins in BAP1-depleted cells. Representative staining of cells at 12 hours post-IR treatment are shown in A) and the data are presented as mean ± SD in B). Dashed white line encircles cells with effectively reduced BAP1 expression. Statistical analysis was performed using Student's t-test, *$P < 0.05$, **$P < 0.01$. C) Protein levels of BRCA1, RAD51 and other proteins were determined by western blotting. D) BAP1 is recruited to chromatin after DNA damage. HeLa cells were treated with IR (15 Gy) and chromatin was isolated and analyzed for the indicated proteins. E) BAP1 is recruited at the proximity of a single DSB in MCF7 cells carrying an I-SceI site. Top, schematic representation of the DSB created by I-SceI and the position of the primers used for the ChIP assay. Bottom, enrichment of endogenous BAP1 and H2Aub on regions at proximity to the DSB was determined by ChIP and calculated as percentage of the input. Experiments were repeated 2 times independently and real-time PCR was performed 3 times for each experiment. Data are presented as mean ± SEM.

Figure 3. BAP1 KO DT40 cells are sensitive to DNA damaging agents and defective in HR-mediated gene conversion at sIgM locus.

A) Schematic for the strategy used to generate BAP1 KO in DT40 cells. B) Southern blot confirming BAP1 targeted alleles. C) DT40 BAP1 KO clones 1 and 2, isolated after Cre-mediated excision of BAP1. D) Clonogenic survival of BAP1 KO DT40 cells treated with IR or Olaparib. Statistical analysis was performed using Student's t-test, **P < 0.01. E) BAP1 KO DT40 cells have increased chromosome breaks after DNA damage. Cells were treated with IR (2 Gy) and fixed after 3.5 hours. Three independent experiments were done and chromosome aberrations (isochromatid/ chromatid gaps and breaks and radial figures) were scored in 100 cells for each experiment. Results are reported as total aberrations per cell. F) Left, schema representing the mechanism of sIgM reversion in DT40 cells by gene conversion. Right, sIgM- cells, isolated by flow cytometry, were expanded for 90 generations and the proportion of sIgM+ revertant cells of each sub-population was determined. The experiment was done 2 times independently and the graph compiles the results of both experiments with medians indicated by horizontal lines. Statistical analysis was performed using Student's t-test, **P < 0.01.

Figure 4. **BAP1 is phosphorylated following DNA damage on multiple sites.**

A) Schematic representation of BAP1 showing its main domains and motifs: ubiquitin C-terminal hydrolase (UCH), HCF-1 binding motif (HBM), C-Terminal Domain (CTD) and nuclear localization signal (NLS) along with the identified phosphorylation sites. B) ATM is required for phosphorylation of BAP1. HeLa cells expressing Flag-HA-BAP1 were incubated with ATM inhibitors and then treated with IR (7.5 Gy). Immunoprecipitated BAP1 was subjected to immunoblotting or PRO-Q stain. C) BAP1 complexes were purified at 3 hours post-IR and subjected to silver staining (left) and western blot analysis (right). D) Top, purified BAP1 complexes were incubated with or without the Ub-VME probe for 2 hours and analyzed by western blot. Bottom, in vitro deubiquitination assay of nucleosomal H2Aub using purified BAP1 complexes. Flag-HA-BAP1 complexes were isolated at different times post-IR and incubated with nucleosomes for 4 hours.

Figure 5. Phosphorylation of BAP1 following IR promotes cellular recovery from DNA damage.

A) Generation of H226 cells stably expressing BAP1 WT and mutants. B) Effects of BAP1 WT and mutant forms on H226 cells proliferation. The same number of cells was seeded and allowed for colony formation visualized by crystal violet staining. Experiment was done at least three times. C) H226 cell lines were treated with IR (20 Gy) and surviving colonies were quantified by crystal violet staining and normalized to the untreated controls. Experiment was done 3 times and data are presented as mean ± SD. Statistical analysis was performed using Student's t-test, **P < 0.01. D) ChIP analysis of the recruitment of phosphorylation-deficient mutants of BAP1 at the proximity of DSB in MCF7 cells carrying an I-SceI site. Experiment was repeated 2 times independently and real-time PCR was performed 3 times for each experiment. Data are presented as mean ± SEM. E) H226 BAP1-deficient cells that express BAP1 WT or mutant forms were treated with IR (15 Gy) and harvested for western blotting. F) Model for the role of BAP1 in the DSB response. BAP1 is phosphorylated after DNA damage, thus promoting its recruitment to the DSB site for H2A deubiquitination allowing the recruitment of downstream DSB signaling and repair proteins.

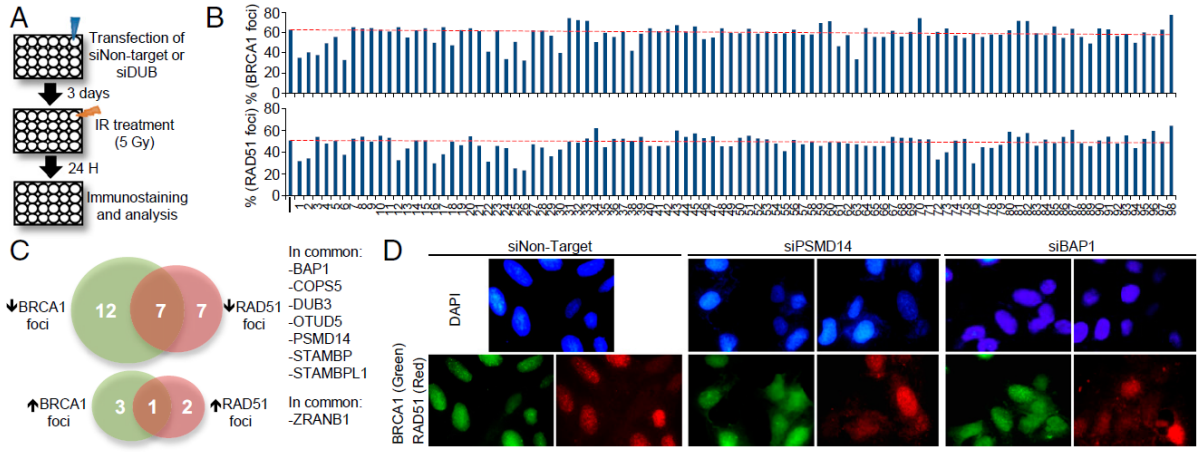
A
Transfection of siNon-target or siDUB
3 days
IR treatment (5 Gy)
24 H
Immunostaining and analysis
B
% (BRCA1 foci)
% (RAD51 foci)
C
BRCA1 foci
12
7
7
RAD51 foci
In common:
-BAP1
-COPS5
-DUB3
-OTUD5
-PSMD14
-STAMBP
-STAMBPL1
BRCA1 foci
3
1
2
RAD51 foci
In common:
-ZRANB1
D
siNon-Target
siPSMD14
siBAP1
DAPI
BRCA1 (Green)
RAD51 (Red)

Figure 1

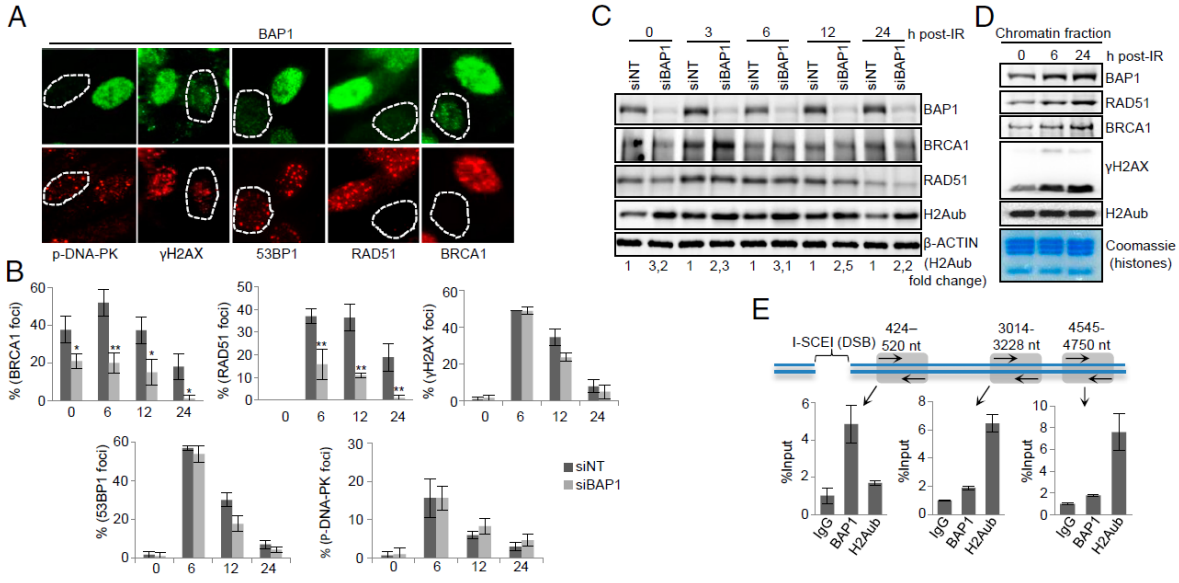
A
BAP1
p-DNA-PK
γH2AX
53BP1
RAD51
BRCA1
B
% (BRCA1 foci)
% (RAD51 foci)
% (γH2AX foci)
% (53BP1 foci)
% (P-DNA-PK foci)
siNT
siBAP1
C
h post-IR
BAP1
BRCA1
RAD51
H2Aub
β-ACTIN
(H2Aub fold change)
D
Chromatin fraction
h post-IR
BAP1
RAD51
BRCA1
γH2AX
H2Aub
Coomassie (histones)
E
I-SCEI (DSB)
424–520 nt
3014-3228 nt
4545-4750 nt
%Input
IgG
BAP1
H2Aub

Figure 2

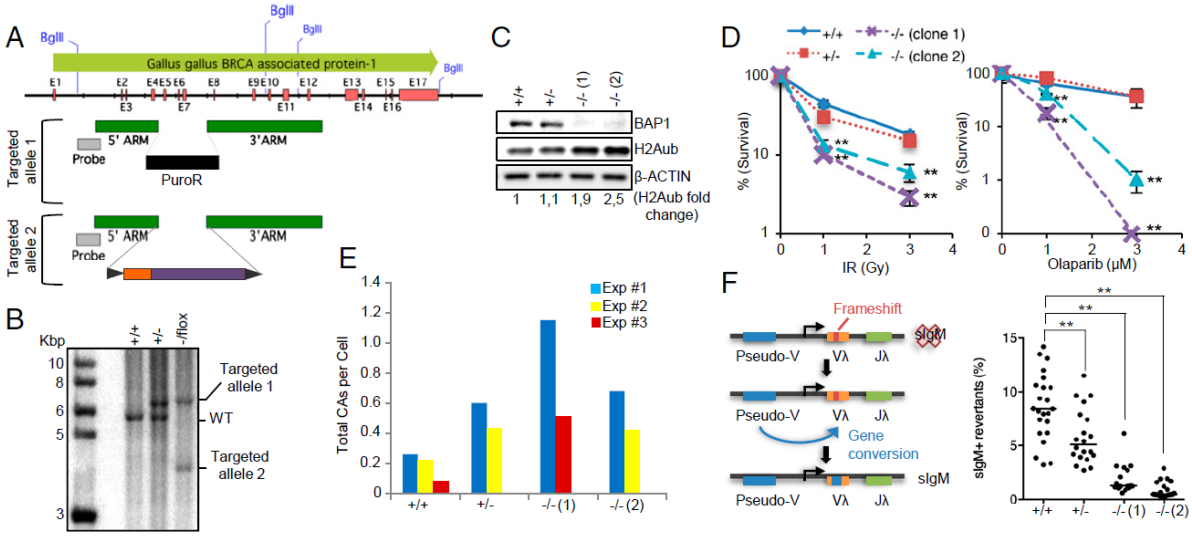
A
BglII
Gallus gallus BRCA associated protein-1
E1 E2 E3 E4E5E6 E7 E8 E9E10 E11 E12 E13 E14 E15 E16 E17
Targeted allele 1
5' ARM
3'ARM
Probe
PuroR
Targeted allele 2
B
Kbp
+/+
+/-
-/flox
Targeted allele 1
WT
Targeted allele 2
C
BAP1
H2Aub
β-ACTIN
1 1,1 1,9 2,5 (H2Aub fold change)
D
+/+
+/-
-/- (clone 1)
-/- (clone 2)
% (Survival)
IR (Gy)
Olaparib (μM)
E
Exp #1
Exp #2
Exp #3
Total CAs per Cell
F
Frameshift
sIgM
Pseudo-V
Vλ
Jλ
Gene conversion
sIgM+ revertants (%)

Figure 3

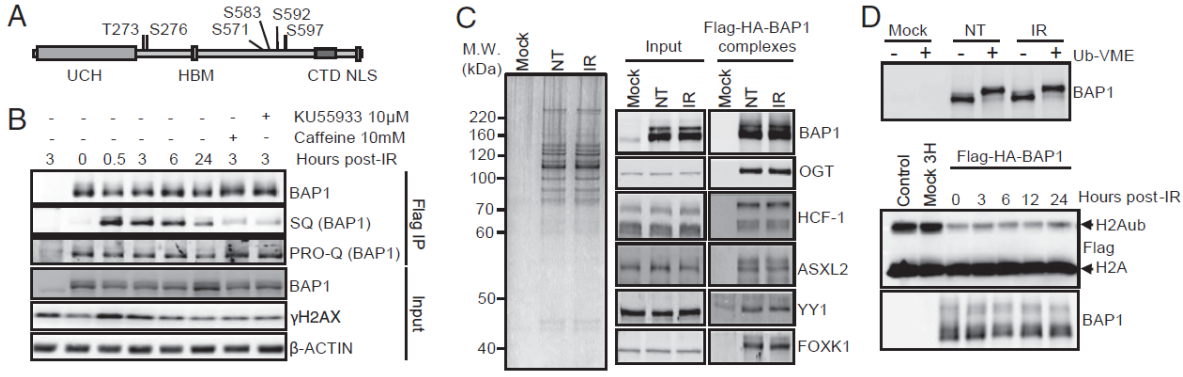
A
T273
S276
S583
S571
S592
S597
UCH
HBM
CTD NLS
B
KU55933 10μM
Caffeine 10mM
Hours post-IR
3 0 0.5 3 6 24 3 3
BAP1
SQ (BAP1)
PRO-Q (BAP1)
BAP1
γH2AX
β-ACTIN
Flag IP
Input
C
M.W. (kDa)
Mock
NT
IR
220
160
120
100
70
60
50
40
Input
Flag-HA-BAP1 complexes
BAP1
OGT
HCF-1
ASXL2
YY1
FOXK1
D
Mock
NT
IR
Ub-VME
BAP1
Control
Mock 3H
Flag-HA-BAP1
0 3 6 12 24 Hours post-IR
H2Aub
Flag
H2A
BAP1

Figure 4

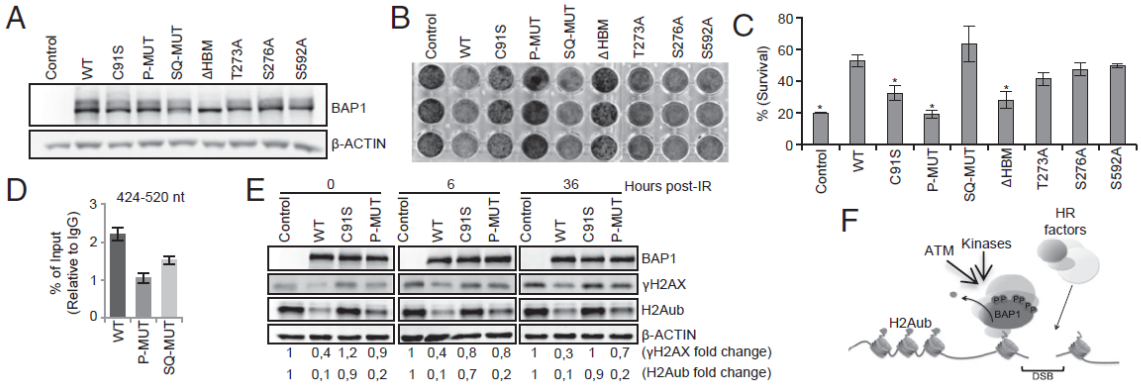
A
Control
WT
C91S
P-MUT
SQ-MUT
ΔHBM
T273A
S276A
S592A
BAP1
β-ACTIN
B
Control
WT
C91S
P-MUT
SQ-MUT
ΔHBM
T273A
S276A
S592A
C
% (Survival)
80
60
40
20
0
Control
WT
C91S
P-MUT
SQ-MUT
ΔHBM
T273A
S276A
S592A
D
424-520 nt
% of Input
(Relative to IgG)
3
2
1
0
WT
P-MUT
SQ-MUT
E
0
6
36
Hours post-IR
Control
WT
C91S
P-MUT
BAP1
γH2AX
H2Aub
β-ACTIN
1 0,4 1,2 0,9 1 0,4 0,8 0,8 1 0,3 1 0,7 (γH2AX fold change)
1 0,1 0,9 0,2 1 0,1 0,7 0,2 1 0,1 0,9 0,2 (H2Aub fold change)
F
HR
factors
ATM
Kinases
BAP1
H2Aub
DSB

Figure 5

SUPPLEMENTAL MATERIALS AND METHODS

Cell culture, plasmids, antibodies and chemicals

Primary human lung fibroblasts LF1, BAP1-deficient human lung squamous carcinoma NCI-H226, cervical cancer HeLa, osteosarcoma U2OS, breast cancer MCF7 carrying an I-SceI cassette and HEK293T cells were cultured in Dulbecco's modified Eagle's medium (DMEM) supplemented with 10 % fetal bovine serum (FBS) and penicillin/streptomycin (Pen/Strep) in 5% CO2 at 37oC. Chicken bursa lymphoma DT40 Cre-1 (1) were cultured in Roswell Park Memorial Institute (RPMI) medium supplemented with 10% FBS, 1% chicken serum, 100 μM β-mercaptoethanol and Pen/Strep in 5% CO2 at 40 oC. Cervical cancer HeLa S3 cells used for complex purification were cultured in Minimum Essential Media (MEM) supplemented with 5% FBS/ Pen/Strep in 5% CO2 at 37 oC.

Cloning of human BAP1 WT and C91S were described (2). BAP1 mutant in phosphorylation sites (P-MUT: T273A, S276A, S571A, S583A, S592A and S597A) was generated using gene synthesis (BioBasic). Other mutants of BAP1 were generated by site directed mutagenesis. BAP1 (WT and mutants) were then subcloned into pENTR D-Topo plasmid (Life Technologies) and recombined into pMSCV-Flag/HA-IRES-Puro. The targeted sequences of shBAP1 #1 and #2 are GGCTGAGATTGCAAACTATGAG and GGTTTCAGCCCTGAGAGCAAAG respectively (2). pCDNA.3 Flag-H2A plasmid was described (3).

Monoclonal anti-BAP1 (C4), polyclonal anti-BAP1 (H300), monoclonal anti-BRCA1 (D9), polyclonal anti-RAD51 (D92), polyclonal anti-53BP1 (H300), polyclonal anti-YY1 (H414), monoclonal anti-p53 (DO.1), polyclonal anti-OGT (H300) antibodies were purchased from Santa Cruz. Polyclonal anti-ubiquityl-histone H2A lysine 119 (#8240), polyclonal anti-phospho histone H3 serine 10 (#3377), Anti-pSQ (#6966), pCHK1 S345 (#2348) and normal rabbit IgG (2729) are from Cell Signaling. Monoclonal anti-phospho-H2A.X serine 139 (05-636) and monoclonal anti-β-actin (C4) antibodies were purchased from Millipore. Polyclonal anti-HCF-1 (A301-400A) and polyclonal anti-ASXL2 (A302-037A) were purchased from

Bethyl laboratories. Monoclonal anti-p21 (556431) was purchased from BD Pharmingen. Monoclonal anti-Flag (M2) was purchased from Sigma and monoclonal anti-HA (HA11) was purchased from Covance. Polyclonal anti-phospho DNA-PK S2056 (ab18192) is from Abcam. Mouse polyclonal anti-FOXK1 antibody was kindly provided by Dr. Xiao-Hua Li (Southwestern University of Texas). Fluorophore-coupled secondary antibodies anti-mouse/anti-rabbit Alexa Fluor 488 and Alexa Fluor 596 were purchased from Life Technologies. The PI3-Kinase inhibitor caffeine (4), was purchased from Sigma-Aldrich. The ATM inhibitor KU-55933 (5), was purchased from Selleck Chemicals. The ATR inhibitor VE-821 (6), was purchased from Selleck Chemicals. The CDK1 inhibitor RO-3306 (7), was purchased from Calbiochem. The CDK1, CDK2 and CDK5 inhibitor Roscovitine (8), was purchased from Cell Signaling. The CDK2 inhibitor Purvalanol A (9) and GW8510 (10), were purchased from Abcam and Sigma-Aldrich respectively. The CDK2, CDK1 and and CDK4 inhibitor SU9516 (11), was purchased from Tocris Bioscience

siDUB screen

U2OS cells were transfected with individual siRNA pool (consisting of 4 pooled siRNA oligonucleotides) targeting DUBs (ON-TARGETplus® SMARTpool® siRNA Library - Human Deubiquitinating Enzymes) or the non-target control from Dharmacon (G-104705, Lot 10138) using Lipofectamine 2000 (Life Technologies). Three days post-transfection, cells were exposed to 5 Gy of ionizing radiation (IR) and collected 24 hours later for immunostaining. Approximately 100 cells were counted for each condition and cells with more than 10 DNA damage foci were considered as positives.

RNAi and immunoblotting

For siRNA experiments, we used ON-TARGETplus® SMARTpool® siRNA against human BAP1 and non-target control (Dharmacon, Thermo Scientific). Transfections of siRNA or shRNA constructs were done using Lipofectamine 2000 (Life Technologies).

Total cell extracts were prepared in lysis buffer (25 mM Tris-HCl, 1% SDS) and protein concentration was determined by bicinchoninic acid (BCA) assay. SDS-PAGE and western

blotting were conducted according to standard procedures. The band signals were acquired using the LAS-3000 LCD camera coupled to the MultiGauge software (Fuji, Standford, CT)

BAP1 gene targeting

The DT40 Cre-1 cell line harboring the fusion protein of Cre and the hormone-binding domain of the mutated estrogen receptor (Mer) (1) was used to generate the BAP1 conditional KO. Gene targeting and southern blotting were done essentially as previously described (12). The targeting constructs were assembled in pBluescript II. The first BAP1 allele was targeted with a puromycin resistance cassette. The second allele was replaced by an insert flanked with two loxP sites that contained the human BAP1 gene under the chicken beta-actin promoter and a blasticidin S resistance cassette. Antibiotic resistance cassettes were previously described (1). Positive clones were screened by southern blot on BglII digested genomic DNA with probes generated by PCR with the following primers: TCCCGCTCAACTGAAGTTCT and CCACAAATGCTCTGAGTGGA. To excise the human BAP1 gene from the conditional BAP1 KO cells, cells were treated with 50 nM of 4-hydroxytamoxifen for 4 days. Cells were then sub-cloned to isolate BAP1 constitutive KO clones.

Clonogenic survival assay

DT40 cells were seeded on plates containing DMEM with 1.5% methylcellulose, 10% FBS, 1% chicken serum, 100 μM β-mercaptoethanol and Pen/Strep. For the IR treatment, the cells were exposed to a cesium-137 source (Gamma Cell; Atomic Energy Canada) at the indicated doses prior seeding. For the Olaparib treatment, cells were seeded in the methylcellulose media containing the indicated concentrations of Olaparib (Selleck chemical). Cells were incubated at 40 oC for 20-30 days to allow colony formation.

H226 stable cell lines expressing Flag-HA-BAP1 WT, C91S or P-MUT were treated with indicated doses of IR and incubated for 5-7 days. The surviving colonies were washed with phosphate-buffered saline (PBS) and fixed with 3 % paraformaldehyde for 20 minutes. Cells were then stained with 0.2 % crystal violet for 10 minutes followed by several washes with PBS. Retained staining was then extracted with 10 % acetic acid and the optical density (OD)

of the extracted dye was determined by spectrophotometry at 540 nm. The population survival rate is determined by the average ratio between the OD of the treated sample and the untreated control sample.

Chromosome aberrations analysis

DT40 cells were treated with 2 Gy of IR and fixed after 3.5 hours. To enrich cells in metaphase, cells were treated with 100 ng/mL of colcemid for 2 hours prior fixation, metaphase spreading and Giemsa staining. Analysis was performed on 100 metaphases of each population. Chromosome abnormalities (isochromatid/ chromatid gaps and breaks and radial figures) were scored.

sIgM phenotype conversion assay

After 20 min incubation with anti-chicken IgM-FITC (Bethyl #A30-102F, 1:800) in phosphate-buffered saline (PBS) containing 2% bovine serum albumin (BSA), DT40 cells were sorted by flow cytometry to obtain homogeneous sIgM negative (sIgM-) populations. Multiple cell populations were cultured in 24-well plates (100 000 cells per well) for 90 doubling times (splitting 1:2 every 1 or 2 days). Their sIgM phenotype is determined by flow cytometry with the same staining procedure used for cell sorting.

Immunofluorescence

Cells were immunostained as previously described (2). The nuclei were stained with 4',6-diamidino-2-phenylindole (DAPI). Images were acquired using the Zeiss Axio Imager Z.2 microscope, Zeiss Acroplan/N-Acroplan 40X/0.65 -0.17 objective and AxioCAM MRm camera.

Flow cytometry analysis

DNA content of cells was analyzed essentially as described (13). Briefly, cells were harvested by trypsinization and fixed with 70 % ethanol. After PBS wash, cells were treated with 100 µg/ml RNase A for 30 min at 37 °C and stained with 50 µg/ml propidium iodide.

DT40 cells intracellular staining for anti-BAP1 (monoclonal) and anti-phospho histone H3 serine 10 was done as follows. Around 1X106 cells were fixed with 70 % of ethanol, blocked with 1 % BSA in PBS and incubated with the indicated primary antibody for 1.5 hours followed by incubation with Alexa Fluor 488-coupled secondary antibody for 1 hour. Between the antibodies incubation, cells were washed with PBS and PBS containing 1 % BSA. DNA was co-stained as described above.

BrdU incorporation in DT40 cells was determined using 1X106 fixed cells following incubation with 20 μM of BrdU for 30 min. DNA of the fixed cells was denatured using HCl 4N/ Triton 0.5 % for 30 min and neutralized by 100 mM Borax pH 8.5. Cells were then blocked with 1 % BSA in PBS followed by incubation with anti-BrdU antibody coupled to Alexa 488 (clone MoBU-1, 1:200, Life Technologies) for 1 hour. DNA was co-stained as described above.

Cells were analyzed using a LSRII flow cytometer (Becton Dickinson) and data were processed with FlowJo V887 software (Tree Star, Inc.).

Chromatin immunoprecipitation on I-SceI-induced double strand break (DSB)

Induction of a single DSB following I-SceI expression, ChIP experiments and real-time PCR were done essentially as previously described (14). Polyclonal anti-BAP1 (H300), polyclonal anti-ubiquitinated histone H2A lysine 119 (DC27C4) and normal rabbit IgG (2729) were used for ChIP experiments. Primers for ChIP experiments were described earlier (15). ChIP on ectopically expressed Flag-HA-BAP1 or mutants was conducted using anti-Flag antibody. First BAP1 constructs were transfected using X-tremeGENE 9 (Roche, #06365779001), then electroporated 24 hours later with the pCAG-ISCEI plasmid before harvesting. Values were calculated as percentage of the input relative to the IgG control, which is set to 1.

Chromatin fractionation

Chromatin fraction was obtained as previously described (16). Briefly, HeLa cells were treated with 15 Gy of IR and fractionated with 50 mM Tris-HCl pH 7.3, 50 mM NaCl, 0.5%

Triton, 5 mM EDTA, 50 mM NaF, 10 mM beta-glycerophosphate, 1 mM Na3VO4, 10 mM 2-mercaptoethanol, 1 mM phenylmethylsulfonyl fluoride (PMSF) and anti-protease cocktail (Sigma). The pellet fraction (the chromatin) was washed several times with the fractionation buffer before sonication. Proteins were quantified and used for western blotting.

Purification of BAP1-associated proteins following DNA damage and identification of phosphorylation sites

Around 3 X 10^9 HeLa S3 cells expressing stably Flag-HA-BAP1 or the empty vector (2) were treated with 10 Gy of IR. Total extracts were prepared 3 hours post-treatment by lysing cells with 50 mM Tris-HCl pH 7.3, 50 mM NaCl, 0.5% NP-40, 50 mM NaF, 10 mM beta-glycerophosphate, 1 mM Na_3VO_4, 10 mM 2-mercaptoethanol, 1 mM PMSF and anti-protease cocktail (Sigma). Lysates were clarified by centrifugation at 20 000g for 30 min and filtration through 0.45 μM filter. Tandem purification (Flag-HA) was done essentially as previously described (17). Mass spectrometry analysis was provided by the Taplin facility at Harvard Medical School (Boston). PRO-Q Diamond phosphoprotein gel stain was purchased from Life Technologies. The polyacrylamide gel was fixed and stained according to the manufacturer's protocol.

Ub-VME hybridization assay

Ubiquitin-Vinyl Methyl Ester (Ub-VME) probe purification and hybridization assay was done as previously described (18). Purified BAP1 complexes or total cell extract were incubated with Ub-VME for 2 hours at room temperature. Reactions were stopped by adding Laemmli buffer and analysed by western blotting.

In vitro ubH2A deubiquitination assay

Native nucleosomes were isolated from HEK293T cells transfected with pCDNA.3 Flag-H2A. As previously described with some modifications, soluble chromatin fraction was obtained by nucleosomes digestion with micrococcal nuclease (MNase, Sigma) (19). Cells were lysed in 420 buffer (50 mM Tris-HCl pH 7.3, 420 mM NaCl, 1% NP-40, 1 mM PMSF, protease inhibitor cocktail (Sigma), and 20 mM of N-ethylmaleimide (NEM) to block any

DUB activity associated with chromatin. After centrifugation, the chromatin pellet was washed twice with the same buffer followed by two washes using MNase buffer (20 mM Tris-HCl pH 7.3, 100 mM KCl, 2 mM MgCl2, 1 mM CaCl2, 0.3 M sucrose, 0.1% NP-40, 1 mM PMSF and protease inhibitor cocktail). Chromatin was then treated with 3 U/ml MNase for 10 min at room temperature and the reaction was stopped with 5 mM EDTA. Following high-speed centrifugation, the soluble chromatin fraction was incubated overnight at 4 °C with Flag M2 agarose beads (Sigma). Beads were then washed several times with EB 300 buffer (50 mM Tris-HCl pH 7.3; 5 mM EDTA; 300 mM NaCl; 10 mM NaF; 1% NP-40; 1 mM PMSF; 1 mM dithiothreitol (DTT); protease inhibitors cocktail (Sigma)) containing 20 mM NEM, followed by several washes with EB 300 buffer without NEM. Beads bound nucleosomes were then eluted with Flag peptides (0.2 μg/ml). The isolated nucleosomes were used for the in vitro deubiquitination assay with Flag-HA BAP1 complexes purified at different times post-IR treatment (5 Gy). The DUB reaction was carried in (50 mM Tris-HCl, pH 7.3; 1mM MgCl2; 50 mM NaCl; 1 mM DTT) for 4 hours at 37°C, stopped by adding 2X Laemmli buffer and analyzed by western blotting.

SUPPLEMENTAL REFERENCES

1. Arakawa H, Lodygin D, & Buerstedde JM (2001) Mutant loxP vectors for selectable marker recycle and conditional knock-outs. (Translated from eng) BMC Biotechnol 1:7 (in eng).

2. Yu H, et al. (2010) The Ubiquitin Carboxyl Hydrolase BAP1 Forms a Ternary Complex with YY1 and HCF-1 and is a Critical Regulator of Gene Expression. (Translated from Eng) Mol Cell Biol (in Eng).

3. Minsky N & Oren M (2004) The RING domain of Mdm2 mediates histone ubiquitylation and transcriptional repression. Mol Cell 16(4):631-639.

4. Sarkaria JN, et al. (1999) Inhibition of ATM and ATR kinase activities by the radiosensitizing agent, caffeine. Cancer Res 59(17):4375-4382.

5. Hickson I, et al. (2004) Identification and characterization of a novel and specific inhibitor of the ataxia-telangiectasia mutated kinase ATM. Cancer Res 64(24):9152-9159.

6. Charrier JD, et al. (2011) Discovery of potent and selective inhibitors of ataxia telangiectasia mutated and Rad3 related (ATR) protein kinase as potential anticancer agents. (Translated from eng) J Med Chem 54(7):2320-2330 (in eng).

7. Johnson N, et al. (2009) Cdk1 participates in BRCA1-dependent S phase checkpoint control in response to DNA damage. Mol Cell 35(3):327-339.

8. Meijer L, et al. (1997) Biochemical and cellular effects of roscovitine, a potent and selective inhibitor of the cyclin-dependent kinases cdc2, cdk2 and cdk5. (Translated from eng) Eur J Biochem 243(1-2):527-536 (in eng).

9. Villerbu N, Gaben AM, Redeuilh G, & Mester J (2002) Cellular effects of purvalanol A: a specific inhibitor of cyclin-dependent kinase activities. (Translated from eng) Int J Cancer 97(6):761-769 (in eng).

10. Johnson K, et al. (2005) Inhibition of neuronal apoptosis by the cyclin-dependent kinase inhibitor GW8510: identification of 3' substituted indolones as a scaffold for the development of neuroprotective drugs. (Translated from eng) J Neurochem 93(3):538-548 (in eng).

11. Lane ME, et al. (2001) A novel cdk2-selective inhibitor, SU9516, induces apoptosis in colon carcinoma cells. (Translated from eng) Cancer Res 61(16):6170-6177 (in eng).

12. Campo VA, et al. (2013) MSH6- or PMS2-deficiency causes re-replication in DT40 B cells, but it has little effect on immunoglobulin gene conversion or on repair of AID-generated uracils. (Translated from eng) Nucleic acids research 41(5):3032-3046 (in eng).
13. Affar EB, et al. (2006) Essential dosage-dependent functions of the transcription factor Yin Yang 1 in late embryonic development and cell cycle progression. Mol. Cell Biol. 26(9):3565-3581.
14. Rodrigue A, et al. (2006) Interplay between human DNA repair proteins at a unique double-strand break in vivo. (Translated from eng) EMBO J 25(1):222-231 (in eng).
15. Krietsch J, et al. (2012) PARP activation regulates the RNA-binding protein NONO in the DNA damage response to DNA double-strand breaks. (Translated from eng) Nucleic acids research 40(20):10287-10301 (in eng).
16. Daou S, et al. (2011) Crosstalk between O-GlcNAcylation and proteolytic cleavage regulates the host cell factor-1 maturation pathway. (Translated from eng) Proc Natl Acad Sci U S A 108(7):2747-2752 (in eng).
17. Nakatani Y & Ogryzko V (2003) Immunoaffinity purification of mammalian protein complexes. Methods Enzymol 370:430-444.
18. Borodovsky A, et al. (2002) Chemistry-based functional proteomics reveals novel members of the deubiquitinating enzyme family. Chem Biol 9(10):1149-1159.
19. Groisman R, et al. (2003) The ubiquitin ligase activity in the DDB2 and CSA complexes is differentially regulated by the COP9 signalosome in response to DNA damage. Cell 113(3):357-367.

SUPPLEMENTAL FIGURES

Figure S1. A) BAP1 depletion using shRNA constructs impairs IRIF formation. U2OS cells were transfected with two different shRNA constructs against BAP1 (shBAP1 #1 and shBAP1 #2) and treated with IR (7.5 Gy). 16 hours post-treatment, cells were fixed for immunostaining of the indicated proteins. Representative images of the experiment are shown. White dashed lines encircle the BAP1-depleted cells. B) BAP1 promotes homologous recombination foci (BRCA1 and RAD51) formation after DNA damage. Original images of Figure 2A are shown. Human fibroblast LF1 cells transfected with control or BAP1 siRNA constructs were combined (1:1) and treated with IR (7.5 Gy). Cells were fixed at different time points post-IR (0h, 6h, 12h and 24h) and subjected to immunostaining of the indicated proteins. BAP1-depleted cells were identified by decreased BAP1 signal and are encircled by white dashed lines. Note that BAP1 RNAi-treated cells were mixed with the control RNAi-treated cells in these immunofluorescence experiments to facilitate the comparison.

Figure S2. A) Depletion of BAP1 does not cause major defects in cell cycle. Human fibroblast LF1 cells were BAP1-depleted by siRNA and subjected for western blotting of the indicated proteins (left panel) and cell cycle profile analysis by flow cytometry using propidium iodide (right panel). Percentage of cell population at each cell cycle phase is shown. B) Depletion of BAP1 does not induce stabilization of p53. LF1 cells were BAP1-depleted using siRNA and treated with IR (7.5 Gy). Cells were collected at different time points following IR treatment and proteins were analyzed by western blot for the indicated proteins. C) BAP1-depleted cells have increased H2A ubiquitination. LF1 cells were treated with siControl (siNT) or siBAP1 and combined (1:1) before fixation and immunostaining of the indicated proteins. Representative images of the stainings are shown. BAP1-depleted cells were identified by decreased BAP1 signal and are encircled by white dashed lines.

Figure S3. A) BAP1 is highly conserved between human and chicken. Alignment of Gallus gallus (NP_001025761.1) and Homo sapiens (NP_004647.1) BAP1 with ClustalW2 and visualized with Geneious software R6.1.4. Identical amino acids (a.a.) are highlighted in

green, similar a.a. are highlighted in yellow and not similar a.a. are in gray. B) Human BAP1 inserted in chicken bap1 locus can be excised by Cre induction. Excision following 3 days of Cre induction was analyzed by flow cytometry using an anti-human BAP1 antibody.

Figure S4. A) BAP1 KO cells proliferate at slower rates. Cells were seeded at the same number at day 0 and counted at days 1, 3 and 5. The experiment was repeated 3 times. Data are presented as mean ± SD. Statistical analysis was performed using Student's t-test, *P < 0.05. B) BAP1 KO cells did not shown any major defect in G1 phase progression. BAP1 KO DT40 cells were incubated with 200 ng/ml of nocodazole to arrest the cells in M phase. Different times after the addition of the drug, cells were fixed and subjected to cell cycle profile analysis by flow cytometry using propidium iodide. C) BAP1 KO cells have a slightly decreased S phase population as revealed by BrdU incorporation. Cells were incubated with BrdU for 30 min prior fixation and co-stained with anti-BrdU antibody and propidium iodide. Cell cycle profile and BrdU uptake were analyzed by flow cytometry. The experiment was repeated 3 times. Data are presented as mean of BrdU positive cells ± SD. Statistical analysis was performed using Student's t-test, *P < 0.05. Representative results of the experiment are shown on the right. D) BAP1 KO cells have similar number of mitotic cells than BAP1 WT cells. Asynchronous cells were fixed and co-stained with anti-phosphorylated H3S10 antibody and propidium iodide. Mitotic population was analyzed by flow cytometry. The experiment was performed 3 times. Data are presented as mean of phosphorylated H3S10 positive cells ± SD. Representative results of the experiment are shown on the right.

Figure S5. BAP1 KO DT40 cells have increased chromosome breaks following DNA damage. BAP1 KO DT40 cells were treated with 2 Gy of IR and fixed after 3.5 hours. Colcemid was added to the cells for 2 hours prior fixation to enrich mitotic cells. A) Representative images of metaphase spreads of each population are shown. Red arrows indicate chromosomal aberrations. B) At least two independent experiments were done and chromosome aberrations of 100 cells were counted in each experiment. Cumulative results of all experiments are shown in Figure 3E.

Figure S6. Phosphorylation of BAP1 following IR treatment. A) G2/M checkpoint was induced by IR treatment in the HeLa S3 cells used for BAP1 complexes purification. Cells were treated with IR (10 Gy) and fixed 24h post-treatment for cell cycle profile analysis by flow cytometry using propidium iodide. This assay was conducted to control for the efficiency of the IR treatment in our large scale complexes purification. B) BAP1 is phosphorylated on specific residues following IR. BAP1 phosphorylated peptide sequences identified by mass spectrometry are shown. Phospho-residues are colored in red and their position in BAP1 sequence are indicated. C) Two BAP1 IR-specific phospho-sites are conserved. Alignment of BAP1 amino acid sequence from different species using Geneious software R6.1.4. Accession numbers are shown. BAP1 IR-specific phospho-residues are squared in red. D) IR treatment does not affect the assembly of major components of the BAP1 complexes. Quantification of protein peptides by MS/MS revealed that the composition of the BAP1 core complex does not change following IR. E) BAP1 DUB activity is not affected by IR. DUB activity was revealed by Ubiquitin-VME (Ub-VME) probe labeling assay. IR-treated HeLa and U2OS total cell extracts were incubated with Ub-VME probe for 2 hours and analyzed by western blot using BAP1 antibody. The shifted-up BAP1 bands are indicative of probe labeling.

Figure S7. Characterization of BAP1 phosphorylation following DNA damage. A) Mutation of BAP1 phosphorylation sites. U2OS cells stably expressing Flag-HA-BAP1 mutants were treated with IR (7.5 Gy) for 3 hours and used for immunoprecipitation using anti-Flag beads. The samples were subjected to western blotting using an anti-pSQ. YY1 was used as a loading control. Note that mutation of the S276 site (also an SQ motif) does not decrease the signal detected with this anti-pSQ (compare the pSQ signal versus BAP1 signal in the immunoprecipitation). This antibody recognizes pS/TQ(G) found at the position 592 of BAP1. B) The role of ATR in the phosphorylation of BAP1. HeLa cells stably expressing Flag-HA-BAP1 were pretreated with the ATR inhibitor VE-821 for 1 hour and then with IR (7.5 Gy) for 3 hours and used for immunoprecipitation using anti-Flag beads. C) DNA-PK is not required for the phosphorylation of BAP1. Immunoprecipitation of BAP1 from DNA-PK-deficient and proficient cells, MO59J and MO59K, respectively before and after IR (7.5 Gy)

treatment. D) HCF-1 is not required for phosphorylation of BAP1. U2OS cells stably expressing Flag-HA-BAP1 WT, ΔHBM or SQ-MUT were treated with IR (7.5 Gy) for 3 hours and used for immunoprecipitation of BAP1 using anti-Flag beads. E) The inhibition of CDKs does not affect BAP1 phosphorylation. HeLa cells stably expressing the empty vector or Flag-HA-BAP1 WT were pretreated with the indicated CDK inhibitors for 1 hour and then with IR (7.5 Gy) for 3 hours and used for immunoprecipitation using anti-Flag beads. The immunoprecipitated BAP1 samples were immunoblotted against anti-pSQ or stained with PRO-Q. F) Characterization of BAP1 P-MUT following IR treatment. HeLa cells stably expressing the empty vector, Flag-HA-BAP1 WT or P-MUT were treated with IR (7.5 Gy). Following immunoprecipitation using anti-Flag beads, the samples were subjected to immunoblotting using anti-SQ or stained with PRO-Q. G) The BAP1 P-MUT does not lose interaction with the major partners of BAP1. HeLa S3 cells stably expressing the empty vector, Flag-HA-BAP1 WT or P-MUT were subjected for immuno-purification using anti-Flag and anti-HA beads followed by silver staining. The major components of the BAP1 complexes were detected by western blot. H) BAP1 P-MUT exhibits H2A DUB activity in vitro. Flag-HA-BAP1 WT or P-MUT complexes were incubated with purified nucleosomes for the indicated time points. H2A deubiquitination was analysed by western blotting.

Figure S8. H226 BAP1-deficient cells reconstituted with BAP1 WT, catalytic inactive (C91S) or phospho-mutant (P-MUT). A) H226 cells stably expressing different Flag-HA-BAP1 mutants were fixed and stained with anti-HA antibody and DAPI. B) Cells were treated with IR (15 Gy) for the indicated time points and harvested for the analysis of apoptosis. The samples were fixed with ethanol, stained with propidium iodide and analyzed by flow cytometry for the sub G1 population. C-D) H226 BAP1-deficient cells harbor intrinsic DNA damage foci and exhibit genomic instability. C) H226 cells were immunostained for γH2AX and DNA was stained with DAPI. H226 cells showed constitutive γH2AX foci. D) Chromosome instability in H226 cells was visualized by DAPI-stained DNA. Presence of micronuclei and inter-nuclear bridges are indicated by the white arrows.

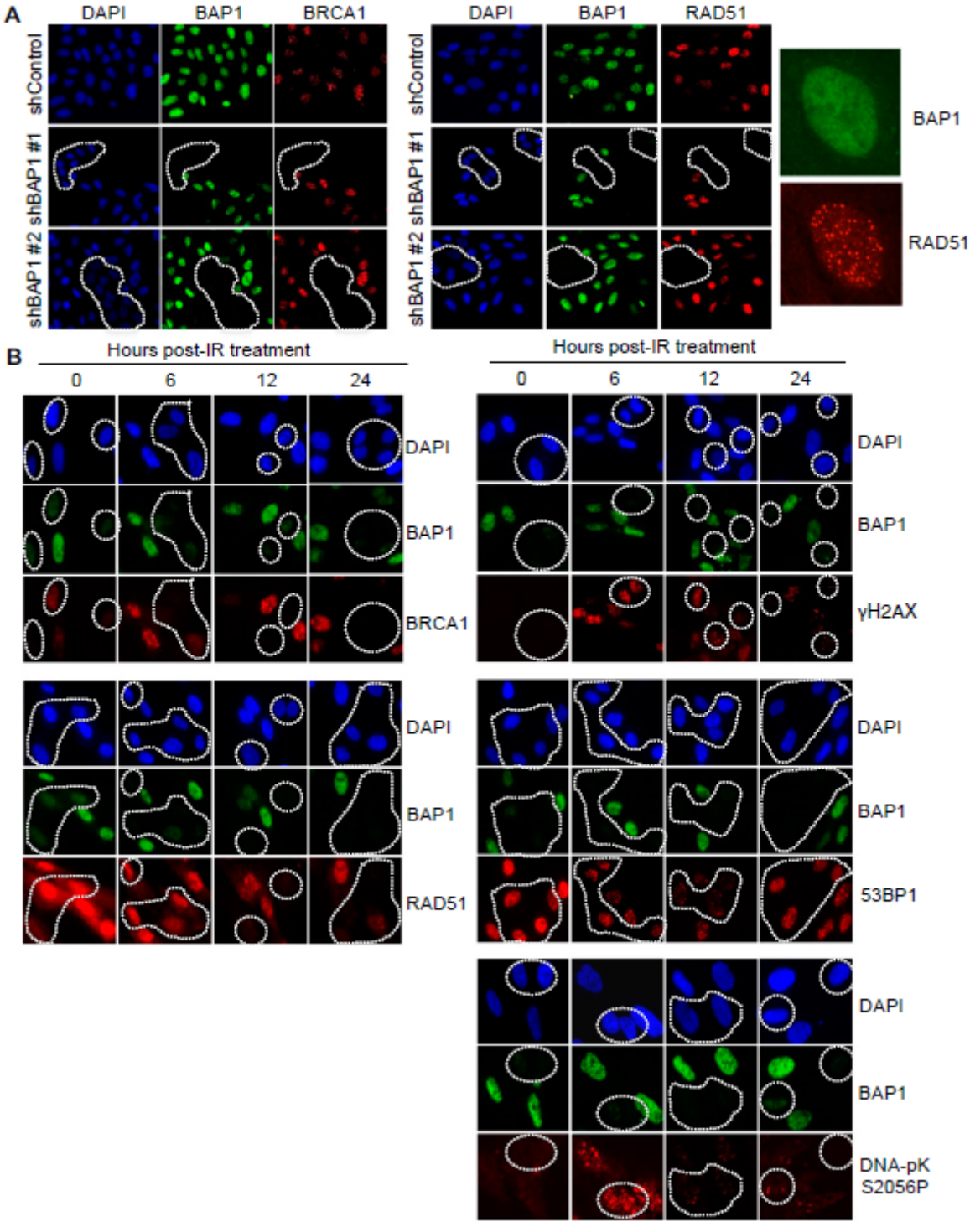
A
DAPI
BAP1
BRCA1
shControl
shBAP1 #1
shBAP1 #2
DAPI
BAP1
RAD51
shControl
shBAP1 #1
shBAP1 #2
BAP1
RAD51
B
Hours post-IR treatment
0
6
12
24
DAPI
BAP1
BRCA1
DAPI
BAP1
γH2AX
DAPI
BAP1
RAD51
DAPI
BAP1
53BP1
DAPI
BAP1
DNA-pK
S2056P

Figure S1

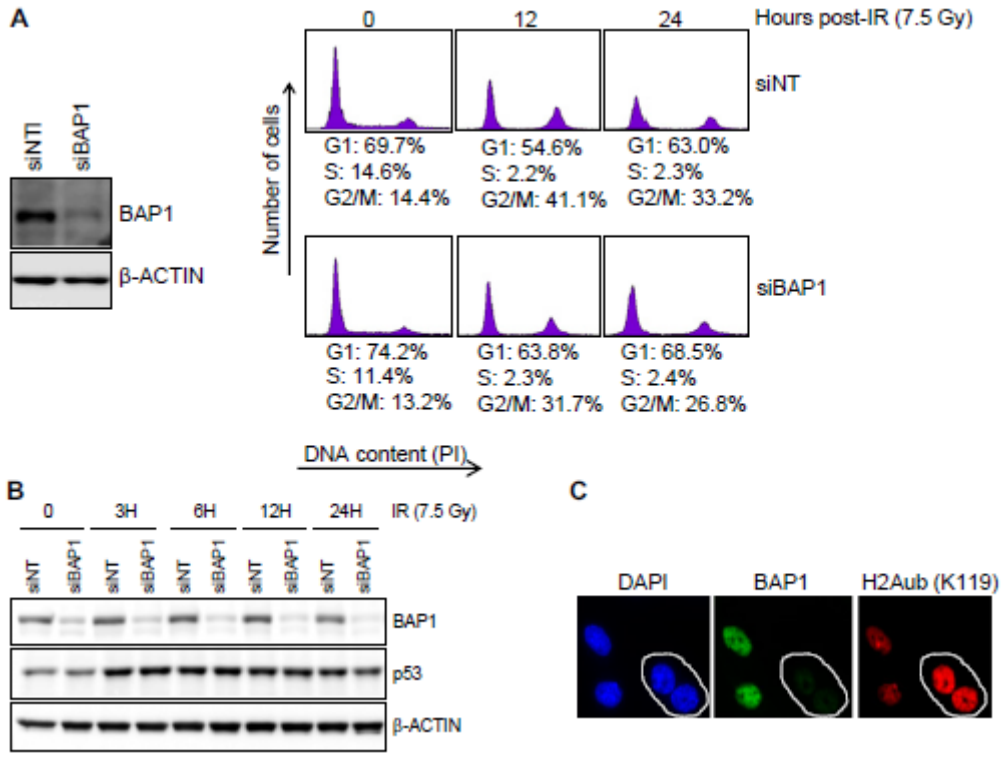
A
siNT
siBAP1
BAP1
β-ACTIN
0
12
24
Hours post-IR (7.5 Gy)
siNT
Number of cells
G1: 69.7%
S: 14.6%
G2/M: 14.4%
G1: 54.6%
S: 2.2%
G2/M: 41.1%
G1: 63.0%
S: 2.3%
G2/M: 33.2%
siBAP1
G1: 74.2%
S: 11.4%
G2/M: 13.2%
G1: 63.8%
S: 2.3%
G2/M: 31.7%
G1: 68.5%
S: 2.4%
G2/M: 26.8%
DNA content (PI)
B
0
3H
6H
12H
24H
IR (7.5 Gy)
siNT
siBAP1
BAP1
p53
β-ACTIN
C
DAPI
BAP1
H2Aub (K119)

Figure S2

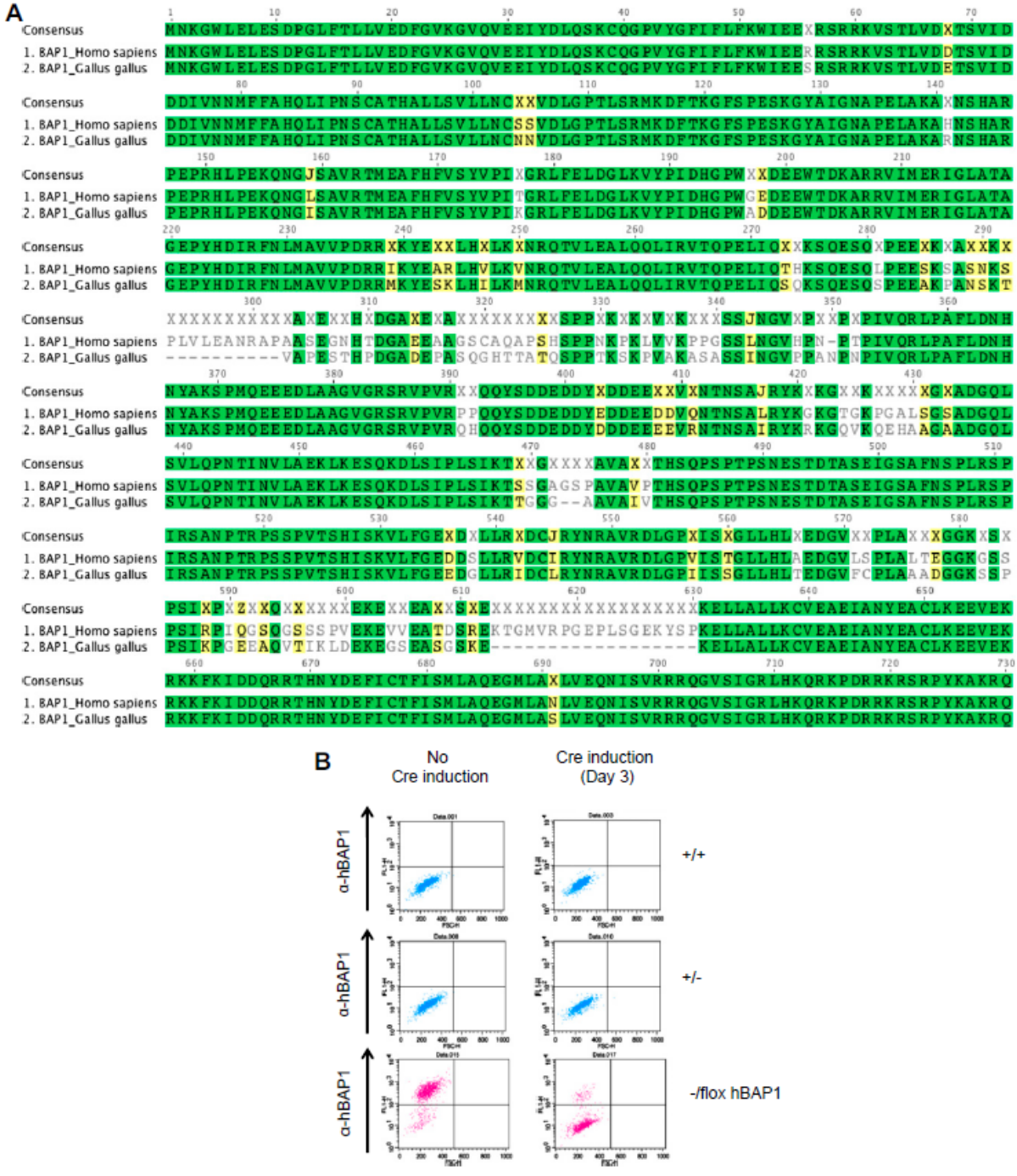
A
Consensus
1. BAP1_Homo sapiens
2. BAP1_Gallus gallus
B
No
Cre induction
Cre induction
(Day 3)
α-hBAP1
+/+
+/-
-/flox hBAP1

Figure S3

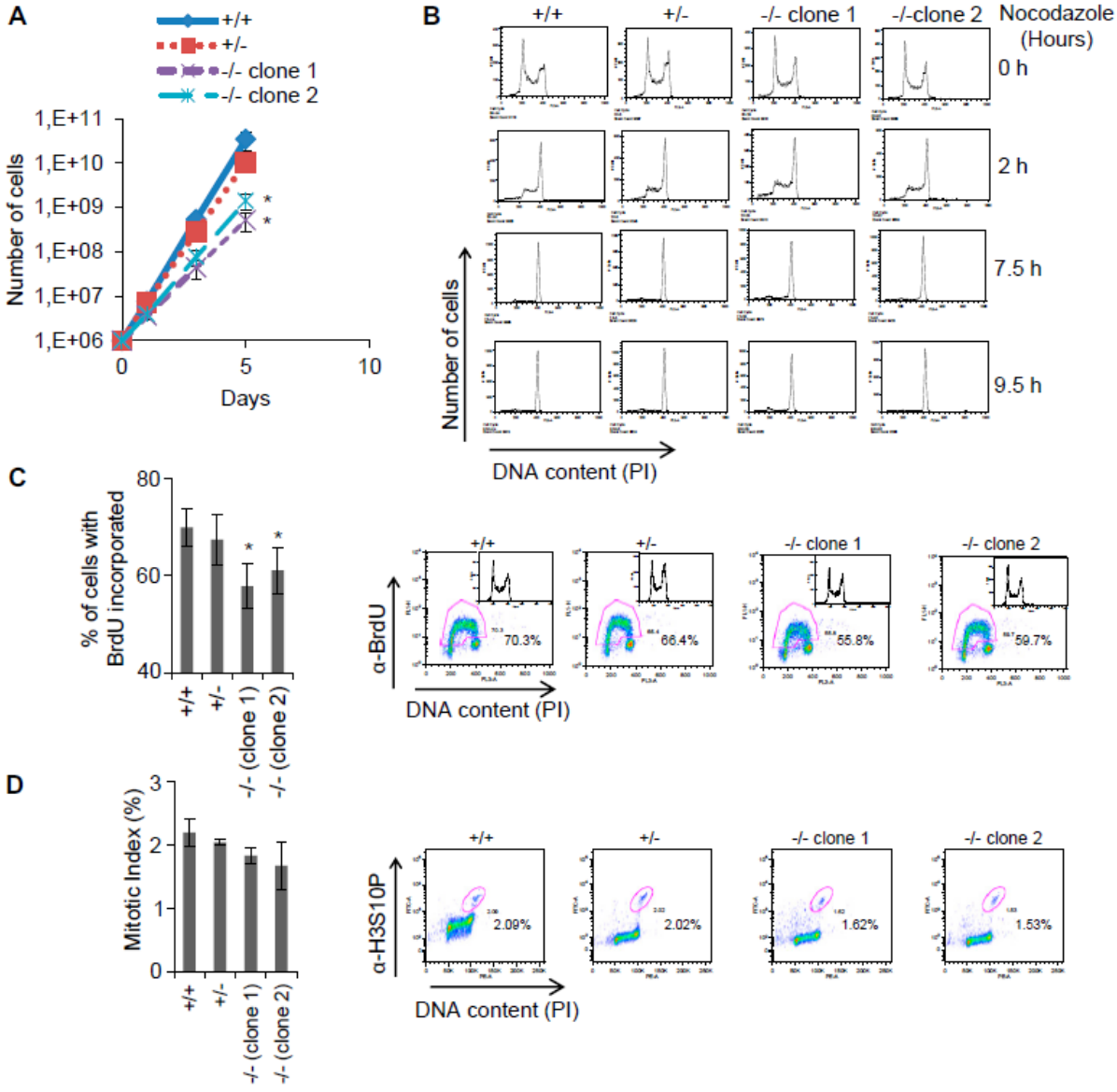
A
+/+
+/-
-/- clone 1
-/- clone 2
Number of cells
1,E+11
1,E+10
1,E+09
1,E+08
1,E+07
1,E+06
0
5
10
Days
B
+/+
+/-
-/- clone 1
-/-clone 2
Nocodazole (Hours)
0 h
2 h
7.5 h
9.5 h
Number of cells
DNA content (PI)
C
% of cells with BrdU incorporated
80
60
40
+/+
+/-
-/- (clone 1)
-/- (clone 2)
α-BrdU
70.3%
66.4%
55.8%
59.7%
DNA content (PI)
D
Mitotic Index (%)
3
2
1
0
α-H3S10P
2.09%
2.02%
1.62%
1.53%
DNA content (PI)

Figure S4

A

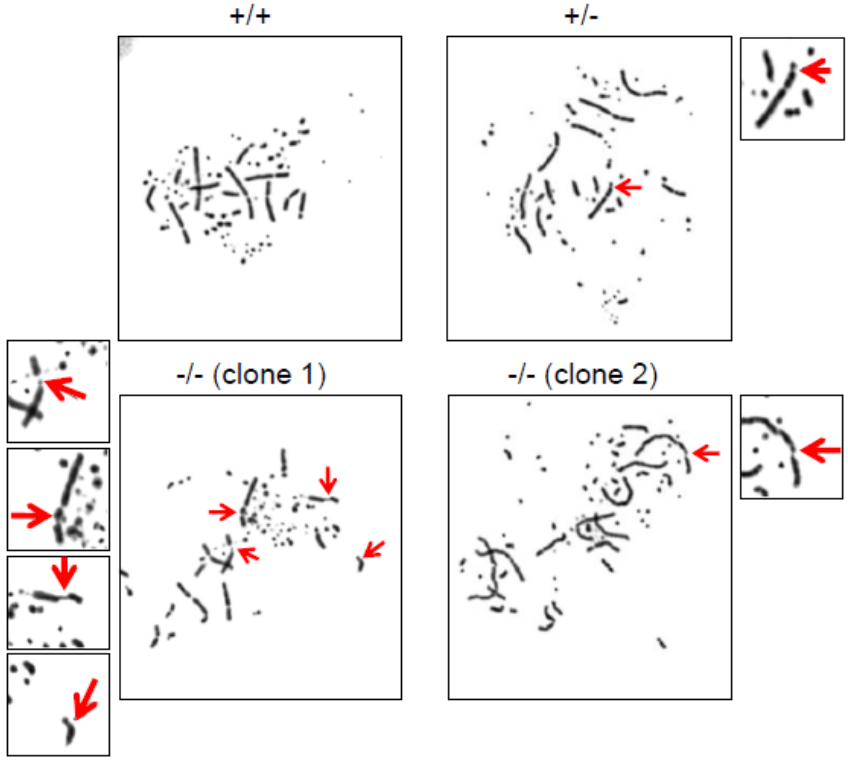

B

Genotype	Isochromatid		Chromatid		Radial figures	Total aberrations (per cell)	
	Breaks	Gaps	Breaks	Gaps		With chromatid gaps	Without chromatid gaps
+/+	(6) (0) (0)	(10) (10) (3)	(4) (9) (5)	(5) (3) (0)	(1) (0) (0)	(0.26) (0.22) (0.08)	(0.22) (0.19) (0.08)
+/-	(3) (5)	(11) (9)	(21) (38)	(8) (9)	(0) (0)	(0.43) (0.60)	(0.35) (0.51)
-/- (clone 1)	(1) (8)	(10) (26)	(25) (73)	(15) (6)	(0) (0)	(0.51) (1.15)	(0.35) (1.09)
-/- (clone 2)	(9) (2)	(21) (12)	(25) (24)	(11) (4)	(1) (0)	(0.68) (0.42)	(0.57) (0.38)

Figure S5

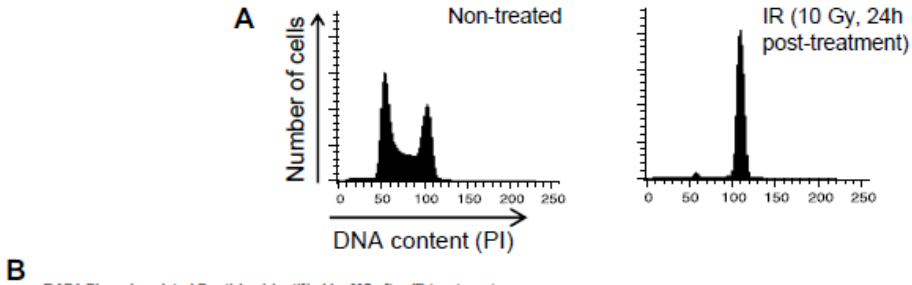

B

BAP1 Phosphorylated Peptides identified by MS after IR treatment.

Amino acid	Non Treated	IR
396	VPVRPPQQYS#DDEDDYEDDEEDDVQNTNSALR	VPVRPPQQYS#DDEDDYEDDEEDDVQNTNSALR
522	SANPTRPSS#PVTSHISK	SANPTRPS#SPVTSHISK
513	S#ANPTRPSS#PVTSHISK	S#ANPTRPSS#PVTSHISK
369	LPAFLDNHNYAKS#PM*QEEEDLAAGVGR	LPAFLDNHNYAKS#PM*QEEEDLAAGVGR
328	APAASEGNHTDGAEEAAGSCAQAPSHS#PPNKPK	APAASEGNHTDGAEEAAGSCAQAPSHS#PPNKPK
509	TSSGAGSPAVAVPTHSQPSPTPSNESTDTASEIGSAFNSPLRS#PIR	TSSGAGSPAVAVPTHSQPSPTPSNESTDTASEIGSAFNSPLRS#PIR
505	TSSGAGSPAVAVPTHSQPSPTPSNESTDTASEIGSAFNS#PLR	TSSGAGSPAVAVPTHSQPSPTPSNESTDTASEIGSAFNS#PLR
487/489	TSSGAGSPAVAVPTHSQPSPTPSNESTDTASEIGSAFNSPLR	TSSGAGSPAVAVPTHSQPSPTPSNESTDTASEIGSAFNSPLR
597	GSSPSIRPIQGSQGSSS#PVEK	GSSPSIRPIQGSQGSSS#PVEK
292	SASNKS#PLVLEANR	SASNKS#PLVLEANR
123	GFS#PESK	GFS#PESK
585	GSSPS#IRPIQGSQGSSSPVEK	
369	S#PM*QEEEDLAAGVGR	
273/276		VTQPELIQTHKSQESQLPEESK
571		DLGPVISTGLLHLAEDGVLS#PLALTEGGK
592		GSSPSIRPIQGS#QGSSSPVEK
592/597		GSSPSIRPIQGS#QGSSS#PVEK
583/597		GSS#PSIRPIQGSQGSSS#PVEK
583		GSS#PSIRPIQGSQGSSSPVEK

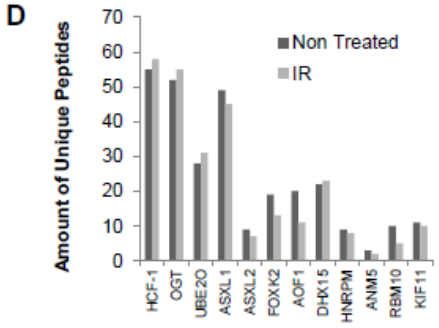

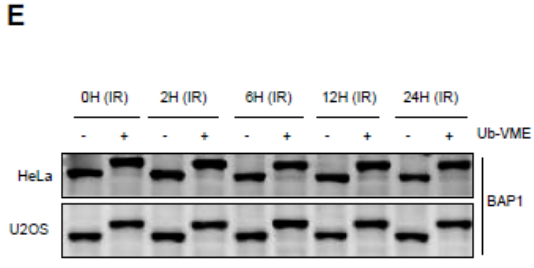

Figure S6

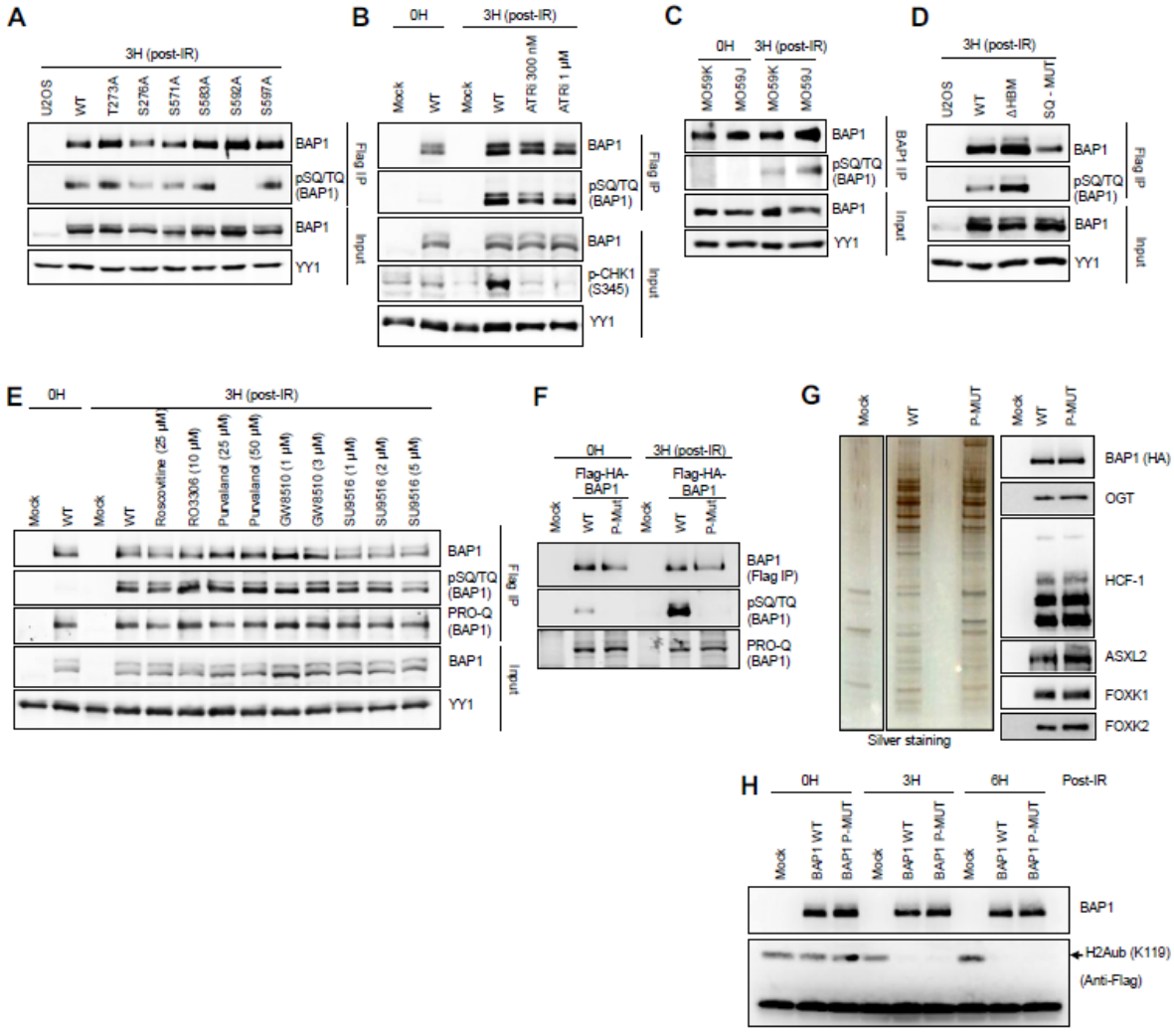
A
3H (post-IR)
U2OS
WT
T273A
S276A
S571A
S583A
S592A
S597A
BAP1
pSQ/TQ (BAP1)
BAP1
YY1
Flag IP
Input
B
0H
3H (post-IR)
Mock
WT
Mock
WT
ATRi 300 nM
ATRi 1 μM
BAP1
pSQ/TQ (BAP1)
BAP1
p-CHK1 (S345)
YY1
Flag IP
Input
C
0H
3H (post-IR)
MO59K
MO59J
MO59K
MO59J
BAP1
pSQ/TQ (BAP1)
BAP1
YY1
BAP1 IP
Input
D
3H (post-IR)
U2OS
WT
ΔHBM
SQ - MUT
BAP1
pSQ/TQ (BAP1)
BAP1
YY1
Flag IP
Input
E
0H
3H (post-IR)
Mock
WT
Mock
WT
Roscovitine (25 μM)
RO3306 (10 μM)
Purvalanol (25 μM)
Purvalanol (50 μM)
GW8510 (1 μM)
GW8510 (3 μM)
SU9516 (1 μM)
SU9516 (2 μM)
SU9516 (5 μM)
BAP1
pSQ/TQ (BAP1)
PRO-Q (BAP1)
BAP1
YY1
Flag IP
Input
F
0H
3H (post-IR)
Flag-HA-BAP1
Flag-HA-BAP1
Mock
WT
P-Mut
Mock
WT
P-Mut
BAP1 (Flag IP)
pSQ/TQ (BAP1)
PRO-Q (BAP1)
G
Mock
WT
P-MUT
Mock
WT
P-MUT
BAP1 (HA)
OGT
HCF-1
ASXL2
FOXK1
FOXK2
Silver staining
H
0H
3H
6H
Post-IR
Mock
BAP1 WT
BAP1 P-MUT
Mock
BAP1 WT
BAP1 P-MUT
Mock
BAP1 WT
BAP1 P-MUT
BAP1
H2Aub (K119)
(Anti-Flag)

Figure S7

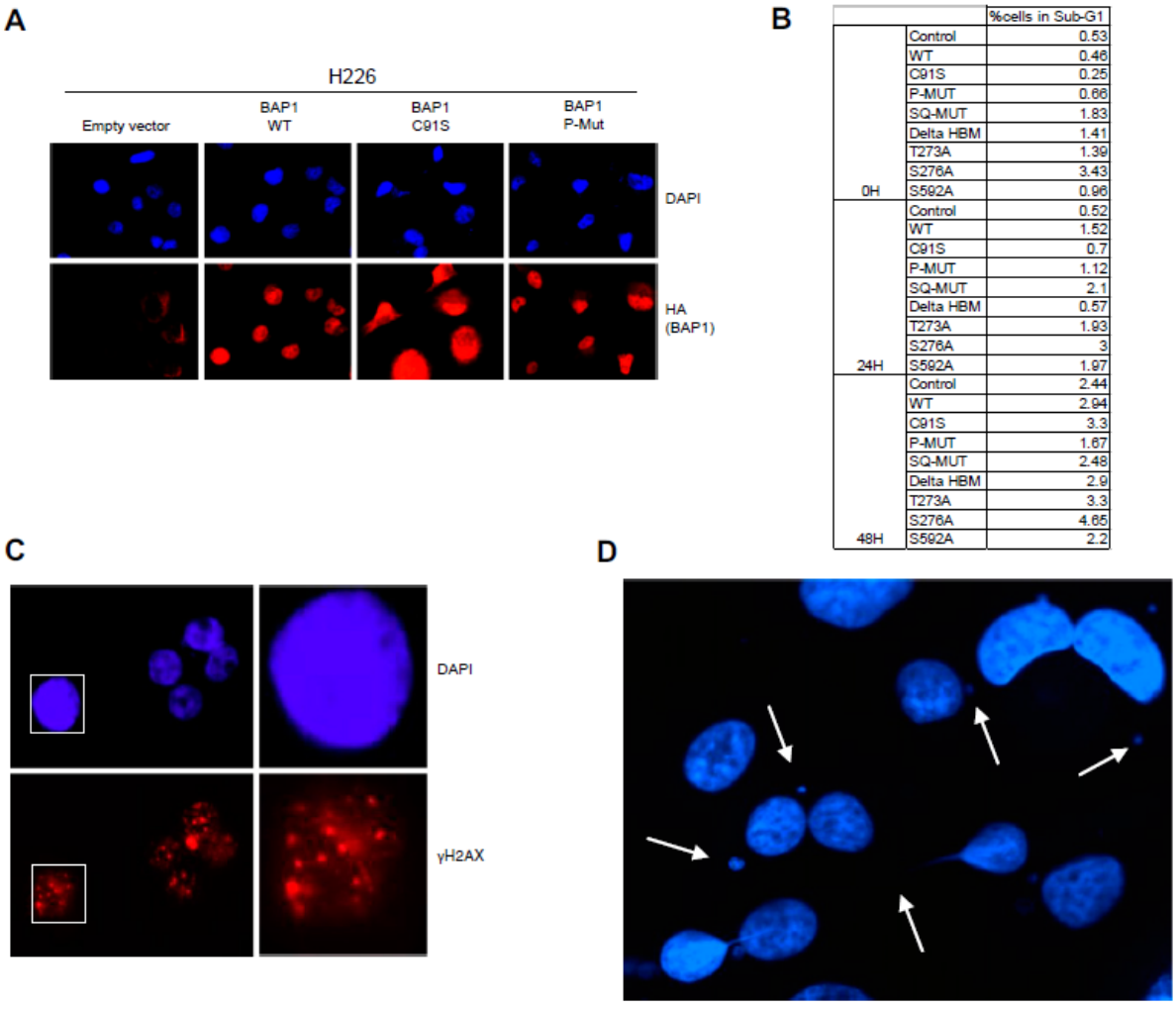

		%cells in Sub-G1
0H	Control	0.53
	WT	0.46
	C91S	0.25
	P-MUT	0.66
	SQ-MUT	1.83
	Delta HBM	1.41
	T273A	1.39
	S276A	3.43
	S592A	0.96
24H	Control	0.52
	WT	1.52
	C91S	0.7
	P-MUT	1.12
	SQ-MUT	2.1
	Delta HBM	0.57
	T273A	1.93
	S276A	3
	S592A	1.97
48H	Control	2.44
	WT	2.94
	C91S	3.3
	P-MUT	1.67
	SQ-MUT	2.48
	Delta HBM	2.9
	T273A	3.3
	S276A	4.65
	S592A	2.2

Figure S8

Table S1. List of DUBs associated with decreased or increased IR-induced foci formation

DUB name	Cells with foci (%)
BRCA1 foci*	
Control	63
BAP1	35
COPS5	41
CXORF53 (BRCC36)	38
CYLD	50
DUB3	33
OTUD5	50
OTUD7	48
PSMD14	41
SENP2	34
STAMBP	51
STAMBPL1	32
UBL5	40
UCHL1	51
UEVLD	42
USP15	53
USP3	47
USP31	33
USP6	49
C13ORF22	50
BRCA1 foci†	
Control	63
UBR1	75
UBTD1	73
USP38	75
ZRANB1	78
RAD51 foci*	
Control	51
BAP1	32
COPS5	35
DUB3	38
OTUB1	33
OTUD5	30
OTUD6B	38
PSMD14	31
STAMBP	25
STAMBPL1	23
UBL4	36
USP24	41
USP4	33
USP40	40
USP43	30
RAD51 foci†	
Control	51
UCHL1	62
USP53	61
ZRANB1	64

*Only DUBs associated with a decrease (BRCA1 foci $\leq$ 53%, RAD51 foci $\leq$ 41%) of at least 10% of cells with foci compared with the control are considered. The 10% cutoff was chosen to maximize chances of hit identification, taking into account that transfection efficiency was not determined because of lack of specific antibodies for all DUBs. Cells with more than 10 foci of the indicated protein were counted.

†Only DUBs associated with an increase (BRCA1 foci $\geq$ 73%, RAD51 foci $\geq$ 61%) of at least 10% of cells with foci compared with the control are considered. The 10% cutoff was chosen to maximize chances of hit identification, taking into account that transfection efficiency was not determined because of lack of specific antibodies for all DUBs. Cells with more than 10 foci of the indicated protein were counted.